

Studies on Interactions of Exported
***Plasmodium falciparum* Membrane Proteins**

Inauguraldissertation

zur

Erlangung der Würde eines Doktors der Philosophie

vorgelegt der

Philosophisch-Naturwissenschaftlichen Fakultät

der Universität Basel

von

Olivier Dietz

aus Basel (BS)

Basel, 2014

Genehmigt von der Philosophisch-Naturwissenschaftlichen Fakultät auf Antrag von Prof.
Hans-Peter Beck und Prof. Tim Gilberger.

Basel, den 10.Dezember 2013

Prof. Dr. Jörg Schibler

Dekan

Table of Contents

Acknowledgements	1
Summary	3
Abbreviations.....	5
Chapter 1: Introduction.....	7
Malaria.....	8
<i>Plasmodium falciparum</i> life cycle.....	9
Genome of <i>P. falciparum</i>	11
Erythrocyte modification by <i>P. falciparum</i>	11
Protein export in <i>P. falciparum</i>	15
Protein-protein interactions.....	18
Protein-protein interactions in <i>P. falciparum</i>	21
Outline	26
References.....	27
Chapter 2: Establishment of the mating-based split-ubiquitin system as a new <i>in vitro</i> interaction platform for <i>Plasmodium falciparum</i> membrane proteins.....	41
Chapter 3: Characterization of the potential MAHRP1 interaction partners PIESP2 & PF3D7_0501000.....	83
Chapter 4: SEMP1: Characterization of a small exported <i>Plasmodium</i> <i>falciparum</i> membrane protein.....	101
Chapter 5: Verification of potential SEMP1 protein-protein interactions by mbSUS pairwise interaction assays.....	147
Chapter 6: General discussion.....	165
Outlook.....	179
Appendix.....	181

Acknowledgements

I would first like to say a very big thank you to my supervisor Hans-Peter Beck for giving me the opportunity to work on this interesting project. I really enjoyed my time in your group and I am very grateful for your support, your enthusiasm, your valuable inputs and all the interesting discussions. Additionally I would like to thank Till Voss not only for joining my thesis committee but especially for all the inspiring conversations throughout my years at the SwissTPH. Further I highly appreciate that Tim Gilberger did join my thesis committee and I want to thank him for taking the long trip to Basel. Other thanks go to Ingrid Felger for her constructive input and for giving me the opportunity to be involved in the P27 project.

I am very grateful to everyone who contributed to my work: Sebastian Rusch for the immunization of mice, Françoise Brand for the great electron microscopy pictures, Esther Mundwiler for providing the PF3D7_0702500-3xHA parasite, Annette Gaida for transfection of the PIESP2-GFP and PF3D7_0501000-GFP parasite lines, Sophie Öhring for providing the SEMP1-3xHA parasite and Till Voss for revising the SEMP1 manuscript.

A big thank you of course goes to all the great people from the lab that I had the pleasure to work with during my time at the SwissTPH. Especially Nicolas Brancucci, who was a great companion throughout all our studies and with whom I shared a lot of great moments, in the lab as well as in our free time. Special mention deserves amongst others also Sebastian Rusch, who with his great knowledge and sheer inexhaustible patience was an irreplaceable support. Thank you for all the laughs and great discussions. The same applies to “Miss MAHRple” Esther Mundwiler, who I would like to thank for her infectious enthusiasm, her valuable input and many interesting conversations. Special thanks also go to Serej Ley for her much appreciated moral support during the writing stage of my thesis and for many interesting discussions about our projects, PNG and everything else. I also would like to thank Nicole Bertschi for all the great conversations and the shared spare time activities (concerts, climbing, hockey etc.). I also want to thank the two great ladies from the Molecular Diagnostics lab Rahel Wampfler and Natalie Hofmann for all the interesting conversations and especially for their infectious

ACKNOWLEDGEMENTS

enthusiasm. Also big thanks go to the two Londoners Kathrin “KW” Witmer for all the laughs and Christian (Chrigu) Flück for the adventurous trip to Nijmegen. Of course many thanks go also to all the other present and former lab members for creating such a great working atmosphere: Alex “Four PHISTs for a Halleluja” Oberli, Françoise Brand (Mrs. Tokuyasu), Dania Müller (real time PCR expert and great help all around), Martin “Chichi” Maire, Caroline Kulangara (thanks for giving me the opportunity to be involved in the P27 project), Annette Gaida, Igor Niederwieser (thanks for your valuable input regarding the work with yeast), Anna Perchuc, Christian Köpfl, Sophie Öhring, Claudia List, Marie Ballif, Pax Masimba, Michael Filarsky, Adrian Najer, Felista Mwingira, Tereza Vieira de Rezende, Pricila Thihara and all the Master students and civil workers: Mussa Maganga, Pablo Scholer, Lincoln Timinao, David Beauparlant, Bianca Bracher, Mirjam Moser, Sandra Brenneisen, Damien Jacot, Patrick Seitz, Samuel Lüdi, Hai Bui, David Stucki, and Grégory Morandi.

I also thank all the great people I met outside the lab who added to the great atmosphere at the Institute: Matthias Rottman (for all the interesting conversations about science, hockey and everything else), Michael Käser (thanks for the laughs in the office), Christoph Schmid (for introducing me into the secrets of Perl), Christian Scheurer, Urs Duthaler, Philipp Ludin, Fabrice Graf, Benjamin Speich, Kathrin Ingram, Lucienne Tritten, Daniel Nyogea, Sergio Wittlin, Pascal Mäser, Yvette Endriss, Beatrice Wäckerlin, Fabien Haas, Dirk Stoll, Paul Haas, Amanda Ross (for her statistical advice) and also the IT crew for their sometimes much needed support.

I am also very grateful to the Rudolf Geigy Foundation for their financial support during the final stage of my thesis and to the Swiss Society of Tropical Medicine and Parasitology (SSTMP) for enabling my participation at the Molecular Parasitology Meeting in Woods Hole.

I am also very thankful to Andrew Dunbar and Bruno Tigani from Novartis for giving me the possibility to use their confocal microscopy facility.

Most of all I would like to thank my family. I am deeply grateful to my mother Ursula, my father Werner and my brother Thierry for their tremendous support throughout my whole live. Very special thanks also go to Olivia Brenzikofer, for her support, love and belief in me.

Summary

Responsible for about 700'000 annual deaths worldwide, malaria today is still one of the major health problems in developing countries. The most deadly form of human malaria called malaria tropica is caused by the apicomplexan parasite *Plasmodium falciparum* that is transmitted by the female *Anopheles* mosquito. Its pathology is associated with the asexual development of the unicellular parasite within the human red blood cell (RBC) that is devoid of all internal organelles and any protein trafficking machinery. Therefore, intraerythrocytic survival and virulence of *P. falciparum* strictly depend on extensive host cell refurbishments mediated by the export of parasite proteins into the erythrocyte cytosol. Although numerous of these proteins have been identified and some extensively studied, still surprisingly little is known about their functions and interactions. It could be shown that many of these proteins are transported to or via parasite-induced membranous structures in the erythrocyte cytosol termed Maurer's clefts (MCs). While these MCs are known to have a crucial role in protein trafficking, probably by acting as secretory organelles that concentrate virulence proteins for delivery to the host cell membrane, their specific functions have yet to be determined.

With this study we aimed at bringing new insight into the functions and interactions of exported *P. falciparum* proteins, with intent to create a basis for the extensive interaction network of the parasite's exportome. Therefore we not only performed interaction studies using classical approaches like co-immunoprecipitation (Co-IP), but also tried to establish the yeast mating-based split-ubiquitin system (mbSUS) as a new *in vitro* interaction platform for *P. falciparum* membrane proteins on the basis of the integral MC protein 'membrane associated histidine rich protein 1' (MAHRP1). To contribute to a better understanding of protein export we further identified and characterized a new MC membrane protein that we termed 'small exported membrane protein 1' (SEMP1).

By Co-IP experiments we identified several potential SEMP1 interaction partners, including REX1 and other membrane-associated proteins that were confirmed to co-localize with SEMP1 at the MCs. Although a number of experiments deemed the quality of the generated *P. falciparum* cDNA library sufficient, we were unsuccessful to identify MAHRP1-binding proteins by mbSUS high-throughput screens. However, we could

SUMMARY

show that even without a functional library the mbSUS provides a useful tool to verify *P. falciparum* membrane protein interactions on a one by one basis by confirming binding of SEMP1 to a protein identified as potential interaction partner by Co-IP. A combination of Co-IP and mbSUS represents a promising new strategy for the identification and confirmation of direct *P. falciparum* membrane protein interactions.

We showed by immunofluorescence and solubility assays that SEMP1 is early exported into the RBC cytosol upon invasion where it inserts into the MCs before it is at least partly translocated to the RBC membrane. Using conventional and conditional loss-of-function approaches we found that SEMP1 is not essential for parasite survival, gametocytogenesis, or export of the major parasite virulence factor ‘*P. falciparum* erythrocyte membrane protein 1’ (*PfEMP1*) under culture conditions. Transcriptome analysis of SEMP1-depleted parasites further showed that expression of a number of exported parasite proteins was up-regulated in its absence, including *PfEMP3* and a ‘*Plasmodium* helical interspersed subtelomeric family’ (PHIST) protein possibly indicating a role for SEMP1 in modulation of the erythrocyte membrane skeleton.

With this thesis we contribute to a better understanding of the export of *P. falciparum* proteins and their interactions within the human RBC. Our findings provide a starting point for numerous follow-up studies which in the end should result in a comprehensive interaction network. By bringing new insight into the complex interactome of exported parasite proteins we will hopefully identify new intervention targets to interfere with the essential refurbishment of the host cell.

Abbreviations

ATS	acidic terminal sequence
BSA	bovine serum albumin
BSD	blasticidin S deaminase
Co-IP	co-immunoprecipitation
Cub	C-terminal split-ubiquitin
DD	destabilization domain
DHFR	dehydrofolate reductase
EBA	erythrocyte binding antigens
EM	electron microscopy
ER	endoplasmic reticulum
FKBP	FK506 binding protein
GFP	green fluorescent protein
HA	hemagglutinin
HPI	hours post invasion
IPTi	intermittent preventive treatment of infants
IPTp	intermittent preventive treatment of pregnant women
ITN	insecticide-treated bed net
KAHRP	knob associated histidine rich protein
KO	knock out
MAHRP	membrane associated histidine rich protein
mbSUS	mating-based split-ubiquitin system
MC	Maurer's cleft
MESA	mature parasite-infected erythrocyte surface antigen
MHC	Major Histocompatibility Complex
MS	mass spectrometry
NPPs	new permeability pathways
Nub	N-terminal split-ubiquitin
ORF	open reading frame
PBS	phosphate buffered saline

ABBREVIATIONS

PCR	polymerase chain reaction
PEXEL	<i>Plasmodium</i> export element
PfEMP	<i>Plasmodium falciparum</i> erythrocyte membrane protein
PHIST	<i>Plasmodium</i> helical interspersed sub-telomeric protein
PI3P	phosphatidylinositol-3-phosphate
PNEP	PEXEL-negative exported protein
PPI	protein-protein interaction
PTEX	<i>Plasmodium</i> translocon of exported proteins
PV	parasitophorous vacuole
PVM	parasitophorous vacuole membrane
RBC	red blood cell
REX	ring exported protein
RG	reporter gene
SBP1	skeleton binding protein 1
SDS	sodiumdodecylsulfate
SEMP1	small exported membrane protein 1
SP	signal peptide
SRP	signal recognition particle
STEVOR	subtelomeric variable open reading frame
TF	transcription factor
TVN	tubovesicular network
UBP	ubiquitin-specific protease
VTS	vacuolar transport signal
WHO	World Health Organization
YPAD	Yeast Extract - Peptone - Dextrose plus Adenine medium
Y2H	yeast-two-hybrid

Chapter 1

Introduction:

Malaria and *Plasmodium falciparum* Cell Biology

INTRODUCTION

Malaria

With over 500 million new yearly infections which cause about 660'000 annual deaths, mainly in children under five, malaria still represents one of the world's most devastating human diseases (1). Besides its severe effects on infected individuals, its presence also leads to a substantial decrease in the annual Gross Domestic Product (GDP) (2,3). This means that in endemic countries malaria affects the uninfected population as well as the infected and that the disease is one of the reasons for poverty in developing countries. 104 countries, mainly in tropical and subtropical regions, were endemic for malaria in 2010. While with 45 countries the WHO African region is the most affected, the disease is also endemic in Asia, Latin America and the Middle East (1). Malaria is caused by a single-celled eukaryotic parasite which belongs to the genus *Plasmodium* and can infect humans, primates and rodents. More than 100 species of this protozoan parasite exist, but only four of them are able to naturally infect humans: *Plasmodium vivax*, *P. ovale*, *P. malariae* and *P. falciparum* (4). However, increased transmission of non-human malaria parasites like *P. knowlesi*, which usually infects monkeys in restricted parts of South-East Asia, is observed (5,6). While *P. falciparum* is mainly responsible for malaria pathology across Sub-Saharan Africa, *P. vivax* is the most prevalent malaria parasite in most other endemic areas like South-East Asia. *P. vivax*, *P. ovale* and *P. malariae* all cause substantial morbidity but the most severe form of human malaria called malaria tropica is caused by *P. falciparum*. Since *P. falciparum* is the only parasite which causes severe malaria, it is responsible for the majority of malaria-associated morbidity and nearly all the mortality (7). Clinical symptoms of the severe malaria are anaemia, cerebral malaria, hypoglycaemia, non-cardiac pulmonary oedema, renal failure and respiratory failure. Responsible for most parasite-related disease symptoms is thereby its asexual development within the human red blood cell (RBC).

Malaria control is a difficult task due to the parasite's extremely complex life cycle and its ability to adapt to the resulting heterogeneous environment. Nevertheless during the last few years the number of malaria cases could be successfully reduced. This was

achieved by control programs which improved access to preventives like insecticide-treated bed nets (ITNs) and preventive treatment of pregnant women and infants (IPTp and IPTi), as well as artemisinin-based combination drug therapy. One of the biggest obstacles regarding malaria control is the lack of an effective vaccine. The most advanced malaria vaccine RTS,S/AS01 which targets the pre-erythrocytic stage of *P. falciparum* offers only limited protection. Recent phase 3 trials showed 50.4 % efficacy in children aged 5 to 17 months (8), and 30.1 % efficacy in infants aged 6 to 12 weeks (9). A new vaccine candidate called PfSPZ which is made by isolating attenuated sporozoites from the salivary glands of irradiated mosquitoes showed promise in preliminary clinical studies: none of six individuals given the highest dose of the vaccine was infected following experimental challenge with malaria (10). Another huge problem regarding malaria control is emerging drug-resistance in the parasite which calls for new antimalarial drugs. However, in order to find new drugs a deeper understanding of the parasite and especially of the disease causing asexual blood stage is necessary.

***Plasmodium falciparum* life cycle**

The apicomplexan parasite *P. falciparum* has a very complex life cycle, which not only comprises generation changes of sexual and asexual stages, but also transmission between a human host and an insect vector (Fig. 1). The parasite is transmitted by the bite of an infected female *Anopheles* mosquito, which injects sporozoites together with anticoagulant-containing saliva into the subcutaneous tissue. The sporozoites then migrate to the liver via the human bloodstream, where they invade liver cells. Within the hepatocytes they undergo an asexual replication called exo-erythrocytic schizogony, during which they develop into polynucleic schizonts. Cell rupture then releases thousands of merozoites into the bloodstream where they immediately invade erythrocytes. Red blood cell invasion involves the release of several protein factors from secretory organelles called rhoptries and micronemes, which enable penetration of the erythrocyte membrane and lead to formation of a parasitophorous vacuole. Within the infected red blood cell the parasite undergoes an asexual development and matures within 48 hours from an early ring over a trophozoite to a late schizont stage, which gives rise to

16-32 merozoites. The infected erythrocyte then bursts and the merozoites are released into the blood stream again, where they immediately invade new red blood cells. The symptoms of severe malaria are only associated with this intraerythrocytic asexual cycle. In order to evade elimination in the spleen, the parasite mediates adhesion of infected RBCs to the host endothelium, which as a side effect causes organ failure and cerebral malaria by clogging of blood capillaries and release of pro-inflammatory cytokines (11). After several cycles of asexual intraerythrocytic development, eventually some newly invaded red blood cells differentiate into sexual forms, male and female gametocytes, which represent the transmission stage of the parasite.

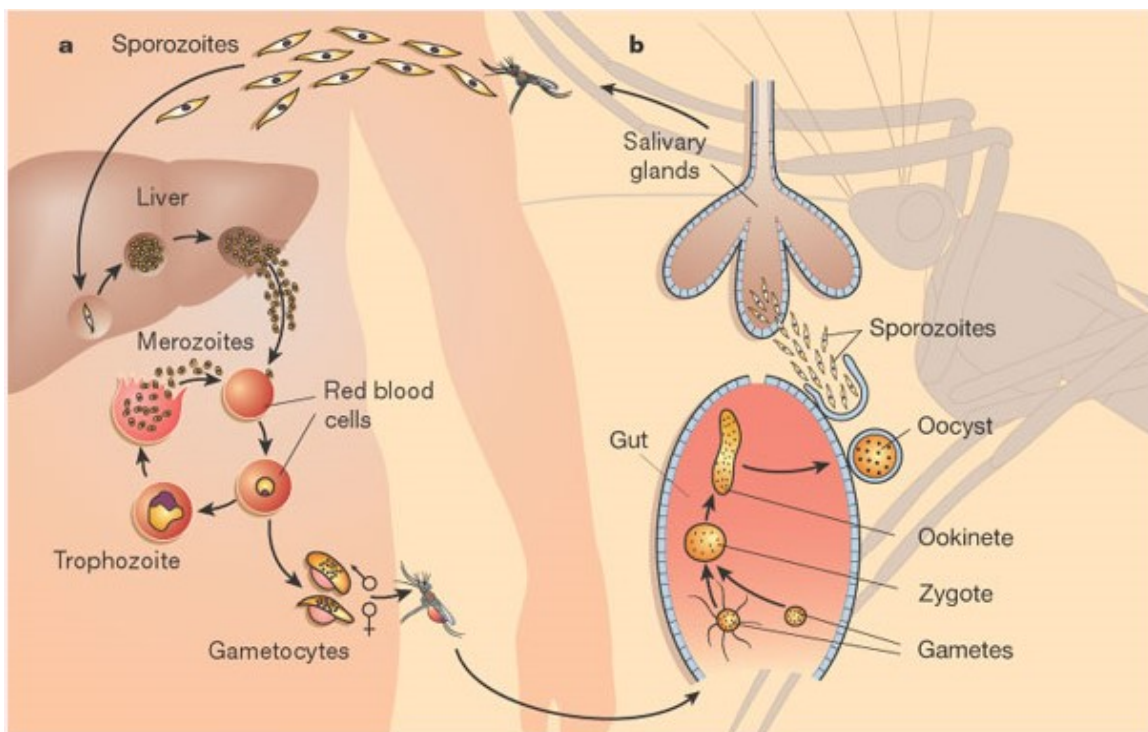


Figure 1: Schematic depiction of the *P. falciparum* life cycle (12).

After uptake by a female *Anopheles* mosquito upon blood meal, the male gametocytes undergo rapid nuclear division and exflagellation to produce microgametes which fertilize the female macrogametes within the mosquito midgut. The resulting zygote transforms further to an ookinete and traverses the mosquito gut wall, where it encysts as an oocyst and produces numerous sporozoites by a process called sporogony. After oocyst rupture the sporozoites are released into the mosquito body cavity from where they migrate to the salivary gland.

Genome of *P. falciparum*

In 2002 the complete sequence of the 22.8 Mb *P. falciparum* genome has been published (13). Analysis revealed approximately 5400 open reading frames (ORFs) which are distributed across 14 chromosomes, a 6 kb linear mitochondrial genome (encoding three proteins plus rRNAs) and a 35 kb circular plastid genome with over 60 ORFs (14). It could be shown that the parasite's DNA has a remarkably high A/T content of about 80 % in coding and even ~ 90 % in non-coding regions. Sequence analysis further revealed a large evolutionary distance between *P. falciparum* and eukaryotic model organisms: about 60 % of all parasite ORFs lack homologies to annotated genes, meaning that their function is still unknown. Insight into the function and interactions of these proteins will provide the basis for the discovery of new drug targets and vaccine development. The completion of the *P. falciparum* genome represented a milestone in malaria research allowing for a much more comprehensive investigation of the parasite's biology by performing genome- and proteome-wide experiments.

Erythrocyte modification by *P. falciparum*

The primary function of human erythrocytes is the transport of oxygen from the lungs to the body tissues. To optimize this function, mature red blood cells lost their internal organelles in order to generate maximum space for haemoglobin, an iron-containing biomolecule which is responsible for oxygen binding. On one hand this characteristic has the big advantage for the parasite that its host cell is also devoid of all major histocompatibility complex (MHC) molecules which allow to hide from immunological detection. On the other hand, since erythrocytes also lack any protein trafficking machinery, survival of *P. falciparum* also strictly depends on extensive structural, biochemical and functional host cell modifications which are responsible for the *P. falciparum* associated disease symptoms. Once inside the RBC the parasite therefore immediately starts to export hundreds of proteins which cause remarkable structural and morphological changes in the infected erythrocyte including increased membrane rigidity, permeability and adhesiveness.

During the intraerythrocytic part of its life cycle the parasite resides in a parasitophorous vacuole (PV) separated from the host cell cytoplasm by the parasitophorous vacuole membrane (PVM). Extensions from the PVM to the erythrocyte form the so called tubovesicular network (TVN) (15,16). Even though questions remain about the function and biogenesis of the TVN, there are indications that it has secretory characteristics (16,17) and might be involved in nutrient import (18,19).

The TVN is not the only parasite derived membranous structure in the RBC cytoplasm. The parasite further generates slender tubes with an electron-lucent lumen and an electron-dense coat (20–23) called Maurer's clefts (MCs). As the parasite matures they are distributed beneath the erythrocyte surface, where they are anchored to the erythrocyte cytoskeleton via tubular structures called tethers (24–29). While some questions remain regarding the specific function of the MCs, they are believed to constitute a surrogate Golgi which concentrates virulence proteins for further transport to the erythrocyte membrane (27,30,31). The basis of this theory is the observation that several parasite RBC surface proteins are exported via the MCs. These proteins include membrane proteins like the erythrocyte membrane protein1 (PfEMP1) and subtelomeric variable open reading frame (STEVOR) as well as soluble proteins like the knob-associated histidine-rich protein (KAHRP) and PfEMP3 (32–36). Further evidence for a Golgi-like function of the MCs comes from the observation that deletion of its proteins 'membrane associated histidine rich protein 1' (MAHRP1) (37), 'skeleton binding protein 1' (SBP1) (38,39) and 'ring exported protein 1' (REX1) (40) prevents PfEMP1 export to the host cell surface. While questions remain regarding the specific function of the MCs, a number of its constituents have been identified by analysis of early transcribed genes (41) and proteomic studies (30,42). However, ongoing research steadily reveals new candidates, which indicates that the current MC proteome is far from complete. In-depth characterization of some of these MC proteins revealed that many of them have a predicted hydrophobic domain. While some of them were shown to be integral membrane proteins like e.g. MAHRP1 (43), SBP1 (44) and REX2 (45), others are rather membrane associated like e.g. REX1 (46). Even though some were shown to be essential for PfEMP1 trafficking, the function of most MC proteins remains elusive. One reason for the difficulty to identify the function of MC proteins is their inapplicability for

yeast-two-hybrid (Y2H) screenings. Due to their hydrophobic nature they are expected to insert into yeast membranes upon expression and thereby prevent reconstitution of a functional transcription factor in the nucleus, which is a prerequisite for the functionality of the system (47). The aim of this study was therefore to establish the yeast mating-based split-ubiquitin system (mbSUS) as a new *in vitro* interaction platform for *P. falciparum* membrane proteins. mbSUS would circumvent the problems associated with the analysis of membrane proteins using the classical yeast two-hybrid approach and provide a very powerful tool not only for the investigation of MC proteins, but also any *P. falciparum* membrane protein of interest.

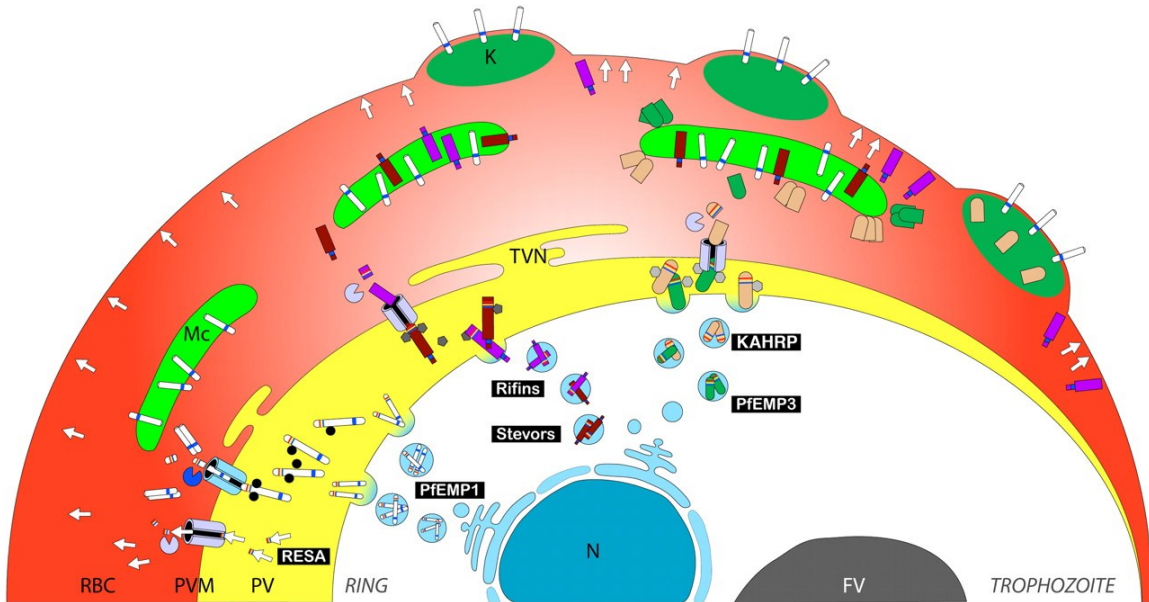


Figure 2: Erythrocyte modification by *P. falciparum*. Survival and virulence of *P. falciparum* critically depend on extensive host cell modifications mediated by the export of numerous parasite proteins into the erythrocyte cytoplasm. Extensions from the PVM form the so called tubovesicular network (TVN). Other parasite derived membranous structures called Maurer's clefts (MC) are believed to constitute a surrogate Golgi which concentrates virulence proteins like the major parasite virulence factor PfEMP1 for further transport to the erythrocyte membrane. The MCs are anchored to the erythrocyte cytoskeleton via tubular structures called tethers (not shown). The parasite further reshapes the erythrocyte membrane by formation of surface protrusions called knobs (K) which anchor PfEMP1. Figure taken from (48).

Adherence of *P. falciparum* infected erythrocytes to vascular endothelial cells is associated with surface protrusions called knobs which consist of electron-dense submembrane cups and the overlying RBC plasma membrane (49). The density of knobs on the surface of infected erythrocytes thereby increases with parasite maturity (50). Knobs consist of several parasite derived proteins but their main component is the knob-associated histidine-rich protein 1 (KAHRP) (51,52) which was shown to be essential for knob formation (53). There is evidence that KAHRP interacts with several cytoskeletal RBC constituents like spectrin, actin, and spectrin-actin band 4.1 complexes (54,55). These interactions could be responsible for the structural alterations of infected erythrocytes. It was recently shown that interaction of KAHRP with the RBC membrane skeleton protein ankyrin R is required for its attachment to the erythrocyte membrane and therefore potentially important for promoting the adhesion of malaria-infected red cells to endothelial surfaces (56). It is further believed that KAHRP anchors PfEMP1 at the knobs by binding to its ATS domain (57–59). However, a recent study was unable to confirm this ATS-KAHRP binding under soluble conditions (60). PfEMP1 was shown to bind various endothelial host cell receptors in order to mediate adhesion of infected erythrocytes to the blood capillaries. While this mechanism enables the parasite to evade elimination in the spleen, it also causes organ failure and cerebral malaria by clogging of blood capillaries and release of pro-inflammatory cytokines (61). PfEMP1 is therefore the major parasite virulence factor.

Between 12 and 16 hours after invasion, the parasite further establishes so called new permeability pathways (NPPs) in the RBC plasma membrane which mediate the uptake of nutrients into the infected cell by increasing the membrane permeability (62–64). While the origin of the NPP forming components is still debated (65–68), there is evidence that exported parasite proteins are involved in their formation (69). It is hypothesized that upon infection these parasite proteins activate otherwise silenced erythrocyte transporters. Studies thereby suggest that not only one single channel type is involved in transport across the RBC membrane (70). However, the nature and number of pathways that underlie the NPPs have yet to be identified.

Protein export in *P. falciparum*

In order to survive within the human erythrocyte, a very specialized cell which is devoid of all internal organelles and any protein trafficking machinery, *P. falciparum* needs to refurbish its host cell by exporting numerous proteins into the red blood cell cytosol. Since the parasite does not reside directly within the erythrocyte cytoplasm but within a parasitophorous vacuole (PV), this export is a complicated process which involves transport across not only one but several membranes: the parasite membrane, the PV membrane (PVM) and for some proteins even the erythrocyte membrane. Although the parasite's Golgi apparatus is highly reduced, homologues for most constituents of the classical secretion pathway are present in *P. falciparum* and most exported proteins contain a conserved N-terminal signal peptide. This hydrophobic peptide is recognized by the signal recognition particle (SRP) which directs it into the endoplasmic reticulum (ER). While this signal sequence is sufficient to direct proteins into the *P. falciparum* ER with default release into the PV, another motif called *Plasmodium* export element (PEXEL) (71) or vacuolar transport signal (VTS) (72) is necessary for further transport across the PVM. This *Plasmodium*-specific export signal is located near the N-terminus, usually about 20 amino acids downstream of the signal peptide, and consists of the conserved sequence R/KxLxE/Q/D where x is a non-charged amino acid. The PEXEL motif was shown to be proteolytically cleaved (73,74) by the ER-resident protease Plasmepsin V (75–77) which produces an acetylated –xE/Q/D N-terminus that plays an important role in export of the mature protein (78). Because it was observed that PEXEL proteins cleaved by other proteases are not exported, even if they produce the same mature protein, Plasmepsin V appears to also have a role in guiding the proteins into this specific export pathway (76). Recent studies revealed that PEXEL-binding by the phosphatidylinositol-3-phosphate (PI(3)P) may also be involved in the export process (79). It was suggested that exported proteins are first guided to an ER export region by PI3P before they are cleaved off the membrane by Plasmepsin V (79). However, the function of PI3P during protein export remains elusive. The identification of the PEXEL motif allowed the prediction of a first *P. falciparum* exportome which comprised up to 8 % of all *P. falciparum* proteins (80). Knock-out studies further revealed that several of

these PEXEL-containing proteins are involved in erythrocyte remodelling processes (81). Even though many questions remain regarding the transport of PEXEL proteins across the PVM, it could be shown that it is an ATP dependant process (82) and that the protein needs to be unfolded (83). It was further shown that it probably involves a putative translocon termed '*P. falciparum* translocon for exported proteins' (PTEX). This multimeric protein complex whose components are *Plasmodium* specific was found on the inside of the PVM (84). While such a translocon based transport across the PVM does make sense for soluble proteins, it seems unsuitable for export of integral membrane proteins. One possible explanation could be that these proteins are synthesized as soluble proteins which do not insert into membranes before reaching their target membrane. However, while some studies support the existence of such a pathway (85), others showed that some PVM and MC proteins are already insoluble in the ER (35,86). How these proteins are exported is still unclear.

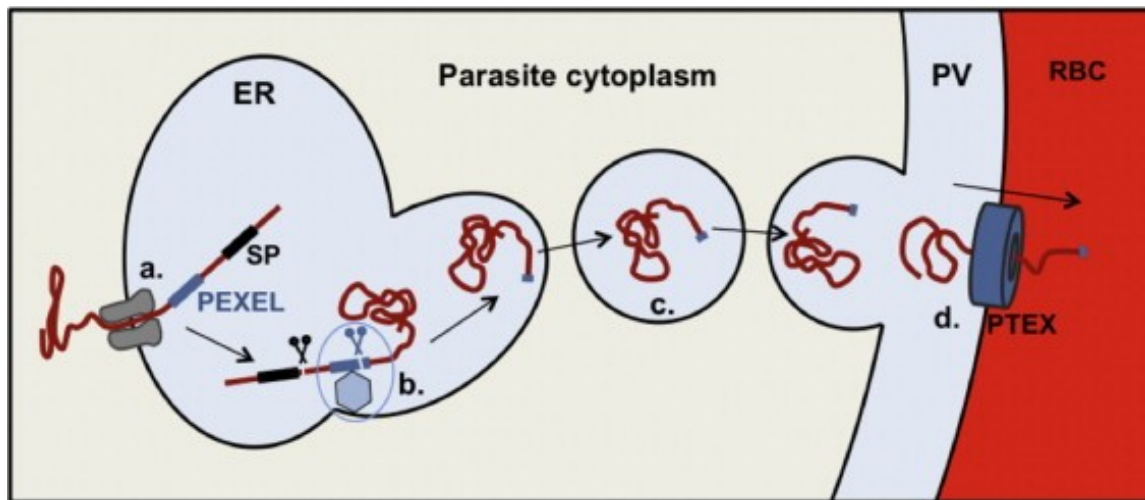


Figure 3: Model for PEXEL protein export in *P. falciparum*. After signal-peptide (SP) cleavage by the signal peptidase (indicated by black scissors), PI3P (b, hexagon) binding and plasmepsin V cleavage (b, blue scissors) guide PEXEL proteins into the export pathway, possibly by sorting the mature protein into export competent ER regions. The protein is then transported into the PV via a vesicular pathway (c, likely involves the Golgi apparatus), where the PVM translocon PTEX mediates its export into the host cell (d) (87).

After export across the PVM into the erythrocyte cytosol, most proteins are further transported to the MCs and the RBC membrane. It was initially suggested that MCs are connected to the PVM and that exported proteins are transported via this network (88), but recent studies indicate that they are rather individual unconnected units (89). Another theory was that membrane proteins might segregate into nascent MCs when they are formed at the PVM (90). However, it was recently shown that the parasite is able to transport newly synthesized proteins to MCs already present in the RBC (89).

The identification of the PEXEL / VTS motif represented a break through which increased our understanding of *P. falciparum* protein export tremendously. However, the parasite also has a sub-set of proteins called PEXEL-negative exported proteins (PNEPs) which is secreted into the host cell despite lacking both a signal peptide and a PEXEL sequence. A consensus sequence necessary for PNEP export has not been found, which makes it impossible to predict how many PNEPs have yet to be identified. However, there is little doubt that the current *P. falciparum* exportome is far from complete. Most PNEPs seem to contain at least one hydrophobic transmembrane (TM) domain (78). These TMs were not only shown to be essential for entry into the secretory pathway, the observation that they are not interchangeable with TM domains from non-exported proteins further indicates an involvement in determining the protein's target location (85,91). While most PNEPs have at least one of these hydrophobic domains, not all of them are integral membrane proteins. Some like the 'membrane-associated histidine rich protein 2' (MAHRP2) and the 'ring-exported protein 1' (REX1) were shown to be rather membrane associated (29,92). Truncation studies further revealed that for most PNEPs not only the TM domain, but also the protein's N-terminus is essential for export (29,37,85,92). However, the length of these essential N-termini varies between different PNEPs and no consensus sequence could be identified within them. While the precise PNEP export mechanisms remain elusive, ER intermediates of PNEPs indicate export via the classical secretory pathway (85,90). Additionally it was shown that the export of some PNEPs is brefeldin A sensitive which also points to ER trafficking before the export (91). After trafficking across the PVM most PNEPs like e.g. MAHRP1, REX1,

REX2 and SBP1 localize to the Maurer's clefts (43–46,91). But PNEPs can also be found at other compartments like e.g. the tethers (29).

Overall it is still unclear how much PNEP export differs from PEXEL protein trafficking, and even different export mechanisms of different PNEPs seems likely. In order to bring new insight into the export mechanisms of PNEPs we investigated the sequence requirements of the newly identified Maurer's clefts resident 'small exported membrane protein 1' (SEMP1) in chapter 4.

Protein-protein interactions

Protein-protein interactions are the building blocks of biological systems and defined as the binding between two or more proteins in order to achieve an energetically and functionally favourable structure. For two components to be able to interact and achieve such a dimeric structure, they need surfaces that are complementary in terms of shape and chemistry. The classical classification for dimeric protein associations can either describe the binding between two components that are identical (homodimer) or different (heterodimer). However, with the number of identified dimeric interactions steadily increasing, a more specific classification seemed necessary. Orfan and Rost therefore included the longevity of a certain association to define four classes of dimeric interactions: 1. homo-obligomer: between permanently interacting identical subunits; 2. homo-complex: between transiently interacting identical subunits; 3. hetero-obligomer: between permanently interacting different subunits; 4. hetero-complex: between transiently interacting different subunits (93) (Fig.4).

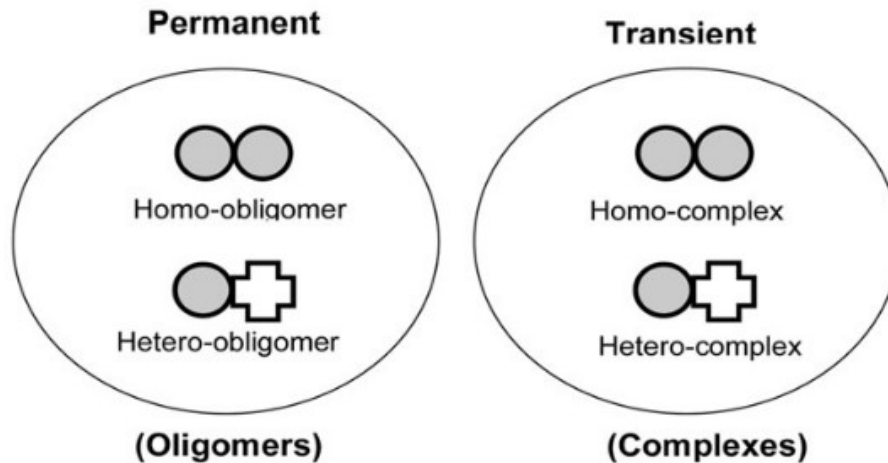


Figure 4: Classification of dimeric protein interactions including longevity of the association according to Orfan and Rost (93). Homo interactions between identical proteins are illustrated by a pair of identical symbols, hetero interactions between non-identical proteins are illustrated by a pair of non-identical symbols (94).

Numerous studies investigating specific protein-protein interactions revealed much information about the protein components and features, as well as forces important to establish the specific bindings. The primary protein structure seems thereby to be crucial: the amino acid distribution within a protein not only differs from the interior to the exterior (95), also the distribution in a protein-protein interface was shown to be different from the rest of the protein surface (96–99). However, there are conflicting reports from different studies in terms of specific amino acid preferences at these interaction sites. It seems like different classes of protein-protein interactions have different amino acid preferences at their binding interfaces which are dependent on energetic properties: Transient interaction partners also exist independently of each other. Therefore they can not have large hydrophobic patches on their surface which are energetically unfavourable. In contrast, obligomer interfaces are permanently shielded from the solvent by their binding-partners. Therefore they can contain hydrophobic patches which in that case are not energetically unfavourable. Further it seems that there also exist amino acid preferences within the protein-protein interface itself which is divided into a core and a rim region. The core is thereby the center of high binding energies which contains high frequencies of tryptophan and tyrosine residues (93,100,101).

The specific properties of residues present at the protein-protein interface generate the forces which are responsible for binding of the two protein components. These forces include hydrogen bonds, electrostatic forces, salt bridges and hydrophobic forces. Many protein-protein interfaces contain water molecules which form hydrogen bonds with both components of the association. While the distribution of water molecules within the protein-protein interface was shown to be very diverse, it is thought that protein-protein bindings involve in general at least as many water mediated contacts as direct ones (102). Electrostatic forces caused by charged and polar residues within the protein-protein interface vary widely between different complexes (103,104). While in some complexes they actually oppose binding, in others they have no or even a positive effect on protein associations (105). Additionally electrostatic forces can combine with hydrogen bonds to form salt bridges. Another important aspect regarding protein associations is that solvent exclusion from the protein-protein interface is an important condition for high affinity binding. The so-called O-ring hypothesis suggests that it is achieved by a ring of hydrophobic residues located around a central core (106).

Additionally to the amino acid composition also the secondary structure of a protein was shown to be important for its binding ability. It was shown that while turns and loop structures are over represented at protein-protein interfaces, the opposite is true for helices and sheet structures (100). A possible explanation for this observation is that turns and loop structures create a flexible environment that might be beneficial for tight packing.

Upon interaction many proteins undergo conformational changes, which range from small side chain conformational changes of core amino acids to changes in orientation of whole protein domains. The causes for these conformational changes are the facilitation of tight packing, to allow the residues to execute a specific function and the formation of hydrogen bonds and salt bridges (107).

Protein-protein interactions in *Plasmodium falciparum*

To completely understand an organism at the molecular level is a big challenge. Cellular machineries are highly dynamic and their proteins are involved in complex interactions which form a highly sensitive regulation system. While generation of a detailed protein-protein interaction (PPI) network is never an easy task, *P. falciparum* has some species specific additional difficulties. Because of its large evolutionary distance to eukaryotic model organisms, only about 40 % of its proteins have homologues which allowed *in silico* studies to generate computationally modelled PPI networks (108–110). The other 60 % of the parasite's genes lack similarity to functionally annotated proteins and could therefore only be annotated as hypothetical proteins with unknown function. For these proteins high-throughput experiments were needed to establish a starting point for further investigations. LaCount et al. used a high-throughput yeast two hybrid (Y2H) system to generate a first *P. falciparum* asexual blood stage PPI network consisting of 1267 proteins and 2823 interactions which were used to computationally identify clusters of functionally related proteins (111). This way several hypothetical proteins were predicted to have a role in cell invasion, RNA processing, splicing or to be potentially exported. However, its accuracy remains unclear because only a few experimentally proven *P. falciparum* PPIs exist which would allow validation of the generated network, an approach used as the gold standard for model organisms. The generated PPI network is a good starting point but further experimental validation of its interactions is inevitable. A limitation of this first *P. falciparum* PPI network is the use of a Y2H system which is not suited for investigation of membrane proteins. Because of their hydrophobic nature they insert into yeast membranes which prevents the attached transcription factor from entering the nucleus. Since the majority of exported *P. falciparum* proteins were shown to be membrane proteins, an alternative approach is needed in order to investigate the PPI network of the parasite's exportome. Therefore we tried to establish the 'mating-based split-ubiquitin system' (mbSUS) as a new *in vitro* interaction platform for *P. falciparum* membrane proteins (chapter 2).

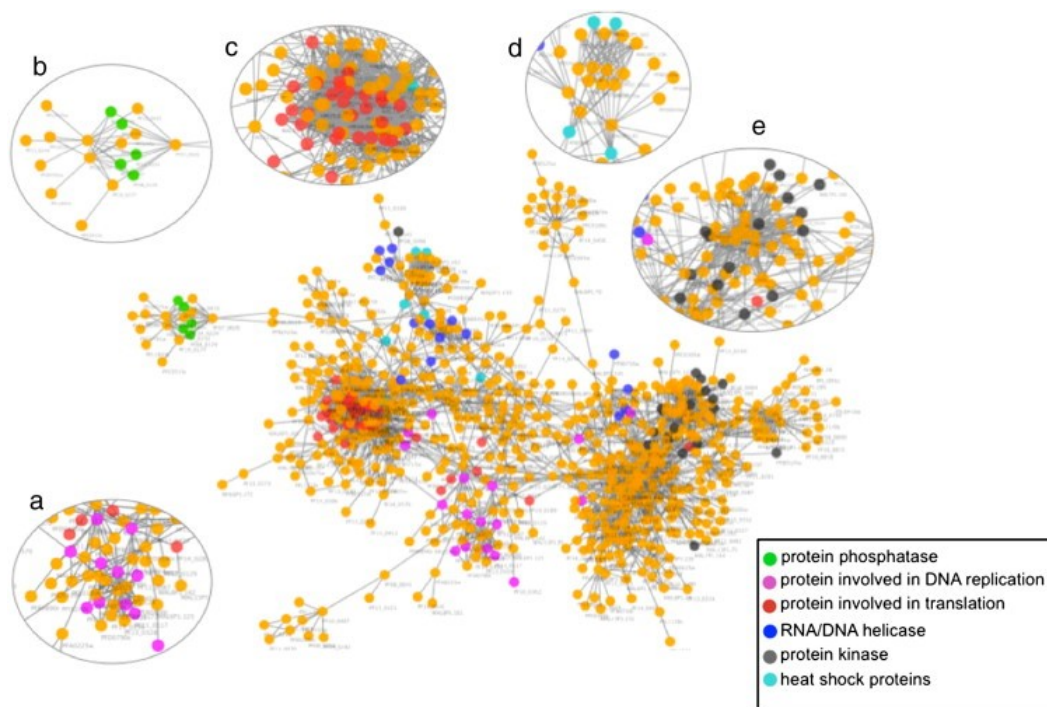


Figure 5: A computationally modeled *P. falciparum* 3D7 protein–protein interaction network. Important groups of annotated proteins are highlighted in different colours: protein phosphatases (green), proteins involved in DNA replication (pink), proteins involved in translation (red), RNA / DNA helicases (dark blue), protein kinases (black) and heat shock proteins (light blue). Insets show a detailed view of some protein clusters which represent a specific cellular or molecular function: DNA replication (a), Phosphatase activity (b), Protein translation (c), Heat-shock machinery (d) and Kinase activity (e) (112).

In spite of the described difficulties, several studies successfully identified and experimentally confirmed interactions between different *P. falciparum* proteins. Some of them are involved in erythrocyte invasion: the apical membrane antigen 1 (AMA1) was shown to interact with the two rhoptry neck proteins RON2 (113) and RON4 (114). Other studies revealed the binding between the actin bridging molecule aldolase and thrombospondin-related anonymous protein (TRAP), both part of the acto-myosin motor responsible for gliding motility (115,116). Another known *P. falciparum* protein interaction between components of this acto-myosin motor is the one between myosin A (MyoA) and myosin tail domain interacting protein (MTIP) (117,118). An additional detected interaction which was shown to be important for erythrocyte invasion is between the reticulocyte binding protein homologue 5 (PfRh5) and the Rh5 interacting protein

(RIPR) (119). However, not only invasion related interactions could be identified: pull-down assays revealed that the leucine rich repeat family member PfLRR1 interacts with the protein phosphatase type 1 (PfPP1) to build a complex which is thought to be important for regulation of cell cycle progression (120). Hain et al. demonstrated binding between the two autophagy-related proteins PfAtg3 and PfAtg8 (121) and the major parasite virulence factor PfEMP1 was recently shown to bind with its ATS domain to the Plasmodium helical interspersed sub-telomeric (PHIST) protein PF3D7_0936800 (60). Further the dynein light chain 1 protein (PfDLC1) was shown to bind to *P. falciparum* myosin A and actin 1 (122) and a recent study revealed an interaction of heat shock protein 90 (Hsp90) with activator of Hsp90 ATPase (Aha1) (123).

P. falciparum proteins not only interact with each other, some also bind to erythrocyte components. Certain interactions were shown to be involved in RBC invasion of merozoites: members of the erythrocyte binding-like (ebl) family called erythrocyte binding antigens (EBAs) are thereby responsible for high affinity binding to glycoproteins on the erythrocyte surface. EBA-175 was shown to bind to glycophorin A (124) and EBA-140 to glycophorin C (125). A second protein family involved in erythrocyte invasion by binding to RBC surface receptors are the reticulocyte binding protein homologues (PfRh): PfRh4 was demonstrated to bind to the complement receptor 1 (CR1) (126) and PfRh5 binds to the Ok blood group antigen basigin (127).

Other studies identified various parasite-erythrocyte protein interactions involved in host cell refurbishment: the erythrocyte cytoskeletal protein spectrin was identified as the primary attachment site for the ring-infected erythrocyte surface antigen (RESA) (128), and also to interact with the major parasite virulence factor PfEMP1 (57) together with the knob-associated histidine-rich protein (KAHRP) (54). Spectrin was further shown to be a binding site for the erythrocyte membrane protein PfEMP3 (128,129), an interaction which was shown to destabilize the RBC skeleton (130). In addition to spectrin also other erythrocyte skeleton proteins were shown to interact with parasite proteins: host cell actin was demonstrated to interact with PfEMP1 (57) and KAHRP (131), while Protein 4.1 interacts with the mature parasite-infected erythrocyte surface antigen (MESA) (132,133)

and the PHIST protein PF3D7_0402000 (134). KAHRP was further shown to bind the adaptor protein Ankyrin (135).

Additionally to erythrocyte components, *P. falciparum* proteins also interact with other host proteins. Binding of parasite ligands on the erythrocyte surface to endothelial host cell receptors mediates cytoadherence of infected RBCs and therefore has a key role in the pathology of *P. falciparum*. The best studied and characterized interactions involve the parasite-derived RBC surface antigen PfEMP1. Two major subtypes of PfEMP1 (group B and C) were shown to bind the scavenger receptor CD36 which is expressed on endothelial and epithelial cells, macrophages, monocytes, platelets, erythrocyte precursor and adipocytes (136–139). A smaller subset of PfEMP1 which contains a pair of DBL β -C2 domains is the parasite ligand for ICAM1, a member of the immunoglobulin superfamily which is expressed on endothelial cells and leukocytes (140–142). Further it could be shown that PfEMP1 binds to the glycoprotein P-selectin found on endothelial cells and activated platelets (143) and to the platelet endothelial cell adhesion molecule 1 PECAM1 (144). PfEMP1 was also demonstrated to bind to the glycosaminoglycan heparan sulphate which is believed to be involved in rosette formation and binding of infected RBCs to endothelial cells (144–147). Finally a unique PfEMP1 protein termed VAR2CSA was shown to bind the chondroitin sulphate A (CSA) receptor in the placenta which results in placental malaria (148,149).

While identification of protein-protein interactions is known to be fundamental to understand an organism at the molecular level, in case of *P. falciparum* it has the potential to be even more important. Since many proteins are only able to execute their function if they are part of a correctly assembled complex, interactions of essential proteins are potential new drug targets. Because usually only small protein regions, so called binding hotspots, are responsible for the binding with an interaction partner (106,150), small molecules can be sufficient to inhibit the interaction if they bind specifically (151). Such small molecules and peptides have already been successfully used to interfere with crucial protein-protein interactions in viruses (152–155), bacteria (156), *Trypanosoma brucei* (157) and were also identified as potential drugs for cancer

treatment (158). For *P. falciparum* it was shown that synthetic triose phosphate isomerase peptides can interfere with formation of the active enzyme (159) and that small synthetic peptides of the cysteine protease falcipain-2 (FP2) produced morphological abnormalities in the parasite's food vacuole (160). Recently Hain et al. were further able to prevent the interaction between autophagy-related proteins Atg3 and Atg8 with low concentrations of the small molecule 1,2,3-trihydroxybenzene (121). The results of these studies indicate that protein interaction inhibiting peptides and molecules have an enormous potential as a new class of antimalarial drugs. Something that is urgently needed in consideration of the increasing spread of drug-resistant parasites.

Outline of this thesis

Aim of this thesis was to bring new insight into the interactions and functions of exported *P. falciparum* proteins. Therefore we investigated the two PEXEL-negative exported proteins MAHRP1 and ‘small exported membrane protein 1’ (SEMP1). MAHRP1 was previously identified as an integral Maurer’s clefts protein, which is essential for export of the major parasite virulence factor PfEMP1 (37). Since not only MAHRP1 but most PNEPs were shown to be membrane proteins, their interactions can not be investigated by classical yeast-two-hybrid assays (Y2H). In chapter 2 we therefore tried to establish the ‘mating-based split-ubiquitin system’ (mbSUS) (161) as a new *in vitro* interaction platform for *P. falciparum* membrane proteins on the basis of MAHRP1. The thereby generated bait was used to investigate binding of MAHRP1 to its two previously identified potential interactors ‘parasite-infected erythrocyte surface protein’ (PIESP2) and PF3D7_0501000 by mbSUS pairwise interaction assays (chapter 3). In order to bring new insight into the processes of host cell refurbishment we further identified and characterized SEMP1. Chapter 4 characterizes SEMP1 which includes the determination of its localization by immunofluorescence assays and electron microscopy, its solubility, and we investigated its function by knockout studies and transcriptional analysis (also chapter 4). Sequence requirements for trafficking of SEMP1 were also analyzed by transfection of parasites with plasmids expressing truncated and mutated versions of the protein fused to a GFP-tag. Since the MAHRP1 mbSUS library screenings described in chapter 2 were unsuccessful, we performed co-immunoprecipitation experiments to identify interaction partners of SEMP1 (also chapter 4). We thereby identified the PNEPs PF3D7_0702500 and PF3D7_0601900 which were investigated for direct binding to SEMP1 by mbSUS pairwise interaction assays in chapter 5.

References

1. World Health Organization. WHO | World Malaria Report 2012. 2009.
2. Sachs J, Malaney P. The economic and social burden of malaria. *Nature*. 2002 Feb 7;415(6872):680–5.
3. Orem JN, Kirigia JM, Azairwe R, Kasirye I, Walker O. Impact of malaria morbidity on gross domestic product in Uganda. *Int Arch Med*. 2012;5(1):12.
4. Tuteja R. Malaria - an overview. *FEBS J*. 2007 Sep;274(18):4670–9.
5. Singh B, Kim Sung L, Matusop A, Radhakrishnan A, Shamsul SSG, Cox-Singh J, et al. A large focus of naturally acquired *Plasmodium knowlesi* infections in human beings. *Lancet*. 2004 Mar 27;363(9414):1017–24.
6. Putaporntip C, Hongsrimumang T, Seethamchai S, Kobasa T, Limkittikul K, Cui L, et al. Differential prevalence of *Plasmodium* infections and cryptic *Plasmodium knowlesi* malaria in humans in Thailand. *J Infect Dis*. 2009 Apr 15;199(8):1143–50.
7. Severe and complicated malaria. World Health Organization, Division of Control of Tropical Diseases. *Trans R Soc Trop Med Hyg*. 1990;84 Suppl 2:1–65.
8. Agnandji ST, Lell B, Soulanoudjingar SS, Fernandes JF, Abossolo BP, Conzelmann C, et al. First results of phase 3 trial of RTS,S/AS01 malaria vaccine in African children. *N Engl J Med*. 2011 Nov 17;365(20):1863–75.
9. RTS,S Clinical Trials Partnership, Agnandji ST, Lell B, Fernandes JF, Abossolo BP, Methogo BGNO, et al. A phase 3 trial of RTS,S/AS01 malaria vaccine in African infants. *N Engl J Med*. 2012 Dec 13;367(24):2284–95.
10. Seder RA, Chang L-J, Enama ME, Zephir KL, Sarwar UN, Gordon IJ, et al. Protection Against Malaria by Intravenous Immunization with a Nonreplicating Sporozoite Vaccine. *Science*. 2013 Sep 20;341(6152):1359–65.
11. Pongponratn E, Riganti M, Punpoowong B, Aikawa M. Microvascular sequestration of parasitized erythrocytes in human falciparum malaria: a pathological study. *Am J Trop Med Hyg*. 1991 Feb;44(2):168–75.
12. Wirth DF. Biological revelations. *Nature*. 2002 Oct 3;419(6906):495–6.
13. Gardner MJ, Hall N, Fung E, White O, Berriman M, Hyman RW, et al. Genome sequence of the human malaria parasite *Plasmodium falciparum*. *Nature*. 2002 Oct 3;419(6906):498–511.

14. Wilson RJ, Denny PW, Preiser PR, Rangachari K, Roberts K, Roy A, et al. Complete gene map of the plastid-like DNA of the malaria parasite *Plasmodium falciparum*. *J Mol Biol*. 1996 Aug 16;261(2):155–72.
15. Behari R, Haldar K. *Plasmodium falciparum*: protein localization along a novel, lipid-rich tubovesicular membrane network in infected erythrocytes. *Exp Parasitol*. 1994 Nov;79(3):250–9.
16. Elmendorf HG, Haldar K. *Plasmodium falciparum* exports the Golgi marker sphingomyelin synthase into a tubovesicular network in the cytoplasm of mature erythrocytes. *J Cell Biol*. 1994 Feb;124(4):449–62.
17. Lauer SA, Ghori N, Haldar K. Sphingolipid synthesis as a target for chemotherapy against malaria parasites. *Proc Natl Acad Sci U S A*. 1995 Sep 26;92(20):9181–5.
18. Lauer SA, Rathod PK, Ghori N, Haldar K. A membrane network for nutrient import in red cells infected with the malaria parasite. *Science*. 1997 May 16;276(5315):1122–5.
19. Tamez PA, Bhattacharjee S, van Ooij C, Hiller NL, Llinás M, Balu B, et al. An erythrocyte vesicle protein exported by the malaria parasite promotes tubovesicular lipid import from the host cell surface. *PLoS Pathog*. 2008;4(8):e1000118.
20. Langreth SG, Jensen JB, Reese RT, Trager W. Fine structure of human malaria in vitro. *J Protozool*. 1978 Nov;25(4):443–52.
21. Atkinson CT, Aikawa M, Perry G, Fujino T, Bennett V, Davidson EA, et al. Ultrastructural localization of erythrocyte cytoskeletal and integral membrane proteins in *Plasmodium falciparum*-infected erythrocytes. *Eur J Cell Biol*. 1988 Feb;45(2):192–9.
22. Elford BC, Cowan GM, Ferguson DJ. Transport and trafficking in malaria-infected erythrocytes. *Trends Microbiol*. 1997 Dec;5(12):463–465; discussion 465–466.
23. Kriek N, Tilley L, Horrocks P, Pinches R, Elford BC, Ferguson DJP, et al. Characterization of the pathway for transport of the cytoadherence-mediating protein, PfEMP1, to the host cell surface in malaria parasite-infected erythrocytes. *Mol Microbiol*. 2003 Nov;50(4):1215–27.
24. Waterkeyn JG, Wickham ME, Davern KM, Cooke BM, Coppel RL, Reeder JC, et al. Targeted mutagenesis of *Plasmodium falciparum* erythrocyte membrane protein 3 (PfEMP3) disrupts cytoadherence of malaria-infected red blood cells. *EMBO J*. 2000 Jun 15;19(12):2813–23.
25. Hanssen E, Sougrat R, Frankland S, Deed S, Klonis N, Lippincott-Schwartz J, et al. Electron tomography of the Maurer’s cleft organelles of *Plasmodium falciparum*-infected erythrocytes reveals novel structural features. *Mol Microbiol*. 2008 Feb;67(4):703–18.

26. Tilley L, Hanssen E. A 3D view of the host cell compartment in *P. falciparum*-infected erythrocytes. *Transfus Clin Biol J Société Fr Transfus Sang*. 2008 Mar;15(1-2):72–81.
27. Tilley L, Sougrat R, Lithgow T, Hanssen E. The twists and turns of Maurer's cleft trafficking in *P. falciparum*-infected erythrocytes. *Traffic Cph Den*. 2008 Feb;9(2):187–97.
28. Hanssen E, Carlton P, Deed S, Klonis N, Sedat J, DeRisi J, et al. Whole cell imaging reveals novel modular features of the exomembrane system of the malaria parasite, *Plasmodium falciparum*. *Int J Parasitol*. 2010 Jan;40(1):123–34.
29. Pachlatko E, Rusch S, Müller A, Hemphill A, Tilley L, Hanssen E, et al. MAHRP2, an exported protein of *Plasmodium falciparum*, is an essential component of Maurer's cleft tethers. *Mol Microbiol*. 2010;77(5):1136–52.
30. Lanzer M, Wickert H, Krohne G, Vincensini L, Braun Breton C. Maurer's clefts: a novel multi-functional organelle in the cytoplasm of *Plasmodium falciparum*-infected erythrocytes. *Int J Parasitol*. 2006 Jan;36(1):23–36.
31. Wickert H, Krohne G. The complex morphology of Maurer's clefts: from discovery to three-dimensional reconstructions. *Trends Parasitol*. 2007 Oct;23(10):502–9.
32. Wickham ME, Rug M, Ralph SA, Klonis N, McFadden GI, Tilley L, et al. Trafficking and assembly of the cytoadherence complex in *Plasmodium falciparum*-infected human erythrocytes. *EMBO J*. 2001 Oct 15;20(20):5636–49.
33. Knuepfer E, Rug M, Klonis N, Tilley L, Cowman AF. Trafficking of the major virulence factor to the surface of transfected *P. falciparum*-infected erythrocytes. *Blood*. 2005 May 15;105(10):4078–87.
34. Knuepfer E, Rug M, Klonis N, Tilley L, Cowman AF. Trafficking determinants for PfEMP3 export and assembly under the *Plasmodium falciparum*-infected red blood cell membrane. *Mol Microbiol*. 2005 Nov;58(4):1039–53.
35. Przyborski JM, Miller SK, Pfahler JM, Henrich PP, Rohrbach P, Crabb BS, et al. Trafficking of STEVOR to the Maurer's clefts in *Plasmodium falciparum*-infected erythrocytes. *EMBO J*. 2005 Jul 6;24(13):2306–17.
36. Lavazec C, Sanyal S, Templeton TJ. Hypervariability within the Rifin, Stevor and Pfmc-2TM superfamilies in *Plasmodium falciparum*. *Nucleic Acids Res*. 2006;34(22):6696–707.
37. Spycher C, Rug M, Pachlatko E, Hanssen E, Ferguson D, Cowman AF, et al. The Maurer's cleft protein MAHRP1 is essential for trafficking of PfEMP1 to the surface of *Plasmodium falciparum*-infected erythrocytes. *Mol Microbiol*. 2008 Jun;68(5):1300–14.

38. Cooke BM, Buckingham DW, Glenister FK, Fernandez KM, Bannister LH, Marti M, et al. A Maurer's cleft-associated protein is essential for expression of the major malaria virulence antigen on the surface of infected red blood cells. *J Cell Biol.* 2006 Mar 13;172(6):899–908.
39. Maier AG, Rug M, O'Neill MT, Beeson JG, Marti M, Reeder J, et al. Skeleton-binding protein 1 functions at the parasitophorous vacuole membrane to traffic PfEMP1 to the Plasmodium falciparum-infected erythrocyte surface. *Blood.* 2007 Feb 1;109(3):1289–97.
40. Dixon MWA, Kenny S, McMillan PJ, Hanssen E, Trenholme KR, Gardiner DL, et al. Genetic ablation of a Maurer's cleft protein prevents assembly of the Plasmodium falciparum virulence complex. *Mol Microbiol.* 2011 Aug;81(4):982–93.
41. Spielmann T, Beck HP. Analysis of stage-specific transcription in Plasmodium falciparum reveals a set of genes exclusively transcribed in ring stage parasites. *Mol Biochem Parasitol.* 2000 Dec 1;111(2):453–8.
42. Vincensini L, Richert S, Blisnick T, Van Dorsselaer A, Leize-Wagner E, Rabilloud T, et al. Proteomic analysis identifies novel proteins of the Maurer's clefts, a secretory compartment delivering Plasmodium falciparum proteins to the surface of its host cell. *Mol Cell Proteomics MCP.* 2005 Apr;4(4):582–93.
43. Spycher C, Klonis N, Spielmann T, Kump E, Steiger S, Tilley L, et al. MAHRP-1, a novel Plasmodium falciparum histidine-rich protein, binds ferriprotoporphyrin IX and localizes to the Maurer's clefts. *J Biol Chem.* 2003 Sep 12;278(37):35373–83.
44. Blisnick T, Morales Betoulle ME, Barale JC, Uzureau P, Berry L, Desroses S, et al. Pfsbp1, a Maurer's cleft Plasmodium falciparum protein, is associated with the erythrocyte skeleton. *Mol Biochem Parasitol.* 2000 Nov;111(1):107–21.
45. Spielmann T, Hawthorne PL, Dixon MWA, Hannemann M, Klotz K, Kemp DJ, et al. A cluster of ring stage-specific genes linked to a locus implicated in cytoadherence in Plasmodium falciparum codes for PEXEL-negative and PEXEL-positive proteins exported into the host cell. *Mol Biol Cell.* 2006 Aug;17(8):3613–24.
46. Hawthorne PL, Trenholme KR, Skinner-Adams TS, Spielmann T, Fischer K, Dixon MWA, et al. A novel Plasmodium falciparum ring stage protein, REX, is located in Maurer's clefts. *Mol Biochem Parasitol.* 2004 Aug;136(2):181–9.
47. Fields S, Song O. A novel genetic system to detect protein-protein interactions. *Nature.* 1989 Jul 20;340(6230):245–6.

48. Marti M, Baum J, Rug M, Tilley L, Cowman AF. Signal-mediated export of proteins from the malaria parasite to the host erythrocyte. *J Cell Biol.* 2005 Nov 21;171(4):587–92.
49. Luse SA, Miller LH. *Plasmodium falciparum* malaria. Ultrastructure of parasitized erythrocytes in cardiac vessels. *Am J Trop Med Hyg.* 1971 Sep;20(5):655–60.
50. Quadt KA, Barfod L, Andersen D, Bruun J, Gyan B, Hassenkam T, et al. The density of knobs on *Plasmodium falciparum*-infected erythrocytes depends on developmental age and varies among isolates. *PloS One.* 2012;7(9):e45658.
51. Culvenor JG, Langford CJ, Crewther PE, Saint RB, Coppel RL, Kemp DJ, et al. *Plasmodium falciparum*: identification and localization of a knob protein antigen expressed by a cDNA clone. *Exp Parasitol.* 1987 Feb;63(1):58–67.
52. Pologe LG, Pavlovec A, Shio H, Ravetch JV. Primary structure and subcellular localization of the knob-associated histidine-rich protein of *Plasmodium falciparum*. *Proc Natl Acad Sci U S A.* 1987 Oct;84(20):7139–43.
53. Crabb BS, Cooke BM, Reeder JC, Waller RF, Caruana SR, Davern KM, et al. Targeted gene disruption shows that knobs enable malaria-infected red cells to cytoadhere under physiological shear stress. *Cell.* 1997 Apr 18;89(2):287–96.
54. Pei X, An X, Guo X, Tarnawski M, Coppel R, Mohandas N. Structural and functional studies of interaction between *Plasmodium falciparum* knob-associated histidine-rich protein (KAHRP) and erythrocyte spectrin. *J Biol Chem.* 2005 Sep 2;280(35):31166–71.
55. Cooke BM, Mohandas N, Coppel RL. The malaria-infected red blood cell: structural and functional changes. *Adv Parasitol.* 2001;50:1–86.
56. Weng H, Guo X, Papoin J, Wang J, Coppel R, Mohandas N, et al. Interaction of *Plasmodium falciparum* knob-associated histidine-rich protein (KAHRP) with erythrocyte ankyrin R is required for its attachment to the erythrocyte membrane. *Biochim Biophys Acta.* 2013 Sep 30;
57. Oh SS, Voigt S, Fisher D, Yi SJ, LeRoy PJ, Derick LH, et al. *Plasmodium falciparum* erythrocyte membrane protein 1 is anchored to the actin-spectrin junction and knob-associated histidine-rich protein in the erythrocyte skeleton. *Mol Biochem Parasitol.* 2000 May;108(2):237–47.
58. Waller KL, Cooke BM, Nunomura W, Mohandas N, Coppel RL. Mapping the binding domains involved in the interaction between the *Plasmodium falciparum* knob-associated histidine-rich protein (KAHRP) and the cytoadherence ligand *P. falciparum* erythrocyte membrane protein 1 (PfEMP1). *J Biol Chem.* 1999 Aug 20;274(34):23808–13.

59. Waller KL, Nunomura W, Cooke BM, Mohandas N, Coppel RL. Mapping the domains of the cytoadherence ligand Plasmodium falciparum erythrocyte membrane protein 1 (PfEMP1) that bind to the knob-associated histidine-rich protein (KAHRP). *Mol Biochem Parasitol*. 2002 Jan;119(1):125–9.
60. Mayer C, Slater L, Erat MC, Konrat R, Vakonakis I. Structural analysis of the Plasmodium falciparum erythrocyte membrane protein 1 (PfEMP1) intracellular domain reveals a conserved interaction epitope. *J Biol Chem*. 2012 Mar 2;287(10):7182–9.
61. Miller LH, Baruch DI, Marsh K, Doumbo OK. The pathogenic basis of malaria. *Nature*. 2002 Feb 7;415(6872):673–9.
62. Martin RE, Kirk K. Transport of the essential nutrient isoleucine in human erythrocytes infected with the malaria parasite Plasmodium falciparum. *Blood*. 2007 Mar 1;109(5):2217–24.
63. Pillai AD, Nguitragool W, Lyko B, Dolinta K, Butler MM, Nguyen ST, et al. Solute restriction reveals an essential role for clag3-associated channels in malaria parasite nutrient acquisition. *Mol Pharmacol*. 2012 Dec;82(6):1104–14.
64. Saliba KJ, Horner HA, Kirk K. Transport and metabolism of the essential vitamin pantothenic acid in human erythrocytes infected with the malaria parasite Plasmodium falciparum. *J Biol Chem*. 1998 Apr 24;273(17):10190–5.
65. Ginsburg H. Oxidative permeabilization? *Trends Parasitol*. 2002 Aug;18(8):346; author reply 346–347.
66. Huber SM, Uhlemann A-C, Gamper NL, Duranton C, Kremsner PG, Lang F. Plasmodium falciparum activates endogenous Cl(-) channels of human erythrocytes by membrane oxidation. *EMBO J*. 2002 Jan 15;21(1-2):22–30.
67. Ginsburg H, Stein WD. The new permeability pathways induced by the malaria parasite in the membrane of the infected erythrocyte: comparison of results using different experimental techniques. *J Membr Biol*. 2004 Jan 15;197(2):113–34.
68. Staines HM, Alkhalil A, Allen RJ, De Jonge HR, Derbyshire E, Egée S, et al. Electrophysiological studies of malaria parasite-infected erythrocytes: Current status. *Int J Parasitol*. 2007 Apr;37(5):475–82.
69. Baumeister S, Winterberg M, Duranton C, Huber SM, Lang F, Kirk K, et al. Evidence for the involvement of Plasmodium falciparum proteins in the formation of new permeability pathways in the erythrocyte membrane. *Mol Microbiol*. 2006 Apr;60(2):493–504.
70. Staines HM, Ashmore S, Felgate H, Moore J, Powell T, Ellory JC. Solute transport via the new permeability pathways in Plasmodium falciparum-infected human red

- blood cells is not consistent with a simple single-channel model. *Blood*. 2006 Nov 1;108(9):3187–94.
71. Marti M, Good RT, Rug M, Knuepfer E, Cowman AF. Targeting malaria virulence and remodeling proteins to the host erythrocyte. *Science*. 2004 Dec 10;306(5703):1930–3.
 72. Hiller NL, Bhattacharjee S, van Ooij C, Liolios K, Harrison T, Lopez-Estraño C, et al. A host-targeting signal in virulence proteins reveals a secretome in malarial infection. *Science*. 2004 Dec 10;306(5703):1934–7.
 73. Chang HH, Falick AM, Carlton PM, Sedat JW, DeRisi JL, Marletta MA. N-terminal processing of proteins exported by malaria parasites. *Mol Biochem Parasitol*. 2008 Aug;160(2):107–15.
 74. Boddey JA, Moritz RL, Simpson RJ, Cowman AF. Role of the Plasmodium Export Element in Trafficking Parasite Proteins to the Infected Erythrocyte. *Traffic*. 2009;10(3):285–99.
 75. Russo I, Babbitt S, Muralidharan V, Butler T, Oksman A, Goldberg DE. Plasmepsin V licenses Plasmodium proteins for export into the host erythrocyte. *Nature*. 2010 Feb 4;463(7281):632–6.
 76. Boddey JA, Hodder AN, Günther S, Gilson PR, Patsiouras H, Kapp EA, et al. An aspartyl protease directs malaria effector proteins to the host cell. *Nature*. 2010 Feb 4;463(7281):627–31.
 77. Boddey JA, Carvalho TG, Hodder AN, Sargeant TJ, Sleebs BE, Marapana D, et al. Role of plasmepsin V in export of diverse protein families from the Plasmodium falciparum exportome. *Traffic Cph Den*. 2013 May;14(5):532–50.
 78. Grüning C, Heiber A, Kruse F, Flemming S, Franci G, Colombo SF, et al. Uncovering common principles in protein export of malaria parasites. *Cell Host Microbe*. 2012 Nov 15;12(5):717–29.
 79. Bhattacharjee S, Stahelin RV, Speicher KD, Speicher DW, Haldar K. Endoplasmic reticulum PI(3)P lipid binding targets malaria proteins to the host cell. *Cell*. 2012 Jan 20;148(1-2):201–12.
 80. Sargeant TJ, Marti M, Caler E, Carlton JM, Simpson K, Speed TP, et al. Lineage-specific expansion of proteins exported to erythrocytes in malaria parasites. *Genome Biol*. 2006;7(2):R12.
 81. Maier AG, Rug M, O'Neill MT, Brown M, Chakravorty S, Szeszak T, et al. Exported proteins required for virulence and rigidity of Plasmodium falciparum-infected human erythrocytes. *Cell*. 2008 Jul 11;134(1):48–61.

82. Ansorge I, Benting J, Bhakdi S, Lingelbach K. Protein sorting in Plasmodium falciparum-infected red blood cells permeabilized with the pore-forming protein streptolysin O. *Biochem J.* 1996 Apr 1;315 (Pt 1):307–14.
83. Gehde N, Hinrichs C, Montilla I, Charpian S, Lingelbach K, Przyborski JM. Protein unfolding is an essential requirement for transport across the parasitophorous vacuolar membrane of Plasmodium falciparum. *Mol Microbiol.* 2009 Feb;71(3):613–28.
84. De Koning-Ward TF, Gilson PR, Boddey JA, Rug M, Smith BJ, Papenfuss AT, et al. A newly discovered protein export machine in malaria parasites. *Nature.* 2009 Jun 18;459(7249):945–9.
85. Saridaki T, Fröhlich KS, Braun-Breton C, Lanzer M. Export of PfSBP1 to the Plasmodium falciparum Maurer’s clefts. *Traffic Cph Den.* 2009 Feb;10(2):137–52.
86. Günther K, Tümmler M, Arnold HH, Ridley R, Goman M, Scaife JG, et al. An exported protein of Plasmodium falciparum is synthesized as an integral membrane protein. *Mol Biochem Parasitol.* 1991 May;46(1):149–57.
87. Deponte M, Hoppe HC, Lee MCS, Maier AG, Richard D, Rug M, et al. Wherever I may roam: protein and membrane trafficking in P. falciparum-infected red blood cells. *Mol Biochem Parasitol.* 2012 Dec;186(2):95–116.
88. Wickert H, Göttler W, Krohne G, Lanzer M. Maurer’s cleft organization in the cytoplasm of plasmodium falciparum-infected erythrocytes: new insights from three-dimensional reconstruction of serial ultrathin sections. *Eur J Cell Biol.* 2004 Oct;83(10):567–82.
89. Grüring C, Heiber A, Kruse F, Ungefehr J, Gilberger T-W, Spielmann T. Development and host cell modifications of Plasmodium falciparum blood stages in four dimensions. *Nat Commun.* 2011 Jan 25;2:165.
90. Spycher C, Rug M, Klonis N, Ferguson DJP, Cowman AF, Beck H-P, et al. Genesis of and trafficking to the Maurer’s clefts of Plasmodium falciparum-infected erythrocytes. *Mol Cell Biol.* 2006 Jun;26(11):4074–85.
91. Haase S, Herrmann S, Grüring C, Heiber A, Jansen PW, Langer C, et al. Sequence requirements for the export of the Plasmodium falciparum Maurer’s clefts protein REX2. *Mol Microbiol.* 2009 Feb;71(4):1003–17.
92. Dixon MWA, Hawthorne PL, Spielmann T, Anderson KL, Trenholme KR, Gardiner DL. Targeting of the ring exported protein 1 to the Maurer’s clefts is mediated by a two-phase process. *Traffic Cph Den.* 2008 Aug;9(8):1316–26.
93. Ofraan Y, Rost B. Analysing six types of protein-protein interfaces. *J Mol Biol.* 2003 Jan 10;325(2):377–87.

94. Jones S. Computational and structural characterisation of protein associations. *Adv Exp Med Biol.* 2012;747:42–54.
95. Chothia C. The nature of the accessible and buried surfaces in proteins. *J Mol Biol.* 1976 Jul 25;105(1):1–12.
96. Lo Conte L, Chothia C, Janin J. The atomic structure of protein-protein recognition sites. *J Mol Biol.* 1999 Feb 5;285(5):2177–98.
97. Jones S, Thornton JM. Protein-protein interactions: a review of protein dimer structures. *Prog Biophys Mol Biol.* 1995;63(1):31–65.
98. Bordner AJ, Abagyan R. Statistical analysis and prediction of protein-protein interfaces. *Proteins.* 2005 Aug 15;60(3):353–66.
99. Jones S, Thornton JM. Analysis of protein-protein interaction sites using surface patches. *J Mol Biol.* 1997 Sep 12;272(1):121–32.
100. Ansari S, Helms V. Statistical analysis of predominantly transient protein-protein interfaces. *Proteins.* 2005 Nov 1;61(2):344–55.
101. Chakrabarti P, Janin J. Dissecting protein-protein recognition sites. *Proteins.* 2002 May 15;47(3):334–43.
102. Janin J. Wet and dry interfaces: the role of solvent in protein-protein and protein-DNA recognition. *Struct Lond Engl* 1993. 1999 Dec 15;7(12):R277–279.
103. Sheinerman FB, Norel R, Honig B. Electrostatic aspects of protein-protein interactions. *Curr Opin Struct Biol.* 2000 Apr;10(2):153–9.
104. Bahar I, Jernigan RL. Inter-residue potentials in globular proteins and the dominance of highly specific hydrophilic interactions at close separation. *J Mol Biol.* 1997 Feb 14;266(1):195–214.
105. Sheinerman FB, Honig B. On the role of electrostatic interactions in the design of protein-protein interfaces. *J Mol Biol.* 2002 Apr 19;318(1):161–77.
106. Bogan AA, Thorn KS. Anatomy of hot spots in protein interfaces. *J Mol Biol.* 1998 Jul 3;280(1):1–9.
107. Janin J, Chothia C. The structure of protein-protein recognition sites. *J Biol Chem.* 1990 Sep 25;265(27):16027–30.
108. Date SV, Stoeckert CJ Jr. Computational modeling of the *Plasmodium falciparum* interactome reveals protein function on a genome-wide scale. *Genome Res.* 2006 Apr;16(4):542–9.

109. Wuchty S, Ipsaro JJ. A draft of protein interactions in the malaria parasite *P. falciparum*. *J Proteome Res.* 2007 Apr;6(4):1461–70.
110. Wuchty S, Adams JH, Ferdig MT. A comprehensive *Plasmodium falciparum* protein interaction map reveals a distinct architecture of a core interactome. *Proteomics.* 2009 Apr;9(7):1841–9.
111. LaCount DJ, Vignali M, Chettier R, Phansalkar A, Bell R, Hesselberth JR, et al. A protein interaction network of the malaria parasite *Plasmodium falciparum*. *Nature.* 2005 Nov 3;438(7064):103–7.
112. Ramaprasad A, Pain A, Ravasi T. Defining the protein interaction network of human malaria parasite *Plasmodium falciparum*. *Genomics.* 2012 Feb;99(2):69–75.
113. Srinivasan P, Beatty WL, Diouf A, Herrera R, Ambroggio X, Moch JK, et al. Binding of *Plasmodium* merozoite proteins RON2 and AMA1 triggers commitment to invasion. *Proc Natl Acad Sci.* 2011 Aug 9;108(32):13275–80.
114. Alexander DL, Arastu-Kapur S, Dubremetz J-F, Boothroyd JC. *Plasmodium falciparum* AMA1 binds a rhoptry neck protein homologous to TgRON4, a component of the moving junction in *Toxoplasma gondii*. *Eukaryot Cell.* 2006 Jul;5(7):1169–73.
115. Buscaglia CA, Coppens I, Hol WGJ, Nussenzweig V. Sites of interaction between aldolase and thrombospondin-related anonymous protein in *plasmodium*. *Mol Biol Cell.* 2003 Dec;14(12):4947–57.
116. Heiss K, Nie H, Kumar S, Daly TM, Bergman LW, Matuschewski K. Functional characterization of a redundant *Plasmodium* TRAP family invasin, TRAP-like protein, by aldolase binding and a genetic complementation test. *Eukaryot Cell.* 2008 Jun;7(6):1062–70.
117. Green JL, Martin SR, Fielden J, Ksagoni A, Grainger M, Yim Lim BYS, et al. The MTIP-myosin A complex in blood stage malaria parasites. *J Mol Biol.* 2006 Feb 3;355(5):933–41.
118. Douse CH, Green JL, Salgado PS, Simpson PJ, Thomas JC, Langsley G, et al. Regulation of the *Plasmodium* motor complex: phosphorylation of myosin A tail-interacting protein (MTIP) loosens its grip on MyoA. *J Biol Chem.* 2012 Oct 26;287(44):36968–77.
119. Chen L, Lopaticki S, Riglar DT, Dekiwadia C, Uboldi AD, Tham W-H, et al. An EGF-like protein forms a complex with PfRh5 and is required for invasion of human erythrocytes by *Plasmodium falciparum*. *PLoS Pathog.* 2011 Sep;7(9):e1002199.

120. Daher W, Browaeys E, Pierrot C, Jouin H, Dive D, Meurice E, et al. Regulation of protein phosphatase type 1 and cell cycle progression by PflRR1, a novel leucine-rich repeat protein of the human malaria parasite *Plasmodium falciparum*. *Mol Microbiol*. 2006 May;60(3):578–90.
121. Hain AUP, Weltzer RR, Hammond H, Jayabalasingham B, Dinglasan RR, Graham DRM, et al. Structural characterization and inhibition of the *Plasmodium* Atg8-Atg3 interaction. *J Struct Biol*. 2012 Dec;180(3):551–62.
122. Daher W, Pierrot C, Kalamou H, Pinder JC, Margos G, Dive D, et al. *Plasmodium falciparum* dynein light chain 1 interacts with actin/myosin during blood stage development. *J Biol Chem*. 2010 Jun 25;285(26):20180–91.
123. Chua CS, Low H, Lehming N, Sim TS. Molecular analysis of *Plasmodium falciparum* co-chaperone Aha1 supports its interaction with and regulation of Hsp90 in the malaria parasite. *Int J Biochem Cell Biol*. 2012 Jan;44(1):233–45.
124. Sim BK, Chitnis CE, Wasniowska K, Hadley TJ, Miller LH. Receptor and ligand domains for invasion of erythrocytes by *Plasmodium falciparum*. *Science*. 1994 Jun 24;264(5167):1941–4.
125. Lobo C-A, Rodriguez M, Reid M, Lustigman S. Glycophorin C is the receptor for the *Plasmodium falciparum* erythrocyte binding ligand PfEBP-2 (baebl). *Blood*. 2003 Jun 1;101(11):4628–31.
126. Tham W-H, Wilson DW, Lopaticki S, Schmidt CQ, Tetteh-Quarcoop PB, Barlow PN, et al. Complement receptor 1 is the host erythrocyte receptor for *Plasmodium falciparum* PfRh4 invasion ligand. *Proc Natl Acad Sci U S A*. 2010 Oct 5;107(40):17327–32.
127. Crosnier C, Bustamante LY, Bartholdson SJ, Bei AK, Theron M, Uchikawa M, et al. Basigin is a receptor essential for erythrocyte invasion by *Plasmodium falciparum*. *Nature*. 2011 Dec 22;480(7378):534–7.
128. Foley M, Tilley L, Sawyer WH, Anders RF. The ring-infected erythrocyte surface antigen of *Plasmodium falciparum* associates with spectrin in the erythrocyte membrane. *Mol Biochem Parasitol*. 1991 May;46(1):137–47.
129. Da Silva E, Foley M, Dluzewski AR, Murray LJ, Anders RF, Tilley L. The *Plasmodium falciparum* protein RESA interacts with the erythrocyte cytoskeleton and modifies erythrocyte thermal stability. *Mol Biochem Parasitol*. 1994 Jul;66(1):59–69.
130. Pei X, Guo X, Coppel R, Mohandas N, An X. *Plasmodium falciparum* erythrocyte membrane protein 3 (PfEMP3) destabilizes erythrocyte membrane skeleton. *J Biol Chem*. 2007 Sep 14;282(37):26754–8.

131. Kilejian A, Rashid MA, Aikawa M, Aji T, Yang YF. Selective association of a fragment of the knob protein with spectrin, actin and the red cell membrane. *Mol Biochem Parasitol*. 1991 Feb;44(2):175–81.
132. Lustigman S, Anders RF, Brown GV, Coppel RL. The mature-parasite-infected erythrocyte surface antigen (MESA) of *Plasmodium falciparum* associates with the erythrocyte membrane skeletal protein, band 4.1. *Mol Biochem Parasitol*. 1990 Jan 15;38(2):261–70.
133. Waller KL, Nunomura W, An X, Cooke BM, Mohandas N, Coppel RL. Mature parasite-infected erythrocyte surface antigen (MESA) of *Plasmodium falciparum* binds to the 30-kDa domain of protein 4.1 in malaria-infected red blood cells. *Blood*. 2003 Sep 1;102(5):1911–4.
134. Parish LA, Mai DW, Jones ML, Kitson EL, Rayner JC. A member of the *Plasmodium falciparum* PHIST family binds to the erythrocyte cytoskeleton component band 4.1. *Malar J*. 2013;12:160.
135. Magowan C, Nunomura W, Waller KL, Yeung J, Liang J, Van Dort H, et al. *Plasmodium falciparum* histidine-rich protein 1 associates with the band 3 binding domain of ankyrin in the infected red cell membrane. *Biochim Biophys Acta*. 2000 Nov 15;1502(3):461–70.
136. Baruch DI, Gormely JA, Ma C, Howard RJ, Pasloske BL. *Plasmodium falciparum* erythrocyte membrane protein 1 is a parasitized erythrocyte receptor for adherence to CD36, thrombospondin, and intercellular adhesion molecule 1. *Proc Natl Acad Sci U S A*. 1996 Apr 16;93(8):3497–502.
137. Oquendo P, Hundt E, Lawler J, Seed B. CD36 directly mediates cytoadherence of *Plasmodium falciparum* parasitized erythrocytes. *Cell*. 1989 Jul 14;58(1):95–101.
138. Barnwell JW, Asch AS, Nachman RL, Yamaya M, Aikawa M, Ingravallo P. A human 88-kD membrane glycoprotein (CD36) functions in vitro as a receptor for a cytoadherence ligand on *Plasmodium falciparum*-infected erythrocytes. *J Clin Invest*. 1989 Sep;84(3):765–72.
139. Robinson BA, Welch TL, Smith JD. Widespread functional specialization of *Plasmodium falciparum* erythrocyte membrane protein 1 family members to bind CD36 analysed across a parasite genome. *Mol Microbiol*. 2003 Mar;47(5):1265–78.
140. Smith JD, Craig AG, Kriek N, Hudson-Taylor D, Kyes S, Fagan T, et al. Identification of a *Plasmodium falciparum* intercellular adhesion molecule-1 binding domain: a parasite adhesion trait implicated in cerebral malaria. *Proc Natl Acad Sci U S A*. 2000 Feb 15;97(4):1766–71.
141. Chattopadhyay R, Taneja T, Chakrabarti K, Pillai CR, Chitnis CE. Molecular analysis of the cytoadherence phenotype of a *Plasmodium falciparum* field isolate

- that binds intercellular adhesion molecule-1. *Mol Biochem Parasitol.* 2004 Feb;133(2):255–65.
142. Springer AL, Smith LM, Mackay DQ, Nelson SO, Smith JD. Functional interdependence of the DBLbeta domain and c2 region for binding of the *Plasmodium falciparum* variant antigen to ICAM-1. *Mol Biochem Parasitol.* 2004 Sep;137(1):55–64.
143. Senczuk AM, Reeder JC, Kosmala MM, Ho M. *Plasmodium falciparum* erythrocyte membrane protein 1 functions as a ligand for P-selectin. *Blood.* 2001 Nov 15;98(10):3132–5.
144. Chen Q, Heddini A, Barragan A, Fernandez V, Pearce SF, Wahlgren M. The semiconserved head structure of *Plasmodium falciparum* erythrocyte membrane protein 1 mediates binding to multiple independent host receptors. *J Exp Med.* 2000 Jul 3;192(1):1–10.
145. Barragan A, Fernandez V, Chen Q, von Euler A, Wahlgren M, Spillmann D. The duffy-binding-like domain 1 of *Plasmodium falciparum* erythrocyte membrane protein 1 (PfEMP1) is a heparan sulfate ligand that requires 12 mers for binding. *Blood.* 2000 Jun 1;95(11):3594–9.
146. Vogt AM, Barragan A, Chen Q, Kironde F, Spillmann D, Wahlgren M. Heparan sulfate on endothelial cells mediates the binding of *Plasmodium falciparum*-infected erythrocytes via the DBL1alpha domain of PfEMP1. *Blood.* 2003 Mar 15;101(6):2405–11.
147. Chen Q, Barragan A, Fernandez V, Sundström A, Schlichtherle M, Sahlén A, et al. Identification of *Plasmodium falciparum* erythrocyte membrane protein 1 (PfEMP1) as the rosetting ligand of the malaria parasite *P. falciparum*. *J Exp Med.* 1998 Jan 5;187(1):15–23.
148. Fried M, Duffy PE. Adherence of *Plasmodium falciparum* to chondroitin sulfate A in the human placenta. *Science.* 1996 Jun 7;272(5267):1502–4.
149. Salanti A, Staalsoe T, Lavstsen T, Jensen ATR, Sowa MPK, Arnot DE, et al. Selective upregulation of a single distinctly structured var gene in chondroitin sulphate A-adhering *Plasmodium falciparum* involved in pregnancy-associated malaria. *Mol Microbiol.* 2003 Jul;49(1):179–91.
150. Clackson T, Wells JA. A hot spot of binding energy in a hormone-receptor interface. *Science.* 1995 Jan 20;267(5196):383–6.
151. Buchwald P. Small-molecule protein-protein interaction inhibitors: therapeutic potential in light of molecular size, chemical space, and ligand binding efficiency considerations. *IUBMB Life.* 2010 Oct;62(10):724–31.

152. Babé LM, Rosé J, Craik CS. Synthetic “interface” peptides alter dimeric assembly of the HIV 1 and 2 proteases. *Protein Sci Publ Protein Soc.* 1992 Oct;1(10):1244–53.
153. Schramm HJ, Boetzel J, Büttner J, Fritsche E, Göhring W, Jaeger E, et al. The inhibition of human immunodeficiency virus proteases by “interface peptides.” *Antiviral Res.* 1996 May;30(2-3):155–70.
154. Rinaldi M, Tintori C, Franchi L, Vignaroli G, Innitzer A, Massa S, et al. A versatile and practical synthesis toward the development of novel HIV-1 integrase inhibitors. *ChemMedChem.* 2011 Feb 7;6(2):343–52.
155. White PW, Faucher A-M, Goudreau N. Small molecule inhibitors of the human papillomavirus E1-E2 interaction. *Curr Top Microbiol Immunol.* 2011;348:61–88.
156. Voet A, Callewaert L, Ulens T, Vanderkelen L, Vanherreweghe JM, Michiels CW, et al. Structure based discovery of small molecule suppressors targeting bacterial lysozyme inhibitors. *Biochem Biophys Res Commun.* 2011 Feb 25;405(4):527–32.
157. Ohkanda J, Buckner FS, Lockman JW, Yokoyama K, Carrico D, Eastman R, et al. Design and synthesis of peptidomimetic protein farnesyltransferase inhibitors as anti-Trypanosoma brucei agents. *J Med Chem.* 2004 Jan 15;47(2):432–45.
158. Vu BT, Vassilev L. Small-molecule inhibitors of the p53-MDM2 interaction. *Curr Top Microbiol Immunol.* 2011;348:151–72.
159. Singh SK, Maithal K, Balaram H, Balaram P. Synthetic peptides as inactivators of multimeric enzymes: inhibition of Plasmodium falciparum triosephosphate isomerase by interface peptides. *FEBS Lett.* 2001 Jul 13;501(1):19–23.
160. Rizzi L, Sundararaman S, Cendic K, Vaiana N, Korde R, Sinha D, et al. Design and synthesis of protein-protein interaction mimics as Plasmodium falciparum cysteine protease, falcipain-2 inhibitors. *Eur J Med Chem.* 2011 Jun;46(6):2083–90.
161. Iyer K, Bürkle L, Auerbach D, Thaminy S, Dinkel M, Engels K, et al. Utilizing the split-ubiquitin membrane yeast two-hybrid system to identify protein-protein interactions of integral membrane proteins. *Sci STKE Signal Transduct Knowl Environ.* 2005 Mar 15;2005(275):p13.

Chapter 2

Establishment of the mating-based split-ubiquitin system as a new *in vitro* interaction platform for *Plasmodium falciparum* membrane proteins

Introduction

The protozoan parasite *Plasmodium falciparum* is the causative agent of malaria tropica, the most severe form of human malaria responsible for nearly 700'000 annual deaths worldwide (1). The pathology of this disease is associated with the asexual development of the unicellular parasite within the human red blood cell. During this intraerythrocytic part of the life cycle the parasite resides in a parasitophorous vacuole (PV) separated from the host cell cytoplasm by the parasitophorous vacuole membrane (PVM). Since erythrocytes do not express the major histocompatibility complex (MHC) the parasite can hide from immunological detection. On the other hand erythrocytes are highly specialized cells, devoid of all internal organelles and any protein-trafficking machinery. Survival within the red blood cell and virulence of *P. falciparum* therefore critically depend on extensive host cell modifications. These are mediated through the export of numerous parasite proteins into the red blood cell (RBC) cytoplasm, including two parasite induced membranous structures: A tubovesicular network (TVN) extending from the PVM (2,3) and slender tubes with an electron-lucent lumen and an electron-dense coat called Maurer's clefts (MCs). These MCs seem to have a crucial role in protein trafficking, probably by functioning as a secretory organelle that concentrates virulence proteins for delivery to the host cell membrane (4,5). One of these proteins exported via the MCs is the variable surface antigen called '*P. falciparum* erythrocyte membrane protein 1' (PfEMP1). PfEMP1 mediates adhesion to a variety of endothelial host cell receptors (6–8) and thus prevents the infected cells from being eliminated in the spleen. PfEMP1 mediated adherence to vascular endothelial cells constrains blood circulation and triggers the release of pro-inflammatory cytokines which leads to damages in various organs like the liver, lungs and the brain (9,10) and thus is the major process of malaria pathology.

The example of PfEMP1 demonstrates how the pathology of Malaria is firmly associated with exported parasite proteins which therefore are of major interest. Numerous of these exported proteins have been identified and some extensively studied. However, still surprisingly little is known about their function. Because proteins often work in pairs or complexes, one possibility to identify a protein's function is to identify its interacting

partners. Today this is often facilitated by high-throughput *in vitro* screening methods. The most common and easiest high-throughput screen for protein interactions is thereby the classical yeast two-hybrid (Y2H) assay (11), which has already been successfully used to generate a first *P. falciparum* blood-stage protein interaction network (12). Y2H consists of two components: the DNA-binding domain of a transcription factor (TF) fused to the investigated (bait) protein and the transcription activation domain of the TF fused to a protein library (prey). When both chimeric proteins are co-expressed in yeast and localized to the nucleus, and if the bait and prey protein interact with each other, they reconstitute a functional TF that activates the transcription of a marker gene which enables growth of the yeast cell on selective medium. However, despite the successful application of the classical Y2H to identify a multitude of protein interactions in various organisms including *P. falciparum*, it has one major drawback: Y2H is depleted of membrane protein interactions. Since the activation domain of the TF will be retained at the membrane when fused to a membrane protein, it is unavailable for reconstitution of the functional TF in the yeast nucleus. As a consequence the classical Y2H not only is unable to investigate membrane bait proteins in full-length, it is also inappropriate to identify interactions with other membrane proteins. Because most of the known exported *P. falciparum* proteins are membrane proteins, an alternative method is therefore required to investigate the interactome of the parasite's exportome. Like the classical Y2H the mating-based split-ubiquitin system (mbSUS) is based on yeast as a heterologous system and has a similar read out. But mbSUS solves the problem that the TF is non-functional when fused to a membrane protein by releasing the TF from the membrane if the investigated membrane protein interacts with the prey protein (13–15). Therefore the system uses an ubiquitin which is split into an N-terminal (Nub) and a C-terminal (Cub) domain (Fig. 1). Ubiquitin is a small conserved protein which serves as a target for degradation by the 26S proteasome and is recognized by ubiquitin-specific proteases (UBPs) present in all eukaryotic cells (16). When the Cub and Nub domains are co-expressed, they are able to reconstitute a functional ubiquitin (17). The mbSUS uses the circumstance that Nub mutants with an isoleucine (I) to glycine (G) exchange at position 13 have a reduced affinity to Cub. Hence they are only able to reconstitute the full-length ubiquitin when brought into proximity via the interaction of an additional protein pair

which is fused to the Nub or the Cub respectively (17). The investigated bait-protein is thereby fused to the Cub which further is fused to an artificial TF. This TF consists of the bacterial LexA-DNA binding domain and the *Herpes simplex* VP16 transactivator protein (LexA-VP16). In case that the investigated membrane protein interacts with a library protein fused to the mutated Nub (soluble and membrane proteins), the Nub and Cub moieties are brought together and a functional ubiquitin molecule can be reconstituted (Fig. 1). This allows cleavage by endogenous ubiquitin-specific proteases, which releases the LexA-VP16 transcription factor from the membrane protein to the cytosol where it diffuses into the nucleus and activates transcription of marker genes. In the used NMY51 yeast reporter strain (18) these marker genes are *his3* and *ade2* whose activation enables the yeast to grow on defined minimal medium lacking histidine and / or adenine (19).

Two species specific challenges must be considered when using *P. falciparum* bait proteins in the mbSUS: first, many exported parasite proteins do not have a conserved eukaryotic export signal. Therefore it is very unlikely that these proteins are efficiently secreted and inserted into yeast membranes on their own. A second *P. falciparum* specific challenge regarding mbSUS is the high AT content (80 %) of the parasite's genome (20) which was shown to hinder protein expression in heterologous systems (21). To overcome these problems we have the possibility to add different yeast derived artificial sequences to the bait's N-terminus by the use of different bait plasmids: either a *Saccharomyces cerevisiae* signal sequence (SUC2) which ensures proper membrane insertion (pBT3-SUC) or a short *S. cerevisiae* leader sequence (STE2) which optimizes expression (pBT3-STE).

We tried to establish mbSUS as a new *in vitro* interaction platform for *P. falciparum* membrane proteins on the basis of the known integral MC protein 'membrane-associated histidine-rich protein 1' (MAHRP1). Besides a central transmembrane domain, MAHRP1 contains an acidic N-terminal and a histidine-rich C-terminal domain which faces the erythrocyte cytoplasm (Type I transmembrane protein). This C-terminal domain has a histidine content of nearly 30% in 3D7 and contains six tandem repeats of the amino acid sequence DHGH, with additional preceding DH repeats (22). Some parasite derived histidine-rich proteins were shown to be involved in detoxification by catalyzing the

ferritroporphyrin (FP) polymerization to haematin and by enhancing its degradation by H_2O_2 (23). Because recombinant MAHRP1 was shown to bind and increase degradation of FP *in vitro* as well (22), it seems likely that it protects the Maurer's clefts and their associated proteins from deleterious effects of FP. MAHRP1 was further shown to have an important role in the translocation of *PfEMP1*, the major parasite virulence factor, from the parasite to the host cell membrane: By knocking out the MAHRP1 gene of 3D7 parasites, Spycher and colleagues (24) demonstrated that *PfEMP1* accumulates within the confines of the plasma membrane / PVM interface and is not transported to the MCs and RBC surface anymore in the absence of MAHRP1. In contrast, the transport of other Maurer's cleft-resident proteins like the skeleton binding protein 1 (SBP1) and transit cargo is unaffected by the absence of MAHRP1. Knock-out of MAHRP1 further revealed that it is not essential for parasite viability *in vitro* and MC formation, but in its absence MCs become disorganized in permeabilized cells (24). Since MAHRP1 contains neither an N-terminal ER entry signal nor a PEXEL/VTS motif other regions seem to be necessary for its export to the RBC. Localization studies of truncated versions of MAHRP1 fused to GFP revealed that the transmembrane domain of the protein is needed to enter the endoplasmic reticulum (ER), the first step of the export pathway. It was further demonstrated that the second half of the N-terminal domain is needed for transfer from the parasite's ER to the MCs. The first half of the C-terminal domain, while not necessary for export, may facilitate delivery to the MCs (25).

It is still a matter of some debate how cargo proteins like *PfEMP1* are trafficked to the Maurer's clefts and further to the host cell membrane. Since MAHRP1 is involved in these processes which are the basis for the parasite's serious pathology, the understanding of this protein and its interactions is of major interest.

The aim of this study was to establish the yeast mbSUS as a new *in vitro* interaction platform for *P. falciparum* membrane proteins. mbSUS would circumvent the problems associated with the analysis of membrane proteins using the classical yeast two-hybrid approach and would provide a very powerful tool not only for the identification of MAHRP1 interaction partners, but also for the investigation of any *P. falciparum* membrane protein of interest. Because many of these proteins are involved in essential

biological functions, this would be a crucial step towards a better understanding of *P. falciparum* biology and virulence.

Methods

Yeast medium

NMY51 reporter strain (18) was cultured in Yeast Extract - Peptone - Dextrose plus Adenine medium (YPAD: 1 % yeast extract (Sigma), 2 % Bacto Peptone (BD), 210 μM adenine hemisulfate, 2 % glucose). NMY51 transfected with a bait vector was cultured in minimal medium lacking leucine (SD-leu: 38 mM ammonium sulphate, 0.17 % Difco yeast nitrogen base w/o amino acids and ammonium sulphate (BD), 115 μM L-arginine, 230 μM L-isoleucine, 164 μM L-lysine-HCl, 135 μM L-methionine, 300 μM L-phenylalanine, 1.68 mM L-threonine, 166 μM L-tyrosine, 178 μM L-uracil, 1.28 mM L-valine, 108.6 μM adenine hemisulfate, 129 μM L-histidine, 100 μM L-tryptophan, 2 % glucose). NMY51 co-transfected with bait and prey vectors was cultured in minimal medium lacking leucine and tryptophan (SD-trp-leu: 38 mM ammonium sulphate, 0.17 % Difco yeast nitrogen base w/o amino acids and ammonium sulphate (BD), 115 μM L-arginine, 230 μM L-isoleucine, 164 μM L-lysine-HCl, 135 μM L-methionine, 300 μM L-phenylalanine, 1.68 mM L-threonine, 166 μM L-tyrosine, 178 μM L-uracil, 1.28 mM L-valine, 108.6 μM adenine hemisulfate, 129 μM L-histidine, 2 % glucose). mbSUS library screenings and functional assays were performed in minimal medium lacking leucine, tryptophan and histidine (SD-trp-leu-his: 38 mM ammonium sulphate, 0.17 % Difco yeast nitrogen base w/o amino acids and ammonium sulphate (BD), 115 μM L-arginine, 230 μM L-isoleucine, 164 μM L-lysine-HCl, 135 μM L-methionine, 300 μM L-phenylalanine, 1.68 mM L-threonine, 166 μM L-tyrosine, 178 μM L-uracil, 1.28 mM L-valine, 108.6 μM adenine hemisulfate, 2 % glucose) or minimal medium lacking leucine, tryptophan, histidine and adenine (SD-trp-leu-his-ade: 38 mM ammonium sulphate, 0.17 % Difco yeast nitrogen base w/o amino acids and ammonium sulphate (BD), 115 μM L-arginine, 230 μM L-isoleucine, 164 μM L-lysine-HCl, 135 μM L-methionine, 300 μM L-phenylalanine, 1.68 mM L-threonine, 166 μM L-tyrosine, 178 μM L-uracil, 1.28 mM L-valine, 2 % glucose).

cDNA library constructionmRNA isolation

EasyClone cDNA library construction kit was used for library generation (18). Synchronized ring-, trophozoit- and schizont-stage parasite cultures (7 % parasitemia, 90 ml each) were centrifuged (700g, 5 min), the supernatant removed and each blood pellet resuspended in 105 ml 0.15 % Saponin in PBS (ice cold) to isolate the parasites. After incubation on ice for 10 min the samples were centrifuged (2600g, 5 min, 4°C) and the supernatant removed. Pellet was washed twice with 20 ml ice cold 0.15 % Saponin in PBS (2600g, 5 min, 4°C) and once with 10 ml ice cold PBS. The resulting parasite pellet was resuspended in 4.5 ml Trizol, vortexed (shortly) and incubated at RT for 10 min. 900 µl Chloroform were added and the sample gently shaken for 1 min. After incubation at RT for 2 min the sample was centrifuged (2600 g, 10 min, 4°C) and the aqueous phase transferred to a new tube. 0.8 volumes 2-Propanol were added before the sample was vortexed (shortly) and precipitated o/n at -20°C. After centrifugation (20'000 g, 1 h, 4°C) the supernatant was discarded and the pellet resuspended in 5.25 ml Trizol. After incubation at 37°C for 5 min, 0.2 volumes Chloroform were added. The sample was mixed by shaking for 1 min, quickly vortexed and incubated at RT for 2 min. After centrifugation (20'000 g, 30 min, 4°C) the upper phase was transferred to a new tube, 0.8 volumes 2-Propanol were added and the sample precipitated o/n at -20°C. After centrifugation (20'000 g, 40 min, 4°C) the supernatant was discarded and the pellet washed in 4.9 ml 75 % EtOH (20'000 g, 10 min, 4°C). The pellet was air dried and resuspended in 266 µl 5 mM TE buffer. After incubation at 50°C for 3 min, 17.5 µl 100 mM DTT, 7 µl RNase inhibitor, 35 µl 10x RQ1 buffer and 24.5 µl RQ1 DNase (Promega) were added. After incubation at 37°C for 30 min, 900 µl Trizol were added and incubated at 37°C for additional 5 min. 280 µl Chloroform were added, and after shaking for 1 min the sample was incubated at RT for 3 min. After centrifugation (12'000g, 60 min, 4°C) the upper phase was transferred to a new tube, 0.8 volumes 2-Propanol were added and the RNA was precipitated at -20°C o/n. After centrifugation (20'000 g, 40 min, 4°C) the supernatant was discarded and the pellet washed in 4.9 ml

75% EtOH (20'000 g, 10 min, 4°C). The pellet was air dried and resuspended in 175 µl 5 mM TE buffer. After incubation at 50°C for 3 min the RNA concentration was measured using Nanodrop. 70 µg total RNA from each stage were mixed and messenger RNA (mRNA) was isolated using the Poly(A)Purist mRNA purification Kit (Ambion). mRNA was eluted with 2x 200 µl "RNA storage solution". mRNA concentration was determined using Nanodrop and the quality analyzed by gel electrophoresis. mRNA was precipitated by addition of 1/10 volume 5M Ammonium Acetate, 1 µl Glycogen and 2.5 volumes 100 % EtOH. After incubation o/n at -20°C mRNA was pelleted at full speed for 40 min at 4°C, the supernatant discarded and the pellet washed in 1 ml 75 % EtOH (full speed, 10 min, 4°C). The pellet was air dried and resuspended in "RNA storage solution" (Ambion) to receive an mRNA concentration of ~ 450 ng /µl.

First strand cDNA synthesis

2 µl mRNA (450 ng / µl) sample were mixed with 1 µl ddH₂O, 1 µl CDS-3M adapter (10 µM, (18)) and 1 µl PlugOligo-3M adapter (15 µM, (18)). After incubation at 70°C for 2 min, followed by 42°C for 2 min, 5 µl RT Master mix were added (2 µl 5x first strand buffer (18), 1 µl DTT (20 mM), 1 µl 10x dNTPs (10 mM each), 1 µl EasyClone reverse transcriptase (18)). After 30 min incubation at 42°C, 5 µl IP solution (18) were added and the sample mixed by pipetting. The sample was incubated at 42°C for an additional 90 min before the tube was placed on ice to stop the reaction.

Double strand cDNA synthesis by PCR amplification

4 µl first strand cDNA were mixed with 160 µl ddH₂O, 20 µl 10x EasyClone PCR buffer (18), 4 µl 50x dNTP mix (10 mM each), 8 µl PCR primer M1 (10 µM) and 4 µl 50x EasyClone Polymerase mix (18). PCR was performed at the following conditions (20 cycles for steps 2-4): 95°C for 1 min, 95°C for 15 sec, 66°C for 20 sec, 72°C for 3 min, 66°C for 15 sec, 72°C for 3 min. Double stranded (ds) cDNA was analyzed by gel electrophoresis and purified using Nucleospin Extract II kit (Clontech). DNA was eluted with 100 µl Elution Buffer (Clontech).

*Sfi*I digest and size fractionation of ds cDNA

80 μ l ds cDNA were digested with 20 units *Sfi*I enzyme for 20 h at 50 °C. To purify the digested ds cDNA and remove fragments < 500 bp, gel extraction was performed using Nucleospin Extract II kit (Clontech). After elution with 120 μ l Elution Buffer (Clontech), ds cDNA was analyzed by gel electrophoresis and concentration measured by Nanodrop. Digested cDNA was precipitated o/n at -20°C after adding 1/10 volume 5 M Ammonium Acetate, 2.5 volumes 100 % EtOH and 1 μ l Glycoblue. After centrifugation (20'000 g, 40 min, 4°C) the supernatant was discarded and the pellet washed in 1 ml 75 % EtOH (20'000 g, 10 min, 4°C). The pellet was air dried and cDNA resuspended in Nuclease free ddH₂O to a concentration of ~ 130 ng / μ l which was used for ligation into the *Sfi*I digested prey-vector pPR3-N.

*Sfi*I digest of prey vector pPR3-N

5 μ g pPR3-N prey vector (18) was *Sfi*I digested and purified by gel extraction using Nucleospin Extract II kit (Clontech). The linearized plasmid was diluted to a concentration of 250 ng / μ l which was used for ligation.

Ligation of ds cDNA library into pPR3-N prey vector

For ligation of the *P. falciparum* blood stage ds cDNA library into the prey vector pPR3-N, the following components were mixed: 2 μ l *Sfi*I digested ds cDNA (130 ng / μ l), 2 μ l *Sfi*I digested pPR3-N vector (250 ng / μ l), 1 μ l 10x T4 buffer (NEB), 1 μ l T4 DNA ligase (400'000 U/ml, NEB) and 4 μ l ddH₂O. After incubation at 16°C for 20 h, the volume was adjusted to 100 μ l with ddH₂O and 1/ 10 volume 5 M Ammonium Acetate, 2.5 volumes 100 % EtOH and 1 μ l Glycoblue were added for precipitation. After incubation o/n at -20°C the ligation was centrifuged (20'000 g, 40 min, 4°C) the supernatant was discarded and the pellet washed in 1 ml 75 % EtOH (20'000 g, 10 min, 4°C). The pellet was air dried and resuspended in 20 μ l Nuclease free ddH₂O for Transformation.

Large scale cDNA-library amplification

With the 20 μ l ligation product, 20 independent transformations were performed (1 μ l ligation product each) using electrocompetent DH10B *E. coli* cells (Sigma). 1 μ l ligation product was transferred into a precooled 1.5 ml tube. Electrocompetent DH10B *E. coli* cells (Sigma) were thawed on wet ice and 20 μ l were added to the ligation. The cells / ligation mix was transferred to a chilled 1 mm cuvette and electroporated with 2000 V, 200 Ω , 25 μ F. The cells were resuspended in 1 ml Recovery medium (Sigma, provided with the *E. coli* cells) and transferred to a shaker flask. 5 transformations were pooled in one 100 ml shaker flask and 6.5 ml SOC medium (Sigma) were added (one flask containing 6.5 ml SOC + 5 x 1 ml cells = 11.5 ml total; 4 Flasks). After incubation at 37°C (225 rpm) for 1h, 300 μ l aliquots were spread on 145 mm LB Agar plates containing 100 μ g/ml Ampicillin (150 plates total). After incubation o/n at 37°C the generated ~4'500'000 independent colonies were collected by adding 2 x 5 ml LB per plate with cells scraped into the liquid using a Drigalski spatula and subsequent transfer into a sterile bottle. During the cell collection the LB medium and the collection bottle were kept on ice to prevent further cell division. The collected cell culture (~1.5 l) was distributed into three 1l shaker flasks and incubated at 30°C (225 rpm) for 2.5 h. The whole cell culture was pooled and mixed by shaking. 10 ml were removed, centrifuged (2600 g, 10 min), the supernatant removed and the pellet was resuspended in 10 ml LB containing 25 % Glycerol. 1 ml aliquots were distributed into screw cap cryotubes and frozen in liquid nitrogen to generate stabilates (stored at -80°C).

The remaining cell culture was centrifuged at 3000 g for 5 min to remove the supernatant. The resulting pellet was used for DNA isolation using the PowerPrep HP Plasmid Maxiprep kit (OriGene). After precipitation each DNA pellet was resuspended in 500 μ l TE buffer and concentration measured by Nanodrop.

Analysis of the *P. falciparum* cDNA library quality

To re-transform the amplified cDNA library into *E. coli*, 50 μ l chemocompetent DH5 α cells were mixed with 5 μ l DNA (10 ng / μ l), incubated on ice for 5 min and distributed

on pre-warmed (37°C) LB Agar plates containing Ampicillin. After incubation o/n at 37°C, 60 different clones were analyzed by screening PCR using pPR3-N vector primers 5'-gtcgaaaattcaagacaagg-3' and 5'-aagcgtgacataactaattac-3'. 20 additional colonies were used to inoculate 5 ml LB containing Ampicillin and incubated o/n at 37°C at 225 rpm. Library plasmids were isolated using the QIAprep Spin Miniprep kit (Qiagen) and sequenced using the pPR3-N vector primers. Additionally the library (10 ng / μ l) was used as a template for several PCRs with primers of different genes summarized in table S1. PCR products were analyzed by gel electrophoresis.

Bait vector construction

Full-length MAHRP1 was PCR amplified from cDNA using primers summarized in table S1 and cloned into the bait vector pBT3-C / pBT3-STE / pBT3-SUC / pBT3-N (18) via SfiI restriction sites.

Transformation of the bait vector into the NMY51 yeast reporter strain

A single colony from a 3 day old NMY51 streak was inoculated in 20 ml of liquid YPAD medium (in a 100 ml Erlenmeyer flask) and incubated o/n on a shaker at 275 rpm and 30°C. The titer of the culture was determined using a Neubauer chamber and 2.5×10^8 cells were added to 50 ml pre-warmed YPAD to give 5×10^6 cells / ml. The cells were incubated at 30°C and 275 rpm till the cell titer was 2×10^7 (~5 h). Then the cells were centrifuged (3000 g, 5 min) and the supernatant removed. After the cells were washed in 25 ml ddH₂O (3000 g, 5 min) they were resuspended in 1 ml dd H₂O. Meanwhile the ss carrier DNA (2 mg / ml: (18)) was boiled at 95°C for 5 min and chilled on ice. The cell suspension was centrifuged (11'000 rpm, 30 sec) and the supernatant discarded. The pellet was resuspended in ddH₂O to a final volume of 1 ml and vortexed vigorously. 100 μ l aliquots were distributed into new tubes, centrifuged (11'000 rpm, 30 sec) and the supernatant removed. 360 μ l transformation mix (33 % PEG 3350, 100 mM LiOAc, 0.1 mg boiled ss carrier DNA, 2.5 μ g bait vector) were added and resuspended by vigorously vortexing. After incubation at 42°C (water bath) for 40 min the cells were pelleted

(11'000 rpm, 30 sec) and the supernatant removed. The cells were resuspended in 200 μ l ddH₂O and 100 μ l were spread on pre-warmed (30°C) SD-Leu Agar plates. Plates were sealed with parafilm and incubated at 30°C for 3-5 days.

Freezing of yeast strains (Glycerol stocks)

20 ml liquid yeast medium (depending on the strain either YPAD, SD-Leu or SD-Trp) were inoculated from a single colony of a 3 day old streak (in a 100 ml Erlenmeyer flask) and incubated o/n on a shaker at 275 rpm and 30°C. After centrifugation (2600 g, 5 min), the supernatant was removed and the pellet resuspended in 10 ml 2x YPAD containing 25 % Glycerol. 1 ml aliquots were distributed into screw cap cryotubes and frozen at -80°C.

mbSUS functional assay

A single colony from a 3 day old NMY51 pBT3-SUC-MAHRP1 or pBT3-STE-MAHRP1 streak was inoculated in 20 ml of liquid YPAD medium (in a 100 ml Erlenmeyer flask) and incubated o/n on a shaker at 275 rpm and 30°C. The titer of the culture was determined and 2.5×10^8 cells were added to 50 ml pre-warmed YPAD to give 5×10^6 cells / ml. The cells were incubated at 30°C and 275 rpm till the cell titer was 2×10^7 . The cells then were centrifuged (3000 g, 5 min) and the supernatant removed. The pellet was washed in 25 ml ddH₂O (3000 g, 5 min) and resuspended in 1 ml dd H₂O. Meanwhile the ss carrier DNA (2 mg / ml) was boiled at 95°C for 5 min and chilled on ice. The cell suspension was centrifuged (11'000 rpm, 30 sec) and the supernatant discarded. The pellet was resuspended in ddH₂O to a final volume of 1 ml and vortexed vigorously. 200 μ l aliquots were distributed into new tubes, centrifuged (11'000 rpm, 30 sec) and the supernatant removed. 360 μ l transformation mix (33 % PEG 3350, 100 mM LiOAc, 0.2 mg boiled ss carrier DNA, 2.5 μ g pPR3-N (empty library plasmid, negative control) / pOst1-NubI (wild type Nub, positive control) plasmid DNA) were added and resuspended by vigorously vortexing. After incubation at 42°C (water bath) for 40 min the cells were pelleted (11'000 rpm, 30 sec) and the supernatant removed. Each pellet was resuspended in 1 ml pre-warmed YPAD and incubated at 30°C for 90 min. After

centrifugation (11'000 rpm, 30 sec) the supernatant was removed, each pellet resuspended in 180 μ l ddH₂O (3 ml total) and 80 μ l aliquots were spread on pre-warmed (30°C) SD-Trp-Leu-His / SD-Trp-Leu-His-Ade Agar plates containing 100 mM 3-AT. Additionally a 1:1000 dilution of the transformation was plated on a SD-Trp-Leu plate to determine the transformation efficiency. Plates were sealed with parafilm and incubated at 30°C for 3 (SD-Trp-Leu) or 5 days (SD-Trp-Leu-His / SD-Trp-Leu-His-Ade) before number of colony forming units was determined.

Library Screenings

For one library transformation a total amount of 48 μ g *P. falciparum* blood-stage library DNA was used and a transformation-efficiency in the range of 2×10^5 clones / μ g DNA was yielded. A single colony from a 3 day old NMY51 pBT3-SUC-MAHRP1 streak was inoculated in 20 ml of liquid YPAD medium (in a 100 ml Erlenmeyer flask) and incubated o/n on a shaker at 275 rpm and 30°C. The titer of the culture was determined and 5×10^8 cells were added to 100 ml pre-warmed YPAD to give 5×10^6 cells / ml. The cells were incubated at 30°C and 275 rpm till the cell titer was 2×10^7 and split into 2 x 50 ml. Then the cells were centrifuged (3000 g, 5 min) and the supernatant removed. After each pellet was washed in 25 ml ddH₂O (3000 g, 5 min) they were resuspended in 1 ml dd H₂O. Meanwhile the ss carrier DNA (2 mg / ml) was boiled at 95°C for 5 min and chilled on ice. The cell suspension was centrifuged (11'000 rpm, 30 sec) and the supernatant discarded. Both pellets were resuspended in ddH₂O to a final volume of 1 ml each and vortexed vigorously. 10 x 200 μ l aliquots were distributed into new tubes, centrifuged (11'000 rpm, 30 sec) and the supernatant removed. 720 μ l transformation mix (33 % PEG 3350, 100 mM LiOAc, 0.2 mg boiled ss carrier DNA, 4.8 μ g cDNA library) were added and resuspended by vigorously vortexing. After incubation at 42°C (water bath) for 40 min the cells were pelleted (11'000 rpm, 30 sec) and the supernatant removed. Each pellet was resuspended in 300 μ l ddH₂O (3 ml total) and 200 μ l aliquots were spread on 15 pre-warmed (30°C) SD-Trp-Leu-His-Ade Agar plates containing 100 mM 3-AT. Additionally a 1:1000 dilution of the library transformation was plated on a

SD-Trp-Leu plate to determine the transformation efficiency. Plates were sealed with parafilm and incubated at 30°C for 3 (SD-Trp-Leu) or 8 days (SD-Trp-Leu-His-Ade).

Library plasmid recovery and transformation into *E. coli* for sequencing

For plasmid recovery buffers and spin columns were taken from QIAprep Spin Miniprep kit (Qiagen). Colonies expressing potential MAHRP1 binding partners were re-streaked on fresh SD-trp-leu-his-ade plates containing 100 mM 3-AT and grown at 30°C for 3 days. A nicely sized colony was then inoculated in 4 ml of liquid SD-trp-leu and incubated o/n on a shaker at 275 rpm and 30°C. Cells were centrifuged (10'000 g, 1 min) and the supernatant removed. After resuspension in 250 µl resuspension buffer (Qiagen) 100µl acid washed glass beads (Sigma) were added and the sample vortexed for 5 min. Then 250 µl lysis buffer (Qiagen) were added and after gentle shaking incubated for 4 min. After Addition of 350 µl neutralization buffer (Qiagen) and gentle shaking the sample was centrifuged for 10 min at 14'000 g. The cleared lysate was transferred to a spin column (Qiagen) and centrifuged at 6000 g for 1 min. After discarding the flow-through 500 µl binding buffer (Qiagen) were loaded onto the spin column and centrifuged at 6000 g for 1 min. The flow-through was discarded and the sample once again washed with 500 µl binding buffer and then with 750 µl wash buffer (6000 g, 1 min). After discarding the flow-through the sample was centrifuged again for 1 min at 14'000 g to eliminate remaining wash buffer. 50 µl Elution buffer (Qiagen) were added onto the membrane and after incubation for 1 min the DNA was eluted by centrifugation (14'000 g, 1 min). The eluted DNA was purified using the Nucleospin Extract II kit (Clontech) and eluted with 15 µl Elution buffer (Clontech). 5 µl of the purified plasmid DNA were then transformed into chemocompetent DH5α *E. coli* cells for amplification. Therefore 50 µl chemocompetent DH5α *E. coli* cells were mixed with 5 µl plasmid DNA (10 ng / µl), incubated in ice for 5 min and distributed on pre-warmed (37°C) LB Agar plates containing Ampicillin. After incubation o/n at 37°C, formed colonies were used to inoculate 5 ml LB containing Ampicillin. After incubation at 37°C o/n at 225 rpm, cells were pelleted and the library plasmids isolated using the QIAprep Spin Miniprep kit

(Qiagen). Plasmids were sequenced using the pPR3-N vector primers 5'-gtcгааattcaagacaagg-3' and 5'-aagcgtgacataactaattac-3'.

Results

***P. falciparum* cDNA library construction**

Messenger RNA (mRNA) was isolated from a mixture containing equal amounts of *P. falciparum* ring-, trophozoite- and schizont-stage total RNA (Fig. 2A). The mRNA then was transcribed into double stranded (ds) cDNA (Fig. 2B), PCR amplified and enriched for fragments > 500 bp by gel extraction (Fig. 2C). Subsequently the cDNA library was ligated into the prey vector pPR3-N (18) which contains the two resistance genes Amp^R and TRP1. These allow selection by growth on medium containing ampicillin (bacteria) or lacking tryptophan (yeast). The prey plasmid pPR3-N adds the coding sequence of an N-terminal split-ubiquitin (Nub) 5' to the library gene's N-terminus.

Identification of the *P. falciparum* cDNA library quality before amplification

To test the quality of the generated *P. falciparum* cDNA library an aliquot was transformed into *E. coli* and plasmids of 10 different clones were isolated, *Sfi*I digested and run on a gel to see the *P. falciparum* cDNA inserts. Nine of 10 clones contained a cDNA insert which had an average size of ~ 600 bp (Fig. 2D). Since ligation was shown to be successful, the library was ready for large scale amplification.

Large scale cDNA library amplification

To amplify the complete *P. falciparum* cDNA library it was transformed into electrocompetent DH10B *E. coli* cells (Sigma) by electroporation. The cells were distributed onto 150 LB Agar plates containing Ampicillin and grown over night at 37°C. The resulting ~ 4'500'000 independent colonies were collected and plasmids isolated which yielded a total of 4.28 mg *P. falciparum* blood-stage pPR3-N cDNA library.

Analysis of the *P. falciparum* cDNA library quality

To test the quality of the pPR3-N cDNA library it was retransformed again into chemocompetent DH5 α *E. coli* cells. Sixty clones were screened by PCR using pPR3-N vector primers that showed that all plasmids contained a DNA insert with an average size of ~ 500 bp (Fig. 3A). To further test the representation of *P. falciparum* genes 20 different clones were isolated and their inserts sequenced. Twelve clones contained a partial *P. falciparum* gene (Table 1), 7 clones contained *P. falciparum* ribosomal RNA (rRNA) and only 1 clone contained no insert. To test if full-length genes were contained in the cDNA library 13 different randomly selected parasite genes were PCR amplified using primers spanning the whole ORF: MAHRP1, five “conserved Plasmodium proteins with unknown function” (PF3D7_0716300, PF3D7_1012900, PF3D7_1124300, PF3D7_1317400 and PF3D7_1468900), a zinc finger protein (PF3D7_1009400), a splicing factor (PF3D7_1123900), a fork head domain protein (PF3D7_1307800), a bromodomain protein (PF3D7_1033700), a multiprotein bridging factor (PF3D7_1128200), a Histone H2A variant (PF3D7_0320900), and a putative vesicle-associated membrane protein (PF3D7_1439800). Ten of the thirteen full-length genes were successfully amplified (Fig. 3B).

Taken together, 95 % of the blood stage cDNA library plasmids contained a *P. falciparum* insert (60 % a partial gene, 35 % parasite derived rRNA) with an average insert size of ~ 500 bp. While the most of the plasmids seemed to contain only gene fragments, we show by PCR that over 10 of 13 randomly selected genes were represented as full-length genes. With approximately $4,5 \times 10^6$ clones from the large scale amplification 60 % or $\sim 2.7 \times 10^6$ clones should contain a parasite coding sequence. Since only 1/6 of them would be expected to be in frame and in the correct orientation the library should have an estimate gene-coverage of about 80 fold with an estimate of 5675 genes. Considering that not all parasite genes are transcribed during the blood stage, the coverage is probably even higher.

Bait vector construction

To produce a read-out in the nucleus, the bait-Cub and prey-Nub fusion proteins must be both present in the cytoplasm. Therefore the topology of the investigated protein has to be considered. Because MAHRP1 is a type 1 transmembrane protein, it was ligated into the plasmid vector 5' to the C-terminal half of ubiquitin (Cub) which itself is fused to a LexA-VP16 TF. This guarantees that the TF is exposed to the cytoplasm and able to diffuse into the yeast nucleus after ubiquitin-cleavage. Two different bait vectors were tested for functionality in two independent experiments: pBT3-STE (18) adds the *Saccharomyces cerevisiae* STE2 leader sequence to the N-terminus of the bait protein, which serves as a short leader sequence to optimize expression. pBT3-SUC (18) adds a *S. cerevisiae* signal sequence (SUC2) to the bait's N-terminus, which ensures proper insertion into yeast membranes. Additional components of both bait-vectors are the two selectable markers Kan^R and LEU2 which allow selection of plasmid-bearing cells on medium containing kanamycin (bacteria) or lacking leucine (yeast).

Functional assay with pBT3-STE-MAHRP1 & pBT3-SUC-MAHRP1 bait vectors

To analyze which bait protein (pBT3-STE-MAHRP1 or pBT3-SUC-MAHRP1) is better expressed and inserted into the yeast membranes, both plasmids were co-transformed with either of the two control plasmids pOst1-NubI (positive control) and pPR3-N (negative control) into the yeast reporter strain NMY51.

pOst1-NubI contains a wild type N-terminal Ubiquitin (Nub) which has a strong affinity for the C-terminal Ubiquitin (Cub) fused to the MAHRP1 bait and therefore enables cleavage resulting in cell growth on selective medium (Fig. 4A).

The empty library vector pPR3-N contains a mutated Nub which lost its affinity for Cub. Therefore no ubiquitin cleavage should occur and the TF should be retained at the yeast membranes, thereby preventing cell growth on selective medium (Fig. 4A). Figure 4B shows that 47 % of the yeast cells co-transformed with pBT3-STE-MAHRP1 and pOST1-NubI (positive control) grew on minimal medium lacking histidine and adenine (SD-trp-leu-his-ade). On the other hand 19 % of the cells co-transformed with pBT3-

STE-MAHRP1 and pPR3-N (negative control) could also grow under the same conditions. For yeast cells containing the bait vector pBT3-SUC-MAHRP1, 30 % of those transformed with pOst1-NubI could grow on minimal medium lacking histidine and adenine. In contrast, only 5 % of the cells transformed with the empty library vector pPR3-N could grow on the selective medium (Fig. 4B).

These results show that pBT3-SUC-MAHRP1 bait vector had a significantly reduced background growth compared to pBT3-STE-MAHRP1 and was therefore the better option for further experiments.

Optimization of the screening stringency

To reduce the number of false positives as much as possible in the subsequent library screens, the screening conditions were optimized. A pilot screen which simulated the conditions of a large library screen was performed. For this the pBT3-SUC-MAHRP1 bait-bearing yeast strain was transformed with the empty library vector pPR3-N and plated onto SD-trp-leu-his and SD-trp-leu-his-ade agar plates containing different concentrations of 3-aminotriazole (3-AT). 3-AT is a competitive inhibitor of the *His3* reporter which enables yeast to grow on selective medium lacking histidine and increased concentration of 3-AT should increase the stringency of *His3* selection. Since the mutated Nub expressed from the empty pPR3-N has no affinity for Cub of the MAHRP1 bait, all colonies which grew on selective medium were background. In order to identify the optimal 3-AT concentration, the transformed cells were spread on SD-trp-leu-his and SD-trp-leu-his-ade plates containing 0, 7.5, 10, 20, 50 and 100 mM 3-AT and incubated at 30°C for 4 days before the number of colonies was determined. Figure 4C shows that while a 3-AT concentration of 10 mM already reduced background growth by over 70 %, a concentration of 50 mM (SD-trp-leu-his-ade) or even 100 mM (SD-trp-leu-his) was needed to completely eliminate background.

Functional assay of pBT3-SUC-MAHRP1 with SD-trp-leu-his-ade (100 mM 3-AT)

To test if the pBT3-SUC-MAHRP1 bait is still functional under the determined stringent screening conditions, another functional assay was performed. Therefore pBT3-SUC-MAHRP1 bearing NMY51 yeast cells were transfected with the two control plasmids pOst1-NubI (positive control) and pPR3-N (negative control) and plated on SD-trp-leu-his-ade containing 100 mM 3-AT. After incubation at 30°C for 4 days, the number of colonies was determined. Figure 4D shows that approximately 7000 colonies containing pOst1-NubI did grow on SD-trp-leu-his-ade containing 100 mM 3-AT whilst not a single one was observed with the negative control vector pPR3-N. This not only confirmed that the MAHRP1-Cub bait is correctly expressed and functional, but also that the screening conditions eliminated background while still allowing growth of true positive clones.

Large scale library screenings with pBT3-SUC-MAHRP1

To identify potential MAHRP1 binding partners, two independent library screens were performed. After transformation of the *P. falciparum* blood-stage cDNA library into the NMY51 yeast reporter strain containing the pBT3-SUC-MAHRP1 bait, cells were plated onto SD-trp-leu-his-ade plates containing 100 mM 3-AT and grown at 30°C for up to 8 days. For the two duplicates screens 10^7 and 5×10^6 colony forming units (cfu) were screened for interacting with the MAHRP1 bait. Considering that ~ 60 % contain a *P. falciparum* gene and only 1/6 are in-frame and in the correct orientation approximately 1.5×10^6 parasite genes were actually screened. Since the *P. falciparum* 3D7 strain has a total number of 5675 genes, on average every single parasite gene was represented over 260 times. After four days incubation at 30°C, only 8 colonies were observed, after 5 days 68 additional colonies appeared, and finally after 7 days over 2700 small colonies grew on the 100 mM 3-AT plates. Plasmids of 49 clones were isolated from the yeast cells and sequenced. Of the 49 potential MAHRP1 interaction partners (PMIs) 24 contained a *P. falciparum* gene (49 %), 18 contained *P. falciparum* rRNA (37 %), 2 contained *P. falciparum* chromosomal non coding DNA (4 %), and 5 plasmids had no insert (10 %) (Table 2). Of the 24 clones with parasite genes, only 4 were in frame with

the N-terminal ubiquitin (Nub) and therefore potentially functional prey proteins. Two of these contained parts of the untranslated region (UTR) which contained a stop codon leaving two clones which potentially expressed a *P. falciparum* gene functional in the mbSUS. One was PF3D7_0402200 (surface-associated interspersed (SURFIN) gene 4.1) which was annotated as pseudogene (PlasmoDB) and the other potential MAHRP1 interactor was the putative YL1 nuclear protein (PF3D7_1464000).

In an attempt to counter the large number of false positives produced by the performed library screens, the 3-AT concentration of the selective growth-medium was increased from 100 to 150 mM to increase stringency. A total of 1.1×10^7 cfu were screened for binding with the MAHRP1 bait, which corresponds to ~200 times the whole parasite genome when adjusted for library quality, orientation and frame. After 4 days at 30°C 2 colonies appeared, 25 additional colonies appeared after 5 days and approximately 300 small cfu after 7 days. The plasmids of 6 colonies were isolated and their insert sequenced. Table 2 shows that 2 of the 6 PMIs contained a *P. falciparum* gene, one contained a *P. falciparum* rRNA, two non-coding *P. falciparum* DNA / RNA and one plasmid had no insert. Only 1 of the two parasite genes, a “conserved *Plasmodium* protein with unknown function” (PF3D7_1451000) was in frame. Since it contained parts of the UTR which contained a stop codon, it was not expected to be functionally for the mbSUS.

Confirmation of positive PMIs

To eliminate false positives, the isolated library plasmids of PMI clones containing a *P. falciparum* insert in frame with the Nub were reintroduced into fresh yeast cells expressing the MAHRP1 bait. Neither PMI PF3D7_0402200 and PF3D7_1464000 (containing only coding sequences for the respective genes), nor PF3D7_1140200 and PF3D7_0617800 (containing a part of the UTR which includes a stop codon) were able to maintain growth on selective medium. Additionally to these in-frame PMIs, plasmids containing the merozoite surface protein 1 (MSP1) were also reintroduced into the library. Although never in frame, *msp1* was identified to be an insert of 4 different PMI

colonies (Table 2). However, also the MSP1 prey was not able to trigger growth of MAHRP1 bearing yeast cells on selective medium after retransfection.

Discussion

Protein-protein interactions are the building blocks of all biological systems. Because of their utmost importance it is not surprising that scores of studies have been undertaken to characterize various interactions in model organisms. The identification of binding partners of investigated candidate proteins is thereby often facilitated by high-throughput *in vitro* screening methods like the Y2H assay, ribosomal display or phage display.

Despite their importance, surprisingly little is known about protein-protein interactions in *P. falciparum*. The reasons for this are manifold: the protozoan parasite has a very complex life cycle which makes handling and sample generation difficult. Further it is generally difficult to recombinantly express *P. falciparum* proteins. Despite these difficulties, LaCount and colleagues successfully established a Y2H assay to generate a *P. falciparum* blood-stage protein interaction network (12). While facing several Y2H-specific problems like a large number of false positives and bias towards yeast homologues, they were able to show the applicability of yeast-based *in vitro* systems for identification of *P. falciparum* protein interactions. However, the classical Y2H has a distinct disadvantage for investigation of membrane bound proteins. Because of their hydrophobic nature they insert into yeast membranes and prevent the attached transcription factor (TF) from entering the nucleus. Therefore investigation of full-length membrane proteins is not possible with Y2H. Since the majority of exported parasite proteins, such as MAHRP1 (22) or SBP1 (26) were shown to be membrane proteins, an alternative approach was needed to generate an interaction network of exported *P. falciparum* proteins. Here we tried to establish the mating-based split-ubiquitin system (mbSUS) (19) as a new *in vitro* protein interaction platform for *P. falciparum* membrane proteins on the basis of the integral MC protein MAHRP1.

Since the mbSUS is based on a split ubiquitin whose N-terminal half (Nub) must be fused to the prey proteins, preexisting *P. falciparum* cDNA libraries could not be used and a new one had to be generated. Therefore full-length-enriched *P. falciparum* blood stage cDNA was synthesized and cloned into a library vector which adds a Nub to the prey protein's N-terminus. Because of the N-terminal placement of the Nub the library is only functional with prey proteins which are either soluble or type II transmembrane proteins,

but not with full-length type I prey proteins. However, since the *P. falciparum* genome is very AT rich (~ 80 %) (20), the oligo (dT) adapter used for transcription of full-length mRNA into cDNA also annealed within coding sequences. Therefore the library did not exclusively contain full-length type I transmembrane (TM) proteins, but also gene fragments without a TM domain which are expressed as soluble proteins functional in the mbSUS. For RNA isolation from infected RBCs efficient saponin lysis was crucial to obtain a library of good quality. Although mature erythrocytes have lost their nucleus together with their other organelles, they still appear to contain transcripts of various genes (27). In a first attempt to generate a *P. falciparum* library, over 80 % of inserts derived from human haemoglobin mRNA but this contamination could almost completely be eliminated by increased saponin lysis. Subsequent analysis of libraries showed a high quality with approximately 60% of plasmids containing either full-length or partial *P. falciparum* genes with an average insert size of 500 bp. Accounting for random reading frame and orientation of the inserts this would represent an approximate 80 fold genome coverage. However, this high coverage is a bit misleading in the sense that not all parasite genes are represented equally. Since the library was generated from cDNA it is expected that due to substantial differences in transcript numbers lowly transcribed genes are underrepresented while highly transcribed genes are overrepresented.

During the intra-erythrocytic cycle MAHRP1 is exported early into the RBC where it inserts into Maurer's clefts (MCs) as a type I TM protein (22). Since only the C-terminal part of type I TM proteins is exposed to the cytoplasm and amenable for potential binding partners in mbSUS, the C-terminal split ubiquitin (Cub) and its adherent TF had to be fused C-terminally to the MAHRP1 bait. The MAHRP1 gene has a relatively high AT content (64 %), a characteristic which is known to hinder expression of *P. falciparum* proteins in heterologous systems (21). To overcome this potential problem we generated a bait plasmid which adds the short *Saccharomyces cerevisiae* leader sequence STE2 to the N-terminus of MAHRP1 which optimizes expression in yeast. Since MAHRP1 is a so called PEXEL-negative exported protein which lacks a classical signal peptide (SP), it was very unlikely that it is efficiently secreted and inserted into yeast membranes on its own. Therefore we further generated a bait plasmid which adds the *S. cerevisiae* signal

sequence SUC2 to the N-terminus of MAHRP1 which ensures proper membrane insertion.

The functionality of both generated baits was tested in functional assays in which growth on selective medium of bait-bearing cells transfected with a positive control plasmid containing the wild type Nub with high Cub-affinity showed that the TF containing bait proteins were both correctly expressed. The reduced growth of bait-bearing cells transfected with the empty library vector containing the mutated Nub with reduced Cub-affinity further showed retention of the TF by membrane insertion of the bait. Although both baits were functional in mbSUS it became clear that only SUC-MAHRP1 had an acceptable small background under optimized screening conditions. This indicated that exported *P. falciparum* proteins without a classical SP do not insert efficiently into yeast membranes and therefore need an artificial yeast signal sequence like SUC2. The remaining background could be eliminated by addition of 3-Aminotriazole (3-AT) which is a heterocyclic compound and a competitive inhibitor of the *his3* marker gene and thus increases the stringency of HIS3 selection (28). However, only the highest 3-AT concentration of 100 mM completely eliminate background growth and therefore a minimal medium lacking histidine and adenine (SD-trp-leu-his-ade) containing at least 100 mM 3-AT was used for all library screens.

By screening 2.6×10^7 library plasmids we only identified one single potential MAHRP1 binding partner, the putative nuclear protein YL1 (PF3D7_1464000). While *P. falciparum* YL1 is still uncharacterized, in mammalian cells this nuclear protein presumably plays multiple roles in chromatin modification and remodelling as part of a multi-protein complex (29). This makes YL1 extremely unlikely to be a direct interaction partner of MAHRP1 which is an exported MC membrane protein. The presumed incorrectness of the MAHRP1-YL1 interaction was confirmed by re-transfecting the isolated prey plasmid into fresh yeast cells expressing the MAHRP1 bait which did not result in growth on selective medium.

It is difficult to speculate why we were unsuccessful to identify MAHRP1-binding proteins using the mbSUS. The system might not be applicable to investigate interactions of *P. falciparum* membrane proteins, because the high AT content of the parasite genome (20) hinders protein expression in heterologous systems (21). Although the functional

assay indicated that the MAHRP1 bait protein was sufficiently expressed in the yeast reporter strain, this by no means allows to conclude that the majority of prey proteins would be expressed correctly. To overcome this problem LaCount and colleagues added an auxotrophic marker to the C-terminus of their library proteins (12) which allowed selection of plasmids encoding expressed *P. falciparum* proteins for their Y2H screenings. This pre-selection has the disadvantage that only 1/3 of all proteins which are in frame with the N-terminal Nub fragment are also in frame with this additional marker and thus eliminates another large proportion of clones available for the screen. We abstained from this selection but in retrospect it could have been beneficial when developing this system.

It is also possible that the quality of the generated library was inadequate. Although a number of experiments deemed the quality sufficient it is still possible that certain genes including the potential MAHRP1 interaction partners might not be present in the library. Sequencing of 55 potential interaction partners revealed that the comparatively long untranslated regions (UTRs) of the parasite (30,31) might have caused problems besides expected frame shifts. These UTRs by chance often contain a stop codon which causes premature termination of transcription of the prey protein sequence after the ubiquitin moiety. Three of the five sequenced prey plasmids contained UTRs with a stop codon. In a worst case this would mean that over 50 % of the prey proteins in-frame with the Nub fragment may still not be expressed for that reason reducing the genome coverage to approximately 200 fold than the predicted 450 fold coverage. Nevertheless, such coverage should still be sufficient for a mbSUS library screen.

To prove the applicability of the mbSUS and the generated library a positive control would have been necessary. However, at that time hardly any interaction of a membrane bound protein was confirmed except the binding of aldolase to the thrombospondin-related anonymous protein (TRAP) (32,33). Due to the fairly large size of the TM containing TRAP (~ 160 kDa), the full-length protein would not have been suitable as bait, but since the aldolase binding-site has been shown to be located at the C-terminus in relatively close proximity to the TM domain, TRAP fragments probably could have been still used as positive control. Recently, interaction of the apical membrane antigen (AMA1) and the rhoptry neck protein 2 (RON2) has been shown (34) and the TM

containing AMA1 with 72 kDa in size would have been better suited as bait and should be seriously considered as a positive control for future experiments. On the other hand, the RON2 as interaction partner with a size of 249 kDa is most probably too large to be expressed as full-length protein but it would be expected that the library might also contain smaller RON2 fragments.

A last possibility why we failed to identify interaction partners could be the inherent problem of the mbSUS or Y2H system with the large number of false positive clones and high background (35). In the mbSUS the complete insertion of the bait into the yeast membranes is fundamental. Only a small portion of the bait soluble in the cell can trigger growth on selective medium on its own. By increasing the 3-AT concentration in the selective medium we reduced this growth by increasing the necessary amount of reporter gene (*his3*) transcription. However, the need to use a maximum concentration of 3-AT to completely eliminate the background indicated that membrane insertion of the MAHRP1 bait was far from perfect. In addition, using the maximum 3-AT concentration reduces sensitivity of the system which then triggers growth only if bait and prey have a strong affinity for each other. It is then possible that binding of MAHRP1 to its interaction partner might not be strong enough to overcome these very stringent screening conditions.

In summary, we have generated a *P. falciparum* pPR3-N blood stage cDNA library, which had an overall good quality as judged by various measurements. We successfully generated and expressed a MAHRP1 bait protein in the yeast reporter NMY51 which was shown to insert into yeast membranes and to be functional in the mbSUS with standard control plasmids. However, the mbSUS library screens to identify MAHRP1 binding proteins remained unsuccessful. Nevertheless, the functionality of our MAHRP1 bait with control prey plasmids indicates that mbSUS is applicable for investigation of *P. falciparum* membrane proteins. While the quality and functionality of our library has to be further confirmed, e.g. by using AMA1 as positive control, it might still provide a powerful tool for identification of new *P. falciparum* membrane protein interactions. Even without a functional library the mbSUS could provide a useful tool to confirm

interaction on a one to one basis between a *P. falciparum* membrane protein and an identified specific protein.

References

1. World Health Organization. WHO | World Malaria Report 2012. 2009.
2. Behari R, Haldar K. Plasmodium falciparum: protein localization along a novel, lipid-rich tubovesicular membrane network in infected erythrocytes. *Exp Parasitol.* 1994 Nov;79(3):250–9.
3. Elmendorf HG, Haldar K. Plasmodium falciparum exports the Golgi marker sphingomyelin synthase into a tubovesicular network in the cytoplasm of mature erythrocytes. *J Cell Biol.* 1994 Feb;124(4):449–62.
4. Przyborski JM, Wickert H, Krohne G, Lanzer M. Maurer's clefts--a novel secretory organelle? *Mol Biochem Parasitol.* 2003 Nov;132(1):17–26.
5. Bhattacharjee S, van Ooij C, Balu B, Adams JH, Haldar K. Maurer's clefts of Plasmodium falciparum are secretory organelles that concentrate virulence protein reporters for delivery to the host erythrocyte. *Blood.* 2008 Feb 15;111(4):2418–26.
6. Baruch DI, Gormely JA, Ma C, Howard RJ, Pasloske BL. Plasmodium falciparum erythrocyte membrane protein 1 is a parasitized erythrocyte receptor for adherence to CD36, thrombospondin, and intercellular adhesion molecule 1. *Proc Natl Acad Sci U S A.* 1996 Apr 16;93(8):3497–502.
7. Rowe JA, Moulds JM, Newbold CI, Miller LH. P. falciparum rosetting mediated by a parasite-variant erythrocyte membrane protein and complement-receptor 1. *Nature.* 1997 Jul 17;388(6639):292–5.
8. Reeder JC, Cowman AF, Davern KM, Beeson JG, Thompson JK, Rogerson SJ, et al. The adhesion of Plasmodium falciparum-infected erythrocytes to chondroitin sulfate A is mediated by P. falciparum erythrocyte membrane protein 1. *Proc Natl Acad Sci U S A.* 1999 Apr 27;96(9):5198–202.
9. MacPherson GG, Warrell MJ, White NJ, Looareesuwan S, Warrell DA. Human cerebral malaria. A quantitative ultrastructural analysis of parasitized erythrocyte sequestration. *Am J Pathol.* 1985 Jun;119(3):385–401.
10. Pongponratn E, Riganti M, Punpoowong B, Aikawa M. Microvascular sequestration of parasitized erythrocytes in human falciparum malaria: a pathological study. *Am J Trop Med Hyg.* 1991 Feb;44(2):168–75.
11. Fields S, Song O. A novel genetic system to detect protein-protein interactions. *Nature.* 1989 Jul 20;340(6230):245–6.
12. LaCount DJ, Vignali M, Chettier R, Phansalkar A, Bell R, Hesselberth JR, et al. A protein interaction network of the malaria parasite Plasmodium falciparum. *Nature.* 2005 Nov 3;438(7064):103–7.

13. Stagljar I, Korostensky C, Johnsson N, Heesen S te. A genetic system based on split-ubiquitin for the analysis of interactions between membrane proteins in vivo. *Proc Natl Acad Sci*. 1998 Apr 28;95(9):5187–92.
14. Grefen C, Lalonde S, Obrdlik P. Split-ubiquitin system for identifying protein-protein interactions in membrane and full-length proteins. *Curr Protoc Neurosci* Editor Board Jacqueline N Crawley Al. 2007 Oct;Chapter 5:Unit 5.27.
15. Grefen C, Obrdlik P, Harter K. The determination of protein-protein interactions by the mating-based split-ubiquitin system (mbSUS). *Methods Mol Biol Clifton NJ*. 2009;479:217–33.
16. Hershko A, Ciechanover A. The ubiquitin system for protein degradation. *Annu Rev Biochem*. 1992;61:761–807.
17. Johnsson N, Varshavsky A. Split ubiquitin as a sensor of protein interactions in vivo. *Proc Natl Acad Sci U S A*. 1994 Oct 25;91(22):10340–4.
18. Dualsystems. DUALmembrane Protein Interaction Kits [Internet]. Available from: http://www.dualsystems.com/fileadmin/user_upload/z_download/manuals/DUAL_membrane-starter-kit_user-manual-A14.pdf
19. Iyer K, Bürkle L, Auerbach D, Thaminy S, Dinkel M, Engels K, et al. Utilizing the split-ubiquitin membrane yeast two-hybrid system to identify protein-protein interactions of integral membrane proteins. *Sci STKE Signal Transduct Knowl Environ*. 2005 Mar 15;2005(275):p13.
20. Gardner MJ, Hall N, Fung E, White O, Berriman M, Hyman RW, et al. Genome sequence of the human malaria parasite *Plasmodium falciparum*. *Nature*. 2002 Oct 3;419(6906):498–511.
21. Sibley CH, Brophy VH, Cheesman S, Hamilton KL, Hankins EG, Wooden JM, et al. Yeast as a model system to study drugs effective against apicomplexan proteins. *Methods San Diego Calif*. 1997 Oct;13(2):190–207.
22. Spycher C, Klonis N, Spielmann T, Kump E, Steiger S, Tilley L, et al. MAHRP-1, a novel *Plasmodium falciparum* histidine-rich protein, binds ferriprotoporphyrin IX and localizes to the Maurer’s clefts. *J Biol Chem*. 2003 Sep 12;278(37):35373–83.
23. Papalexis V, Siomos MA, Campanale N, Guo X, Kocak G, Foley M, et al. Histidine-rich protein 2 of the malaria parasite, *Plasmodium falciparum*, is involved in detoxification of the by-products of haemoglobin degradation. *Mol Biochem Parasitol*. 2001 Jun;115(1):77–86.
24. Spycher C, Rug M, Pachlatko E, Hanssen E, Ferguson D, Cowman AF, et al. The Maurer’s cleft protein MAHRP1 is essential for trafficking of PfEMP1 to the

- surface of *Plasmodium falciparum*-infected erythrocytes. *Mol Microbiol.* 2008 Jun;68(5):1300–14.
25. Spycher C, Rug M, Klonis N, Ferguson DJP, Cowman AF, Beck H-P, et al. Genesis of and trafficking to the Maurer's clefts of *Plasmodium falciparum*-infected erythrocytes. *Mol Cell Biol.* 2006 Jun;26(11):4074–85.
 26. Blisnick T, Morales Betoulle ME, Barale JC, Uzureau P, Berry L, Desroses S, et al. Pfsbp1, a Maurer's cleft *Plasmodium falciparum* protein, is associated with the erythrocyte skeleton. *Mol Biochem Parasitol.* 2000 Nov;111(1):107–21.
 27. Kabanova S, Kleinbongard P, Volkmer J, Andrée B, Kelm M, Jax TW. Gene expression analysis of human red blood cells. *Int J Med Sci.* 2009;6(4):156–9.
 28. Brennan MB, Struhl K. Mechanisms of increasing expression of a yeast gene in *Escherichia coli*. *J Mol Biol.* 1980 Jan 25;136(3):333–8.
 29. Cai Y, Jin J, Florens L, Swanson SK, Kusch T, Li B, et al. The mammalian YL1 protein is a shared subunit of the TRRAP/TIP60 histone acetyltransferase and SRCAP complexes. *J Biol Chem.* 2005 Apr 8;280(14):13665–70.
 30. Horrocks P, Dechering K, Lanzer M. Control of gene expression in *Plasmodium falciparum*. *Mol Biochem Parasitol.* 1998 Sep 15;95(2):171–81.
 31. Horrocks P, Wong E, Russell K, Emes RD. Control of gene expression in *Plasmodium falciparum* - ten years on. *Mol Biochem Parasitol.* 2009 Mar;164(1):9–25.
 32. Buscaglia CA, Coppens I, Hol WGJ, Nussenzweig V. Sites of interaction between aldolase and thrombospondin-related anonymous protein in *Plasmodium*. *Mol Biol Cell.* 2003 Dec;14(12):4947–57.
 33. Heiss K, Nie H, Kumar S, Daly TM, Bergman LW, Matuschewski K. Functional characterization of a redundant *Plasmodium* TRAP family invasin, TRAP-like protein, by aldolase binding and a genetic complementation test. *Eukaryot Cell.* 2008 Jun;7(6):1062–70.
 34. Srinivasan P, Beatty WL, Diouf A, Herrera R, Ambroggio X, Moch JK, et al. Binding of *Plasmodium* merozoite proteins RON2 and AMA1 triggers commitment to invasion. *Proc Natl Acad Sci.* 2011 Aug 9;108(32):13275–80.
 35. Von Mering C, Krause R, Snel B, Cornell M, Oliver SG, Fields S, et al. Comparative assessment of large-scale data sets of protein-protein interactions. *Nature.* 2002 May 23;417(6887):399–403.

Tables

Gene ID	gene product	insert size (bp)	full length ratio	UTR length (bp)	orientation
PF3D7_1414600	RNA guanylyltransferase	282	0.18	145	3'—5'
PF3D7_0719400	conserved Plasmodium protein, unknown function	55	0.01	2	3'—5'
PF3D7_1450100	signal recognition particle SRP54, putative	393	0.26	4	5'—3'
PF3D7_0930300	merozoite surface protein 1 precursor	797	0.15	4	5'—3'
PF3D7_1216400	conserved Plasmodium membrane protein, unknown function	778	0.28	0	5'—3'
PF3D7_1029000	unknown function	52	0.02	3	3'—5'
PF3D7_1428300	proliferation-associated protein 2g4, putative	82	0.07	2	5'—3'
PF3D7_1103800	NOT family protein, putative	119	0.01	4	5'—3'
PF3D7_1126700	conserved Plasmodium protein, unknown function	375	0.13	4	5'—3'
PF3D7_1430200	plasmepsin IX	130	0.07	4	5'—3'
PF3D7_1222300	endoplasmin homolog precursor, putative	694	0.28	8	5'—3'
PF3D7_1324900	L-lactate dehydrogenase	216	0.12	6	5'—3'
average		331.1	0.13	15.5	

Table 1 After large-scale amplification of the blood-stage *P. falciparum* cDNA library, 20 library plasmids were sequenced to identify their insert. Of those 20, 12 plasmids contained a partial *P. falciparum* gene (listed above). On average the library plasmids contained about 13 % of the coding sequence of their respective genes and none of the vectors contained a full-length gene. While an untranslated region (UTR) was part of almost every insert, its length was quite small.

PMI	gene	gene product	size (bp)	fragment size (bp)	in frame	Clone appeared after	conditions
1		Chromosome 5, non coding region		229		4 days	100mM 3-AT
2	PF3D7_0419600	ran binding protein 1	843	545	no	4 days	100mM 3-AT
3	PF3D7_1132200	TCP-1/cpn60 chaperonin family	1635	770	no	4 days	100mM 3-AT
4		mal_rna_17:rRNA		218		4 days	100mM 3-AT
5	PF3D7_0628100	HECT-domain (ubiquitin-transferase)	30864	625	no	4 days	100mM 3-AT
6	PF3D7_1228600	merozoite surface protein 9	2232	780	no	4 days	100mM 3-AT
7	PF3D7_1035500	merozoite surface protein 6	1116	500	no	5 days	100mM 3-AT
8		mal_rna_9:rRNA		90		5 days	100mM 3-AT
9		empty		0		5 days	100mM 3-AT
10		empty		0		5 days	100mM 3-AT
11		mal_rna_19:rRNA		129		5 days	100mM 3-AT
12		empty		0		5 days	100mM 3-AT
13	PF3D7_1035300	glutamate-rich protein	3702	400	no	5 days	100mM 3-AT
14		malmito_rna_RNA5:rRNA		107		5 days	100mM 3-AT
15		mal_rna_17:rRNA		216		5 days	100mM 3-AT
16	PF3D7_0402200	surface-associated interspersed gene 4.1, (SURFIN4.1)	6471	820	yes	5 days	100mM 3-AT
17		empty		0		5 days	100mM 3-AT
18	PF3D7_0930300	merozoite surface protein 1	5163	850	no	5 days	100mM 3-AT
19	PF3D7_1229900.1	conserved Plasmodium protein, unknown function	2055	240	no	5 days	100mM 3-AT
20		Chromosome 10, non coding region		60		5 days	100mM 3-AT
21		malmito_rna_RNA18:rRNA		46		5 days	100mM 3-AT
22	PF3D7_0930300	merozoite surface protein 1	5163	870	no	5 days	100mM 3-AT
23		malmito_rna_LSUG:rRNA		620		5 days	100mM 3-AT
24		malmito_rna_RNA14:rRNA		69		> 6 days	100mM 3-AT
25	PF3D7_0723400	conserved Plasmodium protein, unknown function	4269	255	no	> 6 days	100mM 3-AT
26		mal_rna_10:rRNA		108		> 6 days	100mM 3-AT
27		MAL5_28S		436		> 6 days	100mM 3-AT
28	PF3D7_0617800	histone H2A	399	396	no	> 6 days	100mM 3-AT
29		malmito_rna_LSUC:rRNA		47		> 6 days	100mM 3-AT
30	PF3D7_1106200	conserved Plasmodium protein, unknown function	2046	365	no	> 6 days	100mM 3-AT

PMI	gene	gene product	size (bp)	fragment size (bp)	in frame	Clone appeared after	conditions
31	PF3D7_0930300	merozoite surface protein 1	5163	180	no	> 6 days	100mM 3-AT
32		mal_rna_9:rRNA		88		> 6 days	100mM 3-AT
33		empty		0		> 6 days	100mM 3-AT
34		malmito_rna_RNA4:rRNA		459		> 6 days	100mM 3-AT
35	PF3D7_0103400	zinc-carboxypeptidase	4863	365	no	> 6 days	100mM 3-AT
36		malmito_rna_RNA6:rRNA		77		> 6 days	100mM 3-AT
37	PF3D7_0506900	rhomboid protease ROM4	2280	300	no	> 6 days	100mM 3-AT
38	PF3D7_1140200	conserved Plasmodium protein, unknown function	1344	500	yes (UTR stop)	> 6 days	100mM 3-AT
39		MAL5_18S		816		> 6 days	100mM 3-AT
40	PF3D7_0113600	surface-associated interspersed gene (SURFIN)	5586	800	no	> 6 days	100mM 3-AT
41	PF3D7_0617800	histone H2A	399	540	yes (UTR stop)	> 6 days	100mM 3-AT
42		mal_rna_10:rRNA		82		> 6 days	100mM 3-AT
43		malmito_rna_RNA22:rRNA		61		> 6 days	100mM 3-AT
44	PF3D7_1464000	YL1 nuclear protein, putative	2118	850	yes	> 6 days	100mM 3-AT
45		malmito_rna_1:rRNA		120		> 6 days	100mM 3-AT
46	PF3D7_1216000	Serine--tRNA ligase, putative	1857	617	no	> 6 days	100mM 3-AT
47	PF3D7_1320700	conserved Plasmodium protein, unknown function	4329	870	no	> 6 days	100mM 3-AT
48	PF3D7_1478900	ncRNA	1044	460	no	> 6 days	100mM 3-AT
49	PF3D7_1411000.1	conserved Plasmodium protein, unknown function	7233	660	no	> 6 days	100mM 3-AT
50		empty		0		4 days	150 mM 3-AT
51		malmito_rna_RNA11:rRNA		83		4 days	150 mM 3-AT
52		PF12TR011:ncRNA		126		5 days	150 mM 3-AT
53		Chromosome 1, non coding region		> 161		5 days	150 mM 3-AT
54	PF3D7_0930300	merozoite surface protein 1	5163	710	no	5 days	150 mM 3-AT
55	PF3D7_1451000	conserved Plasmodium protein, unknown function	2415	830	yes (UTR stop)	5 days	150 mM 3-AT

Table 2 Summary of all potential MAHRP1 interactors (PMIs) identified by three independent large-scale *P. falciparum* blood-stage cDNA library screenings with the pBT3-SUC-MAHRP1 bait in the mbSUS. Sequencing of 55 PMI clones revealed that only 26 contained a library plasmid with a (partial) *P. falciparum* coding sequence. Of those 26 only 2 were in frame and potentially expressed.

Figure legends

Figure 1 The mating-based split-ubiquitin system. The bait protein is fused to the C-terminal half (Cub) and the prey to the N-terminal half of a split ubiquitin. If they interact a functional ubiquitin protein is reconstituted which gets cleaved by endogenous ubiquitin-specific proteases (USP). This allows the artificial transcription factor (TF) which was fused to the Cub to enter the nucleus (N) where it starts expression of reporter genes (RG). In order to prevent reconstitution of the split ubiquitin without interaction of the bait and prey proteins, the Nub contains a mutation. The bait protein which is fused to the Cub has to be either an integral transmembrane protein, a peripheral membrane protein or attached to the membrane, otherwise it can enter the nucleus and create a report without an interaction with the prey protein. The prey protein can be a soluble protein (A) as well as a membrane protein (B).

Figure 2 *P. falciparum* blood stage cDNA library generation. mRNA (A) was isolated from *P. falciparum* blood-stage total RNA and transcribed into ds cDNA (B) which was enriched for fragments > 500 bp by gel extraction (C). After ligation of the cDNA into the vector pPR3-N, 10 library plasmids were amplified and *Sfi*I digested to determine the size of their *P. falciparum* insert (D) by gel electrophoresis.

Figure 3 Analysis of the pPR3-N *P. falciparum* cDNA library quality. A: Screening PCRs with pPR3-N vector primers of 60 different library clones showed that all analyzed plasmids contained a DNA insert which has an average size of ~ 500 bp. B: To analyze if the generated library contained full-length genes it was used as a PCR template to amplify 13 different randomly selected parasite full-length genes. 10 of the 13 tested genes were successfully amplified (*) whereas 3 genes could not be amplified (*).

Figure 4 mbSUS functional assays with the two bait vectors pBT3-SUC-MAHRP1 and pBT3-STE-MAHRP1. A: Bait-bearing NMY51 yeast cells were transfected with either the empty library plasmid pPR3-N (negative control) or the positive control plasmid pOst1-NubI. Since pOst1-NubI contains a wild-type N-terminal ubiquitin (NubI)

with strong Cub-affinity a functional ubiquitin is reconstituted. Cleavage by ubiquitin-specific proteases enables the transcription factor (TF) to enter the nucleus (N) where it starts transcription of reporter genes (RG). pPR3-N contains a mutated Nub with reduced Cub-affinity which is not able to reconstitute a functional ubiquitin in absence of bait-prey binding. The transformed cells were spread on selective medium (SD-trp-leu / SD-trp-leu-his / SD-trp-leu-his-ade) and after incubation at 30°C for 4 days the number of colony forming units was determined (B). The number in brackets indicates the ratio of grown cells compared to distributed cells. C: To reduce the number of false positives in library screenings as much as possible, a pilot screen with pBT3-SUC-MAHRP1 bearing NMY51 yeast cells was performed. After transfection with the empty library vector pPR3-N the cells were plated on SD-trp-leu-his(-ade) medium containing different concentrations of 3-AT, a competitive inhibitor of the *HIS3* reporter. Shown is the number of clones grown under the respective conditions after 4 days. Since pPR3-N only contains a mutated N-terminal ubiquitin with no affinity for the C-terminal ubiquitin of the bait, all observed growth is background. D: mbSUS functional assay with pBT3-SUC-MAHRP1 bait bearing NMY51 yeast cells transfected with either the negative control pPR3-N or the positive control pOst1-NubI. Cells were spread on selective medium (SD-trp-leu-his-ade) containing 100 mM 3-AT and after incubation at 30°C for 4 days the number of colony forming units was determined.

Table 1 60 % of analyzed library plasmids contain a *P. falciparum* gene fragment.

After large-scale amplification of the generated blood-stage *P. falciparum* cDNA library, 20 library plasmids were sequenced to identify their insert. Of those 20, 12 plasmids contained a partial *P. falciparum* gene. On average the library plasmids contained about 13 % of the coding sequence of their respective genes and none of the vectors contained a full-length gene. While an untranslated region (UTR) was part of almost every insert, its length was quite small.

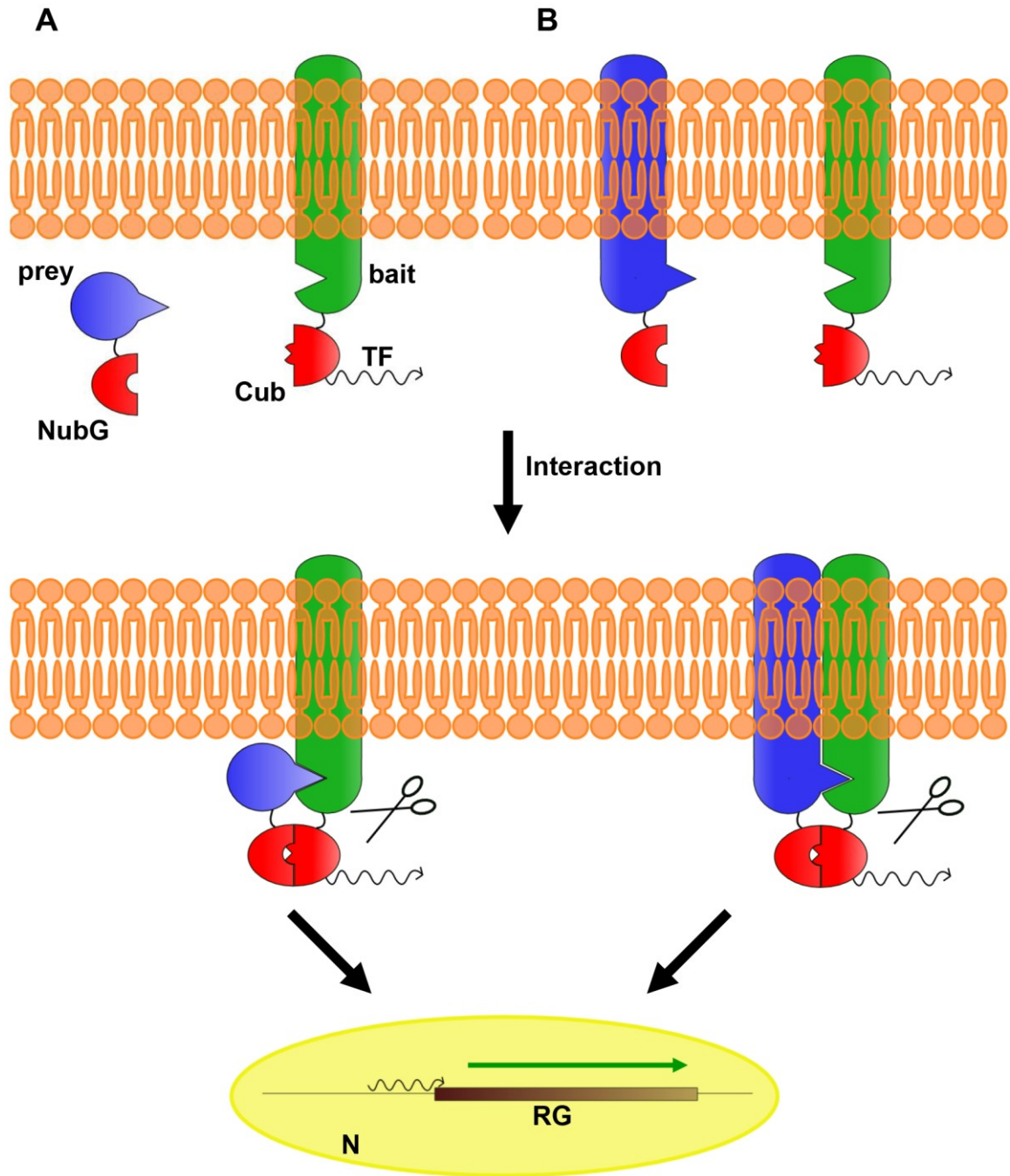


Figure 1

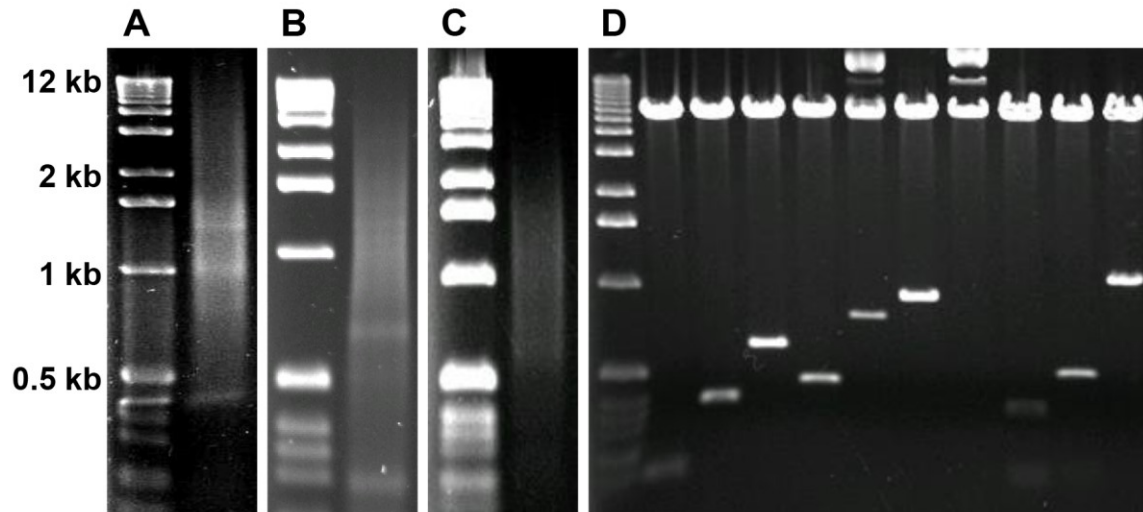


Figure 2

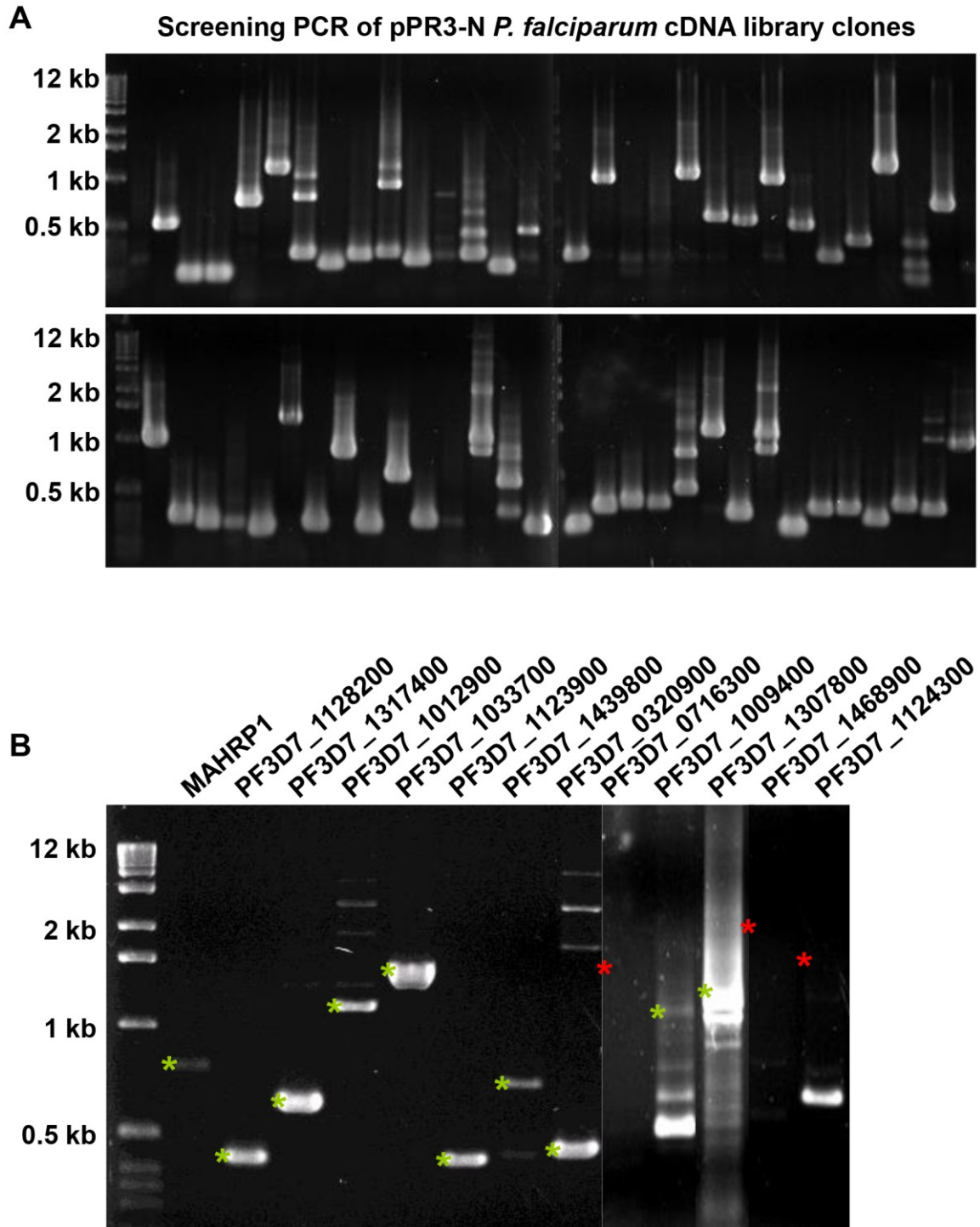


Figure 3

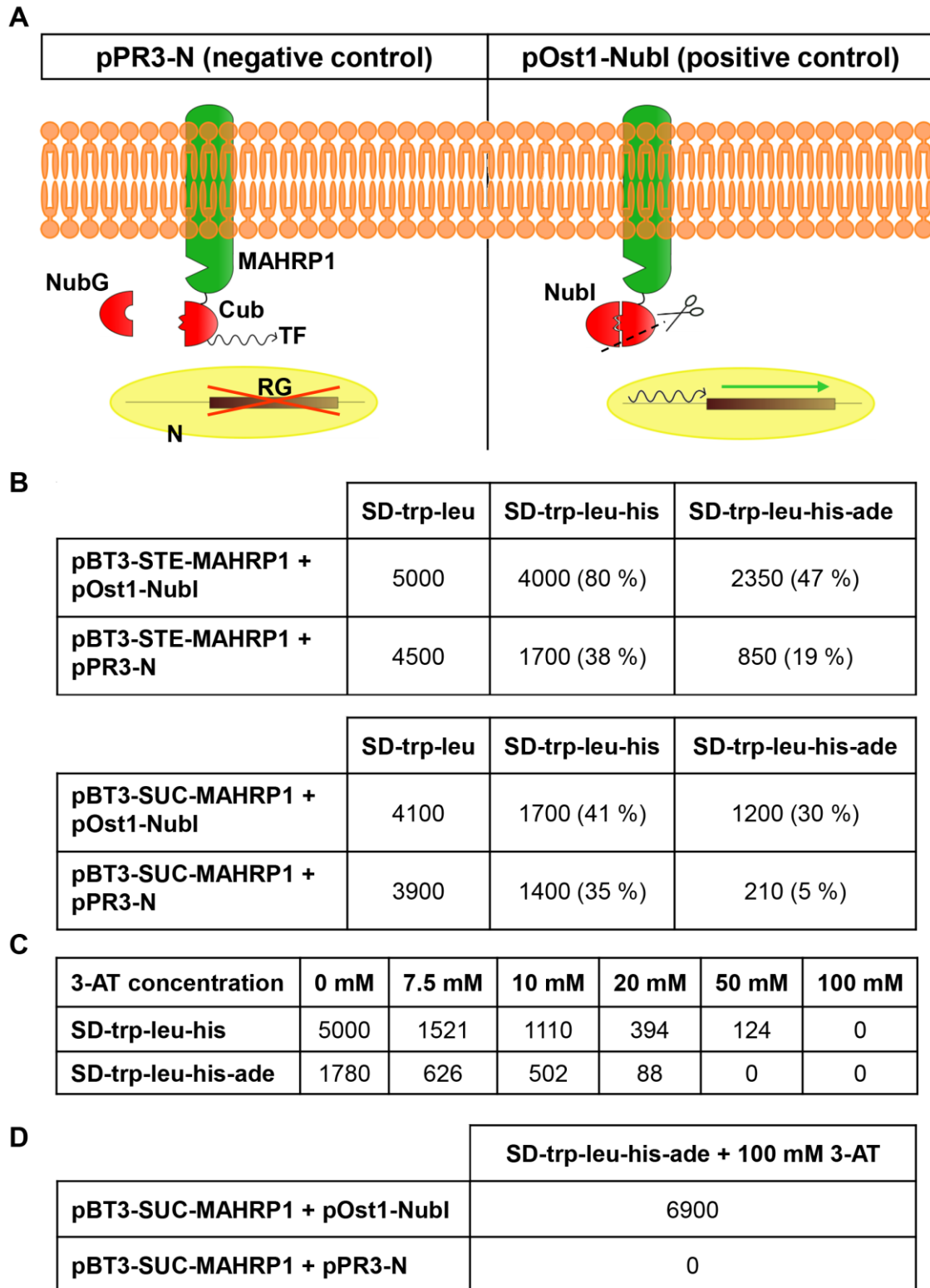


Figure 4

Gene	primer	Sequence	RS	vector	
CDS-3M adapter PlugOligo-3M PCR Primer M1		AAGCAGTGGTATCAACGCAGAGTGGCCGAGGCGGCC(T)20VN AAGCAGTGGTATCAACGCAGAGTGGCCATTACGGCCGGGGG-P AAGCAGTGGTATCAACGCAGAGT	SfiI SfiI		library generation
PF3D7_1033700	F R	CAGTGGATCCTGACCAATGATGCTTGAAG CAGTCCATGGATCTTTTTTTGAACTATCCTC	BamHI NcoI		library quality
PF3D7_1124300	F R	CAGTGGATCCAAAATATGGCTGATAATAACCTAG CAGTCCATGGGTAAAGAATCCTTTGATGAATCG	BamHI NcoI		
PF3D7_1128200	F R	CAGTGGATCCTTATCAATGGATCACCAAGATCTG CAGTCCATGGTTTTTTCTTGGGTGAAGGTAATTG	BamHI NcoI		
PF3D7_1317400	F R	CAGTGGATCCTTAATATGGCTAATACATGGAGATG CAGTCCATGGTGTTTTGTAATTAATTTTTTTTTGTAC	BamHI NcoI		
PF3D7_1468900	F R	CAGTGGATCCAAAAATGAGTCCCCTACTAATG CAGTCCATGGTGATCGTCATAGAAATTTTTGCTC	BamHI NcoI		
PF3D7_0716300	F R	GATCGGATCCTTATGATGAAGGTGTGGGG GATCCCATGGTGAAAATATTTCTTCATAATTTG	BamHI NcoI		
PF3D7_1009400	F R	GATCGGATCCTACTTATGGGTAGAAAGAAG GATCGCTAGCTTCACAATTTGTGTATG	BamHI NheI		
PF3D7_1123900	F R	GATCGGATCCAAAAATGTCCAATACATTAATTTT GATCCCATGGTATTAACATCTGTTCAATTAATC	BamHI NcoI		
PF3D7_1307800	F R	GATCGGATCCTTAAATGAACACCGAAGAAAAAATTAATAC GATCCCATGGATCAGCTTGGCAAGTATCG	BamHI NcoI		
PF3D7_1012900	F R	GATCGGATCCAAAATGGTATCATTAAGATTAG GATCCCATGGATAATCAAACCTGTGTGATG	BamHI NcoI		
PF3D7_0320900	F R	GATCGGATCCAAATGGAAGTTCCAGGAAAAG GATCCCATGGGTTTTTTTTTGGTTTTCTTTGAG	BamHI NcoI		
PF3D7_1439800	F R	CAGTCTTAAGATGAACTTTTAAGAGTAACAC CAGTATCGATCCAGTAACCCATATATTTTGTTA	AflII ClaI		
MAHRP1	F R	ATTAACAAGGCCATTACGGCCGCAGAGCAAGCAGCAGTACA AACTGATTGGCCGAGGCGGCCCCATTATCTTTTTTTCTTGTCTAATTT	SfiI SfiI		
MAHRP1	F F R	ATTAACAAGGCCATTACGGCCGCAGAGCAAGCAGCAGTACA ATTAACAAGGCCATTACGGCCAAAATGCGAGCAAGCAGCAGT AACTGATTGGCCGAGGCGGCCCCATTATCTTTTTTTCTTGTCTAATTT	SfiI SfiI SfiI	pBT3-SUC / -STE pBT3-C pBT3-C / -SUC / -STE	bait

Supplementary table 1. Primers used for library generation, quality testing and bait vector construction

Chapter 3

**Characterization of the potential MAHRP1 interaction
partners PIESP2 & PF3D7_0501000**

Introduction

With over 500 million new yearly infections which cause about 700'000 annual deaths, malaria still represents one of the world's most devastating human diseases (1). The most severe form of human malaria called malaria tropica is caused by the apicomplexan parasite *Plasmodium falciparum*. The symptoms of malaria tropica are strongly associated with the asexual development of the unicellular parasite within the human red blood cell. Erythrocytes are very specialized cells which are devoid of all internal organelles and any protein trafficking machinery in order to accommodate maximum space for haemoglobin. Survival and virulence of *P. falciparum* within RBCs therefore critically depend on extensive host cell refurbishments mediated by the export of parasite proteins into the erythrocyte cytosol. These include parasite derived membranous structures called Maurer's clefts (MC) which have an important role in protein export from the parasite to the erythrocyte membrane. They probably function as a form of a surrogate Golgi which concentrates virulence proteins for delivery to the RBC surface (2,3). One of these virulence proteins exported via MCs is the variable surface antigen *P. falciparum* erythrocyte membrane protein 1 (PfEMP1). After insertion into the host cell membrane it mediates adhesion of the infected RBC to various endothelial host receptors to evade elimination in the spleen (4–6). PfEMP1 mediated binding of iRBCs is also responsible for damages in various organs like the brain, liver and lungs because it hampers blood circulation and induces release of pro-inflammatory cytokines (7,8). Because of its pathological effects PfEMP1 is generally regarded as the major *P. falciparum* virulence factor and therefore of utmost interest.

While the process of PfEMP1 export is still not completely understood, it was shown to be dependent on the presence of the resident integral MC protein 'membrane associated histidine rich protein 1' (MAHRP1): in parasites in which the *mahrp1* gene is deleted PfEMP1 accumulates within the confines of the plasma membrane / PVM interface and is not presented at the RBC surface anymore. This suggests that MAHRP1 could be involved in transport of PfEMP1 in a complex (9). After erythrocyte invasion the 'PEXEL-negative exported protein' (PNEP) MAHRP1 is early expressed and exported into the RBC cytoplasm where it inserts into MC membranes. In addition to a single

central TM domain MAHRP1 contains a histidine rich C-terminal domain which in 3D7 has a histidine content of nearly 30 % and contains six tandem repeats of the amino acid sequence DHGH. Because MAHRP1 is predicted to be a type I TM protein this histidine rich domain faces the erythrocyte cytoplasm where it is believed to protect the MCs and their associated proteins from deleterious effects of ferriprotoporphyrin (FP) by enhancing its degradation to H₂O₂ (10). Knock-out of MAHRP1 not only was shown to have an effect on PfEMP1 transport, its absence further resulted in morphologically different MCs suggesting a role of MAHRP1 as a structural component. (9).

PfEMP1 is known to be the major virulence factor of *P. falciparum*. However, due to its variable nature it might not be suitable as a target for antimalarial interventions. Therefore single copy genes essential for PfEMP1 export like MAHRP1 come into focus. To bring new insight into the function of MAHRP1 and its role in PfEMP1 export we identified by co-immunoprecipitation (co-IP) two exported proteins, namely PF3D7_0501000 (PFE0050w) and ‘parasite-infected erythrocyte surface protein’ (PIESP2) (PF3D7_0501200 / PFE0060w) as potential MAHRP1 binding partners (Annette Gaida, unpublished). The aim of this study was to characterize PIESP2 and PF3D7_0501000 and to confirm their potential interaction with MAHRP1 by a mating-based split-ubiquitin system (mbSUS) pairwise interaction assay using the recently established MAHRP1 bait (chapter 2). This yeast based *in vitro* interaction platform for membrane proteins consists of a split ubiquitin whose moieties are only able to reconstitute a functional protein if brought into proximity via the interaction of the respective proteins that are fused to them (11). Upon bait and prey protein interaction the functional ubiquitin is cleaved off by specific proteases which releases a transcription factor (TF) from yeast membranes. The TF then diffuses to the nucleus and starts transcription of the selection markers *his3* and *ade2* whose activation enables the yeast to grow on defined minimal medium lacking histidine and / or adenine (12).

Methods

Generation of transfection constructs

Full-length PIESP2 / PF3D7_0501000 was PCR amplified using primers summarized in table S1 and cloned 5' to *gfp* into pARL1mGFPmT (13) via AflIII and ClaI / ApaI restriction sites.

P. falciparum transfection

Ring stage 3D7 *P. falciparum* infected erythrocytes (parasitemia ~ 10 %) were transfected with 100 µg plasmid DNA as described (14) and cultured in the presence of 2.5 mg/ml Blasticidin S. Drug resistant parasites were obtained approximately 4 weeks after transfection.

Fluorescence microscopy

Thin smears of parasite infected red blood cells were fixed on glass slides with methanol at -20°C for 2 min, air-dried and blocked with 3 % BSA in PBS. After incubation with mouse anti-GFP (Roche 1:500) and rabbit anti-MAHRP1 serum (1:500) (15) as primary antibodies, slides were washed and incubated with Alexa Fluor 594 (Invitrogen 1:200) conjugated goat anti-mouse and Alexa Fluor 488 (Invitrogen 1:200) conjugated goat anti-rabbit antibodies. After washing, Vectashield Hard Set (Vector Laboratories) containing DAPI was added and covered by a glass coverslip. Images were obtained using a Leica DM 5000B fluorescence microscope. Images were analysed using Photoshop software.

Triton X-114 solubility assay

0.5 ml RBCs infected with 3D7 parasites episomally expressing PIESP2-GFP / PF3D7_0501000-GFP were lysed on ice in 0.15 % saponin. The pellet was resuspended in 200 µl 1 % Triton X-114 in PBS containing protease inhibitors (Roche) and incubated

on ice for 30 min. After centrifugation at 3000 g for 15 min, the supernatant was collected, incubated at 30 °C for 5 min and centrifuged at 20'000 g for 1 min. The supernatant was removed as the aqueous phase and the pellet was washed and resuspended with PBS as detergent phase. Equal amounts of both phases were analyzed by Western blotting (16).

Western blot analysis

Protein samples were resuspended in Laemmli sample buffer, separated on a 12.5 % acrylamide gel and blotted to nitrocellulose (Hybond-C extra; GE Healthcare) using a Trans-Blot semi-dry electroblotter (Bio-Rad). The membrane was blocked in 10 % skim milk + 0.1 % Tween in Tris-buffer. As primary antibodies mouse anti-GFP (Roche 1:1000) or rabbit anti-MAHRP2 serum (1:2000) was used (15). The secondary antibodies used were horseradish peroxidase-conjugated goat anti-mouse (Pierce, 1:20 000) and goat anti-rabbit (Acris, 1:5000) IgG.

Yeast medium

NMY51 reporter strain (17) was cultured in Yeast Extract - Peptone - Dextrose plus Adenine medium (YPAD: 1 % yeast extract (Sigma), 2 % Bacto Peptone (BD), 210 µM adenine hemisulfate, 2 % glucose). NMY51 transfected with a bait vector was cultured in minimal medium lacking leucine (SD-leu: 38 mM ammonium sulphate, 0.17 % Difco yeast nitrogen base w/o amino acids and ammonium sulphate (BD), 115 µM L-arginine, 230 µM L-isoleucine, 164 µM L-lysine-HCl, 135 µM L-methionine, 300 µM L-phenylalanine, 1.68 mM L-threonine, 166 µM L-tyrosine, 178 µM L-uracil, 1.28 mM L-valine, 108.6 µM adenine hemisulfate, 129 µM L-histidine, 100µM L-tryptophan, 2 % glucose). NMY51 co-transfected with bait and prey vectors was cultured in minimal medium lacking leucine and tryptophan (SD-trp-leu: 38 mM ammonium sulphate, 0.17 % Difco yeast nitrogen base w/o amino acids and ammonium sulphate (BD), 115 µM L-arginine, 230 µM L-isoleucine, 164 µM L-lysine-HCl, 135 µM L-methionine, 300 µM L-phenylalanine, 1.68 mM L-threonine, 166 µM L-tyrosine, 178 µM L-uracil, 1.28 mM L-

valine, 108.6 μM adenine hemisulfate, 129 μM L-histidine, 2 % glucose). mbSUS functional assays and pairwise interaction assays were performed in minimal medium lacking leucine, tryptophan, histidine and adenine (SD-trp-leu-his-ade: 38 mM ammonium sulphate, 0.17 % Difco yeast nitrogen base w/o amino acids and ammonium sulphate (BD), 115 μM L-arginine, 230 μM L-isoleucine, 164 μM L-lysine-HCl, 135 μM L-methionine, 300 μM L-phenylalanine, 1.68 mM L-threonine, 166 μM L-tyrosine, 178 μM L-uracil, 1.28 mM L-valine, 2 % glucose, 100 mM 3-aminotriazole).

Bait vector construction

Full-length *mahrp1* was PCR amplified from cDNA using primers shown in table S1 and cloned into the bait vector pBT3-SUC (17) via SfiI restriction sites. To produce a read-out in the nucleus, the bait-Cub fusion protein must be present in the cytoplasm. Therefore the topology of the investigated protein has to be considered. Because MAHRP1 is a type 1 transmembrane protein, it was ligated into the plasmid vector 5' to the C-terminal half of ubiquitin (Cub) which itself is fused to a LexA-VP16 TF. This guarantees that the TF is exposed to the cytoplasm and able to diffuse into the yeast nucleus after ubiquitin-cleavage. pBT3-SUC contains the two selectable markers *kan^R* and *leu2* which allow selection of plasmid-bearing cells on medium containing kanamycin (bacteria) or lacking leucine (yeast). It further adds the *S. cerevisiae* signal sequence (SUC2) to the bait's N-terminus, which ensures proper insertion into yeast membranes.

Transformation of the bait vector into the NMY51 yeast reporter strain

A single colony from a 3 day old NMY51 streak was inoculated into 20 ml of liquid YPAD medium (in a 100 ml Erlenmeyer flask) and incubated o/n on a shaker at 275 rpm and 30°C. The titer of the culture was determined using a Neubauer chamber and 2.5×10^8 cells were added to 50 ml pre-warmed YPAD to give 5×10^6 cells / ml. Cells were incubated at 30°C and 275 rpm till the cell titer was 2×10^7 (~5 h). and subsequently centrifuged (3000 g, 5 min) and the supernatant removed. After washing in 25 ml ddH₂O

(3000 g, 5 min) cells were resuspended in 1 ml dd H₂O. Meanwhile the ss carrier DNA (2 mg / ml) was boiled at 95°C for 5 min and chilled on ice. The cell suspension was centrifuged (11'000 rpm, 30 sec), the supernatant discarded, and the pellet was resuspended in ddH₂O to a final volume of 1 ml and vortexed vigorously. 100 µl aliquots were distributed into new tubes, centrifuged (11'000 rpm, 30 sec) and the supernatant removed. 360 µl transformation mix (33 % PEG 3350, 100 mM LiOAc, 0.1 mg boiled ss carrier DNA, 2.5 µg bait vector) were added and resuspended by vigorously vortexing. After incubation at 42°C (water bath) for 40 min the cells were pelleted (11'000 rpm, 30 sec) and the supernatant removed. The cells were resuspended in 200 µl ddH₂O and 100 µl were spread on pre-warmed (30°C) SD-Leu Agar plates. Plates were sealed with parafilm and incubated at 30°C for 3-5 days.

Freezing of yeast strains (Glycerol stocks)

20 ml liquid yeast medium (depending on the strain either YPAD, SD-Leu or SD-Trp) were inoculated from a single colony from a 3 day old streak (in a 100 ml Erlenmeyer flask) and incubated o/n on a shaker at 275 rpm and 30°C. After centrifugation (2600 g, 5 min), the supernatant was removed and the pellet resuspended in 10 ml 2x YPAD containing 25 % Glycerol. 1 ml aliquots were distributed into screw cap cryotubes and frozen at -80°C.

Prey vector construction

Piesp2 / *pf3d7_0501000* fragments (Fig. 2A) were PCR amplified from cDNA using primers shown in table S1 and cloned into the prey vector pPR3-N (17) via *Sfi*I restriction sites. pPR3-N adds the coding sequence of an N-terminal split-ubiquitin (Nub) 5' to the prey's N-terminus and further contains the two resistance genes *amp^R* and *trp1* which allow selection by growth on medium containing ampicillin (bacteria) or lacking tryptophan (yeast).

mbSUS pairwise interaction assay

A single colony from a 3 day old NMY51 pBT3-SUC-MAHRP1 streak was inoculated into 20 ml of liquid YPAD medium (in a 100 ml Erlenmeyer flask) and incubated o/n on a shaker at 275 rpm and 30°C. The titer of the culture was determined and 2.5×10^8 cells were added to 50 ml pre-warmed YPAD to give 5×10^6 cells / ml. The cells were incubated at 30°C and 275 rpm till the cell titer was 2×10^7 . The cells then were centrifuged (3000 g, 5 min) and the supernatant removed. The pellet was washed in 25 ml ddH₂O (3000 g, 5 min) and resuspended in 1 ml dd H₂O. Meanwhile the ss carrier DNA (2 mg / ml) was boiled at 95°C for 5 min and chilled on ice. The cell suspension was centrifuged (11'000 rpm, 30 sec) and the supernatant discarded. The pellet was resuspended in ddH₂O to a final volume of 1 ml and vortexed vigorously. 200 µl aliquots were distributed into new tubes, centrifuged (11'000 rpm, 30 sec) and the supernatant removed. 360 µl transformation mix (33 % PEG 3350, 100 mM LiOAc, 0.2 mg boiled ss carrier DNA, 2.5 µg prey plasmid DNA) were added and resuspended by vigorously vortexing. After incubation at 42°C (water bath) for 40 min the cells were pelleted (11'000 rpm, 30 sec) and the supernatant removed. Each pellet was resuspended in 1 ml pre-warmed YPAD and incubated at 30°C for 90 min. After centrifugation (11'000 rpm, 30 sec) the supernatant was removed, each pellet resuspended in 180 µl ddH₂O (3 ml total) and 80 µl aliquots were spread on pre-warmed (30°C) SD-Trp-Leu-His-Ade Agar plates containing 100 mM 3-AT. Additionally a 1:1000 dilution of the transformation was plated on a SD-Trp-Leu plate to determine the transformation efficiency. Plates were sealed with parafilm and incubated at 30°C for 3 (SD-Trp-Leu) or 5 days (SD-Trp-Leu-His-Ade) before number of colony forming units was determined.

Results

PIESP2 and PF3D7_0501000 are exported proteins

PIESP2 and PF3D7_0501000 are both located on chromosome 5, separated by only one single gene which is a heat shock protein 40 (HSP40). PIESP2 with 408 amino acids (aa) is considerably larger than PF3D7_0501000 with 260 aa but otherwise both proteins share a number of similarities. They are mainly expressed during the early trophozoite stage, have a PEXEL/VTS motif and a two exon structure with no syntenic genes in other *Plasmodium* species and no annotated functional domains except the transmembrane domains (TMs).

Both proteins have a predicted TM at the N-terminus in PlasmoDB and PIESP2 has two additional TMs near the C-terminus (Fig. 1A). Further analysis with the TM domain prediction software TMHMM (18) showed a high probability of two additional TM domains at the C-terminus of PF3D7_0501000 (Fig. 1B).

Subcellular localization of PIESP2 and PF3D7_0501000

We generated 3D7 transfectants expressing PIESP2 / PF3D7_0501000 C-terminally fused to GFP under the control of the PfCRT5' promoter using the transfection vector pARL (13). When parasite-lysates were probed with antibodies against GFP, a protein of approximately 75 kDa and 50 kDa was observed in PIESP2-GFP or PF3D7_0501000-GFP transfectants, respectively, and no signal was detected in uninfected erythrocytes (not shown).

Subcellular localization of PIESP2-GFP and PF3D7_0501000-GFP was investigated by immunofluorescence assays (IFAs) and transfectants were co-labelled with antibodies against GFP and against MAHRP1 (10). Both, PIESP2-GFP and PF3D7_0501000-GFP co-localized to or close to the MCs with MAHRP1 (Fig. 1C).

Solubility of PIESP2 and PF3D7_0501000

Episomally transfected PIESP2-GFP and PF3D7_0501000-GFP parasites were saponin-lysed and used for a TritonX-114 solubility assay to isolate integral membrane proteins. The soluble and insoluble fractions were analyzed by Western blot using antibodies against GFP and MAHRP2, a PEXEL negative exported protein which behaves like a membrane associated protein despite the presence of a predicted TM domain (15). PIESP2 and PF3D7_0501000 were both detected in the insoluble membrane protein fraction but a substantial amount was also found in the soluble fraction. In contrast, as expected MAHRP2 was found mainly in the soluble protein fraction (Fig. 1D).

mbSUS pairwise interaction assay of MAHRP1 with PIESP2 and PF3D7_0501000

We investigated potential PIESP2 and PF3D7_0501000 binding to MAHRP1 using the mbSUS interaction screen in a pairwise manner. Therefore, we generated for each gene two different prey vectors, one included both predicted C-terminal TM domains whilst the other clone ended just before the TMs. Since PEXEL cleavage does not occur in yeast we generated both prey proteins to start with the cleaved PEXEL motif xE/D (Fig. 2A). After transformation of the prey vectors into the NMY51 reporter strain expressing the SUC-MAHRP1 bait described in chapter 2, cells were plated on SD-trp-leu-his-ade containing 100 mM 3-AT and grown for 6 days at 30°C. We also transfected both control plasmids pPR3-N (negative) and pOst1-NubI (positive) into the MAHRP1-bait strain. Any interaction between MAHRP1 and the two tested prey proteins would have maintained growth but neither PF3D7_0501000 nor PIESP2 could trigger growth of the reporter strain on selective medium (Fig. 2B). Hence, no interaction between MAHRP1 and any of the candidate clones could be confirmed.

Discussion

The MC-resident MAHRP1 was shown to be essential for the export of PfEMP1 to the erythrocyte membrane and is therefore of major interest. However, the specific function of MAHRP1 and its role in PfEMP1 export remain unclear. In an attempt to obtain new insight into the function of MAHRP1 we identified two exported proteins namely PF3D7_0501000 and PIESP2 as potential MAHRP1 binding partners by co-IP (Annette Gaida, unpublished). Both have predicted TM domains and were identified as possible erythrocyte surface proteins in a proteomic screen of tagged proteins (19).

Fluorescence microscopy showed that both candidates, PIESP2 and PF3D7_0501000 at least partially co-localize with MAHRP1 at the MCs. This PIESP2 location confirms a study by Viscensini and colleagues who identified PIESP2 in a proteomic analysis as a MC protein and also showed this by immunofluorescence microscopy (20). In the same study they also obtained peptides of PF3D7_0501000 but did not further study its localization. Besides the confirmed location of PF3D7_0501000 at the MCs we were not able to detect any erythrocyte surface localization of PIESP2 or PF3D7_0501000 as has been reported by Florens and colleagues (19). However, it can not be excluded that weak signals at the surface were overshadowed by the strong MC signal of PIESP2 and PF3D7_0501000.

Solubility assays further confirmed that both proteins were true transmembrane proteins which for PF3D7_0501000 is in contrast to the PlasmoDB annotation showing only a single TM that is cleaved off upon PEXEL cleavage. This solubility assay now confirms the TMHMM prediction of additional TM domains.

Using the mbSUS (Chapter 2) we pairwise tested whether PIESP2 or PF3D7_0501000 interacted with MAHRP1. Since the presence of two transmembrane domains potentially could generate difficulties to correctly insert the protein into the yeast membrane we tested two different prey clones for each protein, one clone including the two C-terminal TMs whilst the sequence of the other clone terminates before the TM domain. Neither of the two PIESP2 or two PF3D7_0501000 constructs could support growth, direct binding of MAHRP1 to either PIESP2 or PF3D7_0501000 could therefore not be confirmed. However, we cannot exclude that any of the three proteins might interact within a protein

complex but without direct binding. Since we were unable to prove that the prey proteins were correctly expressed it is possible that no interaction was detected because of the inability to express PIESP2 or PF3D7_0501000 correctly. The high AT content (80 %) of *P. falciparum* genes (21) might hinder protein expression in such heterologous systems (22). In addition, screening with the MAHRP1 bait requires very stringent screening conditions to eliminate false positive clones and it could be possible that the interaction of MAHRP1 with any of the tested proteins might be too weak to sustain these stringent conditions.

Although we were unable to confirm a direct binding of MAHRP1 to PIESP2 or PF3D7_0501000 we have shown that both proteins localize in a similar pattern and remain interesting candidates for further investigation of the interaction network of exported proteins.

References

1. World Health Organization. WHO | World Malaria Report 2012. 2009.
2. Przyborski JM, Wickert H, Krohne G, Lanzer M. Maurer's clefts--a novel secretory organelle? *Mol Biochem Parasitol*. 2003 Nov;132(1):17–26.
3. Bhattacharjee S, van Ooij C, Balu B, Adams JH, Haldar K. Maurer's clefts of *Plasmodium falciparum* are secretory organelles that concentrate virulence protein reporters for delivery to the host erythrocyte. *Blood*. 2008 Feb 15;111(4):2418–26.
4. Baruch DI, Gormely JA, Ma C, Howard RJ, Pasloske BL. *Plasmodium falciparum* erythrocyte membrane protein 1 is a parasitized erythrocyte receptor for adherence to CD36, thrombospondin, and intercellular adhesion molecule 1. *Proc Natl Acad Sci U S A*. 1996 Apr 16;93(8):3497–502.
5. Rowe JA, Moulds JM, Newbold CI, Miller LH. *P. falciparum* rosetting mediated by a parasite-variant erythrocyte membrane protein and complement-receptor 1. *Nature*. 1997 Jul 17;388(6639):292–5.
6. Reeder JC, Cowman AF, Davern KM, Beeson JG, Thompson JK, Rogerson SJ, et al. The adhesion of *Plasmodium falciparum*-infected erythrocytes to chondroitin sulfate A is mediated by *P. falciparum* erythrocyte membrane protein 1. *Proc Natl Acad Sci U S A*. 1999 Apr 27;96(9):5198–202.
7. MacPherson GG, Warrell MJ, White NJ, Looareesuwan S, Warrell DA. Human cerebral malaria. A quantitative ultrastructural analysis of parasitized erythrocyte sequestration. *Am J Pathol*. 1985 Jun;119(3):385–401.
8. Pongponratn E, Riganti M, Punpoowong B, Aikawa M. Microvascular sequestration of parasitized erythrocytes in human *falciparum* malaria: a pathological study. *Am J Trop Med Hyg*. 1991 Feb;44(2):168–75.
9. Spycher C, Rug M, Pachlatko E, Hanssen E, Ferguson D, Cowman AF, et al. The Maurer's cleft protein MAHRP1 is essential for trafficking of PfEMP1 to the surface of *Plasmodium falciparum*-infected erythrocytes. *Mol Microbiol*. 2008 Jun;68(5):1300–14.
10. Spycher C, Klonis N, Spielmann T, Kump E, Steiger S, Tilley L, et al. MAHRP-1, a novel *Plasmodium falciparum* histidine-rich protein, binds ferriprotoporphyrin IX and localizes to the Maurer's clefts. *J Biol Chem*. 2003 Sep 12;278(37):35373–83.
11. Johnsson N, Varshavsky A. Split ubiquitin as a sensor of protein interactions in vivo. *Proc Natl Acad Sci U S A*. 1994 Oct 25;91(22):10340–4.

12. Iyer K, Bürkle L, Auerbach D, Thaminy S, Dinkel M, Engels K, et al. Utilizing the split-ubiquitin membrane yeast two-hybrid system to identify protein-protein interactions of integral membrane proteins. *Sci STKE Signal Transduct Knowl Environ*. 2005 Mar 15;2005(275):pl3.
13. Crabb BS, Rug M, Gilberger T-W, Thompson JK, Triglia T, Maier AG, et al. Transfection of the human malaria parasite *Plasmodium falciparum*. *Methods Mol Biol Clifton NJ*. 2004;270:263–76.
14. Fidock DA, Wellems TE. Transformation with human dihydrofolate reductase renders malaria parasites insensitive to WR99210 but does not affect the intrinsic activity of proguanil. *Proc Natl Acad Sci U S A*. 1997 Sep 30;94(20):10931–6.
15. Pachlatko E, Rusch S, Müller A, Hemphill A, Tilley L, Hanssen E, et al. MAHRP2, an exported protein of *Plasmodium falciparum*, is an essential component of Maurer's cleft tethers. *Mol Microbiol*. 2010;77(5):1136–52.
16. Bordier C. Phase separation of integral membrane proteins in Triton X-114 solution. *J Biol Chem*. 1981 Feb 25;256(4):1604–7.
17. Dualsystems. DUALmembrane Protein Interaction Kits [Internet]. Available from: http://www.dualsystems.com/fileadmin/user_upload/z_download/manuals/DUAL_membrane-starter-kit_user-manual-A14.pdf
18. Krogh A, Larsson B, von Heijne G, Sonnhammer EL. Predicting transmembrane protein topology with a hidden Markov model: application to complete genomes. *J Mol Biol*. 2001 Jan 19;305(3):567–80.
19. Florens L, Liu X, Wang Y, Yang S, Schwartz O, Peglar M, et al. Proteomics approach reveals novel proteins on the surface of malaria-infected erythrocytes. *Mol Biochem Parasitol*. 2004 May;135(1):1–11.
20. Vincensini L, Richert S, Blisnick T, Dorselaer AV, Leize-Wagner E, Rabilloud T, et al. Proteomic Analysis Identifies Novel Proteins of the Maurer's Clefts, a Secretory Compartment Delivering *Plasmodium falciparum* Proteins to the Surface of Its Host Cell. *Mol Cell Proteomics*. 2005 Apr 1;4(4):582–93.
21. Gardner MJ, Hall N, Fung E, White O, Berriman M, Hyman RW, et al. Genome sequence of the human malaria parasite *Plasmodium falciparum*. *Nature*. 2002 Oct 3;419(6906):498–511.
22. Sibley CH, Brophy VH, Cheesman S, Hamilton KL, Hankins EG, Wooden JM, et al. Yeast as a model system to study drugs effective against apicomplexan proteins. *Methods San Diego Calif*. 1997 Oct;13(2):190–207.

Figure legends

Figure 1 PF3D7_0501000 and PIESP2 are exported membrane proteins. A: schematic representation of the PF3D7_0501000 and PIESP2 proteins. Both proteins have a predicted transmembrane domain (TM) at the N-terminus and only PIESP2 has two additional TM domains predicted near the C-terminus by PlasmoDB. B: Additional analysis also showed a high probability for two C-terminal TM domains in PF3D7_0501000. C: Immunofluorescence assays of MeOH-fixed RBCs infected with 3D7 episomally expressing PF3D7_0501000 or PIESP2 with a C-terminal GFP tag, co-labelled with mouse α -GFP and rabbit α -MAHRP1 antibodies. D: Parasite pellet of 3D7 episomally expressing PF3D7_0501000-GFP or PIESP2-GFP was generated by saponin lysis and partitioned into a soluble protein containing aqueous fraction (a) and a membrane protein fraction contained in the detergent pellet (d). Fractions were analyzed by immunoblot using mouse α -GFP and rabbit α -MAHRP2 antibodies.

Figure 2 mbSUS pairwise interaction assay of MAHRP1 with PF3D7_0501000 & PIESP2. A: Schematic depiction of PF3D7_0501000 and PIESP2 fragments ligated into the prey vector pPR3-N. B: These prey plasmids and the two controls pPR3-N (negative control) & pOST1-NubI (positive control) were transfected into the pBT3-SUC-MAHRP1 bearing yeast reporter NMY51. Transfected cells were spread onto selective medium (SD-trp-leu / SD-trp-leu-his-ade + 100 mM 3-AT) and after incubation for 6 days at 30°C the number of CFUs was determined (B).

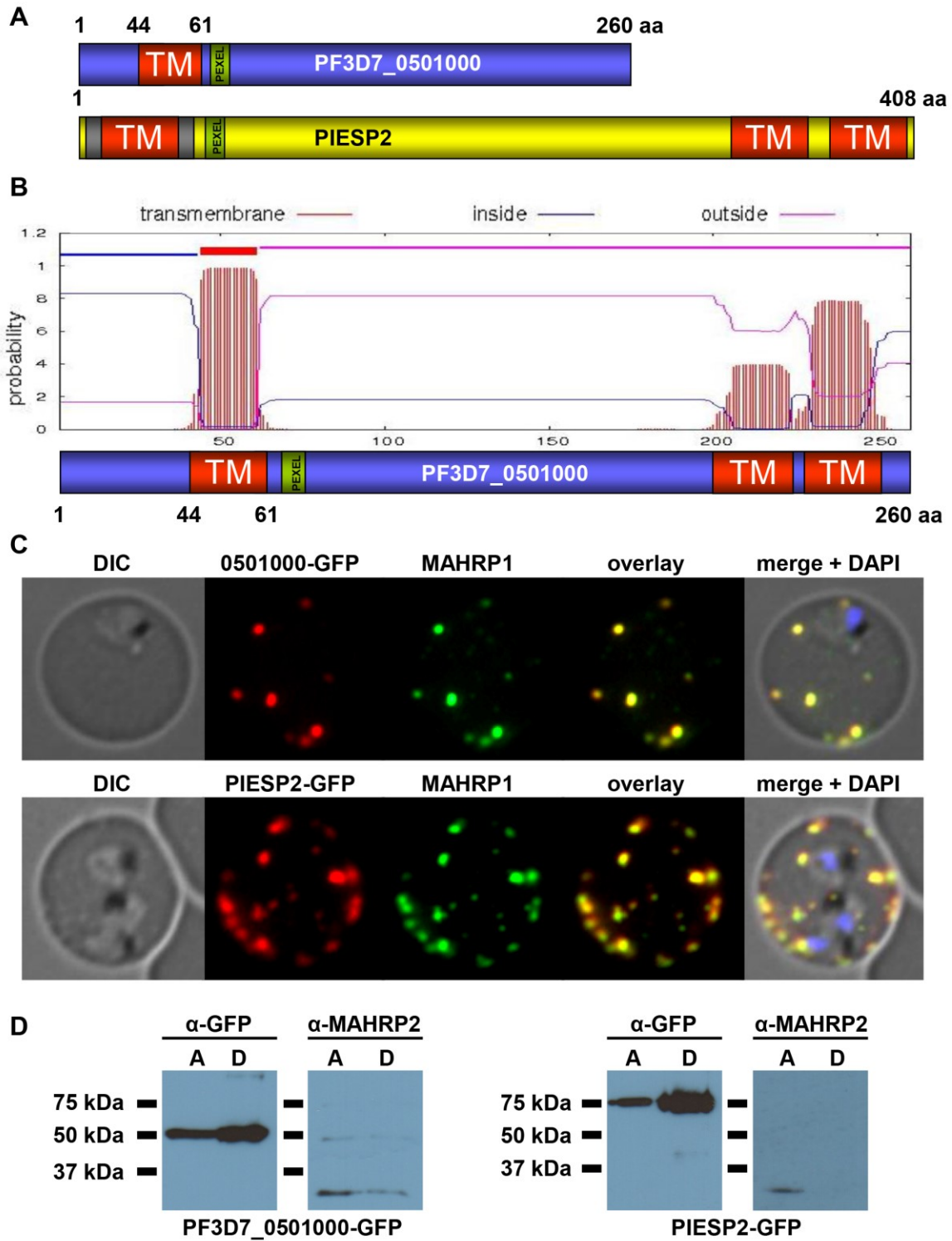
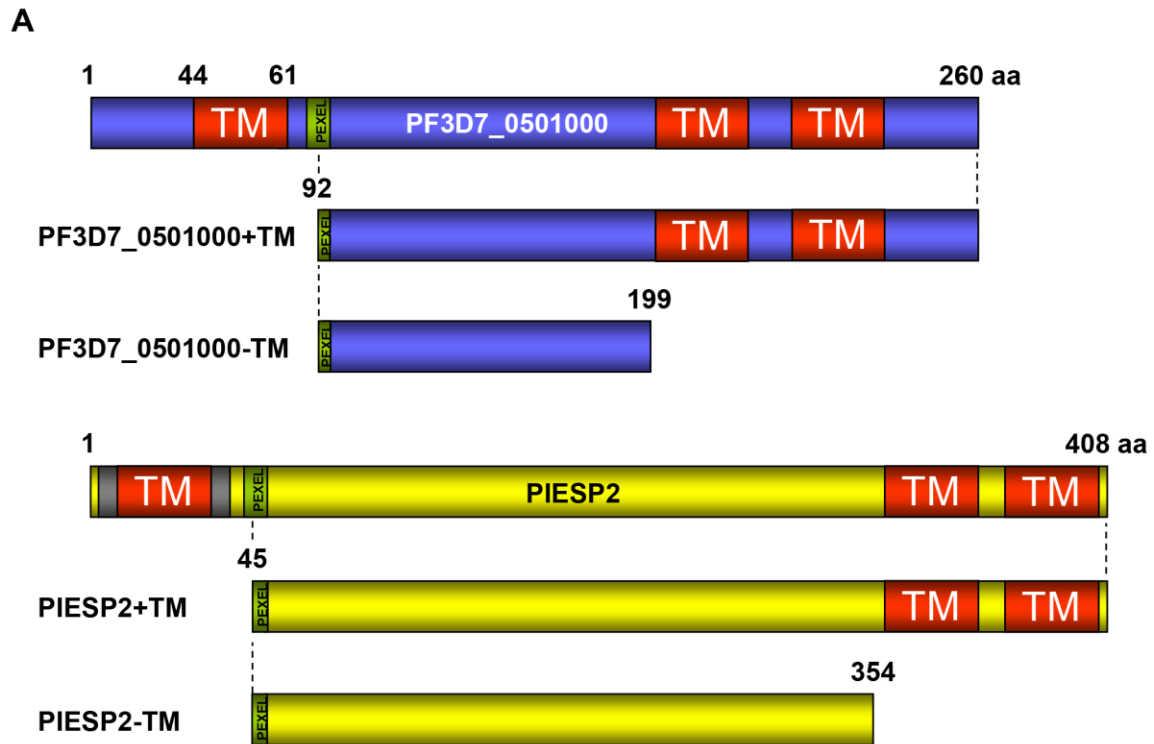


Figure 1



B

	SD-trp-leu-his-ade + 100 mM 3-AT (cfu)	SD-trp-leu (cfu)
pPR3-N	0	11'000
pOst1-Nubl	2300	9500
pPR3-N-PF3D7_0501000+TM	0	8000
pPR3-N-PF3D7_0501000-TM	0	10'000
pPR3-N-PIESP2+TM	0	10'000
pPR3-N-PIESP2-TM	0	8500

Figure 2

Gene	primer	Sequence	RS	vector	
<i>mahrp1</i>	F	ATTAACAAGGCCATTACGGCCGCAGAGCAAGCAGCAGTACA	SfiI	pBT3-SUC / -STE	bait
	F	ATTAACAAGGCCATTACGGCCAAAAATGGCAGAGCAAGCAGCAGT	SfiI	pBT3-C	
	R	AACTGATTGGCCGAGGCGGCCCCATTATCTTTTTTTCTTGTTCTAATTT	SfiI	pBT3-C / -SUC / -STE	
<i>piesp2</i>	F	ATTAACAAGGCCATTACGGCCGCAGATTTTAATGACATGTTTGC	SfiI	pPR3-N	prey
	R+TMs	AACTGATTGGCCGAGGCGGCCTTAAGTTAGTAATAAATTATGAAGAC	SfiI	pPR3-N	
	R-TMs	AACTGATTGGCCGAGGCGGCCTTAAAGTTTCATAACTTCATTAATATATTG	SfiI	pPR3-N	
<i>pf3d7_0501000</i>	F	ATTAACAAGGCCATTACGGCCGCAGAGCAAGAAGATCAATACA	SfiI	pPR3-N	
	R+TMs	AACTGATTGGCCGAGGCGGCCCTATTTATTTGATTCTTGTTTCGTTA	SfiI	pPR3-N	
	R-TMs	AACTGATTGGCCGAGGCGGCCTTAGTTAATTCTTTTTAACTACCAACA	SfiI	pPR3-N	
<i>piesp2</i>	F	ATTAACCTAAGATGTTACTCTTTTTTGCAAAAC	AflII	pARL1mGFPmT	transfection
	R	TAATTATCGATAGTTAGTAATAAATTATGAAGACC	Clal	pARL1mGFPmT	
<i>pf3d7_0501000</i>	F	ATTAACCTAAGATGATGAATAAAAAATCAATG	AflII	pARL1mGFPmT	
	R	TAATTGGGCCCTTTATTTGATTCTTGTTTCG	Apal	pARL1mGFPmT	

Supplementary table 1

Chapter 4

SEMP1: Characterization of a small exported *Plasmodium falciparum* membrane protein

Dietz O^{1,2} Rusch S^{1,2}, Brand F^{1,2}, Mundwiler E^{1,2}, Gaida A^{1,2,3}, Voss T^{1,2},
Beck HP^{1,2,§}

¹ Swiss Tropical and Public Health Institute, Basel, Switzerland

² University of Basel, Basel, Switzerland

³ CSL Behring, Bern, Switzerland

§ corresponding author

Manuscript for submission to Cellular Microbiology

Summary

Survival and virulence of the human malaria parasite *Plasmodium falciparum* during the blood stage of infection critically depend on extensive host cell refurbishments mediated through the export of numerous parasite proteins into the host cell. Parasite-derived membranous structures called Maurer's clefts (MC) presumably play an important role in protein trafficking from the parasite to the red blood cell membrane. However, their specific function has yet to be determined. We identified and characterized a new MC membrane protein, termed small exported membrane protein 1 (SEMP1). Upon invasion it is exported into the RBC cytosol where it inserts into the MCs before it is at least partly translocated to the RBC membrane. Using conventional and conditional loss-of-function approaches we found that SEMP1 is not essential for parasite survival, gametocytogenesis, or PfEMP1 export under culture conditions. Co-IP experiments identified several potential interaction partners, including REX1 and other membrane-associated proteins that were confirmed to co-localize with SEMP1 at the MCs. Transcriptome analysis further showed that expression of a number of exported parasite proteins was up-regulated in SEMP1-depleted parasites. By using Co-IP and transcriptome analysis for functional characterization of an exported parasite protein we provide a new starting point for further detailed dissection and characterisation of MC-associated protein complexes.

Introduction

The protozoan parasite *Plasmodium falciparum* is causing malaria tropica, the most severe form of human malaria responsible for nearly 700'000 annual deaths worldwide (1). Its pathology is associated with the asexual development of the unicellular parasite within the red blood cell (RBC). Because the human erythrocyte is a highly specialized cell which is devoid of all internal organelles, survival of *P. falciparum* critically depends on extensive host cell refurbishments mediated by the export of numerous parasite proteins into the erythrocyte cytoplasm. Some of these proteins like e.g. the major parasite virulence factor PfEMP1, insert into the host cell membrane where they mediate adhesion to endothelial receptors. Thereby the parasite not only prevents elimination of infected RBCs in the spleen, but as a side-effect also causes organ failure and cerebral malaria (2).

Although protein export is the basis of *P. falciparum* pathology, it is still not completely understood. It was shown that many virulence proteins are exported via parasite derived membranous structures in the RBC cytoplasm termed Maurer's clefts (MCs), which are believed to concentrate virulence proteins for delivery to the RBC membrane (3,4). However, while MCs were shown to play a major role in export of virulence proteins (3,4), their precise function remains elusive.

Many exported *P. falciparum* proteins contain a signal peptide (SP) and a PEXEL/VTS export motif (5,6). However, some of the best characterized MC proteins (MAHRP1, SBP1, REX1 & REX2) are PEXEL-negative exported proteins which do not contain a conserved export signal (7–10). While lacking a conserved export motif, these proteins share some similarities among each other: they are expressed early after invasion and mostly possess a transmembrane (TM) domain (MAHRP1, SBP, REX2). Some PEXEL-negative proteins (e.g. REX1, MAHRP2) were shown to be membrane-associated rather than integral membrane proteins but still possess a predicted hydrophobic domain.

In our studies to elucidate the function and composition of MCs, we identified and characterized a new MC-resident protein termed 'small exported membrane protein 1' (SEMP1: PF3D7_0702400 / PF07_0007). SEMP1 is a small PEXEL-negative protein

which is expressed early during blood stage infection and exported to the MCs before being partly translocated further to the RBC membrane where it is suggested to be involved in membrane modification.

Methods

Cell culture

The *P. falciparum* 3D7 strain was cultured *in vitro* at 5 % haematocrit as described (11) using RPMI medium containing 0.5 % Albumax (12). Parasites were synchronized with 5 % sorbitol as described (13).

Plasmid constructs

Full-length *semp1* was PCR amplified using primers 5'-CAGTCTTAAGATGAGTCA-ACCACAAAAACAAC-3' and 5'-CAGTATCGATTTTTGCGTTCTGTAAACTGGCT-3' and cloned 5' to *gfp* into pARL1mGFPmT (14) via AflIII and ClaI restriction sites. PIESP2 was also cloned into pARL1mGFPmT via AflIII and ClaI using primers 5'-ATTAECTTAAGATGTTACTCTTTTTTGCAAAAAC-3' and 5'-TAATTATCGATAGTTAGTAATAAATTATGAAGACC-3'. Truncated and mutated constructs for SEMP1 trafficking studies were generated similarly using primers summarized in table S1.

Primers 5'-GATCGGATCCTGAAAATGAGTCAACCACAAAAAC-3' and 5'-GATCCCATGGTTTTGCGTTCTGTAAACTG-3' were used to clone full-length SEMP1 5' to 3xHA into pBcam-3xHA (15) via BamHI and NcoI restriction sites. Similarly PF3D7_0601900 was cloned into pBcam-3xHA via AflIII and ClaI using primers 5'-CAGTCTTAAGATGACGGACCATTATTGGATTT-3' and 5'-CAGTATCGATATTTTCTGCATTGGCTGAAGCA-3' and PF3D7_0702500 via BamHI and NotI using primers 5'-ATATGGATCCATGGCTTATCCTCTTTTAGAAGATG-3' and 5'-ATATGCGGCCGCTACATGAGCTTCATTAGTGTTTAAAC-3'. To disrupt the SEMP1 gene in 3D7 parasites, a DNA flank of approximately 500 bp starting 78 bp upstream of the SEMP1 start codon was inserted into the transfection vector pH-KO via PstI and EcoRI restriction sites using primers 5'-CAGTCTGCAGCTATTTTCCCTTTAACAATCTTTTT-3' and 5'-CAGTGAATTCGACTTCATGAATTAATTATGCAATA-3'.

To fuse a FKBP destabilization domain (DD) to the C-terminus of the endogenous SEMP1 in 3D7 wild type parasites, an approximately 500 bp DNA flank of the 3' end of SEMP1 was cloned into the transfection vector pARL-DD via BglII and AvrII restriction sites using primers 5'- CAGTAGATCTCCCAAGAAAAGAAATTCAACCC-3' and 5'-CAGTCCTAGGTTTTGCGTTCTGTAAACTGGCT-3'.

***P. falciparum* transfection**

Ring stage 3D7 *P. falciparum* infected erythrocytes (parasitemia ~ 10 %) were transfected with 100 µg plasmid DNA as described (16) and cultured in the presence of either 10 nM WR99210 (pARL1mGFPmT / pH-KO / pARL-DD) or 2.5 mg/ml Blasticidin S (pBcam-3xHA). Drug resistant parasites were obtained approximately 4 weeks after transfection.

To select for integration of the SEMP1 flank into the parasite genome (pH-KO & pARL-DD) transfectants were cycled (3 weeks on / 3 weeks off drug) three times and tested for integration by Southern blot. After integration of the SEMP1 flank into the endogenous gene was observed, a single parasite was isolated by serial dilution.

Triton X-114 solubility assay

0.5 ml RBCs infected with 3D7 parasites episomally expressing SEMP1-3xHA were lysed on ice in 0.15 % saponin. The pellet was resuspended in 200 µl 1 % Triton X-114 in PBS containing protease inhibitors (Roche) and incubated on ice for 30 min. After centrifugation at 3000 g for 15 min, the supernatant was collected, incubated at 30 °C for 5 min and centrifuged at 20'000 g for 1 min. The supernatant was removed as the aqueous phase and the pellet was washed and resuspended with PBS to build the detergent phase. Equal amounts of both phases were analyzed by Western blotting (17).

Generation of SEMP1 mouse polyclonal antibodies

Codon-optimized (for expression in *E. coli*) full-length SEMP1 (Eurofins) was cloned 5' to a 6xHis-tag into the expression vector pSCherry2 (Eurogentec). The SEMP1-6xHis fusion protein was recombinantly expressed in *E. coli* using the CherryTMCodon kit (Eurogentec) and FPLC-purified with an anti-His column. Recombinant SEMP1 protein (0.2 mg/ml) in PBS was mixed with Sigma-Adjuvant-System (S6322, Sigma-Aldrich) according to the manufacturer's protocol. 3 mice (female, balb/c, 16 weeks, Harlan Laboratories) were immunized intra-peritoneally with a 200 µl dose, 3 mice were immunized subcutaneously with a 100 µl dose in each of two sites. All mice were boosted on day 21 and bled on day 31. Blood was collected in heparinised tubes and centrifuged for 10 min at 2000 g. The plasma fraction was removed and stored at -20°C until further use.

Fluorescence microscopy

Thin smears of parasite infected red blood cells were fixed on glass slides with methanol at -20°C for 2 min, air-dried and blocked with 3 % BSA in PBS. After incubation with primary antibodies mouse anti-SEMP1 serum (1:100), mouse anti-GFP (Roche 1:500), rabbit anti-GFP (Abcam 1:200), rat anti-HA (Roche 1:100), rabbit anti-MAHRP1 serum (1:500) (18), rabbit anti-REX1 (1:500) (19), mouse anti-SBP1 (1:200) (20), mouse anti-PfEMP1 (1:50) (21), mouse anti-Pf332 (1:200) (22) and mouse anti-KAHRP (1:500), slides were washed and incubated with Alexa Fluor 488 / 594 (Invitrogen 1:200) conjugated goat anti-mouse antibodies, Alexa Fluor 488 (Invitrogen 1:200) conjugated goat anti-rabbit antibodies or Alexa Fluor 568 (Invitrogen 1:200) conjugated goat anti-rat antibodies. After washing, Vectashield Hard Set (Vector Laboratories) containing DAPI was added and covered by a glass coverslip. Images were obtained using a Leica DM 5000B fluorescence microscope. Images were analysed using Photoshop software.

Alternatively, SEMP1-3xHA infected red blood cells were fixed in 4 % formaldehyde + 0.01 % glutaraldehyde in PBS. After washing in PBS the cells were permeabilized with 0.1 % Triton X-100 in PBS and then blocked with 3 % BSA in PBS. After incubation

with primary antibodies rat anti-HA (Roche 1:100) and rabbit anti-MAHRP1 serum (1:500), cells were washed with PBS and incubated with Alexa Fluor 568 (Invitrogen 1:200) conjugated goat anti-rat and Alexa Fluor 488 (Invitrogen 1:200) conjugated goat anti-rabbit antibodies. After washing cells were resuspended in PBS, mixed with 0.4 volumes Vectashield Hard Set (Vector Laboratories) containing DAPI and mounted on a glass slide with a cover slip. Images were obtained using a Zeiss confocal microscope LSM 700.

Electron microscopy

Immuno-electron microscopy of RBCs infected with 3D7 parasites episomally expressing SEMP1-GFP was performed according to Tokuyasu (23). Cells were chemically fixed in 0.1 M phosphate buffer containing 2 % paraformaldehyde and 0.2 % glutaraldehyde, embedded in gelatin and cryo-preserved in 2.3 M sucrose. Gelatin blocks were frozen in liquid nitrogen and sectioned at -120 °C using an ultramicrotome (UC7, Leica) to generate 70 – 80 nm sections. Immunolabelling was done in 1 % BSA in PBS with rabbit anti-GFP primary antibodies (Abcam, 1:40) and 5 nm immunogold-coupled Protein A (CMC Utrecht, 1:70). After immunolabelling, the sections were stained at 4°C in a 1:9 mixture of 4 % uranyl acetate and 2 % methylcellulose. Images were taken with a CM100 at 80 kV.

Western blot analysis

0.5 ml infected red blood cells were lysed on ice in 0.15 % saponin in PBS. The resulting parasite pellet was resuspended in Laemmli sample buffer, separated on a 12.5 % acrylamide gel or a NuPAGE 4–12 % Bis-Tris gel (Novex) and blotted to nitrocellulose (Hybond-C extra; GE Healthcare) using a Trans-Blot semi-dry electroblotter (Bio-Rad). The membrane was blocked in 10 % skim milk + 0.1 % Tween in Tris-buffer. The used primary antibodies were mouse anti-SEMP1 serum (1:1000), mouse anti-HA (Roche 1:5000), mouse anti-GAPDH (1:20'000) (24), mouse anti-GFP (Roche 1:1000) or rabbit anti-MAHRP2 serum (1:2000) (18). The used secondary antibodies were horseradish

peroxidase-conjugated goat anti-mouse (Pierce, 1:20 000) and goat anti-rabbit (Acris, 1:5000) IgG.

Southern blot analysis

Genomic DNA was isolated by phenol/chloroform extraction of saponin lysed parasites as described (25). DNA was digested with either *Cla*I & *Xma*I (SEMP1-KO) or *Eco*RI (SEMP1-DD) restriction enzymes, separated on a 0.8 % agarose gel and transferred onto a Amersham Hybond-N⁺ membrane (GE Healthcare). Blots were probed with ³²P-dATP-labelled *hdhfr* PCR fragments.

Co-Immunoprecipitation

240 ml culture (5 % hematocrit ,8 % parasitemia) of 3D7 parasites episomally expressing SEMP1-3xHA was cross-linked in 1 % formaldehyde at 37°C. Reaction was stopped after 10 min by addition of 0.125 M glycine and transfer on ice. Cells were pelleted at 700 g for 5 min, washed in ice cold PBS and red blood cells lysed on ice in 0.15 % saponin. After additional washing in PBS the pellet was resuspended in 1.5 ml sonication buffer (50 mM Tris-HCl pH 8.0, 10 mM EDTA, 1 % SDS) containing complete protease inhibitor cocktail and sonicated with a Bioruptor UCD-300 for 10 min (30 sec on / 30 sec off). After centrifugation at 20'000 g for 10 min the supernatant was collected. 650 µl supernatant was mixed with 650 µl 2x binding buffer (50 mM Tris-HCl pH 7.4, 300 mM NaCl, 2 % NP40) and for the negative control additionally 150 µg HA peptide (Sigma) was added. Samples were mixed with 150 µl α-HA affinity matrix (Roche) and incubated at 4°C for 16 h at 25 rpm. The beads were pelleted at 300 g for 1 min and the supernatant removed and collected (supernatant). After washing for 4 x 5 min with 1 ml washing buffer (50 mM Tris-HCl pH 7.4, 150 mM NaCl, 1 mM EDTA, 1 % NP40) the final supernatant was collected (wash) and the beads mixed with 40 µl elution buffer (1x binding buffer containing 0.5 mg / ml HA peptide and protease inhibitors). After incubation at 25 rpm for 2 h the beads were pelleted at 300 g for 1 min and the supernatant collected (elution). The protein content of the elution was subsequently

analyzed by mass-spectrometry from either TCA precipitated pellets or from extracted gel bands after separation on a NuPage 4-12 % Bis-Tris gel (Novex) and Coomassie staining.

Comparative transcriptome analysis by microarray

After Sorbitol-synchronization to an 8 h window, a culture of SEMP1-DD parasites was split and cultured in the presence or absence of Shield. At four specific time points (6-14 hpi, 16-24 hpi, 26-34 hpi & 36-44 hpi) parasite RNA was isolated from 30 ml culture (5 % hematocrit, 5 % parasitemia) using RiboZol RNA extraction reagent (Amresco). RNA was transcribed into cRNA and Cyanine 5-labelled by incorporation of Cy5-CTP using the Quick Amp labelling kit (Agilent). 450 ng Cy5-labelled SEMP1-DD cRNA containing 5 pmol dye were mixed with an equal amount of Cy3-labelled 3D7 reference cRNA generated from mixed stages (equal amounts of ring-, trophozoite- and schizont-stage RNA) and hybridized onto an Agilent *P. falciparum* microarray (AMADID #037237) as described (26). After washing, the slide was air-dried and scanned using a GenePix 4000B microarray scanner and GenePix Pro 7 software. Lowess normalization and background elimination was performed using Acuity 4.0 software (Molecular Devices). SEMP1-dependent transcriptional changes were identified by either Significance Analysis of Microarrays (SAM) (27) or by Student's t-test. Heatmap of candidate genes was generated using Cluster and TreeView software (28).

CD36 binding assay

Recombinant human CD36 (125 µg/ml in PBS) or 1% BSA in PBS (control) was immobilized on a Petri dish as described (29). After incubation in a humid chamber overnight at 4°C, unspecific binding was blocked with 1% BSA in PBS for 30 min at room temperature and washed with RPMI-Hepes. Infected erythrocytes in RPMI-Hepes and 10% serum (5% hematocrit) were added and incubated for 30 min at 37°C. After gentle washing with RPMI-Hepes, bound cells were fixed with 2% glutaraldehyde in RPMI-Hepes for 2 h and stained with 10% Giemsa for 10 min. Bound infected RBCs were

quantified in 8 or 10 different 0.2 mm² areas. The mean value was calculated as infected RBCs per mm² and normalized to a parasitemia of 1%. The experiment was performed three times.

Induction of gametocytogenesis

A 10 ml SEMP1-KO parasite culture (5 % hematocrit, 6 % parasitemia) was sorbitol-synchronized and cultured for 24 h in 20 ml RPMI medium containing 1 % Albumax. After dilution to a parasitemia of ~ 2 % trophozoites, to prevent overgrowth, the committed parasites were cultured in 10 ml normal RPMI medium (0.5 % Albumax) for additional 24 h. Then parasites were cultured for 4 days in 10 ml medium containing 50 mM N-Acetylglucosamine (GlcNac) (replaced daily).

Results

Subcellular localization of SEMP1

SEMP1 (PF3D7_0702400) is located on chromosome 7, contains one intron and encodes a protein of 123 amino acids (aa). This small, early expressed 'Plasmodium protein with unknown function' (PlasmoDB) has no PEXEL motif, no classical signal peptide but a single predicted transmembrane domain (TM) from aa 76 to 98 (Fig. 1A). Like many other PEXEL-negative exported proteins, no syntenic genes in other *Plasmodium* species exist but weak homologies to hypothetical proteins in *P. vixax*, *P. cynomolgi*, and *P. knowlesi* can be found.

We generated 3D7 transfectants expressing SEMP1 with a C-terminal green fluorescent protein (GFP) under the control of the PfCRT5' promoter using the transfection vector pARL (14). Additionally, we also used a parasite line expressing SEMP1 C-terminally fused to a triple Hemagglutinin tag (3xHA) (30). When parasite-lysates were probed with antibodies against 3xHA or GFP, a protein of approximately 20 kDa and 40 kDa in size was observed in SEMP1-3xHA and SEMP1-GFP transfectants (Fig 1B), respectively, and no signal was detected in uninfected erythrocytes.

Live cell imaging of the SEMP1-GFP transfectants showed that the GFP-tagged protein was exported (Fig. 1C). There was also significant fluorescence observed within the parasite which might be due to protein overexpression. We further investigated the subcellular localization of SEMP1-3xHA by IFA using co-labelling with antibodies against the HA-tag and with either antibodies against MAHRP1 (31), REX1 (7) or KAHRP (32). SEMP1-3xHA colocalized with MAHRP1 and REX1 to the MCs (Fig. 1D + 1E). This confirms a study by Heiber and colleagues, which bioinformatically identified new PEXEL-negative proteins and also localized GFP-tagged SEMP1 to the MCs in ring stages and trophozoites (33). Electron microscopy using antibodies against GFP confirmed the localization of SEMP1-GFP at the MCs (Fig 1F). Interestingly, we found that SEMP1-3xHA is further transported to the RBC membrane and partially localizes with KAHRP in later stages (Fig. 2A).

The solubility of SEMP1 was determined in Triton X114-solubility assays where it was detected in the membrane protein fraction as an integral membrane protein but a substantial amount was also found in the soluble fraction. In contrast, MAHRP2, a PEXEL-negative protein shown to be membrane-associated (18), was found exclusively in the soluble protein fraction confirming that the membrane fraction was not contaminated with soluble proteins (Fig. 2B).

To also analyse SEMP1 in wild type parasites, we generated affinity purified mouse antibodies raised against recombinant full-length SEMP1 protein. These antibodies recognized a protein of expected 15 kDa in 3D7 parasite lysates but not in uninfected erythrocytes (Fig. 3A). Double-labeling IFAs of sorbitol-synchronized parasites at 6-14 hours post invasion (hpi), 16–24 hpi, 26–34 hpi and 36–44 hpi showed that SEMP1, similarly to MAHRP1, is exported early after invasion to MCs where it partially co-localizes with MAHRP1 (Fig 3B). In younger stages SEMP1 is not found at all MCs whereas in later stages it is transported further to the RBC membrane. Western blots with parasite lysates taken at corresponding timepoints showed that endogenous SEMP1 is constantly expressed throughout the asexual intra-erythrocytic cycle (Fig 3C).

Requirements for export of SEMP1

To elucidate sequence requirements for SEMP1 export SEMP1-KO parasites (see below) were complemented with transfection constructs expressing full-length, truncated, or mutated versions of SEMP1 with a C-terminal GFP-tag (Fig. 4A). SEMP1-KO parasites were used to avoid interference with the endogenous protein. IFAs to localize these fusion proteins showed that deletion of the complete C-terminus of SEMP1 (SEMP1₁₋₉₇-GFP) did not impair export and resulted in correct localisation whilst deletion of the first 16 amino acids (SEMP1₁₇₋₁₂₃-GFP) of the N-terminus resulted in an impaired export from the parasite. The deletion of 71 amino acids (SEMP1₇₂₋₁₂₃-GFP) of the N-terminus prevented export and resulted in the concentration of SEMP1 in or at the endoplasmic reticulum (Fig. 8B). If the first 16 amino acids of SEMP1 were replaced by the corresponding amino acids of MAHRP2 (M2₁₋₁₆SEMP1₁₇₋₁₂₃-GFP) or the classical signal peptide of MSP1 (MSP1₁₋₁₆SEMP1₁₇₋₁₂₃-GFP) the fusion protein was exported in both

cases albeit with lower efficiency as indicated by the high amount of labelled protein within the parasite confines (Fig. 4B).

Identification of potential SEMP1 interaction partners by Co-IP

In order to reveal proteins interacting with SEMP1 we performed co-immunoprecipitation (Co-IP) experiments followed by mass spectrometry-based protein identification. Protein extracts from formaldehyde-crosslinked trophozoite stage parasites expressing SEMP1-3xHA were incubated with anti-HA affinity matrix. Subsequently, bound SEMP1-3xHA and potential interacting proteins were eluted by competition with soluble HA peptides. As a negative control, an excess of HA peptides was added to the protein extracts during the binding step to prevent binding of SEMP1-3xHA to the affinity matrix. Western blot analysis confirmed that SEMP1-3xHA was successfully purified and eluted (Fig. 5A), and silver staining revealed that additional proteins were co-eluted with SEMP1-3xHA (Fig. 5B). Table 1 summarizes the identified parasite proteins for which ≥ 5 peptides were detected in LC-MS/MS analysis of either TCA precipitated elutions or from Coomassie-stained SDS-PAGE gel slices.

To confirm potential interacting partners 3D7 parasites were transfected with constructs to express candidate proteins with either a C-terminal 3xHA tag (PF3D7_0702500 / PF3D7_0601900), or with a GFP tag (PIESP2).

We determined the subcellular localization of these potential interaction partners by IFAs using mouse anti-SEMP1 antibodies combined with either rat anti-HA antibody for PF3D7_0702500-3xHA and PF3D7_0601900-3xHA or rabbit anti-GFP antibody for PIESP2-GFP. For Pf332 we used mouse anti-Pf332 antibody and rat anti-HA antibody in parasites expressing SEMP1_3xHA. REX1 co-localization was determined using rabbit anti-REX1 antibodies and mouse anti-SEMP1 antibodies. All potential interaction partners co-localized at least partially with SEMP1, but in particular with Pf332 or PIESP2 antibodies only a fraction of SEMP1 positive MCs were labelled with either antibody suggesting that distinct subpopulations of MCs exist (Fig. 6).

Knockout of SEMP1

To investigate the function of SEMP1, the gene was knocked out in 3D7 wild type parasites by single crossover gene disruption. Integration of the human dihydrofolate reductase (*hdhfr*) cassette-containing plasmid pH-SEMP1-KO into the correct location of the parasite genome was confirmed by Southern blot (Fig. 7A) and a parasite clone was isolated by serial dilution. Western blot analysis using polyclonal antibodies against SEMP1 showed that the gene disruption was successful and SEMP1 was absent (Fig 7B). SEMP1-KO parasites were viable in absence of SEMP1 and also showed no adverse growth effects in culture.

In order to test if transport of other proteins was disturbed we analyzed the SEMP1-KO parasite clone by IFA using antibodies against MAHRP1, SBP1, REX1 and PfEMP1. All four tested proteins were still exported in absence of SEMP1 (Fig. 7C). We further tested whether PfEMP1 was correctly exposed on the erythrocyte surface of KO parasites by testing binding of iRBCs to CD36 under static conditions but no differences were observed when compared to the parental parasites (Fig. 7D). Lastly, we tested whether gametocytogenesis could be induced in the SEMP1-KO strain and after five days type II gametocytes appeared and fully matured to stage V gametocytes similarly as in the wild type (Fig. 7E).

To have the ability to investigate the SEMP1 function under controlled conditions and between isogenic populations we also generated a conditional SEMP1 knockdown parasite in 3D7 by fusing a FKBP destabilization domain (DD) to the C-terminus of the endogenous SEMP1. DD confers instability to the fusion protein resulting in its targeted degradation if not stabilised by the small molecule Shield-1 (34,35). Integration of the DD and *hdhfr* cassette-containing plasmid pARL-SEMP1-DD at the correct locus was confirmed by Southern blot (Fig. 8A). Western blot analysis of synchronized SEMP1-DD parasites grown for 2 weeks with or without Shield showed significantly reduced amounts SEMP1 and only minute amounts of protein could be detected (Fig. 8B).

Transcriptional changes in absence of SEMP1

To test if parasites responded to SEMP1 depletion with possible compensatory changes in gene expression we conducted comparative transcriptional profiling using genome-wide microarray technology. Parasite RNA was isolated at four specific time points (6-14 hpi, 16-24 hpi, 26-34 hpi & 36-44 hpi) from synchronized SEMP1-DD parasites cultured with and without Shield. The Cy5-labelled SEMP1-DD cRNA was mixed with an equal amount of Cy3-labelled 3D7 reference cRNA (mixed stages) and hybridized onto an Agilent *P. falciparum* Microarray slide (AMADID #037237) containing oligonucleotides for all *P. falciparum* genes (26). We did not detect any significant transcriptional changes in SEMP1-depleted parasites using Significance Analysis for Microarrays (27). However, using the less stringent Student's t-test, a total of 34 genes were significantly ($p < 0.05$) up-regulated over either two, three or four consecutive time points with a relative average fold change (RAFC) > 1.5 . Down-regulation was observed for twelve parasite genes with a RAFC < 1.5 ($p < 0.05$). The highest fold change of 2.18 was seen for a *var* gene (PF3D7_0900100) between 6 & 14 hours post invasion (hpi). The most highly down-regulated gene codes for a conserved protein with unknown function (PF3D7_1475200) with a 2-fold change between 6 & 14 hpi (Table 2).

A total ten of the up-regulated genes, including the four most highly up-regulated genes, encode known exported proteins (Table 2), namely PfEMP1, HYP12, PHISTb and PfEMP3. In contrast, only one of the twelve down-regulated genes codes for a predicted exported protein with unknown function (PF3D7_0113400). Figure 9 shows that up-regulation of the exported proteins did mostly not peak after invasion but during the trophozoite and schizont stage.

Strikingly, two of the ten up-regulated exported proteins were also identified as potential interaction partners of SEMP1: HSP70-x (PF3D7_0831700) and a protein with unknown function (PF3D7_1353100). Although all other proteins identified as potential SEMP1 interaction partners did not have a RAFC > 1.5 , four of them were still significantly ($p < 0.05$) up-regulated: REX1 (RAFC = 1.20), PF3D7_0702500 (RAFC = 1.33), PF3D7_0601900 (RAFC = 1.35) and GBP (RAFC = 1.44).

Discussion

MCs have a crucial role in protein trafficking to the iRBC membrane and there is evidence that they act as secretory organelles concentrating virulence proteins destined for the host cell membrane (3,4), but further functions have yet to be determined. Similarly, the protein composition of MCs is not well established and there are steadily new proteins revealed, which are either resident or transiently located to the MCs indicating that the current MC proteome is far from complete. Since many of the MC proteins lack a signal peptide (SP) and a PEXEL/VTS motif it is impossible to virtually establish a comprehensive MC proteome.

Here we report the identification and characterization of a new MC protein that we termed SEMP1. It is a small protein with unknown function, has neither a PEXEL-motif nor a SP (PlasmoDB) and the SMART protein domain prediction tool (36) identified a single transmembrane (TM) domain from amino acid 76 to 98 (Fig. 1A). Similar to the MC resident proteins MAHRP1 and SBP1, it is expressed early and exported to the MCs where it integrates into the MC membrane. However, unlike MAHRP1 or SBP1, which persist as integral MC membrane proteins throughout the whole intraerythrocytic cycle (20,31), SEMP1 is translocated further to the RBC membrane in schizonts (Fig. 3B).

Although a number of MC proteins have been identified and extensively studied, surprisingly little is known about their function. Analysis of REX1 null mutants showed that *PfEMP1* is exported to the MCs but not efficiently presented at the RBC surface (37) whilst in MAHRP1 or SBP1 knock-out parasites *PfEMP1* was not translocated to the RBC surface but was retained within the parasite confines or in the MCs (8,21,38). To study the role of SEMP1 in protein export we deleted the protein in two ways. First, we generated a SEMP1 knock-out parasite by single crossover gene disruption and secondly we generated a conditional SEMP1 knock down parasite by fusing the FKBP destabilization domain (DD) to the C-terminus of endogenous SEMP1. In neither parasite line we observed any obvious phenotypic change under *in vitro* culture conditions. All tested proteins (REX1, SBP1, MAHRP1, and *PfEMP1*) were trafficked to their correct destinations in SEMP1-KO parasites, there was no growth reduction, and gametocyte

production was similar to wild type parasites. This suggests that SEMP1 is neither essentially involved in *PfEMP1* export nor in gametocytogenesis. This indicates redundancy of functional pathways in which other proteins might compensate for the loss of SEMP1, and that SEMP1 may have other functions during the intraerythrocytic cycle which escaped our observation such as fitness in natural human infections.

To further elucidate its role we were interested in potential interaction partners of SEMP1. Using Co-IP 13 different *P. falciparum* proteins were identified in two independent experiments. Three proteins were identified in both experiments and hence were priority candidates, namely REX1, PF3D7_0702500, and PF3D7_0601900. While REX1 is a known MC resident protein, both other proteins were uncharacterized so far. Both, PF3D7_0702500 and PF3D7_0601900 have similarities to *semp1* in that they have one intron, are non-syntenic to other *Plasmodium* species and code for small parasite proteins with unknown function (PlasmoDB). They also have a predicted single TM domain and no PEXEL/VTS motif or signal peptide. Their localization to the MCs was recently confirmed by a study that used a bioinformatics approach to identify new PEXEL-negative exported proteins (33), yet we cannot conclude that these proteins are true interaction partners since there is no functional prediction. However, since parasite proteins were extracted with 1 % sodium dodecyl sulphate (SDS), a detergent that breaks down membranes by emulsifying the lipids and proteins, it is conceivable these MC transmembrane proteins were co-precipitated as constituents of the same complex and not just as constituents of the same membrane fragment. None of the other identified exported proteins has been shown to be resident in the MCs. PfHsp70-x is an exported chaperone which in a complex with co-chaperones forms highly mobile structures in the RBC cytosol called J-dots (39,40). MAHRP2 has been described as a PEXEL-negative protein forming cylindrical structures called tethers which are believed to tether the MCs to the erythrocyte skeleton (18). Pf332 is a large *P. falciparum* protein exported into the RBC (41) where it is, similar to SEMP1, closely associated with the MCs (42,43) but also partly with the RBC membrane (43–45). The parasite-infected erythrocyte surface protein 2 (PIESP2) has been identified as a TM protein in the MCs (46) but it also may partly be associated with the RBC membrane (47).

Our study represents one of the first using Co-IP and MS/MS to identify interaction partners of exported *P. falciparum* proteins. While the detected potential SEMP1 interactions need further confirmation, the remarkable cleanliness achieved with HA peptide elution in combination with colocalization of SEMP1 with most identified candidates is very promising.

Since no phenotype could be observed upon knocking out SEMP1, we speculated that the function of SEMP1 might have been compensated for by altered expression of other gene(s). We therefore conducted a comparative transcriptome analysis with SEMP1-DD parasites grown with or without Shield-1. Thus we were able to monitor the effect of loss of SEMP1 in genetically identical parasites at four consecutive time points spanning an entire IDC. In this analysis, 34 genes were identified to be significantly up-regulated over at least two consecutive time points, four of which with the highest RAFC were all exported proteins. Up-regulation of a *var* gene (PF3D7_0900100) is not really surprising since *var* genes regularly switch from expression of one *var* gene to another. In contrast, PF3D7_1301400 codes for an early expressed predicted exported protein containing a SP and PEXEL motif, which belongs to the hypothetical gene family *hyp12*. The three *hyp12* paralogs have no orthologs in any other organism and do not possess any annotated protein domains, making them elusive for functional predictions (48). However, other HYP proteins have been shown to be variantly expressed (49) and it could be conceivable that SEMP1 knockdown parasites switched to the expression of another HYP12. Similarly, PHIST proteins, of which PF3D7_0532300 is a member, also show variant transcriptional expression (49). The PHIST protein encoded by PF3D7_0532300 is expressed early during the IDC and its function is unknown. However, PHIST proteins have been shown to be involved in many functions such as modification of the infected host cell, alteration of membrane rigidity (50), and in the export process itself (50). Some PHIST proteins containing a DnaJ domain might be involved in stabilization of exported proteins (48), and they have been identified in J-dots (40), as constituents of knobs (51), and recently identified to be associated with exosomes (52). In light of these promiscuous functions and localisations of PHIST proteins an involvement in the structure and / or function of MCs is clearly conceivable. PfEMP3 (PF3D7_0201900) is a large PEXEL-

containing protein that is expressed during the ring and trophozoite stage. It associates with MCs and is further transported to the cytoplasmic face of the iRBC where it localizes to knobs but can also be distributed more broadly (53). PfEMP3 seems to be involved in PfEMP1 trafficking (54) and by binding to actin and spectrin contributes to loss of mechanical stability of the erythrocyte membrane (55,56). Together, this gives circumstantial evidence that SEMP1 could potentially be involved similarly in these processes in concert with PfEMP3 and probably also with PHIST proteins. This would also support the identification of Pf332 in our Co-IPs because Pf332 has also been shown to modulate the erythrocyte membrane skeleton (57). Coincidentally, Pf332 expression was moderately up-regulated in SEMP1-depleted parasites but did not reach significance. SEMP1 belongs to the group of PEXEL-negative exported proteins, which also includes proteins such as MAHRP1 (31), SBP1 (38), REX1 (9) and REX2 (10). It is still under debate how these proteins find their destination and no consensus targeting sequence has been found to date. The most common feature is the necessity of most N-terminal region. Similar to REX2 (10) and MAHRP2 (18) deletion of the first 16 amino acids completely abolished export of SEMP1 leaving the protein distributed throughout the parasite. Further truncation of the N-terminal part of SEMP1 up to the TM domain (SEMP1₇₂₋₁₂₃-GFP) leads to an arrest of the protein within the ER. Through this truncation, the TM becomes the N-terminus and might anchor the protein like a non-cleavable SP in the ER membrane. This has also been observed when the MAHRP1 TM domain was fused to GFP (58). As has been shown before with other exported proteins (10,58–60) the first 16 amino acids of SEMP1 could be replaced either with the N-terminal SP of MSP1 or with the first 16 N-terminal residues of MAHRP2.

In conclusion, we identified and characterized a new MC protein termed SEMP1. Upon invasion it is exported early into the iRBC cytosol where it inserts into the MCs before it is at least partly translocated to the RBC membrane. A parasite with knocked out SEMP1 revealed that the protein is not essential for parasite survival, gametocytogenesis or PfEMP1 export under culture conditions. This lack of altered phenotypes after gene knock-out is not an exception but rather the rule. A large-scale study which previously produced knock-out parasites for 39 exported *P. falciparum* proteins only was able to

identify phenotypical changes for 15 clones (38.5 %) (50). By using Co-IP and transcriptome analysis for functional characterization we provide a new starting point for further detailed dissection and characterisation of MC-associated proteins that show no phenotypical changes in knock-out parasites.

Acknowledgements

This project was supported by the Swiss National Science Foundation (31003A_132709 and 31003A_143916). We would like to thank the following colleagues for providing antibodies: Don Gardiner (anti-REX1), Catherine Braun-Breton (anti-SBP1), Brian Cooke (anti-PfEMP1), Mats Wahlgren (anti-Pf332), Claudia Daubenberger (anti-GAPDH) and Diane Taylor (anti-KAHRP). We are grateful to Manual Llinas to grant access to the Agilent microarray.

References

1. World Health Organization. WHO | World Malaria Report 2012. 2009.
2. Miller LH, Baruch DI, Marsh K, Doumbo OK. The pathogenic basis of malaria. *Nature*. 2002 Feb 7;415(6872):673–9.
3. Przyborski JM, Wickert H, Krohne G, Lanzer M. Maurer's clefts--a novel secretory organelle? *Mol Biochem Parasitol*. 2003 Nov;132(1):17–26.
4. Bhattacharjee S, van Ooij C, Balu B, Adams JH, Halder K. Maurer's clefts of *Plasmodium falciparum* are secretory organelles that concentrate virulence protein reporters for delivery to the host erythrocyte. *Blood*. 2008 Feb 15;111(4):2418–26.
5. Hiller NL, Bhattacharjee S, van Ooij C, Liolios K, Harrison T, Lopez-Estraño C, et al. A host-targeting signal in virulence proteins reveals a secretome in malarial infection. *Science*. 2004 Dec 10;306(5703):1934–7.
6. Marti M, Good RT, Rug M, Knuepfer E, Cowman AF. Targeting malaria virulence and remodeling proteins to the host erythrocyte. *Science*. 2004 Dec 10;306(5703):1930–3.
7. Spielmann T, Hawthorne PL, Dixon MWA, Hannemann M, Klotz K, Kemp DJ, et al. A cluster of ring stage-specific genes linked to a locus implicated in cytoadherence in *Plasmodium falciparum* codes for PEXEL-negative and PEXEL-positive proteins exported into the host cell. *Mol Biol Cell*. 2006 Aug;17(8):3613–24.
8. Spycher C, Rug M, Pachlatko E, Hanssen E, Ferguson D, Cowman AF, et al. The Maurer's cleft protein MAHRP1 is essential for trafficking of PfEMP1 to the surface of *Plasmodium falciparum*-infected erythrocytes. *Mol Microbiol*. 2008 Jun;68(5):1300–14.
9. Hawthorne PL, Trenholme KR, Skinner-Adams TS, Spielmann T, Fischer K, Dixon MWA, et al. A novel *Plasmodium falciparum* ring stage protein, REX, is located in Maurer's clefts. *Mol Biochem Parasitol*. 2004 Aug;136(2):181–9.
10. Haase S, Herrmann S, Grüning C, Heiber A, Jansen PW, Langer C, et al. Sequence requirements for the export of the *Plasmodium falciparum* Maurer's clefts protein REX2. *Mol Microbiol*. 2009 Feb;71(4):1003–17.
11. Trager W, Jensen JB. Cultivation of malarial parasites. *Nature*. 1978 Jun 22;273(5664):621–2.

12. Dorn A, Stoffel R, Matile H, Bubendorf A, Ridley RG. Malarial haemozoin/beta-haematin supports haem polymerization in the absence of protein. *Nature*. 1995 Mar 16;374(6519):269–71.
13. Lambros C, Vanderberg JP. Synchronization of *Plasmodium falciparum* erythrocytic stages in culture. *J Parasitol*. 1979 Jun;65(3):418–20.
14. Crabb BS, Rug M, Gilberger T-W, Thompson JK, Triglia T, Maier AG, et al. Transfection of the human malaria parasite *Plasmodium falciparum*. *Methods Mol Biol*. 2004;270:263–76.
15. Flueck C, Bartfai R, Volz J, Niederwieser I, Salcedo-Amaya AM, Alako BTF, et al. *Plasmodium falciparum* Heterochromatin Protein 1 Marks Genomic Loci Linked to Phenotypic Variation of Exported Virulence Factors. *PLoS Pathog* [Internet]. 2009 Sep [cited 2013 Jan 17];5(9). Available from: <http://www.ncbi.nlm.nih.gov/pmc/articles/PMC2731224/>
16. Fidock DA, Wellems TE. Transformation with human dihydrofolate reductase renders malaria parasites insensitive to WR99210 but does not affect the intrinsic activity of proguanil. *Proc Natl Acad Sci USA*. 1997 Sep 30;94(20):10931–6.
17. Bordier C. Phase separation of integral membrane proteins in Triton X-114 solution. *J Biol Chem*. 1981 Feb 25;256(4):1604–7.
18. Pachlatko E, Rusch S, Müller A, Hemphill A, Tilley L, Hanssen E, et al. MAHRP2, an exported protein of *Plasmodium falciparum*, is an essential component of Maurer’s cleft tethers. *Molecular Microbiology*. 2010;77(5):1136–52.
19. Hanssen E, Hawthorne P, Dixon MWA, Trenholme KR, McMillan PJ, Spielmann T, et al. Targeted mutagenesis of the ring-exported protein-1 of *Plasmodium falciparum* disrupts the architecture of Maurer’s cleft organelles. *Mol Microbiol*. 2008 Aug;69(4):938–53.
20. Blisnick T, Morales Betoulle ME, Barale JC, Uzureau P, Berry L, Desroses S, et al. Pfsbp1, a Maurer’s cleft *Plasmodium falciparum* protein, is associated with the erythrocyte skeleton. *Mol Biochem Parasitol*. 2000 Nov;111(1):107–21.
21. Maier AG, Rug M, O’Neill MT, Beeson JG, Marti M, Reeder J, et al. Skeleton-binding protein 1 functions at the parasitophorous vacuole membrane to traffic PfEMP1 to the *Plasmodium falciparum*-infected erythrocyte surface. *Blood*. 2007 Feb 1;109(3):1289–97.
22. Nilsson S, Moll K, Angeletti D, Albrecht L, Kursula I, Jiang N, et al. Characterization of the Duffy-Binding-Like Domain of *Plasmodium falciparum* Blood-Stage Antigen 332. *Malar Res Treat*. 2011;2011:671439.

23. Tokuyasu KT. A technique for ultracytometry of cell suspensions and tissues. *J Cell Biol.* 1973 May;57(2):551–65.
24. Daubenberger CA, Tisdale EJ, Curcic M, Diaz D, Silvie O, Mazier D, et al. The N⁷-terminal domain of glyceraldehyde-3-phosphate dehydrogenase of the apicomplexan *Plasmodium falciparum* mediates GTPase Rab2-dependent recruitment to membranes. *Biol Chem.* 2003 Aug;384(8):1227–37.
25. Beck H-P. Extraction and purification of *Plasmodium* parasite DNA. *Methods Mol Med.* 2002;72:159–63.
26. Painter HJ, Altenhofen LM, Kafsack BFC, Llinás M. Whole-genome analysis of *Plasmodium* spp. Utilizing a new agilent technologies DNA microarray platform. *Methods Mol Biol.* 2013;923:213–9.
27. Tusher VG, Tibshirani R, Chu G. Significance analysis of microarrays applied to the ionizing radiation response. *Proc Natl Acad Sci USA.* 2001 Apr 24;98(9):5116–21.
28. Eisen MB, Spellman PT, Brown PO, Botstein D. Cluster analysis and display of genome-wide expression patterns. *Proc Natl Acad Sci USA.* 1998 Dec 8;95(25):14863–8.
29. Voss TS, Healer J, Marty AJ, Duffy MF, Thompson JK, Beeson JG, et al. A var gene promoter controls allelic exclusion of virulence genes in *Plasmodium falciparum* malaria. *Nature.* 2006 Feb 23;439(7079):1004–8.
30. Oehring SC, Woodcroft BJ, Moes S, Wetzel J, Dietz O, Pulfer A, et al. Organellar proteomics reveals hundreds of novel nuclear proteins in the malaria parasite *Plasmodium falciparum*. *Genome Biol.* 2012 Nov 26;13(11):R108.
31. Spycher C, Klonis N, Spielmann T, Kump E, Steiger S, Tilley L, et al. MAHRP-1, a novel *Plasmodium falciparum* histidine-rich protein, binds ferriprotoporphyrin IX and localizes to the Maurer's clefts. *J Biol Chem.* 2003 Sep 12;278(37):35373–83.
32. Taylor DW, Parra M, Chapman GB, Stearns ME, Rener J, Aikawa M, et al. Localization of *Plasmodium falciparum* histidine-rich protein 1 in the erythrocyte skeleton under knobs. *Mol Biochem Parasitol.* 1987 Sep;25(2):165–74.
33. Heiber A, Kruse F, Pick C, Grüning C, Flemming S, Oberli A, et al. Identification of New PNEPs Indicates a Substantial Non-PEXEL Exportome and Underpins Common Features in *Plasmodium falciparum* Protein Export. *PLoS Pathog.* 2013 Aug 8;9(8):e1003546.
34. Banaszynski LA, Chen L-C, Maynard-Smith LA, Ooi AGL, Wandless TJ. A rapid, reversible, and tunable method to regulate protein function in living cells using synthetic small molecules. *Cell.* 2006 Sep 8;126(5):995–1004.

35. Armstrong CM, Goldberg DE. An FKBP destabilization domain modulates protein levels in *Plasmodium falciparum*. *Nat Methods*. 2007 Dec;4(12):1007–9.
36. Schultz J, Milpetz F, Bork P, Ponting CP. SMART, a simple modular architecture research tool: identification of signaling domains. *Proc Natl Acad Sci USA*. 1998 May 26;95(11):5857–64.
37. Dixon MWA, Kenny S, McMillan PJ, Hanssen E, Trenholme KR, Gardiner DL, et al. Genetic ablation of a Maurer's cleft protein prevents assembly of the *Plasmodium falciparum* virulence complex. *Mol Microbiol*. 2011 Aug;81(4):982–93.
38. Cooke BM, Buckingham DW, Glenister FK, Fernandez KM, Bannister LH, Marti M, et al. A Maurer's cleft-associated protein is essential for expression of the major malaria virulence antigen on the surface of infected red blood cells. *J Cell Biol*. 2006 Mar 13;172(6):899–908.
39. Külzer S, Rug M, Brinkmann K, Cannon P, Cowman A, Lingelbach K, et al. Parasite-encoded Hsp40 proteins define novel mobile structures in the cytosol of the *P. falciparum*-infected erythrocyte. *Cellular Microbiology*. 2010;12(10):1398–420.
40. Külzer S, Charnaud S, Dagan T, Riedel J, Mandal P, Pesce ER, et al. *Plasmodium falciparum*-encoded exported hsp70/hsp40 chaperone/co-chaperone complexes within the host erythrocyte. *Cell Microbiol*. 2012 Nov;14(11):1784–95.
41. Mattei D, Scherf A. The Pf332 gene of *Plasmodium falciparum* codes for a giant protein that is translocated from the parasite to the membrane of infected erythrocytes. *Gene*. 1992 Jan 2;110(1):71–9.
42. Haeggström M, Kironde F, Berzins K, Chen Q, Wahlgren M, Fernandez V. Common trafficking pathway for variant antigens destined for the surface of the *Plasmodium falciparum*-infected erythrocyte. *Molecular and Biochemical Parasitology*. 2004 Jan;133(1):1–14.
43. Hinterberg K, Scherf A, Gysin J, Toyoshima T, Aikawa M, Mazie JC, et al. *Plasmodium falciparum*: - The Pf332 Antigen Is Secreted from the Parasite by a Brefeldin A-Dependent Pathway and Is Translocated to the Erythrocyte Membrane via the Maurer's Clefs. *Experimental Parasitology*. 1994 Nov;79(3):279–91.
44. Mattei D, Scherf A. The Pf332 gene codes for a megadalton protein of *Plasmodium falciparum* asexual blood stages. *Mem Inst Oswaldo Cruz*. 1992;87 Suppl 3:163–8.
45. Moll K, Chêne A, Ribacke U, Kaneko O, Nilsson S, Winter G, et al. A novel DBL-domain of the *P. falciparum* 332 molecule possibly involved in erythrocyte adhesion. *PLoS ONE*. 2007;2(5):e477.

46. Vincensini L, Richert S, Blisnick T, Van Dorsselaer A, Leize-Wagner E, Rabilloud T, et al. Proteomic analysis identifies novel proteins of the Maurer's clefts, a secretory compartment delivering *Plasmodium falciparum* proteins to the surface of its host cell. *Mol Cell Proteomics*. 2005 Apr;4(4):582–93.
47. Florens L, Liu X, Wang Y, Yang S, Schwartz O, Peglar M, et al. Proteomics approach reveals novel proteins on the surface of malaria-infected erythrocytes. *Mol Biochem Parasitol*. 2004 May;135(1):1–11.
48. Sargeant TJ, Marti M, Caler E, Carlton JM, Simpson K, Speed TP, et al. Lineage-specific expansion of proteins exported to erythrocytes in malaria parasites. *Genome Biol*. 2006;7(2):R12.
49. Rovira-Graells N, Gupta AP, Planet E, Crowley VM, Mok S, Ribas de Pouplana L, et al. Transcriptional variation in the malaria parasite *Plasmodium falciparum*. *Genome Res*. 2012 May;22(5):925–38.
50. Maier AG, Rug M, O'Neill MT, Brown M, Chakravorty S, Szeszak T, et al. Exported proteins required for virulence and rigidity of *Plasmodium falciparum*-infected human erythrocytes. *Cell*. 2008 Jul 11;134(1):48–61.
51. Mayer C, Slater L, Erat MC, Konrat R, Vakonakis I. Structural analysis of the *Plasmodium falciparum* erythrocyte membrane protein 1 (PfEMP1) intracellular domain reveals a conserved interaction epitope. *J Biol Chem*. 2012 Mar 2;287(10):7182–9.
52. Regev-Rudzki N, Wilson DW, Carvalho TG, Sisquella X, Coleman BM, Rug M, et al. Cell-cell communication between malaria-infected red blood cells via exosome-like vesicles. *Cell*. 2013 May 23;153(5):1120–33.
53. Pasloske BL, Baruch DI, van Schravendijk MR, Handunnetti SM, Aikawa M, Fujioka H, et al. Cloning and characterization of a *Plasmodium falciparum* gene encoding a novel high-molecular weight host membrane-associated protein, PfEMP3. *Mol Biochem Parasitol*. 1993 May;59(1):59–72.
54. Waterkeyn JG, Wickham ME, Davern KM, Cooke BM, Coppel RL, Reeder JC, et al. Targeted mutagenesis of *Plasmodium falciparum* erythrocyte membrane protein 3 (PfEMP3) disrupts cytoadherence of malaria-infected red blood cells. *EMBO J*. 2000 Jun 15;19(12):2813–23.
55. Glenister FK, Coppel RL, Cowman AF, Mohandas N, Cooke BM. Contribution of parasite proteins to altered mechanical properties of malaria-infected red blood cells. *Blood*. 2002 Feb 1;99(3):1060–3.
56. Cooke BM, Glenister FK, Mohandas N, Coppel RL. Assignment of functional roles to parasite proteins in malaria-infected red blood cells by competitive flow-based adhesion assay. *Br J Haematol*. 2002 Apr;117(1):203–11.

57. Glenister FK, Fernandez KM, Kats LM, Hanssen E, Mohandas N, Coppel RL, et al. Functional alteration of red blood cells by a megadalton protein of *Plasmodium falciparum*. *Blood*. 2009 Jan 22;113(4):919–28.
58. Spycher C, Rug M, Klonis N, Ferguson DJP, Cowman AF, Beck H-P, et al. Genesis of and trafficking to the Maurer's clefts of *Plasmodium falciparum*-infected erythrocytes. *Mol Cell Biol*. 2006 Jun;26(11):4074–85.
59. Saridaki T, Fröhlich KS, Braun-Breton C, Lanzer M. Export of PfSBP1 to the *Plasmodium falciparum* Maurer's clefts. *Traffic*. 2009 Feb;10(2):137–52.
60. Dixon MWA, Hawthorne PL, Spielmann T, Anderson KL, Trenholme KR, Gardiner DL. Targeting of the ring exported protein 1 to the Maurer's clefts is mediated by a two-phase process. *Traffic*. 2008 Aug;9(8):1316–26.

Table 1 Identification of potential SEMP1 interaction partners by Co-IP

Gene ID	Gene product	# of detected peptides			Exported to RBC cytosol
		precipitation		Gel extraction	
		elution	elution (c-)		
PF3D7_0702400	SEMP1	12	0	67	MC
PF3D7_0935900 *	REX1	5	0	29	MC
PF3D7_0702500 *	Plasmodium exported protein	6	0	19	MC
PF3D7_0601900 *	Conserved Plasmodium protein	5	0	13	MC
PF3D7_0831700	PfHsp70-x	0	0	31	J-dots
PF3D7_0818900	HSP70	0	0	15	no
PF3D7_0708400	HSP90	0	0	15	no
PF3D7_1353200	MAHRP2	0	0	12	tethers
PF3D7_1149000 *	Pf332	0	0	11	MC
PF3D7_1016300	Glycophorin Binding Protein GBP	0	0	11	RBC
PF3D7_0507100	60S ribosomal protein L4	0	0	9	no
PF3D7_0517000	60S ribosomal protein L12	0	0	6	no
PF3D7_0501200 *	PIESP2	0	0	5	MC
PF3D7_1462800	GAPDH	0	0	5	no

Identified potential SEMP1 interaction partners with the number of detected peptides in each MS analysis and their localization during the asexual intraerythrocytic cycle (MC = Maurer's clefts; RBC = soluble in the erythrocyte, no = not exported). Marked (*) candidates were investigated for colocalization with SEMP1 by Immunofluorescence assays.

Table 2 Microarray analysis: Transcriptional changes in absence of SEMP1

GeneID	FC 1	FC 2	FC 3	FC 4	RAFC	Product Description
PF3D7_0900100	2.18	1.26	1.08	2.00	2.09	PfEMP1
PF3D7_1301400	0.79	1.77	1.84	2.02	1.93	P. exported protein (hyp12)
PF3D7_0532300	0.74	2.15	1.56	1.59	1.77	P. exported protein (PHISTb)
PF3D7_0201900	0.56	1.71	1.69	1.27	1.70	PfEMP3
PF3D7_0618200	1.15	1.08	1.75	1.63	1.69	conserved Plasmodium protein
PF3D7_0903700	0.95	0.70	1.62	1.72	1.67	alpha tubulin 1
PF3D7_1468200	1.00	1.41	1.60	1.70	1.65	conserved protein,
PF3D7_0831700	1.02	1.27	1.62	1.66	1.64	heat shock protein 70 (HSP70-x)
PF3D7_0113000	0.71	1.60	1.65	1.62	1.64	glutamic acid-rich protein (GARP)
PF3D7_0319900	1.63	1.38	1.16	1.61	1.62	conserved Plasmodium protein,
PF3D7_0821700	1.15	1.47	1.47	1.91	1.61	60S ribosomal protein L22
PF3D7_1226300	1.83	1.36	1.62	1.24	1.60	cof-like hydrolase
PF3D7_1415700	1.21	1.62	1.53	1.42	1.57	serine C-palmitoyltransferase
PF3D7_0804800	1.55	1.10	1.57	1.57	1.57	peptidyl-prolyl isomerase (CYP24)
PF3D7_1200600	1.41	1.49	1.79	0.89	1.56	PfEMP1 (VAR2CSA)
PF3D7_1242700	0.97	1.19	1.56	1.57	1.56	40S ribosomal protein S17
PF3D7_0629100	1.56	0.74	1.25	1.56	1.56	phosphoribosyltransferase
PF3D7_0936800	0.85	1.57	1.38	1.71	1.55	P. exported protein (PHISTc)
PF3D7_0323000	1.52	0.87	1.39	1.59	1.55	conserved Plasmodium protein
PF3D7_1317900	0.87	1.53	1.58	1.38	1.55	nuclear export protein
PF3D7_1476200	1.22	1.42	1.84	1.38	1.55	P. exported protein (PHISTb)
PF3D7_0210900	1.11	1.04	1.49	1.58	1.54	conserved Plasmodium protein
PF3D7_0403700	1.23	1.11	1.52	1.55	1.53	CGI-201 protein, short form
PF3D7_0218100	1.70	1.47	0.80	1.43	1.53	conserved P. membrane protein
PF3D7_1138500	1.53	1.51	1.16	1.36	1.52	protein phosphatase 2c
PF3D7_0402000	0.96	0.85	1.47	1.56	1.52	P. exported protein (PHISTa)
PF3D7_1305400	1.53	1.38	1.65	1.16	1.52	conserved Plasmodium protein
PF3D7_1474000	1.50	1.52	1.07	0.95	1.51	probable protein
PF3D7_0708800	1.04	0.84	1.49	1.53	1.51	heat shock protein 70 (HSP70-z)
PF3D7_1353100	1.07	1.45	1.50	1.51	1.51	Plasmodium exported protein,
PF3D7_1426600	1.55	1.28	1.69	1.24	1.51	conserved Plasmodium protein
PF3D7_1443900	1.09	0.77	1.49	1.52	1.51	heat shock protein 90 (HSP90)
PF3D7_1011800	1.42	0.99	1.64	1.46	1.51	QF122 antigen
PF3D7_1237900	1.24	1.51	1.50	0.50	1.50	conserved Plasmodium protein
PF3D7_0113400	0.60	0.79	1.34	0.60	0.60	Plasmodium exported protein
PF3D7_0930300	1.26	1.14	0.61	0.58	0.59	merozoite surface protein 1
PF3D7_0503200	0.59	0.60	0.70	1.30	0.59	conserved Plasmodium protein
PF3D7_0827600	0.60	0.56	1.08	1.55	0.58	conserved Plasmodium protein
PF3D7_1231300	0.50	0.60	0.61	0.60	0.57	conserved Plasmodium protein
PF3D7_1216500	0.58	0.55	0.84	1.08	0.56	male development gene 1 (MDV1)
PF3D7_0302200	1.01	1.04	0.57	0.56	0.56	cytoadherence linked protein 3.2
PF3D7_0728800	0.57	0.55	1.25	1.55	0.56	conserved Plasmodium protein
PF3D7_0217500	0.79	1.12	0.56	0.54	0.55	calcium dependent protein kinase 1
PF3D7_1307500	0.56	0.78	0.93	0.52	0.54	conserved Plasmodium protein
PF3D7_1112200	0.54	0.53	0.88	1.34	0.54	coq4 homolog, putative
PF3D7_1475200	0.50	0.54	0.83	1.28	0.52	conserved protein

Summary of all significantly ($p < 0.05$) up- (red) and down-regulated (green) parasite genes with a respective average fold change (RAFC) > 1.5 or < 0.6 . The RAFC is thereby the average FC over the significantly up- / down-regulated time points only. The time points were 6-14 hpi (FC1), 16-24 hpi (FC2), 26-34 hpi (FC3) and 36-44 hpi (FC4). Exported parasite proteins are highlighted in yellow.

Figure legends

Figure 1 A: schematic representation of the *semp1* gene (top) and SEMP1 protein structure (bottom). TM, transmembrane protein. B: lysates of 3D7 parasites expressing SEMP1-3xHA or SEMP1-GFP. Detection was by mouse α -HA or mouse α -GFP antibodies. C: Live cell imaging of 3D7 parasites expressing SEMP1 with C-terminal tagged GFP. D: Immunofluorescence assays of MeOH-fixed RBCs infected with 3D7 expressing SEMP1 with a C-terminal 3xHA tag, co-labelled with rat α -HA and either rabbit α -MAHRP1 or rabbit α -REX1 antibodies. E: Scatter plot of co-localization of SEMP1 and REX1 in SEMP1-3xHA parasites. F: Electron microscopy (EM) of RBCs infected with 3D7 expressing SEMP1 with a C-terminal GFP tag labelled with rabbit α -GFP antibodies and decorated with 5 nm gold conjugated Protein A.

Figure 2 A: Immunofluorescence assays of MeOH-fixed RBCs infected with 3D7 expressing SEMP1 with a C-terminal 3xHA tag, co-labelled with rat α -HA and mouse α -KAHRP antibodies. B: Parasite protein pellet of 3D7 expressing SEMP1-3xHA was fractionated using TritonX-114 into a soluble (aqueous phase) (a) and an insoluble (membrane) fraction (d). Proteins were visualized using mouse α -HA and rabbit α -MAHRP2 antibodies.

Figure 3 Localization and expression of endogenous SEMP1 in 3D7 wild-type parasites A: 3D7 wild-type parasite lysate (3D7) and uninfected red blood cells (RBC) were analyzed by immunoblotting and probed with mouse serum raised against recombinant full-length SEMP1. B: IFAs of MeOH-fixed RBCs infected with 3D7 wild-

type parasites synchronized at timepoints 6-14 hours post invasion (hpi), 16-24 hpi, 26-34 hpi and 36-44 hpi. Cells were co-labelled with mouse α -SEMP1 and rabbit α -MAHRP1 serum. C: 3D7 parasite pellets were generated at the respective timepoints by saponin lysis and analyzed by immunoblot using mouse α -SEMP1 serum and mouse α -GAPDH (PF3D7_1462800) antibodies.

Figure 4 Requirements for SEMP1 export into the RBC. A: Lysates of SEMP1-KO parasites expressing full-length and truncated or mutated forms of SEMP1 C-terminally fused to GFP were generated by saponin lysis and analyzed by immunoblotting using mouse α -GFP antibodies. Lane 1: SEMP1₁₋₁₂₃-GFP (full-length), lane 2: SEMP1₁₇₋₁₂₃-GFP, lane3: SEMP1₇₂₋₁₂₃GFP, lane4: SEMP1₁₋₉₇-GFP, lane 5: MSP1₁₋₁₆SEMP1₁₇₋₁₂₃-GFP, lane 6: MAHRP2₁₋₁₆SEMP1₁₇₋₁₂₃-GFP. B: Immunofluorescence assays of MeOH-fixed RBCs infected with SEMP1-KO parasites expressing full-length and truncated or mutated forms of SEMP1 C-terminally fused to GFP. Expressed SEMP1 was labelled with rabbit α -GFP antibodies. The transmembrane domain is depicted in red (TM), a MSP1 signal peptide in brown (MSP1) and the MAHRP2 N-terminus in blue (M2).

Figure 5 Identification of potential SEMP1 interaction partners by Co-IP. Co-IP was performed with 3D7 parasites expressing SEMP1 with a C-terminal 3xHA tag. Cultures were cross-linked with 1 % formaldehyde and parasites were released by saponin treatment, lysed in 1%SDS followed by sonication. Lysate (Input) was incubated with α -HA affinity matrix. After centrifugation the matrix was washed three times with washing buffer (Wash) and proteins were eluted from by HA peptide elution. As a negative control, an excess of soluble HA peptides was added to the input to block the HA binding sites of the matrix (c-). Samples were analyzed by Western blot with α -HA antibodies (A) and by silver staining (B). Proteins co-eluted with SEMP1-3xHA were identified by MS analysis of both TCA precipitated total elution (precipitation) and Coomassie-stained gel slices (gel extraction).

Figure 6 Localization of potential SEMP1 interacting proteins. Immunofluorescence assays of MeOH-fixed RBCs infected with 3D7 expressing SEMP1 / PF3D7_0702500 /

PF3D7_0601900 with a C-terminal 3xHA tag and 3D7 expressing PIESP2 with a C-terminal GFP-tag, co-labelled with mouse α -SEMP1 and rat α -HA (PF3D7_0702500-3xHA & PF3D7_0601900-3xHA) / α -GFP (PIESP2-GFP). For co-labelling of SEMP1-3xHA with REX1 and Pf332, rat α -HA and rabbit α -REX1 / mouse α -Pf332 antibodies were used.

Figure 7 Knockout of SEMP1 by gene disruption has no detectable phenotype. A: *Cla*I- and *Xma*I-digested gDNA isolated from a SEMP1-KO clone (KO) pH-KO plasmid (DP) were analyzed by Southern blot and probed with radioactively labelled *hdhfr*. In case of an integration of the KO plasmid into the parasite genome the expected fragment size is 3927 bp. B: lysates of 3D7 wild type and SEMP1-KO (KO) parasites were generated by saponin lysis and analyzed by Western blot with α -SEMP1 and α -GAPDH (loading control) antibodies. C: Immunofluorescence assays of fixed RBCs infected with SEMP1-KO parasites, probed with α -MAHRP1, α -SBP1, α -REX1 and α -PfEMP1 antibodies. The parasite nuclei were stained with DAPI. D: Bar graph depicting differential binding to CD36 of RBCs infected with wild-type 3D7 and SEMP1-KO parasites. CD36 (or BSA as control) was immobilized on Petri dishes and bound infected RBCs (iRBCs) were calculated as iRBCs per mm² for 1 % parasitemia. E: Upon gametocytogenesis induction of SEMP1-KO parasites by anoxic stress the parasites were followed for 8 days to test for gametocyte formation.

Figure 8 Conditional Knockdown of SEMP1. A: *Eco*RI-digested gDNA isolated from SEMP1-DD parasites (DD) was analyzed by Southern blot and probed with radioactively labelled *hdhfr*. B: A culture of 3D7 parasites expressing SEMP1-DD was split and cultured for 2 weeks in presence (Shld +) or absence (Shld -) of the small molecule Shield-1. Whole parasite-lysates were generated after saponin lysis and analyzed by Western blot using α -SEMP1. As a loading control the blot was additionally probed with antibodies against the housekeeping protein GAPDH.

Figure 9 Transcriptional changes in absence of SEMP1 identified by microarray analysis. Summary of all significantly ($p < 0.05$) up- and down-regulated parasite genes

with a respective average fold change (RAFC) > 1.5 or < 0.6 . The RAFC is thereby the average FC over the significantly up- / down-regulated time points (TPs) only. A graphic depiction of their FCs throughout the four time points (TPs) is shown in form of a heat map. Up-regulation (FC > 1) is indicated in red, down-regulation (FC < 1) in green. The time points were 6-14 hpi (TP1), 16-24 hpi (TP2), 26-34 hpi (TP3) and 36-44 hpi (TP4). Exported proteins are highlighted in yellow.

Supplementary Material

Construct	Primer name	Primer sequence	RS
 SEMP1 ₁₇₋₁₂₃ -GFP	17-123-F	CAGTCTTAAGATGGCCAATACCCAAGAAAAGAAATT	AfIII
	17-123-R	CAGTATCGATTTTTGCGTTCTGTAAACTGGCT	ClaI
 SEMP1 ₇₂₋₁₂₃ -GFP	72-123-F	CAGTCTTAAGATGGAGTTGGTTGAATTTGGTTTAAAC	AfIII
	72-123-R	CAGTATCGATTTTTGCGTTCTGTAAACTGGCT	ClaI
 SEMP1 ₁₋₉₇ -GFP	1-97-F	CAGTCTTAAGATGAGTCAACCACAAAAACAAC	AfIII
	1-97-R	CAGTATCGATTACGTAATCATATATTTGTAAGGC	ClaI
 MSP1 ₁₋₁₆ SEMP1 ₁₇₋₁₂₃ -GFP	MSP1-F	CAGTCTTAAGATGAAGATCATATTCTTTTTATGTTC ATTTCTTTTTTTATTATAAATACACAATGTGTAG CCAATACCCAAGAAAAGAAATT	AfIII
	MSP1-R	CAGTATCGATTTTTGCGTTCTGTAAACTGGCT	ClaI
 M2 ₁₋₁₆ SEMP1 ₁₇₋₁₂₃ -GFP	M2-F	CAGTCTTAAGATGCAGCCTTGCCATATGATGTATA CAATCAAATAAACCATGTAGGAACTCATTGGGCTGC CAATACCCAAGAAAAGAAATT	AfIII
	M2-R	CAGTATCGATTTTTGCGTTCTGTAAACTGGCT	ClaI

Table S1. Primers used to generate truncated and mutated constructs for SEMP1 trafficking studies. *AfIII* and *ClaI* restriction sites (RS) thereby allowed directional cloning into the pARL1mGFPmT transfection vector.

Codon-optimized SEMP1 sequence

ATGAGTCAACCGCAGAAACAGCAGAATGAAGAAGGGGCTGCTACTGCGGCA
AACACCCAGGAGAAGAAATTCAATCCGACACGCAATCCTTCGCAATCTGGTC
CCTATCGTCACCATGGACCACAGGGTCGTACCCCGTATATGCAACTGCACAA
GAATCAGAACAACAACATGGTCAACAAAATCAGCAACTATCTCGGCATTGAG

AACAAAGAACTGGTGGAATTTGGCCTGAATCTGTTTACGTACATCATTGCCAT
TTTCTTAGCCCTGCAAATCTACGACTATGTAACCCATCGCAAATGCGGCTATT
ACAAAGATATGCTGGCGAAAATTGTTTCGCTTTCAGGCATCACTTCAGAATGC
GAAA

Supplementary Figure legends

Figure S1. A: Lysates of 3D7 parasites expressing PF3D7_0702500-3xHA (0702500-3xHA), PF3D7_0601900-3xHA (0601900-3xHA) and PIESP2-GFP generated by saponin lysis and analyzed by Western blot using rat α -HA / mouse α -GFP antibodies.

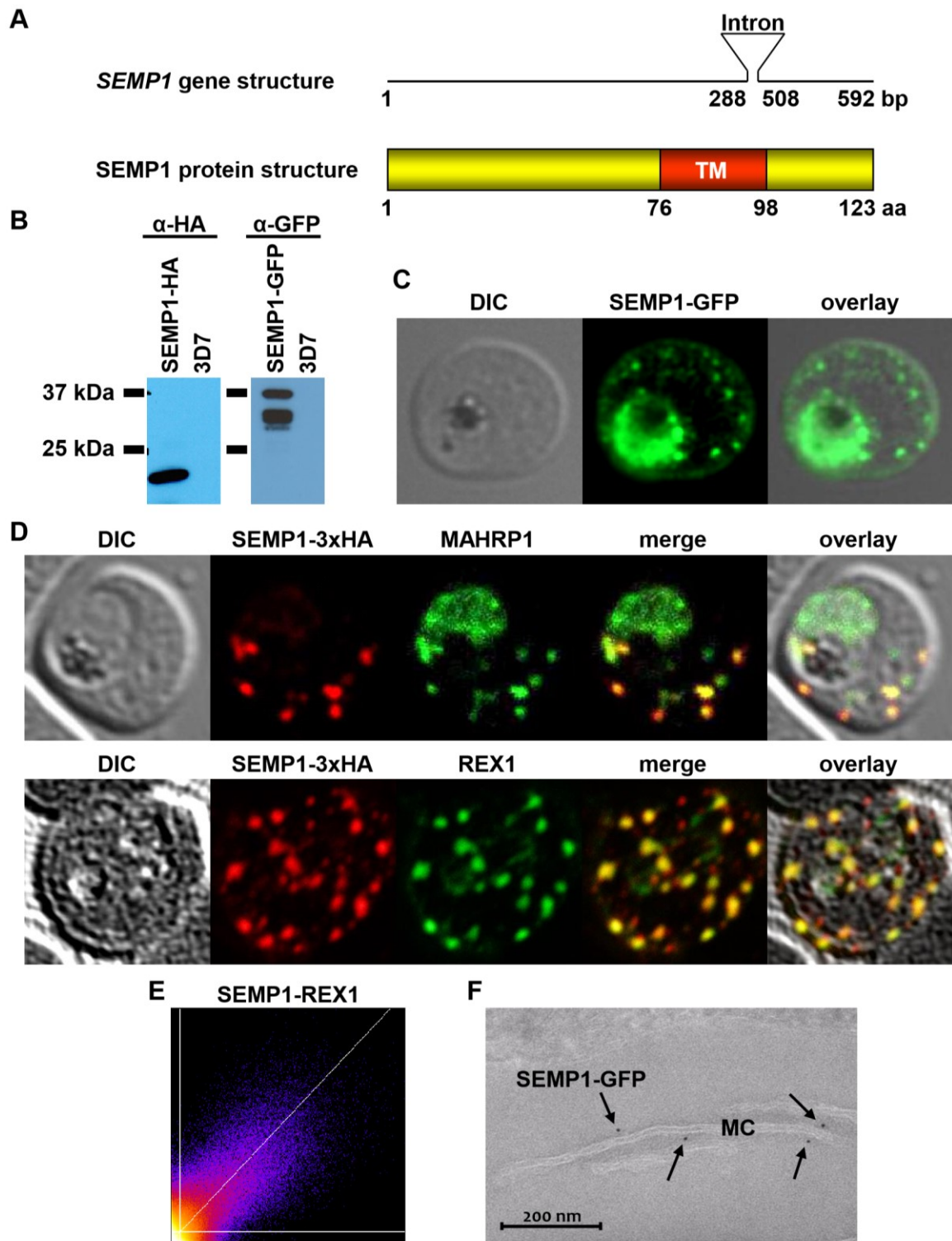


Figure 1

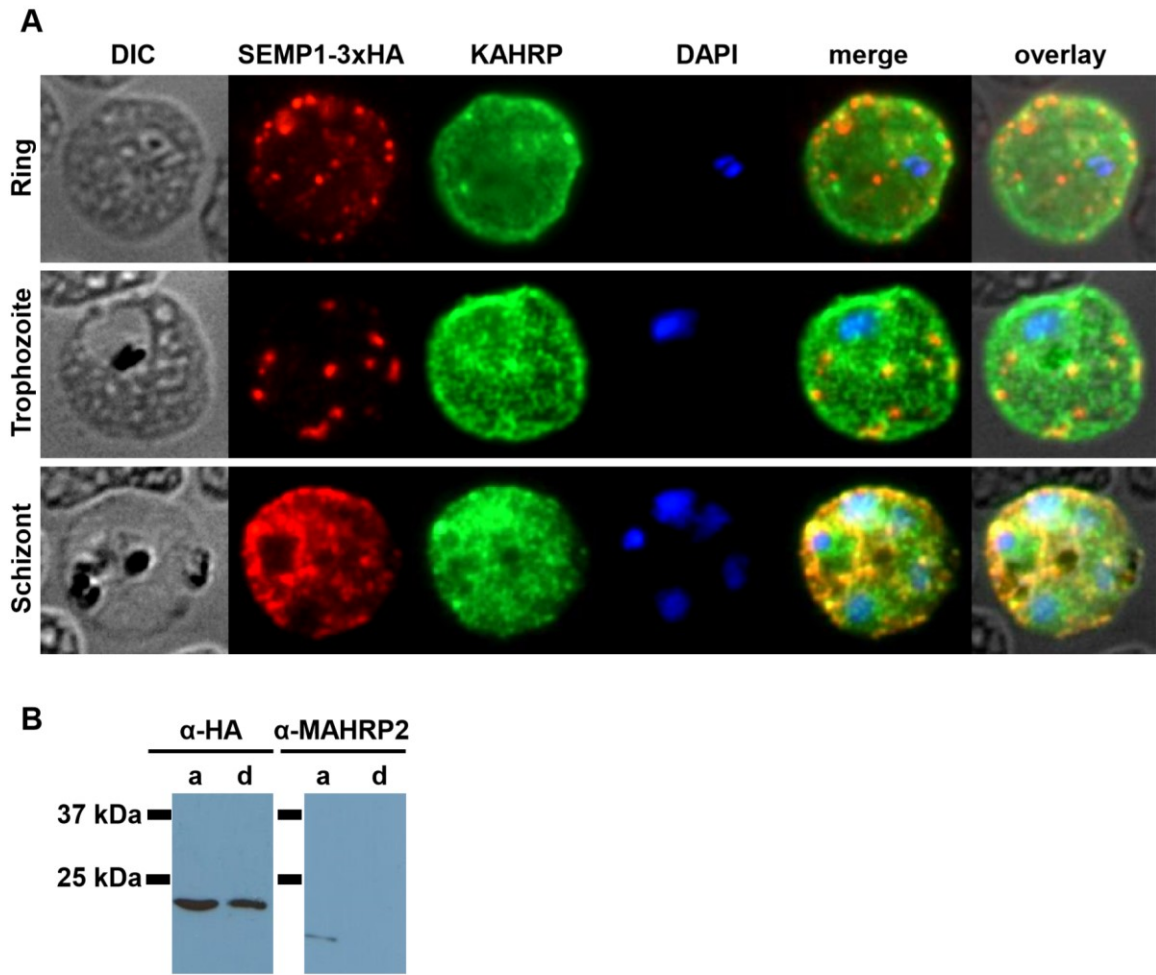


Figure 2

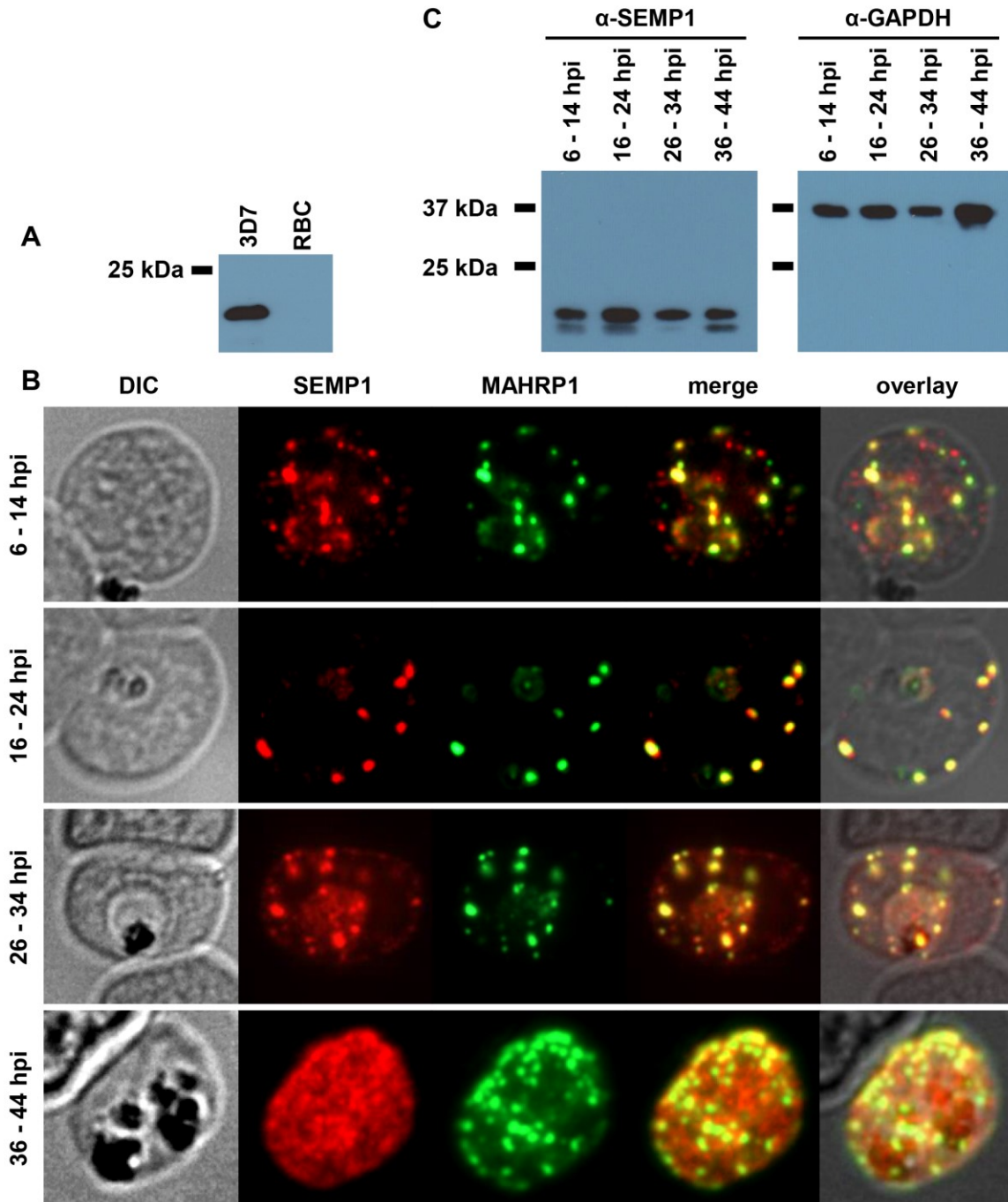


Figure 3

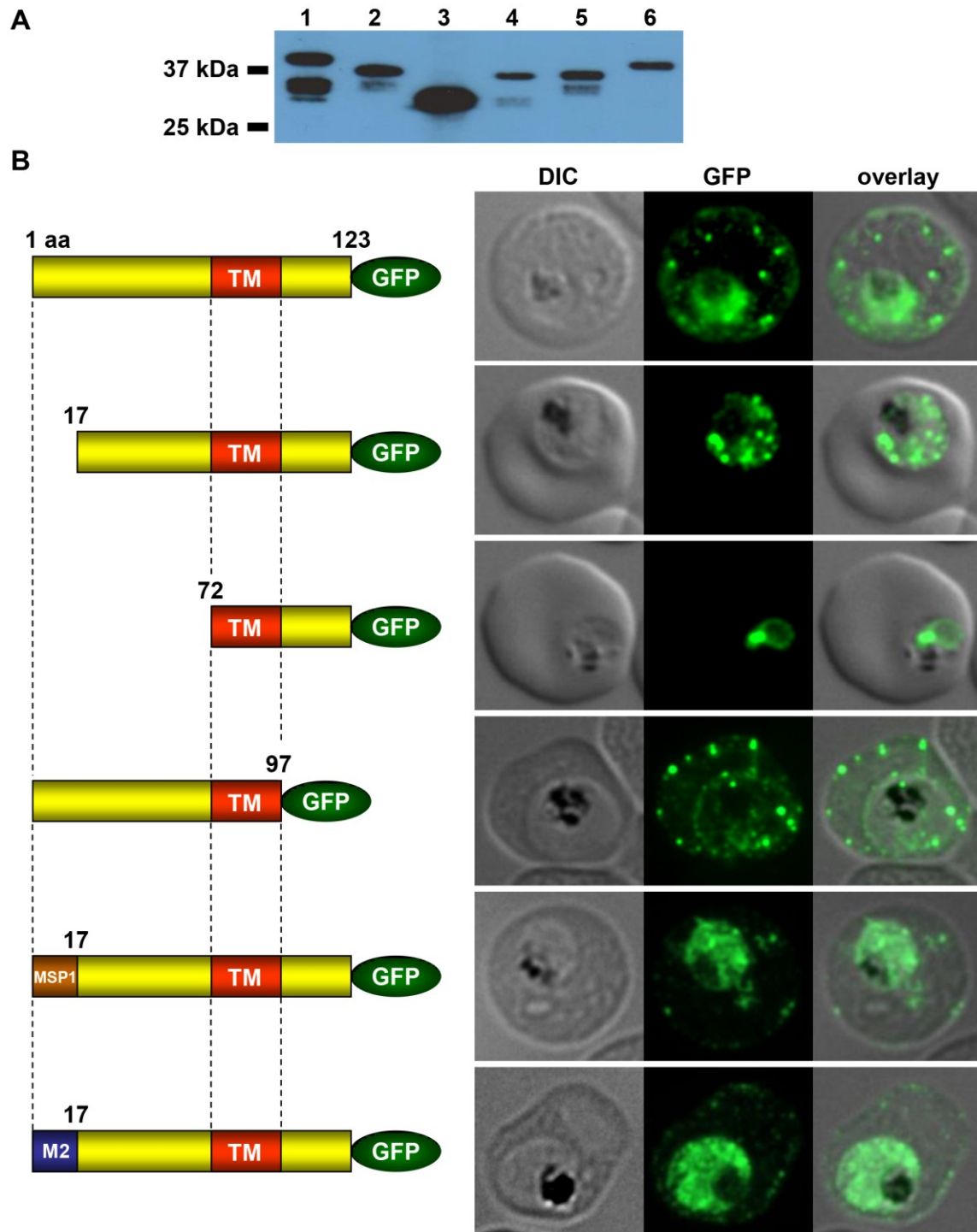


Figure 4

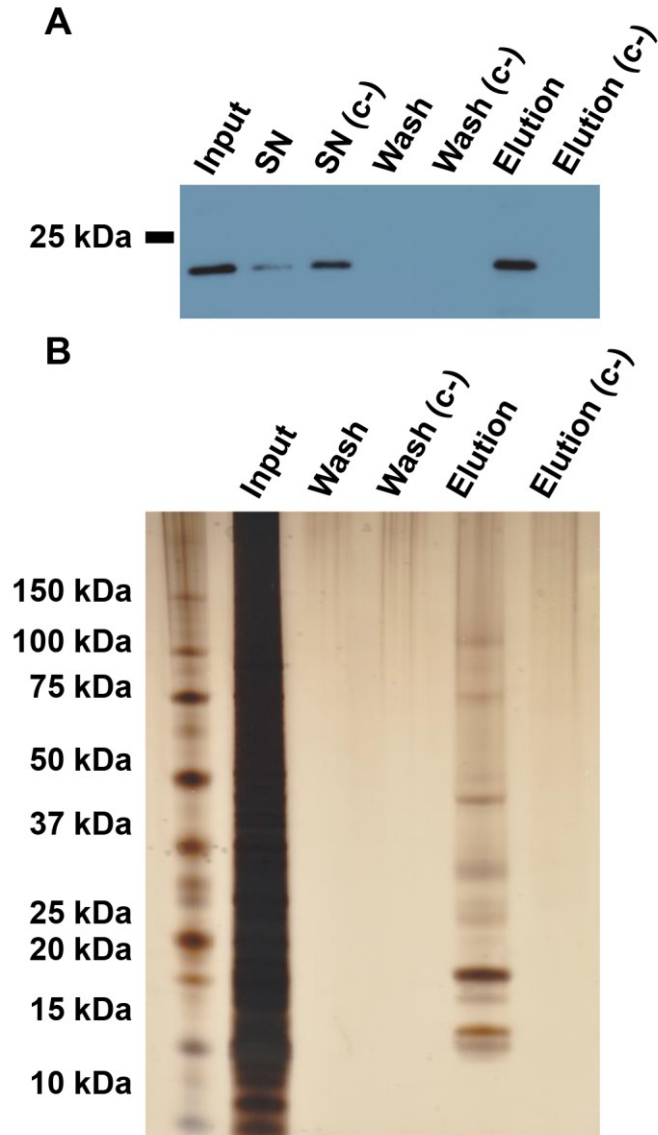


Figure 5

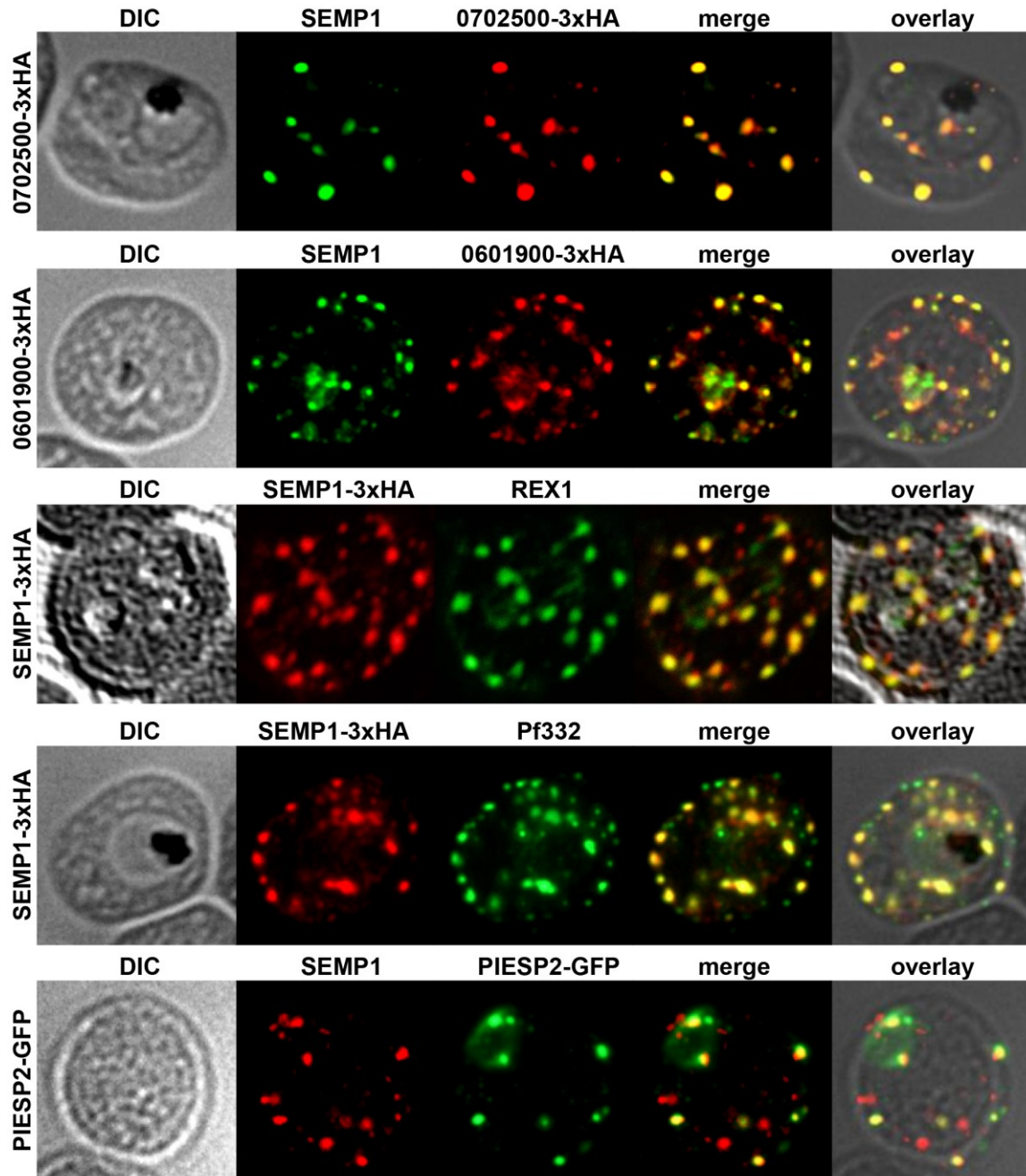


Figure 6

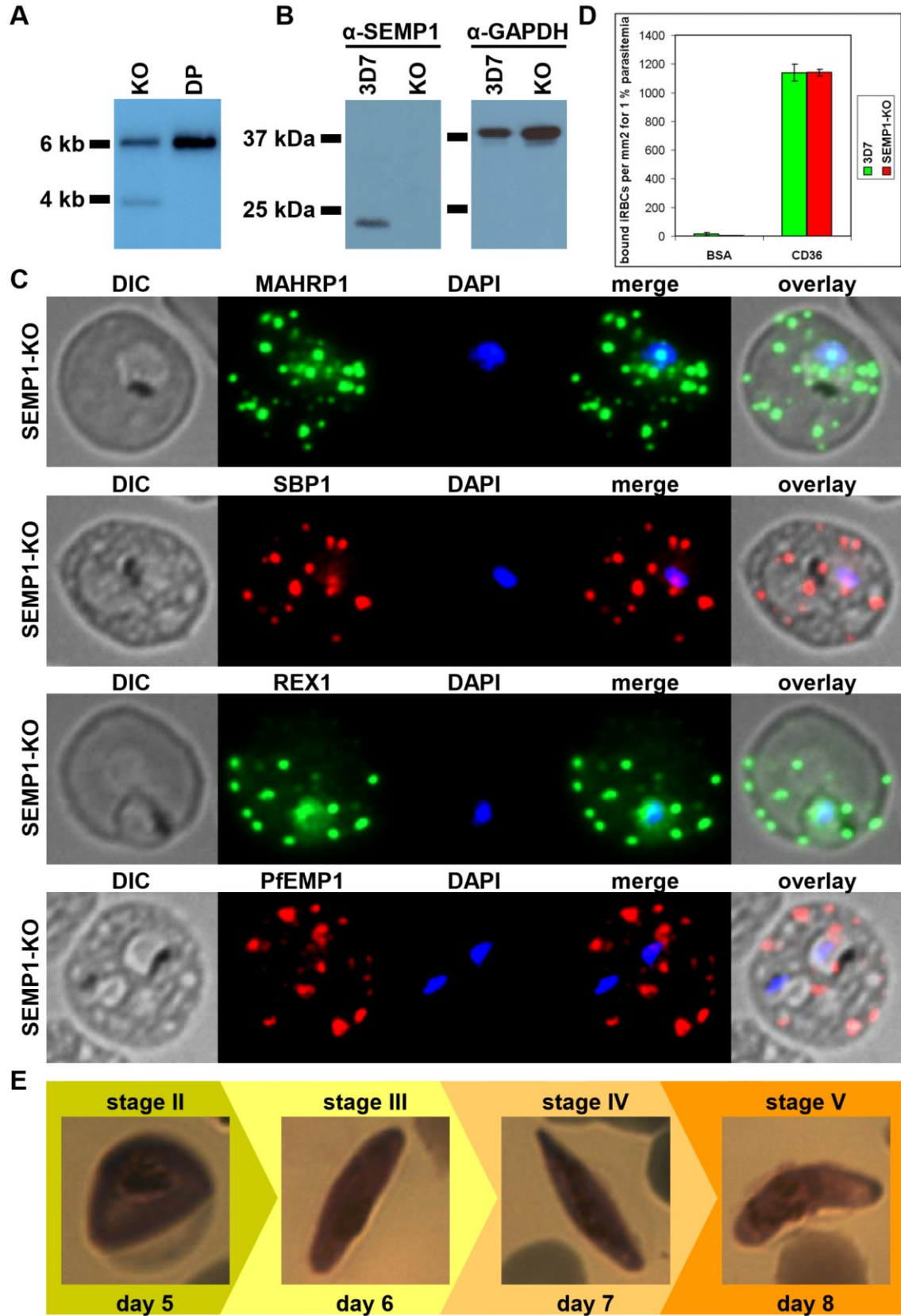


Figure 7

Figure 3

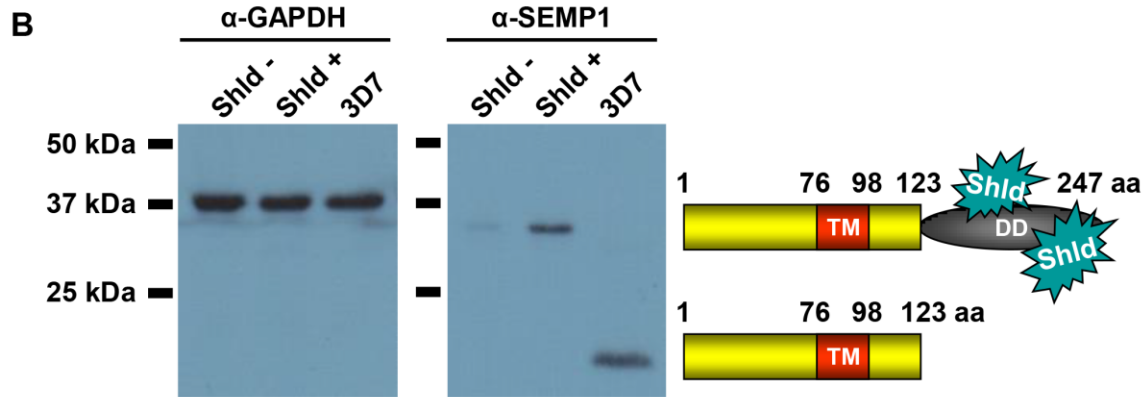
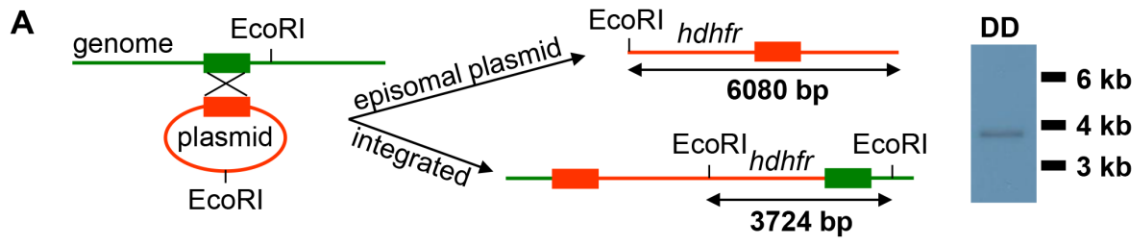


Figure 8

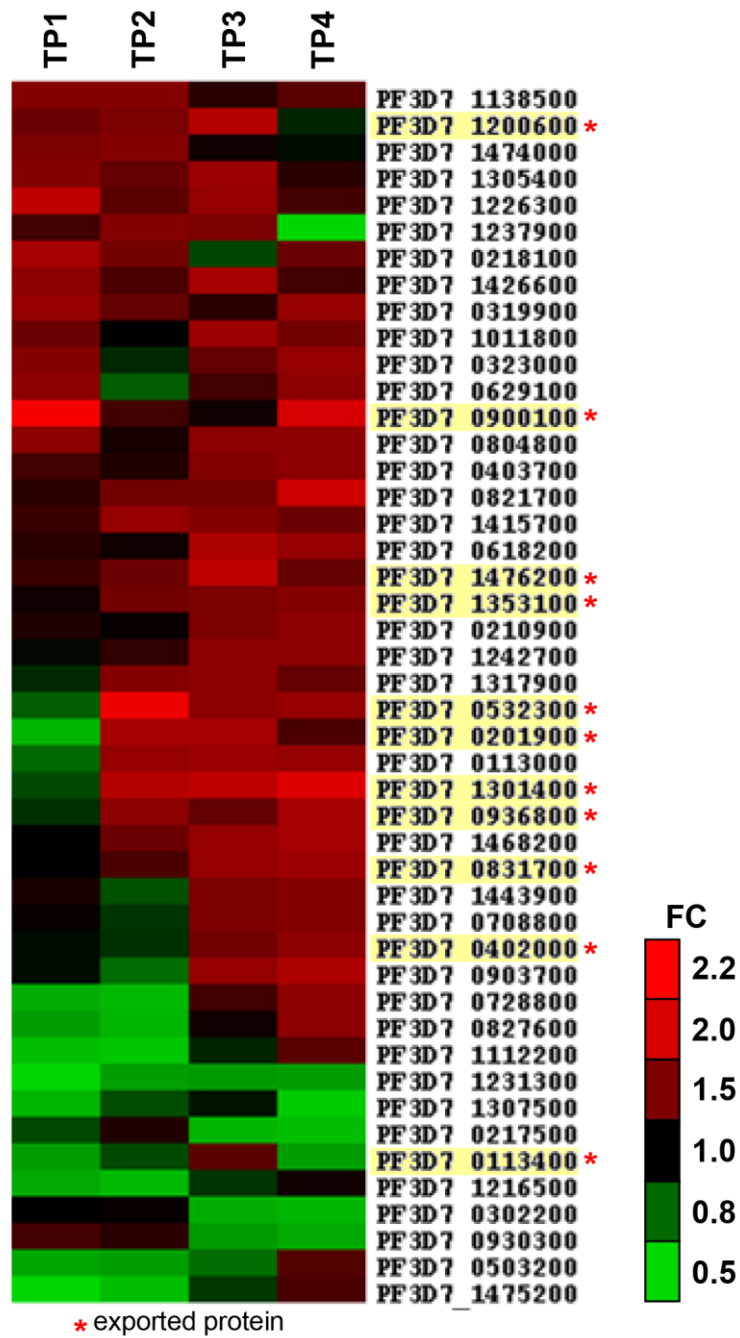


Figure 9

Supplementary Material

Construct	Primer name	Primer sequence	RS
SEMP1 ₁₇₋₁₂₃ -GFP 	17-123-F	CAGTCTTAAGATGGCCAATACCCAAGAAAAGAAATT	AfIII
	17-123-R	CAGTATCGATTTTTGCGTTCTGTAAACTGGCT	Clal
SEMP1 ₇₂₋₁₂₃ -GFP 	72-123-F	CAGTCTTAAGATGGAGTTGGTTGAATTTGGTTTAAAC	AfIII
	72-123-R	CAGTATCGATTTTTGCGTTCTGTAAACTGGCT	Clal
SEMP1 ₁₋₉₇ -GFP 	1-97-F	CAGTCTTAAGATGAGTCAACCACAAAACAAC	AfIII
	1-97-R	CAGTATCGATTACGTAATCATATATTTGTAAGGC	Clal
MSP ₁₋₁₆ SEMP1 ₁₇₋₁₂₃ -GFP 	MSP1-F	CAGTCTTAAGATGAAGATCATATTCTTTTTATGTTT ATTTCTTTTTTTTATTATAAATACACAATGTGTAG CCAATACCCAAGAAAAGAAATT	AfIII
	MSP1-R	CAGTATCGATTTTTGCGTTCTGTAAACTGGCT	Clal
M2 ₁₋₁₆ SEMP1 ₁₇₋₁₂₃ -GFP 	M2-F	CAGTCTTAAGATGCAGCCTTGCCATATGATGTATA CAATCAAATAAACCATGTAGGAACTCATTGGGCTGC CAATACCCAAGAAAAGAAATT	AfIII
	M2-R	CAGTATCGATTTTTGCGTTCTGTAAACTGGCT	Clal

Table S1. Primers used to generate truncated and mutated constructs for SEMP1 trafficking studies. *AfIII* and *Clal* restriction sites (RS) thereby allowed directional cloning into the pARL1mGFPmT transfection vector.

Codon-optimized SEMP1 sequence

ATGAGTCAACCGCAGAAACAGCAGAATGAAGAAGGGGCTGCTACTGCGGCA
AACACCCAGGAGAAGAAATTCAATCCGACACGCAATCCTTCGCAATCTGGTC
CCTATCGTCACCATGGACCACAGGGTCGTACCCCGTATATGCAACTGCACAA
GAATCAGAACAACAACATGGTCAACAAAATCAGCAACTATCTCGGCATTGAG
AACAAAGAACTGGTGGAAATTTGGCCTGAATCTGTTTACGTACATCATTGCCAT
TTTCTTAGCCCTGCAAATCTACGACTATGTAACCCATCGCAAATGCGGCTATT
ACAAAGATATGCTGGCGAAAATTGTTCGCTTTCAGGCATCACTTCAGAATGC
GAAA

Supplementary Figure legends

Figure S1. Lysates of 3D7 parasites expressing PF3D7_0702500-3xHA (0702500-3xHA), PF3D7_0601900-3xHA (0601900-3xHA) and PIESP2-GFP generated by saponin lysis and analyzed by Western blot using α -HA / mouse α -GFP antibodies.

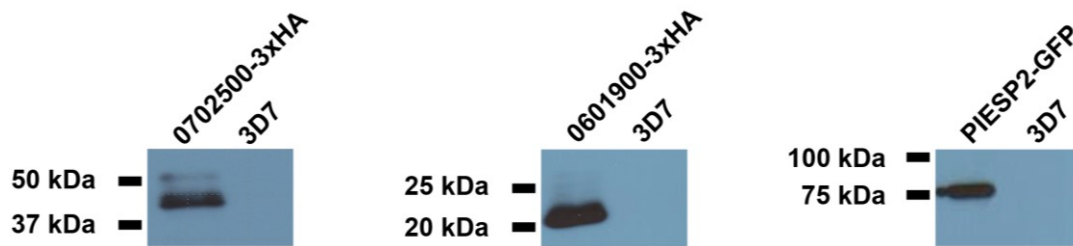


Figure S1

Chapter 5

**Verification of potential SEMP1 protein-protein interactions
by mbSUS pairwise interaction assays**

Introduction

The apicomplexan parasite *Plasmodium falciparum* is the pathogenic agent causing the most severe form of human malaria called malaria tropica, which is responsible for almost 700'000 deaths annually worldwide (1). Once in the blood stream the protozoan parasite undergoes an asexual developmental cycle consisting of repeated erythrocyte invasion, multiplication and release by cell rupture. The disease symptoms are strongly associated with this development within the human red blood cells. Since human erythrocytes are devoid of internal organelles and any protein trafficking machinery, parasite survival and virulence depend on substantial host cell modifications. These are mediated by exporting a large number of parasite proteins into the RBC cytosol and to the RBC membrane. The latter were shown to be transported via parasite derived membranous structures in the RBC cytosol called Maurer's clefts (MCs) which are thought to function as a form of a surrogate Golgi which concentrates virulence proteins for delivery to the RBC surface (2,3). However, their specific function has yet to be determined.

In an attempt to bring new insight into the function and composition of MCs we identified and characterized the MC resident small exported membrane protein 1 (SEMP1, accession number). Although lacking a classical signal peptide (SP) and a PEXEL motif, SEMP1 is exported into the host cell (4) early after erythrocyte invasion. There it inserts into the MCs as a transmembrane (TM) protein before it appears to be partly further exported to the RBC membrane. Knock out studies revealed that SEMP1 is not essential for parasite survival, PfEMP1 export, or gametocytogenesis under culture conditions. Transcriptomic analysis revealed that in absence of SEMP1 transcription of a number of exported parasite proteins is up-regulated, including PfEMP3. Since PfEMP3 was shown to be involved in determining the rigidity of the host cell membrane by binding to actin and spectrin (5,6) its upregulation in a SEMP1 knock out could indicate that PfEMP3 might compensate for the loss of SEMP1. In order to further investigate the function of SEMP1 we performed co-immunoprecipitation (co-IP) and identified several potential interaction partners, including the two previously uncharacterized MC proteins

PF3D7_0702500 (PF07_0008) and PF0601900 (PFF0090w). The aim of this study was to investigate the potential binding of SEMP1 to PF3D7_0702500 and PF3D7_0601900 by the mating-based split-ubiquitin system (mbSUS) (7) in a pairwise interaction assay. This yeast based *in vitro* interaction platform for membrane proteins consists of a split ubiquitin whose moieties are only able to reconstitute a functional protein if brought into proximity via the interaction of the respective proteins that are fused to them (8). Upon bait and prey protein interaction the functional ubiquitin is cleaved off by specific proteases which releases a transcription factor (TF) from yeast membranes. The TF then diffuses to the nucleus and starts transcription of the selection markers *his3* and *ade2* whose activation enables the yeast to grow on defined minimal medium lacking histidine and / or adenine (7).

Methods

Yeast medium

NMY51 reporter strain (9) was cultured in Yeast Extract - Peptone - Dextrose plus Adenine medium (YPAD: 1 % yeast extract (Sigma), 2 % Bacto Peptone (BD), 210 μ M adenine hemisulfate, 2 % glucose). NMY51 transfected with a bait vector was cultured in minimal medium lacking leucine (SD-leu: 38 mM ammonium sulphate, 0.17 % Difco yeast nitrogen base w/o amino acids and ammonium sulphate (BD), 115 μ M L-arginine, 230 μ M L-isoleucine, 164 μ M L-lysine-HCl, 135 μ M L-methionine, 300 μ M L-phenylalanine, 1.68 mM L-threonine, 166 μ M L-tyrosine, 178 μ M L-uracil, 1.28 mM L-valine, 108.6 μ M adenine hemisulfate, 129 μ M L-histidine, 100 μ M L-tryptophan, 2 % glucose). NMY51 co-transfected with bait and prey vectors was cultured in minimal medium lacking leucine and tryptophan (SD-trp-leu: 38 mM ammonium sulphate, 0.17 % Difco yeast nitrogen base w/o amino acids and ammonium sulphate (BD), 115 μ M L-arginine, 230 μ M L-isoleucine, 164 μ M L-lysine-HCl, 135 μ M L-methionine, 300 μ M L-phenylalanine, 1.68 mM L-threonine, 166 μ M L-tyrosine, 178 μ M L-uracil, 1.28 mM L-valine, 108.6 μ M adenine hemisulfate, 129 μ M L-histidine, 2 % glucose). mbSUS library screenings and functional assays were performed in minimal medium lacking leucine, tryptophan and histidine (SD-trp-leu-his: 38 mM ammonium sulphate, 0.17 % Difco yeast nitrogen base w/o amino acids and ammonium sulphate (BD), 115 μ M L-arginine, 230 μ M L-isoleucine, 164 μ M L-lysine-HCl, 135 μ M L-methionine, 300 μ M L-phenylalanine, 1.68 mM L-threonine, 166 μ M L-tyrosine, 178 μ M L-uracil, 1.28 mM L-valine, 108.6 μ M adenine hemisulfate, 2 % glucose) or minimal medium lacking leucine, tryptophan, histidine and adenine (SD-trp-leu-his-ade: 38 mM ammonium sulphate, 0.17 % Difco yeast nitrogen base w/o amino acids and ammonium sulphate (BD), 115 μ M L-arginine, 230 μ M L-isoleucine, 164 μ M L-lysine-HCl, 135 μ M L-methionine, 300 μ M L-phenylalanine, 1.68 mM L-threonine, 166 μ M L-tyrosine, 178 μ M L-uracil, 1.28 mM L-valine, 2 % glucose).

Bait vector construction

Since the prediction programs MEMSAT2 (10) and TMHMM (11) made conflicting predictions of the membrane orientation of SEMP1 (Fig 1A), two prey vectors were generated to facilitate both orientations (Fig. 1B). Therefore full-length *semp1* was PCR amplified from cDNA using primers summarized in table S1 and cloned into the bait vectors pBT3-SUC and pBT3-N (9) via SfiI restriction sites. pBT3-N adds the C-terminal half of ubiquitin (Cub) which itself is fused to a LexA-VP16 TF 5' to *semp1*, pBT3-SUC adds it 3' to *semp1*. Both bait vectors contain the two selectable markers *kan^R* and *leu2* which allow selection of plasmid-bearing cells on medium containing kanamycin (bacteria) or lacking leucine (yeast). pBT3-SUC additionally adds the *S. cerevisiae* signal sequence (SUC2) to the bait's N-terminus, which ensures proper insertion into yeast membranes.

Transformation of the bait vector into the NMY51 yeast reporter strain

A single colony from a 3 day old NMY51 streak was inoculated in 20 ml of liquid YPAD medium (in a 100 ml Erlenmeyer flask) and incubated o/n on a shaker at 275 rpm and 30°C. The titer of the culture was determined using a Neubauer chamber and 2.5×10^8 cells were added to 50 ml pre-warmed YPAD to give 5×10^6 cells / ml. The cells were incubated at 30°C and 275 rpm till the cell titer was 2×10^7 (~5 h). Then the cells were centrifuged (3000 g, 5 min) and the supernatant removed. After the cells were washed in 25 ml ddH₂O (3000 g, 5 min) they were resuspended in 1 ml dd H₂O. Meanwhile single stranded (ss) carrier DNA (2 mg / ml) was boiled at 95°C for 5 min and chilled on ice. The cell suspension was centrifuged (11'000 rpm, 30 sec) and the supernatant discarded. The pellet was resuspended in ddH₂O to a final volume of 1 ml and vortexed vigorously. 100 µl aliquots were distributed into new tubes, centrifuged (11'000 rpm, 30 sec) and the supernatant removed. 360 µl transformation mix (33 % PEG 3350, 100 mM LiOAc, 0.1 mg boiled ss carrier DNA, 2.5 µg bait vector) were added and resuspended by vigorously vortexing. After incubation at 42°C (water bath) for 40 min the cells were pelleted (11'000 rpm, 30 sec) and the supernatant removed. The cells were resuspended in 200 µl

ddH₂O and 100 µl were spread on pre-warmed (30°C) SD-Leu Agar plates. Plates were sealed with parafilm and incubated at 30°C for 3-5 days.

Freezing of yeast strains (Glycerol stocks)

20 ml liquid yeast medium (depending on the strain either YPAD, SD-Leu or SD-Trp) were inoculated from a single colony of a 3 day old streak (in a 100 ml Erlenmeyer flask) and incubated o/n on a shaker at 275 rpm and 30°C. After centrifugation (2600 g, 5 min), the supernatant was removed and the pellet resuspended in 10 ml 2x YPAD containing 25 % Glycerol. 1 ml aliquots were distributed into screw cap cryotubes and frozen at -80°C.

Prey vector construction

Full-length *pf3d7_0702500* and *pf3d7_0601900* were PCR amplified from cDNA using primers summarized in table S1 and cloned into the prey vectors pPR3-N and pPR3-SUC (9) via *SfiI* restriction sites. pPR3-N adds the coding sequence of an N-terminal split-ubiquitin (Nub) 5' to the prey's N-terminus, pPR3-SUC to the C-terminus. Both prey vectors contain the two resistance genes *amp^R* and *trp1* which allow selection by growth on medium containing ampicillin (bacteria) or lacking tryptophan (yeast). pPR3-SUC additionally adds the *S. cerevisiae* signal sequence (SUC2) to the prey's N-terminus, which ensures proper insertion into yeast membranes.

mbSUS functional assay and pairwise interaction assay

To test if SEMP1 inserted correctly into the yeast membrane and was functional in the mbSUS assay, pBT3-SUC-SEMP1 and pBT3-N-SEMP1 were both co-transformed into the NMY51 yeast reporter strain with either of the two control plasmids pOst1-NubI (positive control) and pPR3-N (negative control) to perform a functional assay. A single colony from a 3 day old NMY51 pBT3-SUC-SEMP1 or pBT3-N-SEMP1 streak was inoculated in 20 ml of liquid YPAD medium (in a 100 ml Erlenmeyer flask) and incubated o/n on a shaker at 275 rpm and 30°C. The titer of the culture was determined

and 2.5×10^8 cells were added to 50 ml pre-warmed YPAD to give 5×10^6 cells / ml. The cells were incubated at 30°C and 275 rpm till the cell titer was 2×10^7 . The cells then were centrifuged (3000 g, 5 min) and the supernatant removed. The pellet was washed in 25 ml ddH₂O (3000 g, 5 min) and resuspended in 1 ml dd H₂O. Meanwhile the ss carrier DNA (2 mg / ml) was boiled at 95°C for 5 min and chilled on ice. The cell suspension was centrifuged (11'000 rpm, 30 sec) and the supernatant discarded. The pellet was resuspended in ddH₂O to a final volume of 1 ml and vortexed vigorously. 200 µl aliquots were distributed into new tubes, centrifuged (11'000 rpm, 30 sec) and the supernatant removed. 360 µl transformation mix (33 % PEG 3350, 100 mM LiOAc, 0.2 mg boiled ss carrier DNA, 2.5 µg of either pPR3-N (empty prey vector: negative control) or pOst1-NubI (wild type Nub with strong affinity for Cub: positive control) or prey plasmid DNA) were added and resuspended by vigorously vortexing. After incubation at 42°C (water bath) for 40 min the cells were pelleted (11'000 rpm, 30 sec) and the supernatant removed. Each pellet was resuspended in 1 ml pre-warmed YPAD and incubated at 30°C for 90 min. After centrifugation (11'000 rpm, 30 sec) the supernatant was removed, each pellet resuspended in 180 µl ddH₂O (3 ml total) and 80 µl aliquots were spread on pre-warmed (30°C) SD-Trp-Leu-His / SD-Trp-Leu-His-Ade Agar plates containing 100 mM 3-AT. Additionally a 1:1000 dilution of the transformation was plated on a SD-Trp-Leu plate to determine the transformation efficiency. Plates were sealed with parafilm and incubated at 30°C for 3 (SD-Trp-Leu) or 5 days (SD-Trp-Leu-His / SD-Trp-Leu-His-Ade) before number of colony forming units was determined. Significance of difference in cell growth on selective medium compared to the negative control pPR3-N was determined by Fisher's exact tests.

Results

Functional assay of pBT3-SUC-SEMP1 and pBT3-N-SEMP1

To test if SEMP1 inserted correctly into the yeast membrane and was functional in the mbSUS assay, pBT3-SUC-SEMP1 and pBT3-N-SEMP1 were both co-transformed into the NMY51 yeast reporter strain with either of the two control plasmids pOst1-NubI (positive control) and pPR3-N (negative control). The transformed cells were plated onto selective medium (SD-trp-leu, SD-trp-leu-his and SD-trp-leu-his-ade) and after incubation at 30°C for 5 days the number of grown colonies was determined. Figure 1C shows that 9 % of the yeast cells co-transformed with pBT3-SUC-SEMP1 and pOST1-NubI (positive control) grew on minimal medium lacking histidine (SD-trp-leu-his). In contrast no colony was obtained with the empty prey vector pPR3-N (negative control) under the same conditions. While the pBT3-SUC-SEMP1 bait seems to be correctly expressed and functional to a certain degree, the ratio of pOst1-NubI bearing cells which grow on selective medium is with ~ 9 %, respectively 0.5 % under more stringent conditions (SD-trp-leu-his-ade) quite low. The pBT3-N-SEMP1 bait seems to be not functional in this assay. This would suggest that SEMP1 is a type I transmembrane protein.

mbSUS pairwise interaction assay of SEMP1 with PF3D7_0702500 or PPF3D7_0601900

Both TM domain-bearing PEXEL-negative exported proteins (PNEPs) PF3D7_0702500 and PPF3D7_0601900 were identified by Co-IP as potential interaction partners of the integral MC protein SEMP1. To investigate potential binding of SEMP1 with either of the two candidates, a mbSUS pairwise interaction assay was performed. Since the different TM prediction tools gave conflicting results about membrane orientation of PF3D7_0702500 and PPF3D7_0601900 (either type I or type II TM proteins), two prey vectors were generated for each gene facilitating either direction and tested for potential interaction (Fig. 2A). After transformation of the pPR3-N-PF3D7_0702500 or

PPF3D7_0601900 and pPR3-SUC-PF3D7_0702500 or PPF3D7_0601900 prey vectors into the pBT3-SUC-SEMP1 bearing NMY51 yeast reporter strain cells were plated onto SD-trp-leu-his. After incubation at 30°C for 5 days the number of grown colonies was determined for each combination. Although only few colonies were obtained in all four screens the number of colonies obtained with pPR3-N-PPF3D7_0601900 bearing cells were significantly higher ($p < 0.001$) than with pPR3-N containing cells (negative control) when grown on selective medium (SD-trp-leu-his) (Figure 2B). This could indicate that direct binding between SEMP1 and PF3D7_0601900 occurred and would also suggest that PF3D7_0601900 is a type II transmembrane protein.

Discussion

Parasite derived membranous structures called Maurer's clefts are important for protein trafficking from the parasite to the RBC membrane, probably by acting as secretory organelles that concentrate virulence proteins for further export. However, their specific function in the export process has yet to be determined (2,3). The same applies to their protein composition: while previous studies successfully identified numerous MC resident proteins (12–14), the fact that ongoing research steadily reveals new candidates (15) indicates that the current MC proteome is far from complete. Since many of these newly identified MC proteins are so called PEXEL-negative exported proteins (PNEPs) which lack a SP and a PEXEL/VTS motif, it is impossible to estimate how many additional MC proteins have yet to be identified.

In an attempt to bring new insight into the function and composition of the MCs we have characterized the new MC protein SEMP1 and thereby identified two potential interaction partners namely PF3D7_0702500 and PF3D7_0601900 by Co-IP experiments. Both have similarities to SEMP1 in that they co-localize at the MCs, all have a two exon structure, they are non syntenic to other *Plasmodium* species, they code for small parasite proteins with unknown function (PlasmoDB), and all three proteins have a predicted single TM domain and neither a PEXEL/VTS motif nor a SP.

To investigate PF3D7_0702500 and PF3D7_0601900 for interaction with SEMP1 a mbSUS pairwise interaction assay was performed. The basic requirement of the mbSUS is exposure of the split ubiquitin into the cytoplasm (7) which makes bait protein orientation within the yeast membrane a crucial selection criteria for the bait vector that determines to which end the Cub is added. Since it was unclear in which orientation SEMP1 would integrate into the membrane two different baits were generated to cover both possibilities. Because SEMP1 lacks a classical SP, the *S. cerevisiae* signal sequence SUC2 was added to the N-terminus of the SEMP1 bait clone which had the Cub fragment fused to its C-terminus to ensure membrane insertion. Functional assays revealed that both baits seemed to be correctly expressed but only the one with the C-terminal Cub was functional. From this we concluded that SEMP1 is a type I TM protein similar to e.g. MAHRP1 (12).

The functional pBT3-SUC-SEMP1 bait clones were used in a mbSUS pairwise interaction assay to test binding to PF3D7_0702500 or PF3D7_0601900. Since membrane orientation of these proteins was also unclear, prey vectors were generated to facilitate both orientations and used in the screen. No binding could be detected between SEMP1 and PF3D7_0702500 ($p = 0.549$) whilst pRR3-N-PF3D7_0601900 bearing cells together with SEMP1 produced significantly ($p < 0.001$) more colonies on selective medium than the negative control. Although these results suggested specific binding between SEMP1 and PF3D7_0601900, the small number of colonies is of concern. It could indicate that the interaction of both proteins is weak, the bait is inefficiently expressed, or the Cub fragment is poorly accessible. The latter two reasons are likely since even under non-stringent screening conditions the SEMP1 bait only achieved a growth ratio of 9 % in the functional assay and it is possible that the bait-prey interaction hinders reconstitution of a functional ubiquitin. With the available control it was not possible to confirm the correct expression of the prey protein and the high AT content of 80 % of *P. falciparum* genes (16) could have hindered protein expression in yeast (17) leading to an inefficient prey expression. However, the significant number of colonies with PF3D7_0601900 gives strong evidence for a direct interaction but the lack of growth does not exclude such interaction between SEMP1 and PF3D7_0702500. Further examination is therefore needed, e.g. by pull-down assays or Far-western-blot experiments. For quantification of the detected interactions more complex analyses should be considered: Surface Plasmon Resonance (SPR) studies (18) would allow investigation of very small protein amounts without labelling and thereby not only determine association but also dissociation rates. The disadvantage of SPR is that immobilized proteins may be inactivated. Isothermal Titration Calorimetry (ITC) is the most quantitative technique available for measuring the thermodynamic properties of protein-protein interactions and would allow investigation of proteins in solution. However, application for membrane proteins was shown to be difficult (19). Spectroscopy study by NMR would also allow investigation of proteins in solution and in addition was already successfully used to verify interactions of exported *P. falciparum* proteins (20).

The preceding co-IPs and Immunofluorescence assays (chapter 4) indicate that SEMP1, PF3D7_0601900, PF3D7_0702500 and ‘ring exported protein 1’ (REX1) might all be part of the same protein complex. mbSUS analysis should therefore be expanded to test direct binding between all these proteins. Further, substantiation of the correctness of the co-IP results by this mbSUS study gives reason to characterize PF3D7_0601900 and PF3D7_0702500 in more detail. Generation of specific antibodies would allow localization of the endogenous protein instead of an episomally overexpressed one (chapter 4) and knockout studies might enable functional characterization. Finally co-IP experiments would expand our knowledge of the interaction network centred around SEMP1.

In conclusion, the results from the pairwise interaction assay with SEMP1 and PF3D7_0601900 using the mbSUS need to be confirmed again but showed the applicability of this system to investigate membrane protein interactions in *P. falciparum*. The results from the co-IP presented in chapter 4 also add strong evidence for this interaction and support the notion that the mbSUS pairwise interaction assays could become a powerful tool for the confirmation of membrane protein interactions. However, the performed experiments made it also apparent that probably not all *P. falciparum* membrane proteins are suited for investigation by mbSUS. Since the investigated SEMP1 bait protein appeared to be suboptimal for investigation by mbSUS, either because of ineffective expression or hindered accessibility of the split ubiquitin, it has to be assumed that several *P. falciparum* membrane proteins are completely inapplicable for this promising system. However, in the absence of flawless alternatives mbSUS remains an intriguing strategy for verification of *P. falciparum* membrane protein interactions.

References

1. World Health Organization. WHO | World Malaria Report 2012. 2009.
2. Przyborski JM, Wickert H, Krohne G, Lanzer M. Maurer's clefts--a novel secretory organelle? *Mol Biochem Parasitol*. 2003 Nov;132(1):17–26.
3. Bhattacharjee S, van Ooij C, Balu B, Adams JH, Haldar K. Maurer's clefts of *Plasmodium falciparum* are secretory organelles that concentrate virulence protein reporters for delivery to the host erythrocyte. *Blood*. 2008 Feb 15;111(4):2418–26.
4. Heiber A, Kruse F, Pick C, Grüring C, Flemming S, Oberli A, et al. Identification of New PNEPs Indicates a Substantial Non-PEXEL Exportome and Underpins Common Features in *Plasmodium falciparum* Protein Export. *PLoS Pathog*. 2013 Aug 8;9(8):e1003546.
5. Glenister FK, Coppel RL, Cowman AF, Mohandas N, Cooke BM. Contribution of parasite proteins to altered mechanical properties of malaria-infected red blood cells. *Blood*. 2002 Feb 1;99(3):1060–3.
6. Cooke BM, Glenister FK, Mohandas N, Coppel RL. Assignment of functional roles to parasite proteins in malaria-infected red blood cells by competitive flow-based adhesion assay. *Br J Haematol*. 2002 Apr;117(1):203–11.
7. Iyer K, Bürkle L, Auerbach D, Thaminy S, Dinkel M, Engels K, et al. Utilizing the split-ubiquitin membrane yeast two-hybrid system to identify protein-protein interactions of integral membrane proteins. *Sci STKE Signal Transduct Knowl Environ*. 2005 Mar 15;2005(275):pl3.
8. Johnsson N, Varshavsky A. Split ubiquitin as a sensor of protein interactions in vivo. *Proc Natl Acad Sci U S A*. 1994 Oct 25;91(22):10340–4.
9. Dualsystems. DUALmembrane Protein Interaction Kits [Internet]. Available from: http://www.dualsystems.com/fileadmin/user_upload/z_download/manuals/DUAL_membrane-starter-kit_user-manual-A14.pdf
10. Jones DT, Taylor WR, Thornton JM. A model recognition approach to the prediction of all-helical membrane protein structure and topology. *Biochemistry (Mosc)*. 1994 Mar 15;33(10):3038–49.
11. Krogh A, Larsson B, von Heijne G, Sonnhammer EL. Predicting transmembrane protein topology with a hidden Markov model: application to complete genomes. *J Mol Biol*. 2001 Jan 19;305(3):567–80.

12. Spycher C, Klonis N, Spielmann T, Kump E, Steiger S, Tilley L, et al. MAHRP-1, a novel *Plasmodium falciparum* histidine-rich protein, binds ferriprotoporphyrin IX and localizes to the Maurer's clefts. *J Biol Chem*. 2003 Sep 12;278(37):35373–83.
13. Blisnick T, Morales Betoulle ME, Barale JC, Uzureau P, Berry L, Desroses S, et al. Pfsbp1, a Maurer's cleft *Plasmodium falciparum* protein, is associated with the erythrocyte skeleton. *Mol Biochem Parasitol*. 2000 Nov;111(1):107–21.
14. Hawthorne PL, Trenholme KR, Skinner-Adams TS, Spielmann T, Fischer K, Dixon MWA, et al. A novel *Plasmodium falciparum* ring stage protein, REX, is located in Maurer's clefts. *Mol Biochem Parasitol*. 2004 Aug;136(2):181–9.
15. Mbengue A, Audiger N, Violla E, Dubremetz J-F, Braun-Breton C. Novel *Plasmodium falciparum* Maurer's clefts protein families implicated in the release of infectious merozoites. *Mol Microbiol*. 2013 Apr;88(2):425–42.
16. Gardner MJ, Hall N, Fung E, White O, Berriman M, Hyman RW, et al. Genome sequence of the human malaria parasite *Plasmodium falciparum*. *Nature*. 2002 Oct 3;419(6906):498–511.
17. Sibley CH, Brophy VH, Cheesman S, Hamilton KL, Hankins EG, Wooden JM, et al. Yeast as a model system to study drugs effective against apicomplexan proteins. *Methods San Diego Calif*. 1997 Oct;13(2):190–207.
18. Szabo A, Stolz L, Granzow R. Surface plasmon resonance and its use in biomolecular interaction analysis (BIA). *Curr Opin Struct Biol*. 1995 Oct;5(5):699–705.
19. Rajarathnam K, Rösger J. Isothermal titration calorimetry of membrane proteins - Progress and challenges. *Biochim Biophys Acta*. 2014 Jan;1838(1):69–77.
20. Mayer C, Slater L, Erat MC, Konrat R, Vakonakis I. Structural analysis of the *Plasmodium falciparum* erythrocyte membrane protein 1 (PfEMP1) intracellular domain reveals a conserved interaction epitope. *J Biol Chem*. 2012 Mar 2;287(10):7182–9.

Figure legends

Figure 1 Orientation of SEMP1 in the yeast membrane. A. Different prediction program gave contrasting results for the orientation of SEMP1. MEMSAT (left) predicted SEMP1 as a type I TM protein, while TMHMM (right) predicted SEMP1 to be a type II TM protein. B. Two SEMP1-bait vectors were generated to facilitate both orientations: pBT3-SUC-SEMP1 to facilitate a type I TM protein, pBT3-N-SEMP1 to facilitate a type II TM protein. Cub = C-terminal split ubiquitin, NubI = wild type N-terminal ubiquitin, N = nucleus, RG = reporter gene, TF = transcription factor. C. Both baits were co-transformed into the yeast reporter strain NMY51 with either the empty library plasmid pPR3-N (negative control) or the control plasmid pOst1-NubI which contains a wild-type N-terminal ubiquitin (NubI) which has a strong Cub-affinity (positive control). The transformed cells were spread on selective medium (SD-trp-leu / SD-trp-leu-his / SD-trp-leu-his-ade) and the number of colony forming units was determined after incubation at 30°C for 4 days. The number in brackets indicates the ratio of grown cells compared to distributed cells (SD-trp-leu).

Figure 2 mbSUS pairwise interaction assay of SEMP1 with either PF3D7_0702500 or PF3D7_0601900. A. For both PF3D7_0702500 and PF3D7_0601900 two prey vectors were generated to also facilitate the unknown transmembrane orientation: pBT3-SUC-PF3D7_0702500 and PF3D7_0601900 to facilitate a type I TM protein, pBT3-N-PF3D7_0702500 and PF3D7_0601900 to facilitate a type II TM protein. Cub = C-terminal split ubiquitin, Nub = N-terminal ubiquitin with point mutation, N = nucleus, RG = reporter gene, TF = transcription factor. B: These prey vectors and the empty pPR3-N plasmid (negative control) were transformed into the pBT3-SUC-SEMP1 bearing yeast reporter NMY51. Transformed cells were spread onto selective medium (SD-trp-leu / SD-trp-leu-his) and after incubation for 5 days at 30°C the number of CFUs was determined. Significance of difference in cell growth compared to the negative control pPR3-N was determined by Fisher's exact test and p-values are shown in brackets.

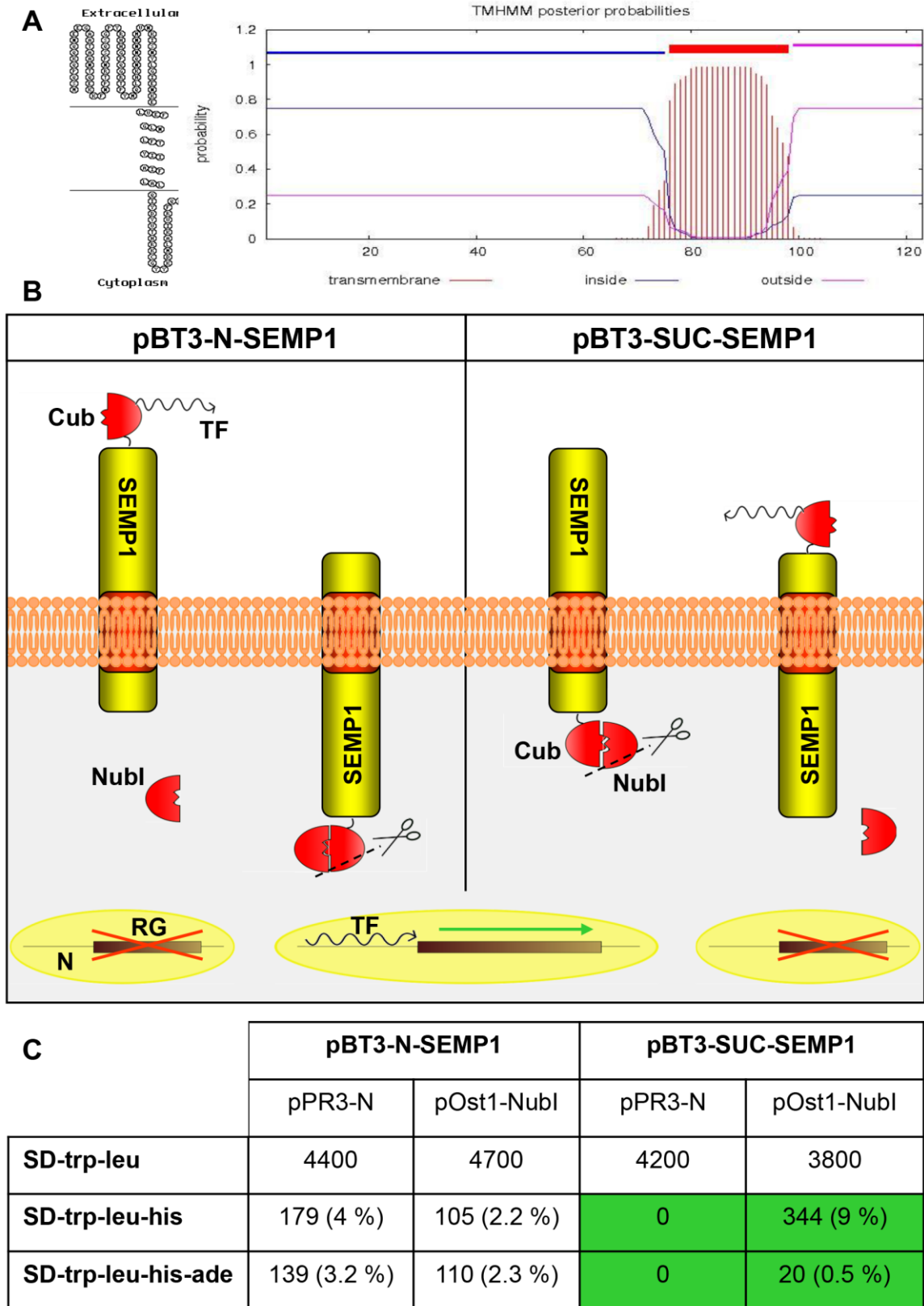


Figure 1

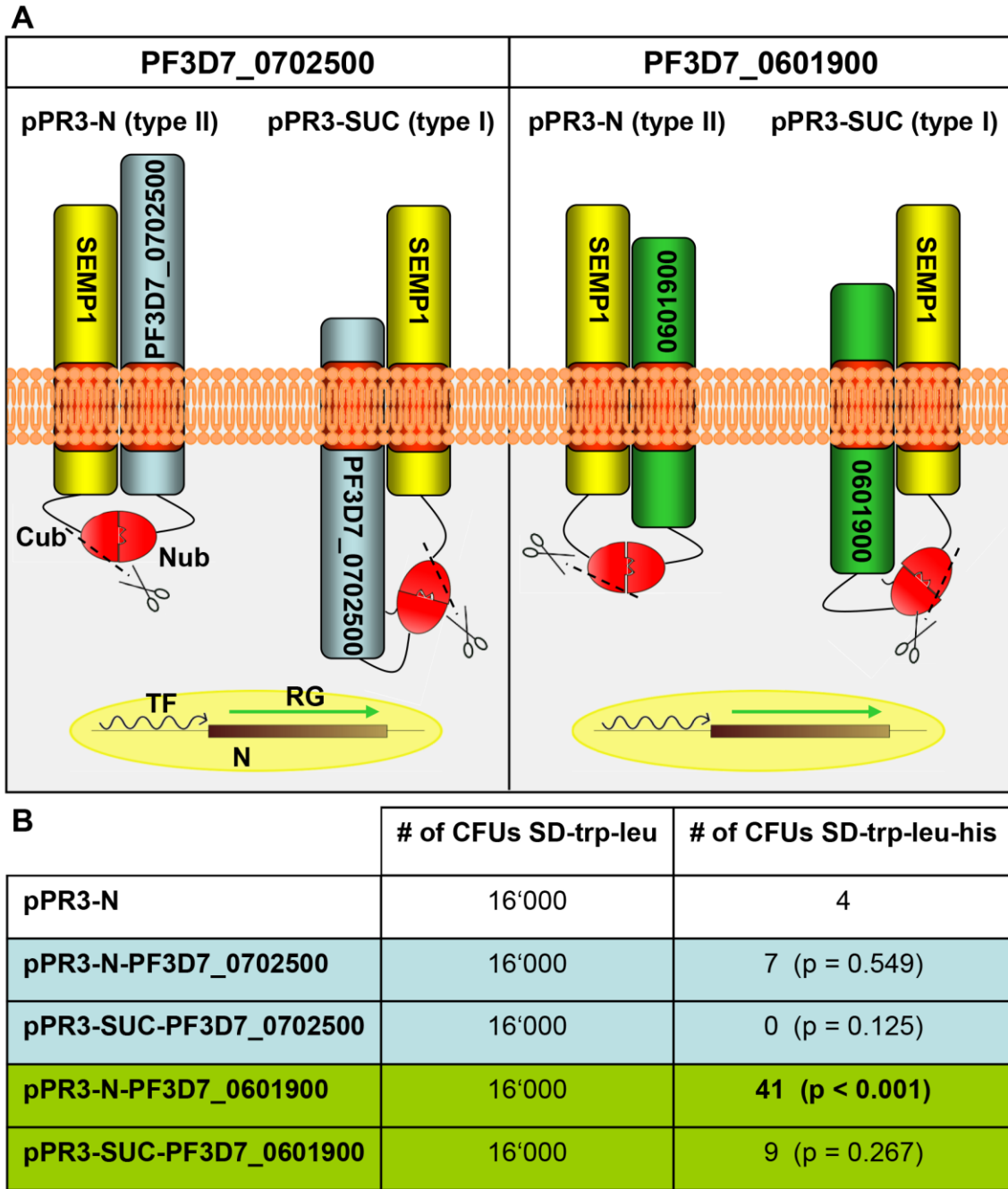


Figure 2

Supplementary table 1. Primers used for mbSUS bait and prey vector generation

Gene	Primer	Sequence	RS	vector	
SEMP1	F	ATTAACAAGGCCATTACGGCCAGTCAACCACAAAAACAACAAAAC	Sfil	pBT3-SUC	bait
	R	AACTGATTGGCCGAGGCGGCCCTTTTGC GTTCTGTAAACTGGCTT	Sfil	pBT3-SUC	
	F	ATTAACAAGGCCATTACGGCCATGAGTCAACCACAAAAACAACA	Sfil	pBT3-N	
	R	AACTGATTGGCCGAGGCGGCCCTTATTTTGC GTTCTGTAAACTGG	Sfil	pBT3-N	
PF3D7_0702500	F	ATTAACAAGGCCATTACGGCCATGGCTTATCCTCTTTTAGAAGA	Sfil	pPR3-N	prey
	R	AACTGATTGGCCGAGGCGGCCCTTATACATGAGCTTCATTAGTGTT	Sfil	pPR3-N	
	F	ATTAACAAGGCCATTACGGCCGCTTATCCTCTTTTAGAAGATGA	Sfil	pPR3-SUC	
	R	AACTGATTGGCCGAGGCGGCCCTACATGAGCTTCATTAGTGTTTAA	Sfil	pPR3-SUC	
PF3D7_0601900	F	ATTAACAAGGCCATTACGGCCATGACGGACCATTTATTGGATTT	Sfil	pPR3-N	
	R	AACTGATTGGCCGAGGCGGCCCTAATTTTCTGCATTGGCTGAAG	Sfil	pPR3-N	
	F	ATTAACAAGGCCATTACGGCCACGGACCATTTATTGGATTTAAT	Sfil	pPR3-SUC	
	R	AACTGATTGGCCGAGGCGGCCCTTTTCTGCATTGGCTGAAGCA	Sfil	pPR3-SUC	

Chapter 6

General Discussion

General Discussion

Despite enormous control efforts Malaria remains one of the world's most devastating human infectious diseases. The causative agent of the most deadly form called malaria tropica is the apicomplexan parasite *Plasmodium falciparum*. Most of the parasite's pathology is associated with its asexual development within the red blood cell. Because the human erythrocyte is a highly specialized cell which is devoid of all internal organelles, survival of *P. falciparum* critically depends on extensive host cell refurbishments. These are mediated by the export of numerous parasite proteins into the erythrocyte cytoplasm, including parasite derived membranous structures termed Maurer's clefts (MCs) which are believed to function as a surrogate Golgi by concentrating virulence proteins for delivery to the RBC membrane (1,2). One of these virulence proteins is the variable surface antigen 'P. falciparum erythrocyte membrane protein 1' (PfEMP1), which after insertion into the erythrocyte membrane mediates adhesion to endothelial receptors. Thereby it not only prevents elimination of infected RBCs in the spleen, but as a side-effect also causes organ failure and cerebral malaria (3). Because this transport of parasite proteins into the host cell is the source of severe *P. falciparum* pathology, identification and characterization of the components of the transport system is of major interest. Although MCs were shown to play a major role in export of virulence proteins (1,2), their precise function remains elusive. In an attempt to bring new insight into the function and composition of these important structures, we identified and characterized the new integral MC protein 'small exported membrane protein 1' (SEMP1) by immunofluorescence assays, knockout studies, co-immunoprecipitation (co-IP) and transcriptional analysis (chapter 4).

Studies on model organisms revealed that protein-protein interactions (PPIs) play a major role in eukaryotic protein secretion which is so important that for their identification James Rothman, Randy Schekman and Thomas Südhof were honoured with the Nobel Prize in Physiology or Medicine in 2013 (4,5). Despite their prime importance, still very little is known about PPIs of secreted *P. falciparum* proteins. The reasons for that are manifold. Because of the parasite's large evolutionary distance to eukaryotic model organisms, about 60 % of its genes lack similarity to functionally annotated genes (6).

Interaction partners of their proteins can therefore only be experimentally identified, which is additionally hindered by the complexity of the parasite's intracellular life cycle. To overcome the described difficulties, high throughput yeast-two-hybrid (Y2H) screenings were undertaken to generate a first *P. falciparum* PPI network (7). However, due to the hydrophobic nature, membrane proteins are not suitable for investigation by Y2H since they insert into the yeast membranes. *P. falciparum* membrane protein interactions have therefore so far been largely ignored. Since the many exported parasite proteins were shown to be membrane proteins, like the 'membrane associated histidine-rich protein 1' (MAHRP1) (8), an alternative approach is needed in order to generate an extensive interaction network of exported *P. falciparum* proteins. With this study we aimed at bringing new insight into interactions of exported *P. falciparum* proteins and thereby establishing a basis for the generation of the interactome of the parasite's exportome. Therefore we not only performed interaction studies using classical approaches like co-IP, but also tried to establish the mating-based split-ubiquitin system (mbSUS) (9) as a new *in vitro* interaction platform for *P. falciparum* membrane proteins on the basis of the integral Maurer's cleft protein MAHRP1.

Generation of a new interaction network of exported *P. falciparum* proteins

In order to expand our knowledge on interactions of exported *P. falciparum* proteins and to create a starting point for generation of a new protein-protein interaction network (Fig. 1), we performed two independent co-IP experiments with the integral MC resident SEMP1. Thereby peptides of three different parasite proteins, namely the 'ring exported protein 1' (REX1), PF3D7_0702500 and PF3D7_0601900 could be detected in both experiments. While REX1 is a well characterized MC protein which was shown to be essential for PfEMP1 export to the RBC membrane (10), the other two proteins were previously uncharacterized. All three candidates were PEXEL-negative exported proteins (PNEPs) which co-localized with SEMP1 at the MCs and had a predicted single transmembrane (TM) domain. Additionally to these three top candidates, peptides of four other exported proteins could be detected in either one of the two experiments: the parasite-infected erythrocyte surface protein (PIESP2), the *P. falciparum* antigen 332

(Pf332), the membrane associated histidine rich protein 2 (MAHRP2) and the heat shock protein 70-x (HSP70-x). Like SEMP1 the two exported proteins PIESP2 and Pf332 are mainly associated with MCs, but also with the erythrocyte membrane. Although these proteins could only be detected in the second co-IP experiment which was more sensitive, their co-localization with SEMP1 (chapter 4) makes them interesting candidates. Due to their localization to different compartments of the infected erythrocyte, an interaction of SEMP1 with MAHRP2 found at tethers, or HSP70-x found in J-dots seems less likely.

PIESP2 as a potential SEMP1 interactor was previously also co-precipitated in two independent experiments with the integral MC protein MAHRP1 (Annette Gaida, unpublished). MAHRP1 was not co-precipitated with SEMP1 but it appears that these two proteins could be indirectly connected via the common interactor PIESP2. MAHRP1 co-IP experiments also identified PF3D7_0501000 as a potential MAHRP1 interactor which was supported by the finding presented in chapter 3 where both PIESP2 and PF3D7_0501000 were shown to be membrane proteins co-localizing with MAHRP1 at the MCs. Although this is circumstantial evidence it could suggest a MAHRP1-PIESP2 / PF3D7_0501000 interaction.

Co-IP experiments with membrane proteins always bear the risk that identified proteins are not real interactors but co-precipitated as constituents of the same membrane fragment. To counteract this problem we extracted parasite proteins with 1 % sodium dodecyl sulphate (SDS), a detergent that breaks down membranes by emulsifying the lipids and proteins. However, although extraction with SDS reduced the described risk significantly, the identified interactions should be further analyzed to resolve all doubt. To investigate if some of the potential PPIs identified by co-IP were binding directly, pairwise interaction assays using the mbSUS were performed. While neither the MAHRP1 – PIESP2 or PF3D7_0501000 nor the SEMP1 – PF3D7_0702500 interaction could be confirmed, the mbSUS assays showed a weak but significant interaction of SEMP1 with another MC protein (PF3D7_0601900). This was in agreement with the previously described co-IP results which together strongly suggested an interaction between SEMP1 and PF3D7_0601900. Possible follow-up experiments for further verification are pull-down assays or NMR spectroscopy studies which would even allow quantification of the detected interactions.

The comparison of our data on this small preliminary PPI network of exported *P. falciparum* proteins to the large-scale Y2H data of LaCount et al (7) showed three new potential interaction partners for Pf332 which were all uncharacterized. These were the PHIST protein PF3D7_0936800, the exported protein with unknown function PF3D7_0730800.1, and the conserved *Plasmodium* protein with unknown function PF3D7_1325800. LaCount et al. (7) predicted in addition an interaction between MAHRP2 and the putative CCR4-NOT transcription complex subunit 4 PF3D7_1235300. For all other members which we had identified in this PPI network they either found no interactions or they were observed once and therefore not reliable. In particular, none of the potential interaction partners we had identified by co-IP was detected in the Y2H study proving again the non-suitability of the Y2H for the investigation of exported parasite proteins.

In summary, we have potentially generated a small PPI network of exported parasite proteins centred around the two integral MC proteins SEMP1 and MAHRP1 by combining co-IPs, mbSUS assays and the results from a previous large-scale- Y2H study (Fig.1). While most of the identified potential interactions still need further confirmation, e.g. by pull down assays, Far Western blotting, fluorescence resonance energy transfer (FRET), NMR spectroscopy studies, Isothermal Titration Calorimetry (ITC) or Surface Plasmon Resonance (SPR) studies, this could be the basis for numerous follow-up studies which in the end will result in a comprehensive PPI network of exported *P. falciparum* proteins.

Functional characterization of SEMP1

Since disruption of the *semp1* gene did not result in any obvious phenotypic changes under culture conditions we decided to investigate the function of SEMP1 by interaction studies. By two independent co-IP experiments we identified several potential SEMP1 interaction partners: the five Maurer's clefts proteins REX1, Pf332, PIESP2, PF3D7_0702500 and PF3D7_0601900, as well as the tether protein MAHRP2 and the J-dot protein HSP70-x. Additional co-IPs further revealed a potential indirect interaction between SEMP1 and the integral MC protein MAHRP1 via the common interactor

PIESP2. While for some of these identified potential interacting proteins the function is unknown, others have been extensively studied and functionally characterized. Both MC proteins REX1 and MAHRP1 were shown to be essential for PfEMP1 trafficking and maintaining the MC ultrastructure. In REX1 knockout parasites PfEMP1 was still exported to the MCs but not efficiently presented at the erythrocyte membrane (1), while MAHRP1 deletion abolished PfEMP1 export to the MCs (2). Pf332 is a large peripheral MC protein which also associates with the RBC membrane similar to SEMP1. Knock-out studies showed that it also disrupted PfEMP1 transport and the structure of the MCs, but additionally modulated the erythrocyte membrane rigidity (3,4). The exported chaperone HSP70-x has been shown to be a component of highly mobile structures in the erythrocyte cytoplasm called J-dots and could probably also be involved in PfEMP1 transport (5,6). It is important to note that the four potential SEMP1 interactors REX1, MAHRP1, Pf322, and HSP70-x are all involved in PfEMP1 export, and in determining MC ultrastructure or modulating erythrocyte membrane rigidity. Whether this suggests any indirect involvement of SEMP1 in PfEMP1 trafficking remains to be elucidated but seems unlikely since knock-out of SEMP1 had no effect on PfEMP1 export to the RBC surface and binding of infected erythrocytes to CD36 under static conditions. Nevertheless, it might be possible that SEMP1 is involved in determining MC structure or modulation of erythrocyte membrane rigidity. For the latter there is some evidence from the transcriptional analysis which revealed up-regulation of PfEMP3 in absence of SEMP1. Similar to SEMP1 the exported parasite protein PfEMP3 first associates with MCs but is later transported further to the cytoplasmic face of the RBC membrane (7). PfEMP3 seems to be involved in PfEMP1 trafficking (8) but was also shown to mediate loss of mechanical stability of the RBC membrane by binding to actin and spectrin (9,10). In the absence of SEMP1 not only PfEMP3 potentially involved in modulation of the RBC membrane rigidity was transcriptionally up-regulated but also a *Plasmodium* helical interspersed subtelomeric (PHIST) protein (PF3D7_0532300) which has not been characterized but some other members of the PHIST family have been shown to be involved in alteration of the RBC membrane (11). If we speculate that *pfemp3* and *phist* transcription were altered by the parasite to compensate for the loss of SEMP1, this would indicate an involvement of SEMP1 in similar functions.

Taking together co-IP results and the transcriptome analysis, there is some evidence that SEMP1 might be indirectly involved in PfEMP1 trafficking and/or modulation of RBC membrane rigidity and determination of MC structure. However, knock out studies proved that SEMP1 is not essential for PfEMP1 export and insertion into the RBC membrane. Its involvement in altering RBC membrane rigidity or MC structure remains to be determined. Further investigation into these two possibilities is needed e.g. by deformability testing with atomic force microscopy (AFM), an artificial spleen system (12), a laser-assisted optical rotational cell analyzer (LORCA) (13) or electron microscopy (EM).

Combination of co-IP and mbSUS: a new strategy for identification and verification of direct *P. falciparum* membrane protein interactions?

Because we could not prove the functionality of our *P. falciparum* blood stage cDNA library (chapter 2) the mbSUS can yet not be used to identify new interaction partners. However, if it would be functional in pairwise interaction assays, as suggested by the significant increase in growth of yeast cells co-expressing SEMP1 and PF3D7_0601900 (chapter 5), it would provide a new tool to verify potential direct binding of two implicated interacting proteins. Those candidates for pairwise mbSUS testing could be identified using the optimized co-IP protocol described in chapter 4 which showed a remarkable specific elution due to usage of HA peptides and anti-HA matrix. Such combination of co-IP and mbSUS could represent a new strategy for identification and confirmation of direct *P. falciparum* membrane protein interactions.

However, it became apparent that not all *P. falciparum* membrane proteins seemed to be suited for the mbSUS. While the MAHRP1 bait was able to trigger growth in 30 % yeast cells containing the positive control under stringent screening conditions, SEMP1 yielded only 0.5 % under the same conditions. While this could be improved to 9 % by reducing stringency, the observation that of two investigated bait proteins only one is functional under stringent conditions indicates that several *P. falciparum* membrane proteins might be inapplicable for this promising system. The mbSUS might therefore only be used to confirm but not refute direct binding between two potential interactors. However, the

proposed combination of co-IP and mbSUS remains an intriguing strategy for identification and verification of *P. falciparum* membrane protein interactions.

Functional characterization of exported *P. falciparum* proteins by comparative transcriptome analysis

With SEMP1 we identified a non-essential exported *P. falciparum* protein for which no phenotypical changes could be observed in knock-out parasites. Disruption of the *semp1* gene was shown to neither have an effect on export of the major parasite virulence factor PfEMP1 nor on gametocyte formation. The lack of altered phenotypes after gene knock-out is not an exception but rather the rule. A large-scale study which previously produced knock-out parasites for 39 exported *P. falciparum* proteins only was able to identify phenotypical changes for 15 clones (38.5 %) (20). In our lab we have made similar experience with a number of knock out clones as with SEMP1. At first glance these observations might suggest that many exported parasite proteins are redundant but the expression and export of proteins is associated with high energy costs for the parasite, and makes this rather unlikely. One possible explanation would be that these proteins are involved in processes others than observed under culture conditions. The *in vitro* cultivation of *P. falciparum* used for studying the intraerythrocytic cycle of the parasite (22) does not reflect the conditions found in the human body. All nutrients abound and interactions with the immune system are completely missing, hence it is possible that these proteins are involved in processes such as signal transduction or other immune evasion mechanisms which are difficult to be investigated under culture conditions. It becomes very difficult to investigate these processes and one possibility to overcome these problems would be to do *in vivo* studies in monkeys (23). However, such experiments are too difficult, ethically problematic, and expensive to be performed on a routine basis.

The lack of phenotypical changes in parasites with various genes knocked-out could also be due to compensatory mechanisms by up-regulating transcription of other genes with similar function. This could be examined by comparative transcriptome analysis and by using this approach we showed that in absence of SEMP1 the transcription of several

parasite genes is slightly up-regulated, including PfEMP3 which contributes to a loss of mechanical stability of the RBC membrane via binding to spectrin and actin (18,19). This gives circumstantial evidence that SEMP1 potentially could be involved in modifying RBC membrane rigidity in concert with PfEMP3.

However, since the conditional SEMP1 knock-out parasite grew normally after withdrawal of shield, the transcriptional changes cannot have been resulted by selection but would require feedback-driven transcriptional regulation of exported *P. falciparum* proteins. This increased PfEMP3 transcription needs to be confirmed e.g. by qPCR to speculate on such feedback regulation.

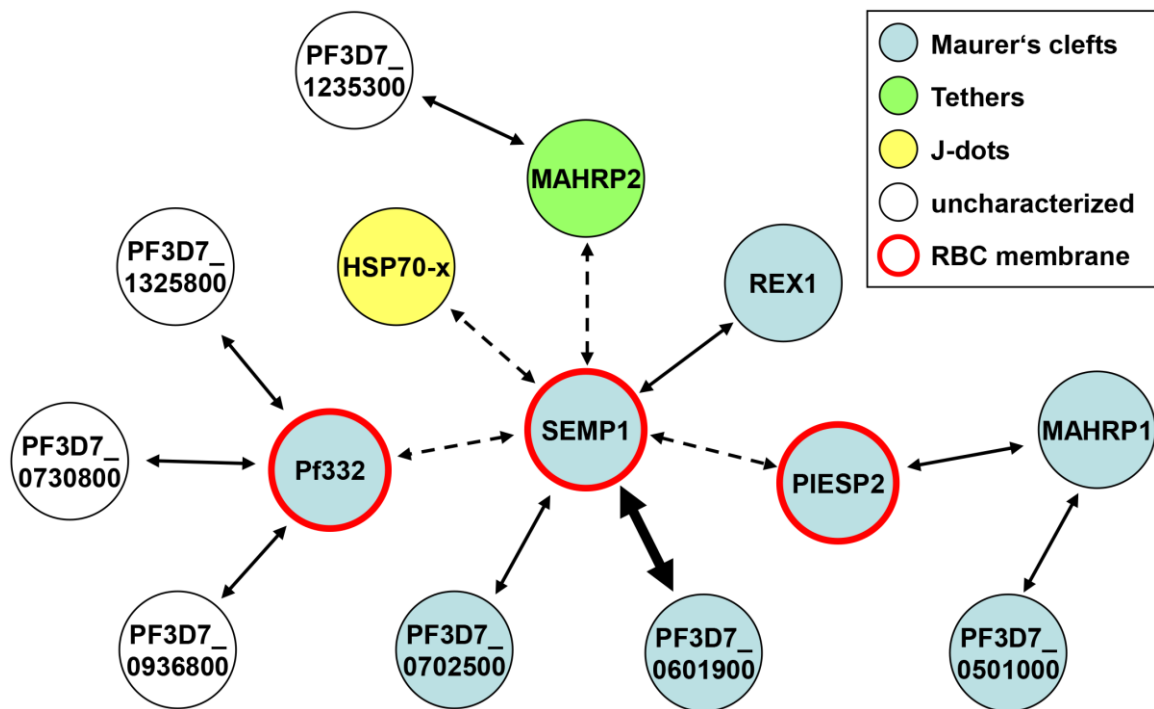


Figure 1 Interaction network of exported *P. falciparum* proteins. By combining co-immunoprecipitation (co-IP) and mating-based split ubiquitin system (mbSUS) results a small network of potential protein-protein (PPI) interactions was generated. The arrows thereby indicate the likelihood of the respective interaction: dashed arrows represent interactions only detected once by co-IP, fine solid arrows stand for interactions either observed twice by co-IP or at least five times in a large-scale yeast-two-hybrid study by LaCount et al. (7), and the thick arrow indicates an interaction detected twice by co-IP and significant ($p < 0.001$) in an mbSUS pairwise interaction assay. The colours indicate the subcellular localization of the respective protein.

References

1. Przyborski JM, Wickert H, Krohne G, Lanzer M. Maurer's clefts--a novel secretory organelle? *Mol Biochem Parasitol*. 2003 Nov;132(1):17–26.
2. Bhattacharjee S, van Ooij C, Balu B, Adams JH, Halder K. Maurer's clefts of *Plasmodium falciparum* are secretory organelles that concentrate virulence protein reporters for delivery to the host erythrocyte. *Blood*. 2008 Feb 15;111(4):2418–26.
3. Miller LH, Baruch DI, Marsh K, Doumbo OK. The pathogenic basis of malaria. *Nature*. 2002 Feb 7;415(6872):673–9.
4. Rothman JE. Mechanisms of intracellular protein transport. *Nature*. 1994 Nov 3;372(6501):55–63.
5. Schekman R, Orci L. Coat proteins and vesicle budding. *Science*. 1996 Mar 15;271(5255):1526–33.
6. Gardner MJ, Hall N, Fung E, White O, Berriman M, Hyman RW, et al. Genome sequence of the human malaria parasite *Plasmodium falciparum*. *Nature*. 2002 Oct 3;419(6906):498–511.
7. LaCount DJ, Vignali M, Chettier R, Phansalkar A, Bell R, Hesselberth JR, et al. A protein interaction network of the malaria parasite *Plasmodium falciparum*. *Nature*. 2005 Nov 3;438(7064):103–7.
8. Spycher C, Klonis N, Spielmann T, Kump E, Steiger S, Tilley L, et al. MAHRP-1, a novel *Plasmodium falciparum* histidine-rich protein, binds ferriprotoporphyrin IX and localizes to the Maurer's clefts. *J Biol Chem*. 2003 Sep 12;278(37):35373–83.
9. Iyer K, Bürkle L, Auerbach D, Thaminy S, Dinkel M, Engels K, et al. Utilizing the split-ubiquitin membrane yeast two-hybrid system to identify protein-protein interactions of integral membrane proteins. *Sci STKE Signal Transduct Knowl Environ*. 2005 Mar 15;2005(275):pl3.
10. Dixon MWA, Kenny S, McMillan PJ, Hanssen E, Trenholme KR, Gardiner DL, et al. Genetic ablation of a Maurer's cleft protein prevents assembly of the *Plasmodium falciparum* virulence complex. *Mol Microbiol*. 2011 Aug;81(4):982–93.
11. Spycher C, Rug M, Pachlatko E, Hanssen E, Ferguson D, Cowman AF, et al. The Maurer's cleft protein MAHRP1 is essential for trafficking of PfEMP1 to the surface of *Plasmodium falciparum*-infected erythrocytes. *Mol Microbiol*. 2008 Jun;68(5):1300–14.

12. Glenister FK, Fernandez KM, Kats LM, Hanssen E, Mohandas N, Coppel RL, et al. Functional alteration of red blood cells by a megadalton protein of *Plasmodium falciparum*. *Blood*. 2009 Jan 22;113(4):919–28.
13. Nilsson S, Angeletti D, Wahlgren M, Chen Q, Moll K. *Plasmodium falciparum* Antigen 332 Is a Resident Peripheral Membrane Protein of Maurer's Clefts. *PLoS ONE*. 2012 Nov 20;7(11):e46980.
14. Külzer S, Rug M, Brinkmann K, Cannon P, Cowman A, Lingelbach K, et al. Parasite-encoded Hsp40 proteins define novel mobile structures in the cytosol of the *P. falciparum*-infected erythrocyte. *Cell Microbiol*. 2010;12(10):1398–420.
15. Külzer S, Charnaud S, Dagan T, Riedel J, Mandal P, Pesce ER, et al. *Plasmodium falciparum*-encoded exported hsp70/hsp40 chaperone/co-chaperone complexes within the host erythrocyte. *Cell Microbiol*. 2012 Nov;14(11):1784–95.
16. Pasloske BL, Baruch DI, van Schravendijk MR, Handunnetti SM, Aikawa M, Fujioka H, et al. Cloning and characterization of a *Plasmodium falciparum* gene encoding a novel high-molecular weight host membrane-associated protein, PfEMP3. *Mol Biochem Parasitol*. 1993 May;59(1):59–72.
17. Waterkeyn JG, Wickham ME, Davern KM, Cooke BM, Coppel RL, Reeder JC, et al. Targeted mutagenesis of *Plasmodium falciparum* erythrocyte membrane protein 3 (PfEMP3) disrupts cytoadherence of malaria-infected red blood cells. *EMBO J*. 2000 Jun 15;19(12):2813–23.
18. Glenister FK, Coppel RL, Cowman AF, Mohandas N, Cooke BM. Contribution of parasite proteins to altered mechanical properties of malaria-infected red blood cells. *Blood*. 2002 Feb 1;99(3):1060–3.
19. Cooke BM, Glenister FK, Mohandas N, Coppel RL. Assignment of functional roles to parasite proteins in malaria-infected red blood cells by competitive flow-based adhesion assay. *Br J Haematol*. 2002 Apr;117(1):203–11.
20. Maier AG, Rug M, O'Neill MT, Brown M, Chakravorty S, Szeszak T, et al. Exported proteins required for virulence and rigidity of *Plasmodium falciparum*-infected human erythrocytes. *Cell*. 2008 Jul 11;134(1):48–61.
21. Hardeman MR, Meinardi MM, Ince C, Vreeken J. Red blood cell rigidification during cyclosporin therapy: a possible early warning signal for adverse reactions. *Scand J Clin Lab Invest*. 1998 Dec;58(8):617–23.
22. Trager W, Jensen JB. Cultivation of malarial parasites. *Nature*. 1978 Jun 22;273(5664):621–2.
23. Herrera S, Perlaza BL, Bonelo A, Arévalo-Herrera M. Aotus monkeys: their great value for anti-malaria vaccines and drug testing. *Int J Parasitol*. 2002 Dec 4;32(13):1625–35.

24. Pologe LG, Ravetch JV. A chromosomal rearrangement in a *P. falciparum* histidine-rich protein gene is associated with the knobless phenotype. *Nature*. 1986 Aug 31;322(6078):474–7.
25. Biggs BA, Kemp DJ, Brown GV. Subtelomeric chromosome deletions in field isolates of *Plasmodium falciparum* and their relationship to loss of cytoadherence in vitro. *Proc Natl Acad Sci U S A*. 1989 Apr;86(7):2428–32.

Outlook

The aim of this thesis was to increase our understanding of the mechanisms involved in erythrocyte modification by the malaria parasite *Plasmodium falciparum*. In order to verify our hypotheses and to bring new insight into the interactions and functions of exported parasite proteins I suggest the following experiments:

- All three previously isolated SEMP1-KO parasite clones contain a subtelomeric chromosome 2 truncation which among others leads to a loss of the *kahrp* gene. These parasites are therefore unqualified to investigate potential deleterious effects of SEMP1 disruption on Knob formation. Hence a *kahrp* containing parasite clone needs to be isolated from a non-clonal culture. This SEMP1-KO clone then should be analyzed for:
 - involvement of SEMP1 in knob formation and Maurer's clefts ultrastructure determination by electron microscopy.
 - involvement of SEMP1 in modification of erythrocyte membrane rigidity by deformability testing with a laser-assisted optical rotational cell analyzer (LORCA).
 - involvement of SEMP1 in stress response by nutrient starvation.
- In order to confirm the by microarray detected transcriptional up- or down-regulation of several *P. falciparum* genes including PfEMP3, qPCR should be performed from the corresponding timepoints.
- The in chapter 3 and 5 described mbSUS pairwise interaction assays need to be repeated in order to confirm the supposed binding between SEMP1 and PF3D7_0601900.

OUTLOOK

- Before further mbSUS library screenings make sense the quality and functionality of the generated *P. falciparum* blood stage cDNA library needs to be further evaluated. I therefore propose to PCR screen it for presence of rhoptry neck protein 2 (RON2) fragments. If the library contains such fragments, an apical membrane antigen (AMA1) bait should be generated and used for a library screen. The thereby generated yeast clones can be analyzed for true positives by PCR screens using RON2 primers. Alternatively the newly identified SEMP1 – PF3D7_0601900 interaction can be used as a positive control if it can be confirmed by a repeated mbSUS pairwise interaction assay.
- The potential interactions between SEMP1 and REX1 / PF3D7_0702500 / PF3D7_0601900 / PIESP2 / Pf332 / Hsp70-x / MAHRP2 need to be further investigated by either by pull-down or NMR experiments.
- In order to expand the generated small potential interaction network of exported *P. falciparum* proteins, co-IP experiments with the already available PF3D7_0601900-3xHA and PF3D7_0702500-3xHA parasites should be performed.

Appendix

Cell biological characterization of the malaria vaccine candidate trophozoite exported protein 1

During the course of this thesis contributions to a research manuscript published in ‘PLoS One’ were made. It characterizes the malaria vaccine candidate ‘trophozoite exported protein 1’ (Tex1) which was localized at the Maurer’s clefts.

Cell Biological Characterization of the Malaria Vaccine Candidate Trophozoite Exported Protein 1

Caroline Kulangara^{1,2}, Samuel Luedin^{1,2}, Olivier Dietz^{1,2}, Sebastian Rusch^{1,2}, Geraldine Frank³, Dania Mueller^{1,2}, Mirjam Moser^{1,2}, Andrey V. Kajava⁴, Giampietro Corradin³, Hans-Peter Beck^{1,2}, Ingrid Felger^{1,2*}

1 Medical Parasitology and Infection Biology, Swiss Tropical and Public Health Institute, Basel, Switzerland, **2** University of Basel, Basel, Switzerland, **3** Department of Biochemistry, University of Lausanne, Epalinges, Switzerland, **4** Centre de Recherches de Biochimie Macromoléculaire, Centre national de la recherche scientifique, University of Montpellier 1 and 2, Montpellier, France

Abstract

In a genome-wide screen for alpha-helical coiled coil motifs aiming at structurally defined vaccine candidates we identified PFF0165c. This protein is exported in the trophozoite stage and was named accordingly Trophozoite exported protein 1 (Tex1). In an extensive preclinical evaluation of its coiled coil peptides Tex1 was identified as promising novel malaria vaccine candidate providing the rationale for a comprehensive cell biological characterization of Tex1. Antibodies generated against an intrinsically unstructured N-terminal region of Tex1 and against a coiled coil domain were used to investigate cytological localization, solubility and expression profile. Co-localization experiments revealed that Tex1 is exported across the parasitophorous vacuole membrane and located to Maurer's clefts. Change in location is accompanied by a change in solubility: from a soluble state within the parasite to a membrane-associated state after export to Maurer's clefts. No classical export motifs such as PEXEL, signal sequence/anchor or transmembrane domain was identified for Tex1.

Citation: Kulangara C, Luedin S, Dietz O, Rusch S, Frank G, et al. (2012) Cell Biological Characterization of the Malaria Vaccine Candidate Trophozoite Exported Protein 1. *PLoS ONE* 7(10): e46112. doi:10.1371/journal.pone.0046112

Editor: Erika Martins Braga, Universidade Federal de Minas Gerais, Brazil

Received: May 13, 2011; **Accepted:** August 28, 2012; **Published:** October 8, 2012

Copyright: © 2012 Kulangara et al. This is an open-access article distributed under the terms of the Creative Commons Attribution License, which permits unrestricted use, distribution, and reproduction in any medium, provided the original author and source are credited.

Funding: The project was supported by the Swiss National Science Foundation (<http://www.snf.ch/>) grant number 310030-112244, by the Novartis Stiftung für Medizinisch-Biologische Forschung (<http://www.stiftungmedbiol.novartis.com/>) and EMVI (<http://www.emvi.org>). This study was funded by the Novartis Stiftung für Medizinisch-Biologische Forschung (<http://www.stiftungmedbiol.novartis.com/>). The funders had no role in study design, data collection and analysis, decision to publish, or preparation of the manuscript.

Competing Interests: This project was partly funded by the Novartis Stiftung für Medizinisch-Biologische Forschung (<http://www.stiftungmedbiol.novartis.com/>). This does not alter the authors' adherence to all the PLOS ONE policies on sharing data and materials.

* E-mail: ingrid.felger@unibas.ch

Introduction

In the past few years Tex1 encoded by PFF0165c was characterized as a novel malaria vaccine candidate. According to PlasmoDB version 6.5 (<http://plasmodb.org>) *tex1* spans nucleotide positions 133'147 to 136'458 on chromosome 6. Tex1 had been identified originally in a genome-wide screen of alpha-helical coiled coil domains in a search for novel vaccine candidates against the blood stage of *P. falciparum* [1,2]. Chemically synthesized short peptides consisting of such a motif can fold into their native structure in aqueous environment and therefore mimic structurally native epitopes. Two regions of Tex1 were chemically synthesized. One of the synthetic peptides, P27, is spanning the coiled coil domain (K845 to T871), the other, P27A, corresponds to N-terminal intrinsically unstructured region (H223 to S326). Both peptides were tested in an extensive preclinical evaluation protocol to analyze the properties of anti-P27 and anti-P27A antibodies regarding *in vitro* parasite killing in presence of monocytes [1,3], correlation with protection in adults and children [3,4], prevalence of peptide recognition by sera from semi-immune adults from different endemic region throughout the world [1,3] and sequence conservation in different culture strains and field isolates [3,5]. Both fragments of Tex1, peptides P27A and P27, are considered promising novel malaria blood stage

vaccine candidates. A phase 1 clinical study of P27A is scheduled in 2011.

In view of the promising outcome of preclinical evaluation and the imminent phase 1 clinical trial, a comprehensive biological characterization of Tex1 was called for. Here we present results of a cell biological analysis characterizing Tex1 in relation to other known exported parasite proteins. We show that Tex1 associates to Maurer's clefts (MC) membrane facing the cytosol of the RBC. Tex1 export depends on the classical secretory pathway. But it seems to lack a classical signal sequence as well as a PEXEL motif, suggesting the presence of alternative sequences involved in protein export to the PV and across the PVM to the RBC cytosol.

Materials and Methods

Ethical treatment of animals

The animal work has been carried out according to relevant national and international guidelines. The immunization experiments in CB6F1 mice and the immunization protocol was approved by the Canton de Vaud (Permit number: 805.6). Immunization of rabbits were performed by the commercial company Eurogentec, 4102 Seraing, Belgium.

Cell culture and protein extracts

P. falciparum 3D7 strain was cultured at 5% haematocrit as described [6], using RPMI medium supplemented with 0.5% Albumax [7]. Parasites were synchronized with 5% sorbitol [8]. To obtain protein extract of mixed stage infected erythrocytes parasites (10 ml petri-dish) were grown to 5% to 10% parasitemia, lysed on ice in 0.03% saponin in phosphate-buffered saline (PBS, pH 7.4) for 10 min, washed with ice cold PBS for complete removal of hemoglobin, and resuspended in Laemmli sample buffer. The protein extracts of late-stage parasites (trophozoites and schizonts) were obtained from *P. falciparum* 3D7-infected erythrocytes in a 30-ml petri dish (5% hematocrit, 6% parasitemia) which was enriched using a magnetic cell sorter (Miltenyi Biotec, Bergisch Gladbach, Germany). The enriched infected erythrocytes were lysed in a 200 μ l volume of PBS, 0.03% saponin (Fluka) in the presence of protease inhibitors (Roche Diagnostics, Basel, Switzerland) for 5 min at 4°C. The parasites were pelleted by centrifugation at 4,000 \times g for 10 min, the supernatant was collected and mixed with sample buffer. The parasite pellet was resuspended in 0.1 M Tris, pH 6.8, and an equal volume of 2 \times Laemmli sample buffer. For protein expression profiling 5 ml of tightly synchronized culture (2 h time frame; 8% parasitemia) was harvested in a 4 hours interval, parasites were lysed on ice in 0.03% saponin in PBS for 10 min and wash 3 times in ice-cold PBS. Parasite pellet was resuspended in cold 0.1 M Tris, pH 6.8, and an equal volume of 2 \times Laemmli sample buffer.

Recombinant expression and purification of recP27 fragment

The C-terminal fragment of Tex1 containing the coiled coil motif P27 (Figure 1A, M681 to E910) was amplified from 3D7 genomic DNA by PCR and cloned into the pQE60 plasmid via the NcoI and BamHI restriction sites (primers used are listed in **Table S1**). Recombinant expression was performed following the manufacturer's protocol (Qiagen Inc.).

Generation of anti-P27, anti-P27A and anti-recPf27 polyclonal rabbit sera and anti-P27 polyclonal mouse sera

Rabbit sera were produced by Eurogentec, Seraing, Belgium. In short, the recPf27 protein (250 μ g) was used for immunization with Freud's adjuvant into two New Zealand white rabbits. Sera samples (20 ml) were affinity purified using recPf27-6xHis protein or the P27 coiled coil peptide coupled to HiTrap NHS-activated HP columns (GE-Healthcare, 1 ml). After antibody binding columns were washed with 50 ml PBS, bound IgG was eluted with 0.1 M glycine, pH 2.5, and the buffer was subsequently changed to PBS using HiTrap Desalting Columns (GE Healthcare). Purified antibodies were stored at -80°C until further use. Polyclonal mouse sera was obtained by immunization of CB6F1 mice. CB6F1 mice were injected 3 times with 20 μ g of the P27 peptide in Montanide ISA 720 at the base of the tail on day 1, 22 and 78. Bleeding was performed 10 days after the second and third immunization. Affinity purification of P27A-specific rabbit has previously been described [1,3].

Western blot analysis

Protein extracts were separated on a 10% sodium dodecyl sulfate-polyacrylamide gel and transferred to nitrocellulose (Hybond-C extra; GE Healthcare) at 4°C for 1 h at 80 V and an additional hour at 100 V. The membrane was blocked for 1 h in 5% skim milk, 0.1% Tween in Tris-buffer. Antibodies used were: Polyclonal rabbit anti-P27A (1:5000); anti-P27 (1:2500) and

anti-Pf27rec (1:2500); anti-MAHRP1 (1:5000), monoclonal mouse anti-MSP1 ([9], 1:1000); anti-SERA5 ([10], 1:2000); horseradish peroxidase-conjugated goat anti-mouse (Pierce, 1:20 000), goat anti-rabbit (Acris, 1:10000).

Solubility analysis

P. falciparum 3D7-infected erythrocytes (30-ml petri dish; 6% parasitemia) were enriched using a magnetic cell sorter (Miltenyi Biotec, Bergisch Gladbach, Germany). Purified mature stages were resuspended in 200 μ l 5 mM Tris pH 8 in the presence of protease inhibitors (Roche Diagnostics, Basel, Switzerland) and lysed by 3 freezing-thawing cycles. Soluble protein fraction was separated by centrifugation 30 min at 20 000 \times g at 4°C. The membrane-containing pellet was resuspended in 200 μ l 0.1 M Na₂CO₃ and incubated for 30 min on ice to extract peripheral membrane proteins. Supernatant containing peripheral proteins was separated by centrifugation (30 min at 20 000 \times g at 4°C). Integral membrane proteins were extracted from the pellet with 1% Triton X-100 on ice for 30 min. Supernatant containing integral proteins was separated by centrifugation (30 min at 20 000 \times g at 4°C) The remaining proteins were extracted with 4% SDS, 0.5% TritonX-114 in 0.5 \times PBS for 30 min at room temperature and separated from the pellet by centrifugation. The supernatant was analyzed as insoluble protein fraction. 10 μ l of each fraction was analyzed by Western Blot.

RNA isolation, cDNA synthesis and real time PCR

3D7-infected erythrocytes were tightly synchronized using 5% D-sorbitol [8]. Three rounds of 5% D-sorbitol treatment was applied (2nd and 3rd treatment was applied 8 hours and 14 hours after the 1st D-sorbitol treatment). Parasites were grown to 8–10% parasitemia (5% haematocrit). 1.5 ml culture was taken in 4 h intervals. In brief, parasite RNA was extracted using TRIzol (Invitrogen) according to the manufacturer's instructions. TRIzol extraction was repeated. Residual gDNA was digested twice with RQ1 DNase (Promega) according to the manufacturer's protocol. Reverse transcription was done by AffinityScript Multiple Temperature Reverse Transcriptase (Stratagene) with random primers (Invitrogen) as described by the manufacturer. To control for gDNA contamination, the target sequence was amplified from the RNA solution prior to reverse transcription. Absolute transcript quantification was performed at final primer concentrations of 0.4 μ M using SYBR[®] Green Master Mix (Applied Biosystems) on a StepOnePlus[™] Real-Time PCR System (Applied Biosystems) in a reaction volume of 12 μ l. All reactions were performed in triplicate yielding virtually identical Ct values. A serial dilution of gDNA was used as standard for absolute quantification. Relative transcript profiles were calculated by normalization against transcript levels of the house-keeping gene PF13_0170 (glutamyl-tRNA synthetase). Validation of synchronization procedure was obtained by analyzing transcript levels of the merozoite surface protein 8 (*msh8*). The primers used for qPCR of *tex1*, PF13_0170 and *msh8* are shown in **Table S2**. The time points of harvest (1–14), the corresponding age of parasites (in hours post infection) and the corresponding parasite stages are illustrated in **Table 1** and were confirmed by Giemsa staining before RNA and Protein extraction.

Indirect immunofluorescence assay (IFA)

Infected erythrocytes were fixed with 4% paraformaldehyde (Polyscience) and 0.0075% glutaraldehyde (Polyscience) for 30 min under constant agitation, permeabilized using 0.1% Triton X-100/PBS for 10 min and blocked with sodium borohydride (NaBH₄)/PBS for 10 min followed by an additional

APPENDIX

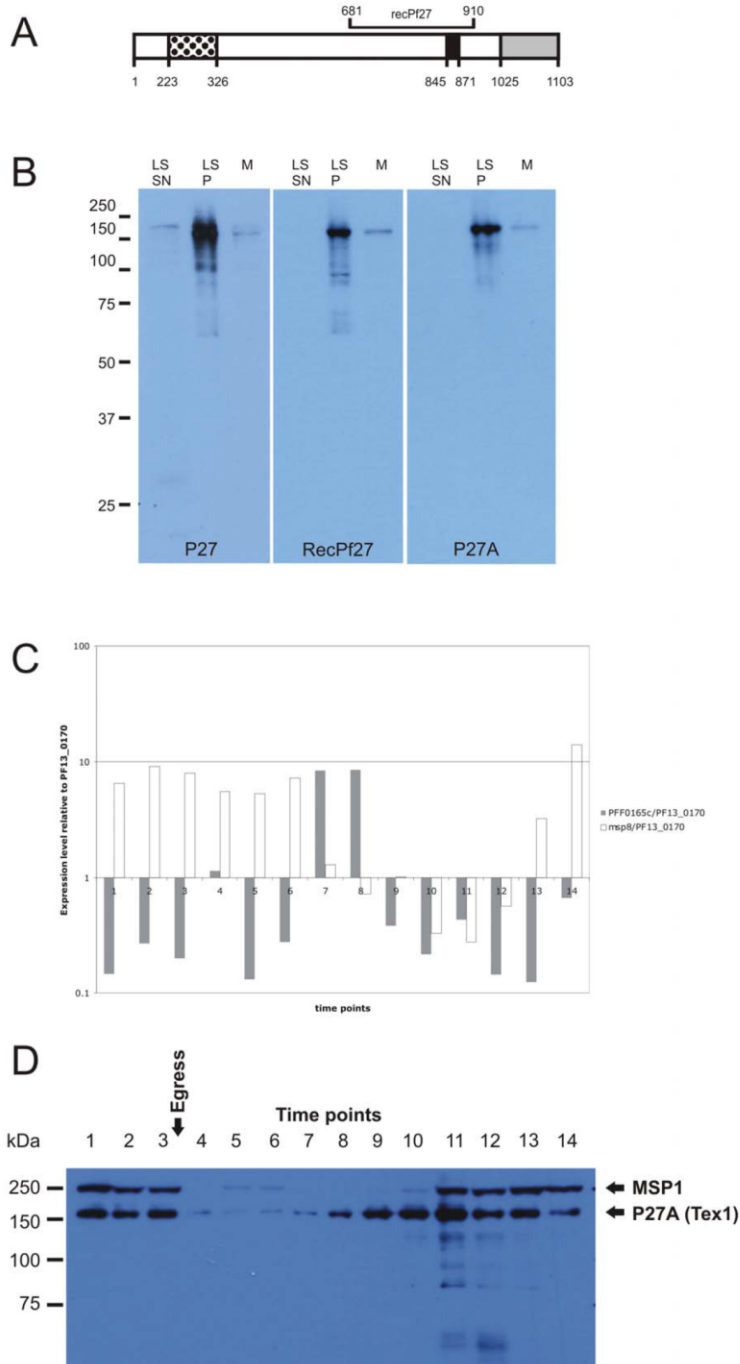


Figure 1. *Tex1* structure and expression dynamics on transcriptional and protein level. A) Schematic representation of *Tex1*. Black dotted: intrinsically unstructured region P27A; Black: coiled coil domain P27; grey: RING motif. B) Western Blot analysis of antibodies specific for P27A and P27 on the pellet fraction after saponin lysis of mixed stage parasite (M) and late stage parasite (LS). The late stage parasites were fractionated into a supernatant (SN) and a pellet (P) fraction after saponin lysis. M: marker C) Abundance of *tex1* transcripts by gRT-PCR. RNA was isolated from tightly synchronized culture in a 4h interval (table 1). *Tex1* transcript levels (grey bars) were normalized to the transcript abundance of the constitutively expressed glutamyl-tRNA synthetase (PF13_0170). As a control for the level of synchronization *msp8* transcripts were measured and compared to

the PF13_0170 transcript level (white bars). D) Protein level was analyzed throughout the intraerythrocytic development cycle in a 4 h interval by Western Blot analysis using antibodies against P27A and compared to protein abundance of MSP1. The parasite age (in hours post infection) and the parasite stages (confirmed by Giemsa staining) corresponding to the time points of harvest are illustrated in table 1. doi:10.1371/journal.pone.0046112.g001

blocking step using 3% BSA in PBS for 1 h as described in [11]. Primary antibodies were used with the following concentrations: polyclonal rabbit sera anti-P27A (1:2000); anti-P27 (1:1000), anti-MAHRP2 ([12], 1:100); anti-REX1 (kind gift from Prof. Don Gardiner, 1:500); mouse polyclonal antibodies anti-P27 (1:200); anti-SBP1 N-terminus specific (kind gift from Prof. Catherine Braun-Breton, 1:200); anti-MAHRP1 (1:200). Secondary antibodies used: Alexa Fluor 488 (Invitrogen; 1:400); Texas Red (Invitrogen; 1:400). Cells were mounted in Vectashield Hard Set supplemented with DAPI (Vector Laboratories) for staining of the nuclear DNA. For the Equinotoxin II assay infected erythrocytes were lightly fixed with 2% paraformaldehyde in RPMI medium (10 min), permeabilized with Equinotoxin II [13], and re-fixed with 4% formaldehyde and 0.00075% glutaraldehyde in PBS (pH 7.4, Gibbco). Cells were blocked with 3% BSA (Sigma) in PBS. Cells were split and one half was additionally treated with 0.1% triton (Merck) for complete permeabilization. Synchronized Ring stage parasites (aged 4 h to 8 h post invasion) were treated with Brefeldin A solved in 100% ethanol (Fluka) to a final concentration of 5 $\mu\text{g ml}^{-1}$. Control cultures were incubated in the presence of equivalent amounts of ethanol. After 18 h parasites were fixed for IFA. BFA was removed from the remaining parasites which were further cultured to ensure viability after treatment. Images were obtained by the Zeiss confocal microscope LSM 700 or Leica DM 5000B fluorescence microscope. Images were processed by ImageJ software or the Huygens Essential Software (Scientific Volume Imaging, The Netherlands). Quantitative analysis of co-localization was done with Huygens Essential Software (Scientific Volume Imaging, The Netherlands).

Results

According to PlasmoDB version 6.5 (<http://plasmodb.org>), the predicted protein has a length of 1103 amino acids (aa) and contains 3 predicted coiled coil domains. Alpha-helical coiled coils share the heptad motif **(abcdefg)_n**, with positions **a** and **d** representing hydrophobic residues, whereas the remaining positions are generally polar. Depending on slight variations in their sequences the coiled coil bundles consist of 2 to 7 alpha-helices that spontaneously self assemble in aqueous solutions. One of the 3 coiled coil domains in Tex1 is the P27 region from position K845 to T871 (in black, **Figure 1A**), which has been identified as potential malaria vaccine candidate previously [1]. The C-terminus of Tex1 consists of a predicted RING (Really Interesting New Gene) domain, spanning amino acids K1025 to L1102 (in grey, **Figure 1A**). Furthermore, a large portion of the C-terminal half of this protein (650–1040) has sequence similarity to several proteins with known 3D structure which have elongated alpha-helical domains capped by the RING-domains (e.g. [14]). This supports correctness of our previous prediction of alpha-helical coiled coil regions in Tex1 (Villard et al., 2007). A long intrinsically unstructured region (IUR) named P27A, ranging from position H223 to S326 (black dotted, **Figure 1A**), corresponds to the second identified potential vaccine candidate within Tex1 [3]. P27A is currently under clinical development and a phase 1 clinical trial is scheduled for 2011.

Tex1 is expressed in intraerythrocytic blood stage parasites and its transcription is up-regulated in the early trophozoite stage

In order to characterize the protein by IFA and Western Blot, rabbit antibodies were generated against P27A and a 240 aa long (including linker and His-tag) recombinant protein (recPf27) encompassing amino acid M681 to E910 (**Figure 1A**) in the C-terminal part of Tex1 and including the P27 coiled coil domain (K845 to T871). Both polyclonal rabbit sera were affinity purified on the respective immunogens. In addition, recPf27 rabbit serum was alternatively affinity purified on the P27 peptide. Thus, three polyclonal rabbit sera were available with specificities to P27A, recPf27 and P27.

Previously, we showed that P27A specific mouse and rabbit sera both detected a protein with the mass of 160 kDa in Western Blot broadly consistent with the predicted mass of 132 kDa [3]. When using several sera raised against different parts of Tex1, all sera recognized a band at about 160 kDa both, in the pellet fraction of mixed parasite stages and in late stage parasites (**Figure 1B**).

The transcription profile was analyzed by quantitative real-time PCR on RNA from tightly synchronized cultures harvested in 4 h intervals covering the 48 h intra-erythrocytic developmental cycle. The collected time points, the corresponding age of the parasites (in hours post invasion) and the respective parasite stages are listed in table 1. The transcription level of *tex1* was analyzed in relation to that of a constitutively transcribed gene, *glutaminyt-tRNA synthetase* (PF13_0170). *Tex1*-specific transcripts were detected throughout the intra-erythrocytic development cycle, but an up-regulation of transcript abundance was detected in early trophozoites (gray bars, **Figure 1C**). To validate the synchronization procedure, transcript levels of the merozoite surface protein 8 (*msp8*) were analyzed at each time point. The *msp8* profile obtained

Table 1. Time points of harvest of synchronized 3D7 *in vitro* culture.

Time points	Hours post infection	Parasite stage
1	46–48	Schizont/Ring
2	0–2	Schizont/Ring
3	4–6	
4	8–10	Ring
5	12–14	
6	16–18	Late Ring
7	20–22	Early Trophozoite
8	24–26	
9	28–30	Trophozoite
10	32–34	
11	36–38	Late Trophozoite
12	40–42	Late Trophozoite/Schizont
13	44–46	Schizont
14	48–50	Schizont/Ring

Synchronized *P. falciparum* 3D7 parasite culture were harvested in 4 h interval. Time points of harvest 1–14 (column 1), the corresponding age of synchronized parasites at each time point of harvest (in hours post invasion, column 2) and the corresponding parasite stage (column 3). doi:10.1371/journal.pone.0046112.t001

(white bars, **Figure 1C**) showed an up-regulation in ring stages and in very late schizont stages as shown in PlasmoDB. The RNA levels of *tex1* were compared with a time course of Tex1 protein abundance analyzed by Western Blot during the intra-erythrocytic cycle. Tex1 protein levels detected in 4 h intervals were highest during early trophozoite stage at time point 8 (**Figure 1D**). The protein persisted until egress, reflected, in the presence of the full length merozoite surface protein 1 (MSP1) [15].

Tex1 is exported to the host cell cytosol and localizes to Maurer's clefts

Previously we reported that Tex1 was exported and accumulated at structures in the cytosol of the infected RBC [3]. To study the exact subcellular localization of Tex1 during the intra-erythrocytic cycle, synchronized 3D7 parasites were analyzed by IFA. In early ring stages (0–6 hours post invasion) the protein was absent (data not shown), whereas in late ring stages (12–16 hours post invasion) Tex1 was detected in punctuated structures within the parasite (**Figure 2A**). In trophozoite stages, Tex1 is exported to the host cell cytosol and associates with elongated structures in the cytosol of the infected RBC (**Figure 2B**) suggestive of Maurer's clefts (MC) staining [16]. In schizont stages the protein was much less focused and seemed to associate to the periphery of the host cell in vicinity to the host cell membrane (**Figure 2C**).

To prove the localization to MC, co-localization experiments were performed using antibodies against known MC markers. In late ring stages the ring exported protein 1 (Rex1) (**Figure 3A**), SBP1 (**Figure 4A**) and MAHRP1 (**Figure 5A**) associated with MC, whereas Tex1 still remained within the parasite. In trophozoite, schizont and late schizont stages, Tex1 appeared to associate with MC as demonstrated by co-localization with Rex1 (**Figure 3B, 3C, 3D**), SBP1 (**Figure 4B, 4C**) and MAHRP1 (**Figure 5B and 5C**). In schizont stages Tex1 signal was detected similar to Rex1 adjacent to the RBC membrane. Tex1 was also detected in close proximity to new structures called tethers (**Figure 6A**) that are characterized by the membrane-associated histidine rich protein 2 (MAHRP2, [12]). However, Tex1 is not found anymore in close proximity to MAHRP2 in schizont stage

parasites (**Figure 6B**). Antibodies directed against Tex1 failed to detect the protein at the surface of infected RBCs in unpermeabilized cells (**Figure S1**) suggesting that in schizonts the protein resides inside of the infected cell in close proximity to the RBC membrane.

Tex1 occurs in two conditions: as soluble protein and in association with membrane structures

Late parasite stages were purified by magnetic cell sorting and were lysed by repeated freeze thaw cycles to release all soluble proteins of the parasite and the RBC. The peripheral, membrane-associated proteins were extracted from the pellet fraction containing the membranes by sodium carbonate buffer (pH 11). The remaining integral membrane proteins were extracted with Triton X-100. This fractionation revealed that Tex1 was partly found soluble but equal amounts of the protein could only be extracted by carbonate buffer indicating that Tex1 associated with membranes (**Figure 7**). As control for the integrity of our fractions we used monoclonal antibodies against serine-rich antigen 5 (SERA5), a soluble protein found in the PV [17,18,19]; MAHRP1 was used as control representing an integral membrane protein [20,21]; MSP1 served as control representing a glycosylphosphatidylinositol lipid anchored protein on the merozoite surface and also as marker for the integral membrane fraction [22].

In order to analyze the localization of Tex1 at the MC, infected RBCs were lysed with Equinatoxin II (EqII), a pore-forming toxin binding preferentially to sphingomyelin-containing membranes [13]. It lyses the RBC membrane ensuring integrity of PVM and MC membranes [23]. SBP1 is an integral membrane protein localizing to MCs. The C-terminus of SBP1 is directed to the RBC cytosol, whereas the N-terminus is directed to the lumen of MCs. The upper panel of **Figure 8** shows Tex1 localization in EqII lysed parasite infected RBC. In these EqII treated parasites the N-terminus of SBP1 is not detected because antibodies specific to this part cannot access their target due to intact MC membranes.

SBP1 staining was performed to demonstrate the integrity of the MC membrane. P27-specific antibodies detected Tex1 in cells

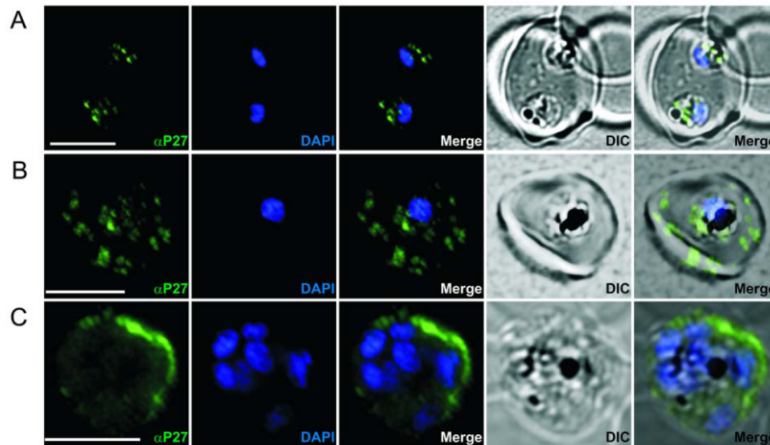


Figure 2. Immunofluorescence staining of erythrocytes infected by *P. falciparum* (ring, trophozoites and schizont stages) using P27-specific polyclonal rabbit sera. P27-specific polyclonal rabbit sera was used to detect Tex1 (green) A) in late ring stages B) in trophozoite stages C) in schizont stages. Nucleus stained with DAPI (blue), transmission picture of the infected red blood cell (DIC) and merged picture of the two signals or the signals merged with transmission picture (merge), Scale bar: 5 μ m.
doi:10.1371/journal.pone.0046112.g002

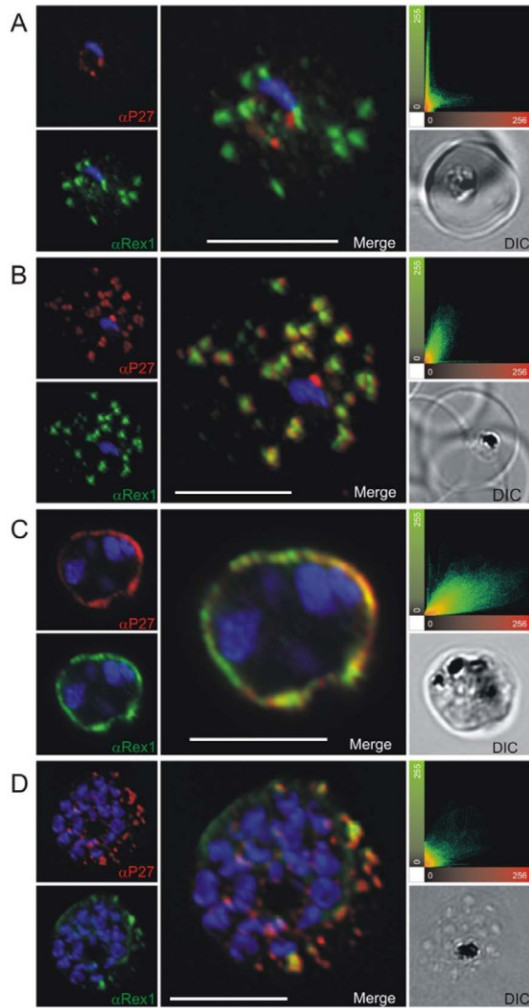


Figure 3. Co-localization of Tex1 with Rex1. P27-specific polyclonal mouse sera (in red) was used to detect TEX1. Rex1 polyclonal rabbit sera (in green). (A) Ring stage parasites; (B) trophozoite stages; (C) schizont stages. Scatter plots show the degree of co-localization of the Tex1 with Rex1 signal. Nuclear DNA was stained with DAPI (blue), Transmission image (DIC), Scale bar: 5 μ m. doi:10.1371/journal.pone.0046112.g003

treated with EqII at the MC. This demonstrated the localization of Tex1 at the surface of MC facing the RBC cytosol (**Figure 8**).

In the lower panel of **Figure 8**, the parasites were further lysed with Triton X-100, which permeabilized also the MCs membrane, therefore SBP1 can be detected with antibodies directed against the N-terminus of the protein (**Figure 8**).

Export of Tex1 is Brefeldin A sensitive

Protein secretion pathways in the eukaryotic cell are classified into the classical and nonclassical secretory pathway as reviewed by [24]. Whereas the classical secretory pathway involves co-translational translocation of proteins into the ER or posttranslational insertion into the ER followed by vesicular transport from

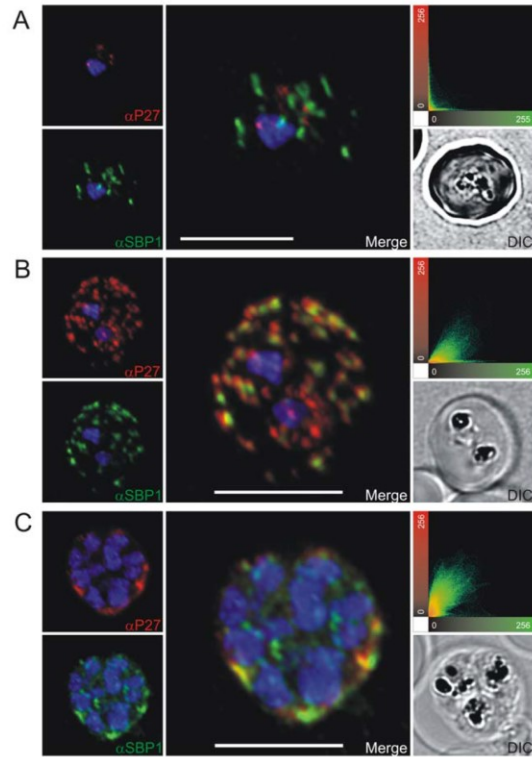


Figure 4. Co-localization of Tex1 with SBP1. P27-specific polyclonal rabbit sera was used to detect Tex1 (red). Co-localization was performed using SBP1 polyclonal mouse sera (green). Co-localization was performed in ring (A) trophozoite (B) and schizont stage (C) infected RBCs. Nuclear DNA was stained with DAPI (blue), Transmission image (DIC), Scale bar: 5 μ m. doi:10.1371/journal.pone.0046112.g004

the ER via Golgi to the cell surface or the extracellular space reviewed in [25], the molecular mechanisms involved in the nonclassical protein secretion are independent of the ER/Golgi system [26,27]. To test by which route Tex1 is exported, infected RBCs were treated with Brefeldin A (BFA), a fungal metabolite shown to block the classical protein secretion pathway [28]. BFA treatment blocked Tex1 export (**Figure 9**) suggesting that Tex1 export depends on components of the classical secretory pathway.

Discussion

Extensive preclinical evaluation of the annotated hypothetical protein Tex1 revealed that two regions, the intrinsically unstructured region P27A and the coiled coil domain P27, show great potential as new malaria vaccine candidates [1,3,5]. Its clinical development, currently in phase 1, called for an in depth analysis of the cytological characteristics of Tex1, which was named ‘‘Trophozoite exported protein 1’’ due to its localization to MC at the trophozoite stage. Association to MC was confirmed by co-localization with Rex1 and other MC proteins. Tex1 associated with the MC membranes facing the cytosol of the RBC. This was demonstrated by EqII lysis of infected RBCs, which in contrast to Triton X-100 permeabilizes exclusively the RBC membrane. While antibodies detected Tex1, other antibodies, directed against

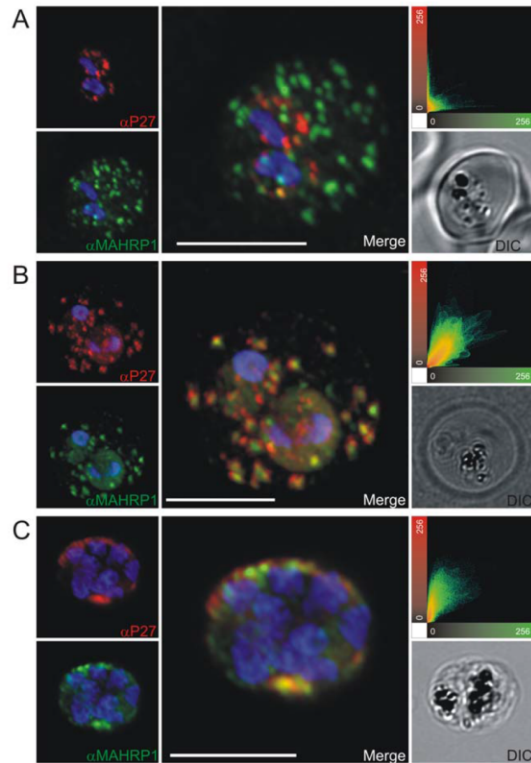


Figure 5. Co-localization of Tex1 with MAHRP1. P27-specific polyclonal rabbit sera was used to detect Tex1 (red). Co-localization was performed using MAHRP1 polyclonal mouse sera (green). Co-localization was performed in ring stage (A) trophozoite (B) and schizont stage (C) infected RBC. Nuclear DNA was stained with DAPI (blue), Transmission image (DIC), Scale bar: 5 μ m. doi:10.1371/journal.pone.0046112.g005

the luminal N-terminus of SBP1, could not access the lumen of MCs and thus gave no signal.

Exported proteins in *P. falciparum* are classified based on the presence or absence of the PEXEL motif which is mostly located downstream of a hydrophobic stretch. Recently, an increasing number of PEXEL-negative exported proteins (PNEPs) were identified [12,16,29,30]. Tex1 also is a PEXEL negative exported protein. To date it is only poorly understood how PNEPs are trafficked across the PVM, and sequence signatures responsible for export across the PVM and to the MC remain to be identified, if these exist at all.

A common characteristic of PNEPs seems to be the presence of either N-terminal signal sequence or a transmembrane domain [31]. For Tex1 no classical signal sequence, nor PEXEL motif, could be identified. The Tex1 expression pattern varies from that of PNEPs. Whereas Tex1 is expressed in trophozoites, PNEPs are expressed early in the intra-erythrocytic developmental cycle. We identified a potential alternative start site at position -43 in respect to the predicted translational start site (PlasmoDB, **Figure S2**). This stretch of 43 aa was predicted by SignalP (<http://www.cbs.dtu.dk/services/SignalP/>) to function as signal anchor and is unique for *P. falciparum* Tex1. No such preceding sequence stretch was detected in the orthologues of *P. vivax* (PVX_113335) and *P.*

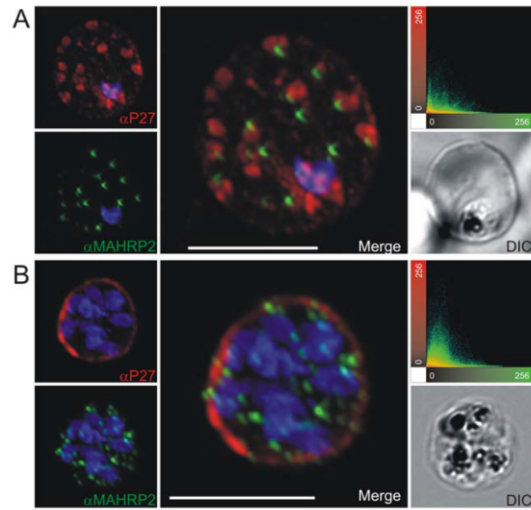


Figure 6. Tex1 localization in trophozoite and schizont stages with respect to newly described structures called tethers. Co-localization of Tex1 (red) with MAHRP2 (green) (A) in trophozoite stages and (B) in schizont stages. Nuclear DNA was stained with DAPI (blue), Transmission image (DIC), Scale bar: 5 μ m. doi:10.1371/journal.pone.0046112.g006

knowlesi (PKH_114650, **Figure S2**). Constructs of Tex1 including a GFP tag at the C-terminus were generated with or without the 43 aa hydrophobic stretch and episomally expressed. However, the GFP signals of both variants remained inside the parasite. More experimental data is needed to further investigate sequences responsible for Tex1 export. GFP-tagging of Tex1 might have interfered with the function of the RING domain at its very C-terminus. This would suggest that the RING domain plays an important role in Tex1 export. Brefeldin A treatment resulted in the accumulation of Tex1 at close proximity to the nucleus suggestive for ER or ER exit sites, indicating the involvement of the classical secretory pathway in the export of Tex1.

Tex1 exhibited a differential solubility pattern, whereby a portion of the protein was found in the soluble fraction, while the rest was present as peripheral membrane protein. No soluble Tex1 was detected in the RBC cytosol or PV, as demonstrated in the fractionation experiment using saponin lysed infected RBCs (**Figure 1B**), suggesting that the soluble pool of Tex1 is present exclusively within the parasite. This finding suggests that Tex1 changes its solubility during export: Tex1 is exported as a soluble protein, but associates with MC membranes after export. Our solubility assay showed equal amounts of soluble Tex1 and membrane-associated Tex1. However, the soluble portion likely is overrated due to freeze/thaw-mediated release of Tex1 from its MC's association.

Also for other proteins a solubility change after export has been reported, e.g. for Rex1 [32]. Similar to Tex1, Rex1 was found to associate with MCs via protein-protein interaction [32]. Rex 1 has a predicted transmembrane domain and its alpha-coiled coil region (amino acids 160–370) seems to be responsible for MC association [32]. Tex1 contains three putative coiled coil domains (**Table S3**). The alpha-helical coiled coil motif is a very abundant protein motif present in around 10% of all proteins [33]. Coiled coils have been shown to function as protein-protein interaction sites and to be involved in oligomerization and complex formation

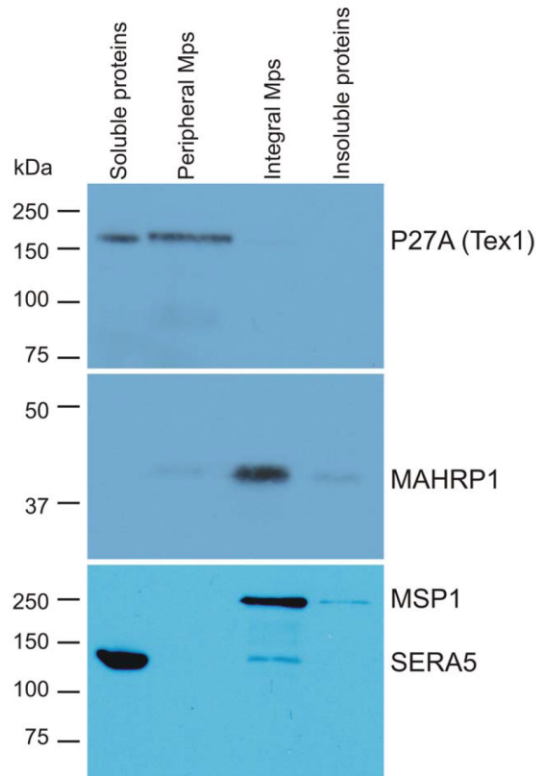


Figure 7. Dual solubility pattern of Tex1 shown by Western blot analysis of membrane fractionation assay of late stage parasites. Soluble proteins from membranes of RBCs infected with late stage parasites lysed by freezing thawing cycles (lane 1). Peripheral membrane proteins extracted by sodium carbonate buffer, (lane 2). Integral membrane proteins obtained by additional 1% Triton X-100 extraction (lane 3). Insoluble proteins (remaining membrane proteins after Triton X-100 extraction) (lane 4). Blot was probed with P27A-specific polyclonal rabbit sera (panel 1), anti-MAHRP1 polyclonal rabbit sera (panel 2) and SERA5 and MSP1 mouse monoclonal antibodies (panel 3).

doi:10.1371/journal.pone.0046112.g007

[34]. Thus, coiled coils participate in many cellular processes, such as membrane fusion, vesicular trafficking and cell motility. Further experiments are needed to elucidate the function of Tex1 coiled coil domains for MC membrane association.

Also for PfEMP1 a change in solubility during export had been reported [35]. Despite the presence of a transmembrane domain, PfEMP1 seems to be synthesized as a carbonate extractable protein. After export PfEMP1 becomes increasingly insoluble [35].

Noteworthy was the observation of very good co-localization of both peripheral membrane proteins Tex1 and Rex1, in contrast to the incomplete/partial co-localization of Tex1 with the integral membrane proteins MAHRP1 and SBP1 at MC's. This provides further evidence for a peripheral membrane association of Tex1.

We investigated, whether the export of Tex1 is influenced by other exported proteins. Tex1 export was not altered in D10 parasites (data not shown), which have a partial deletion of chromosome 9 and a truncation of chromosome 2, eliminating 22 genes, including Rex1, 2, 3, 4 and KAHRP, and resulting in loss of cytoadherence [36,37,38,39] and alteration of the MC structure [40,41]. Similarly, in MAHRP1 knock out parasites, where PfEMP1 trafficking to the RBC membrane is blocked [16], Tex1 was correctly exported and its association with the MC remained intact (data not shown).

Tex1 orthologues were found in *P. vivax* and *P. knowlesi* as well as in *P. berghei*, *P. chabaudi* or *P. yoelii*. P27 was highly conserved among *Plasmodium* species (**Figure S3A**). Interestingly, the unstructured region was present exclusively in *P. falciparum* (**Figure S3B**). Many of the other ring stage exported proteins of *P. falciparum*, such as MAHRP1 and 2, SBP1 and Rex1, 2, 3, and 4, as well as the *resamulti* gene family, do not have orthologues in *P. vivax*. Discrepancies were found also in a comparison of *P. falciparum* and *P. vivax* transcription profiles [42]. Eleven percent of syntenic genes of *P. vivax* and *P. falciparum* differed in gene expression during the intra-erythrocytic developmental cycle [42]. Similar results were obtained for *tex1* transcripts. According to PlasmoDB the *P. vivax* orthologue showed a completely different transcriptional profile with transcripts up-regulated in ring stage parasites suggesting a divergent evolution of Tex1 function.

Antibodies directed against P27 and P27A of Tex1 were effective in *in vitro* parasite killing in the presence of monocytes [1,3] and both P27 and P27A were recognized by serum from semi-immune adults from various endemic settings [1,3]. These results suggested that Tex1 holds a crucial immunological function. However, we found that Tex1 was absent on the surface of the infected RBC. The effector function of Tex1-specific

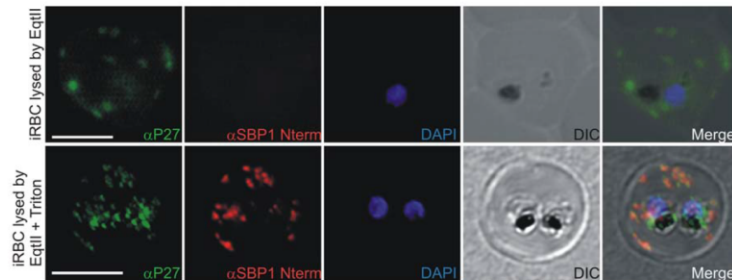


Figure 8. Equinatoxin II assay. A) 3D7 infected RBC lysed with equinatoxin II. Integrity of MCs is demonstrated by the absence of the SBP1 signal after using SBP1 N-terminus specific polyclonal mouse sera (note: N-terminus of SBP1 faces the lumen of MCs). Tex1 signal on the MC surface was obtained with P27-specific polyclonal rabbit sera (in green). B) 3D7 infected RBC lysed with equinatoxin followed by Triton lysis. MC lumen is now accessible for antibodies as shown by the SBP1 signal (in red). Nuclear DNA stained with DAPI (blue), Transmission image (DIC). Scale bar: 5 μ m.

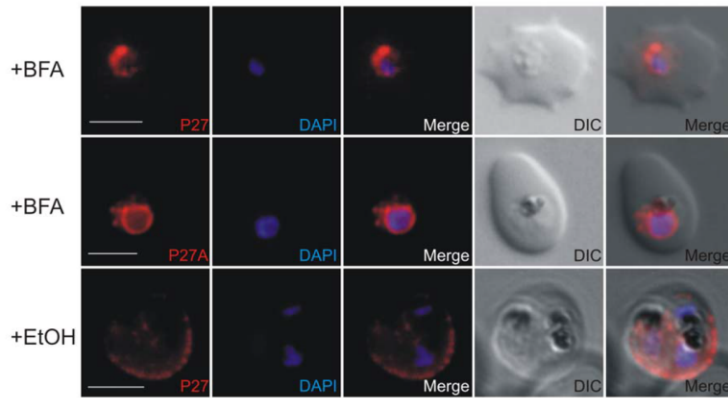


Figure 9. Brefeldin A sensitivity of *Tex1* export. 3D7 infected RBC were treated with BFA and fixed (+BFA). *Tex1* was stained using P27 or P27A-specific mouse antibodies (in red, upper panel: early trophozoite, middle panel: trophozoite). *Tex1* visible inside the parasite in close proximity to the nucleus. A control culture (+EtOH) was incubated with equivalent concentration of ethanol, the solvent of Brefeldin A. In the control culture *Tex1* was correctly exported and associated to MC (in red). The nucleus was stained with DAPI (in blue). Transmission image (DIC). scale bar: 5 μ m. doi:10.1371/journal.pone.0046112.g009

antibodies excludes therefore blocking of cytoadherence or opsonization and destruction of iRBC by phagocytic cells, but involves monocytes. We conclude that the activation of monocytes by P27/P27A-specific antibodies may occur after parasite egress.

The persistence of *Tex1* until egress could indicate functional activity at the end of the 48 h blood stage cycle. To elucidate the biological function of *Tex1*, we attempted to knock-out *tex1*. These attempts failed indicating that the *tex1* locus resists recombination events due to an essential role of *Tex1* for parasite survival.

Conclusion

Tex1 was identified based of extensive preclinical evaluation as promising novel vaccine candidate against *P. falciparum* blood stage infection. In the past, malaria blood-stage vaccine development has focused on antigens located on the surfaces of iRBC or free merozoites. This approach assumed that protective antibodies would opsonize, block invasion or prevent sequestration. *Tex1* was not found to be surface exposed, but instead localized to the surface of MC. Upon egress, *Tex1* gets exposed to the host immune system. A *Tex1*-specific antibody effector function remains to be elucidated, but likely involves the presence of monocytes.

Supporting Information

Figure S1 Absence of surface exposure of *Tex1*. The absence of *Tex1* from the surface of infected RBCs was shown by incubating live cells with P27-specific polyclonal mouse sera directed against *Tex1* (panel A). *Tex1* signal was detected only in a lysed cell (panel A, white arrow). Nucleus stained with DAPI (panel B). Merged pictures of both signals and the transmission image (panel C). Scale bar: 5 μ m. (TIF)

References

- Villard V, Agak GW, Frank G, Jafarshad A, Servis C, et al. (2007) Rapid identification of malaria vaccine candidates based on alpha-helical coiled coil protein motif. *PLoS One* 2: e645.
- Corradin G, Villard V, Kajava AV (2007) Protein structure based strategies for antigen discovery and vaccine development against malaria and other pathogens. *Endocr Metab Immune Disord Drug Targets* 7: 259–265.

Figure S2 Upstream region of *Tex1* and its orthologues in *P. vivax* (PVX_113335) and *P. knowlesi* (PKH_114650). Sequence highlighted in gray represents the region upstream of the predicted start Methionine. Stars (*) represent stop codons. (TIF)

Figure S3 Sequence alignment of the *P. falciparum* *Tex1* with the *P. vivax* orthologue. A) Sequence alignment of the *Tex1* C-terminus, P27 highlighted in grey. B) Sequence alignment of the *Tex1* N-terminus, predicted signal sequence highlighted in light grey; P27A highlighted in bold. (TIF)

Table S1 Oligonucleotide sequences used for cloning (restriction sites in bold). (DOCX)

Table S2 Oligonucleotide sequences used for qRT-PCR. (DOCX)

Table S3 Alpha-helical coiled coil domains in *Tex1* (P27 in bold). (DOC)

Acknowledgments

We acknowledge following colleagues for providing antibodies: Don Gardiner (anti-Rex1); Catherine Braun-Breton (anti-SBP1). We are grateful to Bruno Tigani of Novartis International for substantial assistance at the confocal microscope.

Author Contributions

Conceived and designed the experiments: GC IF HPB. Performed the experiments: CK SL SR GF DM MM OD. Analyzed the data: CK SL AK HPB IF. Contributed reagents/materials/analysis tools: HPB GC. Wrote the paper: CK IF.

- Olugbile S, Kulangara C, Bang G, Bertholet S, Suzarte E, et al. (2009) Vaccine potentials of an intrinsically unstructured fragment derived from the blood stage-associated *Plasmodium falciparum* protein PFF0165c. *Infect Immun* 77: 5701–5709.
- Agak GW, Bejon P, Fegan G, Gicheru N, Villard V, et al. (2008) Longitudinal analyses of immune responses to *Plasmodium falciparum* derived peptides

- corresponding to novel blood stage antigens in coastal Kenya. *Vaccine* 26: 1963–1971.
5. Kulangara C, Kajava AV, Corradin G, Felger I (2009) Sequence conservation in *Plasmodium falciparum* alpha-helical coiled coil domains proposed for vaccine development. *PLoS One* 4: e5419.
 6. Jensen JB, Trager W (1978) *Plasmodium falciparum* in culture: establishment of additional strains. *Am J Trop Med Hyg* 27: 743–746.
 7. Dorn A, Stoffel R, Matile H, Bubendorf A, Ridley RG (1995) Malarial haemozoin/beta-haematin supports haem polymerization in the absence of protein. *Nature* 374: 269–271.
 8. Lambros C, Vanderberg JP (1979) Synchronization of *Plasmodium falciparum* erythrocytic stages in culture. *J Parasitol* 65: 418–420.
 9. Helg A, Mueller MS, Joss A, Pold-Frank F, Stuart F, et al. (2003) Comparison of analytical methods for the evaluation of antibody responses against epitopes of polymorphic protein antigens. *J Immunol Methods* 276: 19–31.
 10. Okitsu SL, Boato F, Mueller MS, Li DB, Vogel D, et al. (2007) Antibodies elicited by a virosomally formulated *Plasmodium falciparum* serine repeat antigen-5 derived peptide detect the processed 47 kDa fragment both in sporozoites and merozoites. *Peptides* 28: 2051–2060.
 11. Tonkin CJ, van Dooren GG, Spurck TP, Struck NS, Good RT, et al. (2004) Localization of organellar proteins in *Plasmodium falciparum* using a novel set of transfection vectors and a new immunofluorescence fixation method. *Mol Biochem Parasitol* 137: 13–21.
 12. Pachlatko E, Rusch S, Muller A, Hemphill A, Tilley L, et al. (2010) MAHRP2, an exported protein of *Plasmodium falciparum*, is an essential component of Maurer's cleft tethers. *Mol Microbiol* 77(5): 1136–1152.
 13. Anderluh G, Pungercar J, Strukelj B, Macek P, Gubensek F (1996) Cloning, sequencing, and expression of equinatoxin II. *Biochem Biophys Res Commun* 220: 437–442.
 14. Cally DL, O'Toole PW, Moore SA (2010) The 2.2-A structure of the HP0958 protein from *Helicobacter pylori* reveals a kinked anti-parallel coiled-coil hairpin domain and a highly conserved ZN-ribbon domain. *J Mol Biol* 403: 405–419.
 15. Child MA, Epp C, Bujard H, Blackman MJ (2010) Regulated maturation of malaria merozoite surface protein-1 is essential for parasite growth. *Mol Microbiol* 78: 187–202.
 16. Spycher C, Rug M, Pachlatko E, Hanssen E, Ferguson D, et al. (2008) The Maurer's cleft protein MAHRP1 is essential for trafficking of P1EMP1 to the surface of *Plasmodium falciparum*-infected erythrocytes. *Mol Microbiol* 68: 1300–1314.
 17. Knapp B, Hundt E, Kupper HA (1989) A new blood stage antigen of *Plasmodium falciparum* transported to the erythrocyte surface. *Mol Biochem Parasitol* 37: 47–56.
 18. Yeoh S, O'Donnell RA, Koussis K, Dluzewski AR, Ansell KH, et al. (2007) Subcellular discharge of a serine protease mediates release of invasive malaria parasites from host erythrocytes. *Cell* 131: 1072–1083.
 19. Blackman MJ (2008) Malarial proteases and host cell egress: an 'emerging' cascade. *Cell Microbiol* 10: 1925–1934.
 20. Spycher C, Klonis N, Spielmann T, Kump E, Steiger S, et al. (2003) MAHRP-1, a novel *Plasmodium falciparum* histidine-rich protein, binds ferriprotoporphyrin IX and localizes to the Maurer's clefts. *J Biol Chem* 278: 35373–35383.
 21. Spycher C, Rug M, Klonis N, Ferguson DJ, Cowman AF, et al. (2006) Genesis of and trafficking to the Maurer's clefts of *Plasmodium falciparum*-infected erythrocytes. *Mol Cell Biol* 26: 4074–4085.
 22. Gerold P, Schofield L, Blackman MJ, Holder AA, Schwarz RT (1996) Structural analysis of the glycosyl-phosphatidylinositol membrane anchor of the merozoite surface proteins-1 and -2 of *Plasmodium falciparum*. *Mol Biochem Parasitol* 75: 131–143.
 23. Jackson KE, Spielmann T, Hanssen E, Adisa A, Separovic F, et al. (2007) Selective permeabilization of the host cell membrane of *Plasmodium falciparum*-infected red blood cells with streptolysin O and equinatoxin II. *Biochem J* 403: 167–175.
 24. Nickel W (2003) The mystery of nonclassical protein secretion. A current view on cargo proteins and potential export routes. *Eur J Biochem* 270: 2109–2119.
 25. Mellman I, Warren G (2000) The road taken: past and future foundations of membrane traffic. *Cell* 100: 99–112.
 26. Rubartelli A, Cozzolino F, Talio M, Sitia R (1990) A novel secretory pathway for interleukin-1 beta, a protein lacking a signal sequence. *Embo J* 9: 1503–1510.
 27. Cooper DN, Barondes SH (1990) Evidence for export of a muscle lectin from cytosol to extracellular matrix and for a novel secretory mechanism. *J Cell Biol* 110: 1681–1691.
 28. Lippincott-Schwartz J, Yuan LC, Bonifacino JS, Klausner RD (1989) Rapid redistribution of Golgi proteins into the ER in cells treated with brefeldin A: evidence for membrane cycling from Golgi to ER. *Cell* 56: 801–813.
 29. Haase S, Herrmann S, Gruring C, Heiber A, Jansen PW, et al. (2009) Sequence requirements for the export of the *Plasmodium falciparum* Maurer's clefts protein REX2. *Mol Microbiol* 71: 1003–1017.
 30. Saridaki T, Frohlich KS, Braun-Breton C, Lanzer M (2009) Export of P1SBP1 to the *Plasmodium falciparum* Maurer's clefts. *Traffic* 10: 137–152.
 31. Spielmann T, Gilberger TW (2010) Protein export in malaria parasites: do multiple export motifs add up to multiple export pathways? *Trends Parasitol* 26: 6–10.
 32. Dixon MW, Hawthorne PL, Spielmann T, Anderson KL, Trenholme KR, et al. (2008) Targeting of the ring exported protein 1 to the Maurer's clefts is mediated by a two-phase process. *Traffic* 9: 1316–1326.
 33. Walshaw J, Woolfson DN (2001) Open-and-shut cases in coiled-coil assembly: alpha-sheets and alpha-cylinders. *Protein Sci* 10: 668–673.
 34. Burkhard P, Stetefeld J, Strelkov SV (2001) Coiled coils: a highly versatile protein folding motif. *Trends Cell Biol* 11: 82–88.
 35. Papakrivovs J, Newbold CI, Lingelbach K (2005) A potential novel mechanism for the insertion of a membrane protein revealed by a biochemical analysis of the *Plasmodium falciparum* cytoadherence molecule P1EMP-1. *Mol Microbiol* 55: 1272–1284.
 36. Day KP, Karamalis F, Thompson J, Barnes DA, Peterson C, et al. (1993) Genes necessary for expression of a virulence determinant and for transmission of *Plasmodium falciparum* are located on a 0.3-megabase region of chromosome 9. *Proc Natl Acad Sci U S A* 90: 8292–8296.
 37. Barnes DA, Thompson J, Triglia T, Day K, Kemp DJ (1994) Mapping the genetic locus implicated in cytoadherence of *Plasmodium falciparum* to melanoma cells. *Mol Biochem Parasitol* 66: 21–29.
 38. Bourke PF, Holt DC, Sutherland CJ, Kemp DJ (1996) Disruption of a novel open reading frame of *Plasmodium falciparum* chromosome 9 by subtelomeric and internal deletions can lead to loss or maintenance of cytoadherence. *Mol Biochem Parasitol* 82: 25–36.
 39. Spielmann T, Hawthorne PL, Dixon MW, Hannemann M, Klotz K, et al. (2006) A cluster of ring stage-specific genes linked to a locus implicated in cytoadherence in *Plasmodium falciparum* codes for PEXEL-negative and PEXEL-positive proteins exported into the host cell. *Mol Biol Cell* 17: 3613–3624.
 40. Culvenor JG, Langford CJ, Crewther PE, Saint RB, Coppel RL, et al. (1987) *Plasmodium falciparum*: identification and localization of a knob protein antigen expressed by a cDNA clone. *Exp Parasitol* 63: 58–67.
 41. Hanssen E, Hawthorne P, Dixon MW, Trenholme KR, McMillan PJ, et al. (2008) Targeted mutagenesis of the ring-exported protein-1 of *Plasmodium falciparum* disrupts the architecture of Maurer's cleft organelles. *Mol Microbiol* 69: 938–953.
 42. Bozdech Z, Mok S, Hu G, Imwong M, Jaidee A, et al. (2008) The transcriptome of *Plasmodium vivax* reveals divergence and diversity of transcriptional regulation in malaria parasites. *Proc Natl Acad Sci U S A* 105: 16290–16295.